MODELLING THE IMPACT OF CONSERVATION STRUCTURES AND CLIMATE CHANGE ON WATER YIELD IN A WATERSHED

by

FOUSIYA

Department of Irrigation and Drainage Engineering

KELAPPAJI COLLEGE OF AGRICULTURAL ENGINEERING AND TECHNOLOGY

TAVANUR, MALAPPURAM- 679573

KERALA, INDIA

2020

MODELLING THE IMPACT OF CONSERVATION STRUCTURES AND CLIMATE CHANGE ON WATER YIELD IN A WATERSHED

by

FOUSIYA
(2018-18-001)

THESIS

Submitted in partial fulfilment of the requirement for the degree of

MASTER OF TECHNOLOGY

IN

AGRICULTURAL ENGINEERING

(Soil and Water Engineering)

Faculty of Agricultural Engineering and Technology

Kerala Agricultural University

Department of Irrigation and Drainage Engineering

KELAPPAJI COLLEGE OF AGRICULTURAL ENGINEERING AND TECHNOLOGY

TAVANUR, MALAPPURAM- 679573

KERALA, INDIA

2020

DECLARATION

I, hereby declare that this thesis entitled **"MODELLING THE IMPACT OF CONSERVATION STRUCTURES AND CLIMATE CHANGE ON WATER YIELD IN A WATERSHED"** is a bonafide record of research work done by me during the course of research and the thesis has not previously formed the basis for the award to me of any degree, diploma, associateship, fellowship or other similar title, of any other University or Society.

Place: Tavanur **Fousiya**

Date: **(2018-18-001)**

CERTIFICATE

Certified that this thesis entitled **"MODELLING THE IMPACT OF CONSERVATION STRUCTURES AND CLIMATE CHANGE ON WATER YIELD IN A WATERSHED"** is a record of research work done independently by **Smt. Fousiya (2018-18-001)** under my guidance and supervision and that it has not previously formed the basis for the award of any degree, diploma, fellowship or associateship to her.

Place: Tavanur

Date:

Dr. Anu Varughese
(Major Advisor, Advisory Committee)
Assistant Professor
Dept of IDE
KCAET, Tavanur.

CERTIFICATE

We, the undersigned members of the advisory committee of Ms. Fousiya, a candidate for the degree of **Master of Technology in Agricultural Engineering** with major in Soil and Water Engineering, agree that the thesis entitled **"MODELLING THE IMPACT OF CONSERVATION STRUCTURES AND CLIMATE CHANGE ON WATER YIELD IN A WATERSHED"** may be submitted by Ms. Fousiya, in partial fulfilment of the requirement for the degree.

Dr. Anu Varughese
(Chairman, Advisory Committee)
Assistant Professor
Dept of IDE
KCAET, Tavanur.

Dr. Ajith Kumar B
(Member, Advisory Committee)
Assistant Professor & Head
Dept of Agricultural Meteorology
College of Horticulture, Vellanikara.

Dr. Sasikala D
(Member, Advisory Committee)
Professor & Head
Dept of IDE, KCAET, Tavanur.

Er. Gilsha Bai E.B
(Member, Advisory Committee)
Assistant Professor (SWE)
RARS, Pattambi.

Dr. Suma Nair
(Member, Advisory Committee)
Assistant Professor (FPM)
Krishi Vigyan Kendra, Thrissur.

EXTERNAL EXAMINER
(Name and Address)

ACKNOWLEDGMENT

While bringing out this thesis to its final form, I came across a number of people whose contributions in various ways helped my field of research and they deserve special thanks. It is a pleasure to express my deep sense of gratitude towards all those who have made it possible for me to complete this project with success.

First and foremost, I bow my heads before God Almighty for the blessings bestowed upon me to materialize this endeavour. I am deeply indebted to the Kerala Agricultural University for providing this opportunity to do the project work.

I would like to express my deep sense of gratitude and indebtedness to my chairman **Dr. Anu Varughese**, Assistant Professor, Dept of IDE, KCAET, Tavanur, for her valuable encouragement, suggestions and support from an early stage of this research and providing me extraordinary experiences throughout the work. Above all, her priceless and meticulous supervision at each and every phase of the work inspired me in innumerable ways. I specially acknowledge her for her advice, supervision, and the vital contribution as and when required during this research. Her involvement with originality has triggered and nourished my intellectual maturity that will help me for a long time to come. I am proud to record that I had the opportunity to work with an experienced Assistant Professor like her.

I extend my sincere thanks to **Dr. Sasikala, D**, Professor and Head, Department of Irrigation and Drainage Engineering, for the kind cooperation. I also owe my sincere thanks to all my Advisory Committee members for their valuable suggestions and guidance during my thesis work. I would also like to express my sincere gratitude to **Dr. Ajithkumar, B**, Assistant Professor and Head, Department of Meteorology, College of Horticulture, Vellanikkara and **Er. Gilsha Bai, E.B,** Assistant Professor (SWE), RARS, Pattambi, for rendering timely advices and support during the entire period of my research work. I am extremely grateful and utmost indebted to **Dr. Suma Nair**, Assistant Professor (FPM), Krishi Vigyan Kendra, Thrissur, for her valuable comments and support especially in my thesis correction. I am highly grateful to **Dr. Sathian K.K**., Professor and Dean, KCAET, Tavanur for his kind support and permission to collect data from different

departments. I also express my sincere gratitude for the technical and moral support rendered by Dr. Asha Joseph, Dr. Rema K.P and Dr. Jinu. A, during the period of research.

I wish to extend my sincere thanks to all the faculty of Surface Water Division of Centre for Water Resources Development and Management (CWRDM), Kunnamangalam, Kozhikode for rendering the needed technical help.
I also owe my sincere thanks to all the staffs of Kerala State Land Use Board, Thrissur, especially **Ginu, T. K,** Geological Assistant, for his kind cooperation.
I would also like to thank my classmate **Ms. Riyola George** and my senior **Mrs. Mamatha Prabhakar** for their valuable suggestions and helpful discussions.
I also express my sincere thanks to all staff members of library, KCAET, Tavanur for their ever willing help and cooperation.

Last but not the least, I must express my gratitude to my parents and family members for being with me at every moment and providing continuous moral boosting and affection during thesis work. This accomplishment would not have been possible without them. I must add that it has been a great experience studying at KCAET campus and all the time spent in this campus will remain in my memory for years to come. I once again express my heartfelt thanks to all those who helped me in completing this venture in time.

Fousiya

Dedicated to
The faculty of Agricultural Engineering

CONTENTS

Chapter No.	Title	Page No.
	LIST OF TABLES	
	LIST OF FIGURES	
	LIST OF APPENDICES	
I	INTRODUCTION	1-7
II	REVIEW OF LITERATURE	8-35
III	MATERIALS AND METHODS	36-65
IV	RESULTS AND DISCUSSION	66-134
V	SUMMARY AND CONCLUSION	135-140
	REFERENCES	i-xxviii
	APPENDICES	xxix-xlvi
	ABSTRACT	

LIST OF TABLES

Table No.	Title of Table	Page No.
2.1.	Parameters used for the representation of conservation practices in SWAT	24
3.1	Bias correction methods used for precipitation and temperature	44
3.2	General performance rating of statistical measures	62
3.3	Classification of drought based on SPI values	64
4.1	DEM properties	67
4.2	Land use distribution in the study area	68
4.3	Slope class distribution	70
4.4	Parameters raking after sensitivity analysis and fitted range of values	76
4.5	Model evaluation statistics	79
4.6	Statistical comparison of different bias correction methods of future climate datasets (CMIP5 and CORDEX-SA) with observed precipitation	90
4.7	Statistical comparison of different bias correction methods of future climate datasets (CMIP5 and CORDEX-SA) with observed maximum temperature	93
4.8	Statistical comparison of different bias correction methods of future climate datasets (CMIP5 and CORDEX-SA) with observed minimum temperature	95
4.9	Water balance components under different climate scenarios	107
4.10	SPI analysis of observed period	112
4.11	RDIst analysis of observed period	114
4.12	Number of drought events using SPI index and RDI index	116
4.13	Number of drought events and duration from 2021-40 under different scenarios using SPI	121
4.14	Number of drought events and duration from 2041-70 under different scenarios using SPI	122
4.15	Surface area and volume of conservation practices summed up at each subbasin outlet	126
4.16	Details of Kanjirapuzha dam needed as input to SWAT	127

LIST OF FIGURES

Fig. No.	Title of figure	Page No.
2.1	Linkage between optimisation program and SWAT in SWAT-CUP	20
2.2	RCP CO_2 Emission Scenarios	31
3.1	Location map of study area	38
3.2	Location map of meteorological and rain gauge stations of Thuthapuzha	41
3.3	ArcMap interface showing ArcSWAT menu	46
3.4	ERDAS IMAGINE 2014 interface	47
3.5	SWAT-CUP interface	48
3.6	CMhyd interface	49
3.7	DrinC software interface	51
3.8	Schematic representation of the hydrologic cycle in SWAT	53
3.9	Project setup menu in SWAT	55
3.10	Watershed delineation sub menu in ArcSWAT	55
3.11	Overlay menu in ArcSWAT	56
3.12	HRU Definition menu in ArcSWAT	57
3.13	Weather data definition menu in ArcSWAT	57
3.14	Write SWAT input tables menu in SWAT model	58
3.15	Setup menu for the process of running SWAT model in ArcSWAT	59
4.1	Digital Elevation Model of Thuthapuzha watershed	66
4.2	(A) Land use map (B) Lookup table of land use map	68
4.3	(A) Soil map of the study area (B) Lookup table showing area and soil series	69 70
4.4	Slope map of the study area	70
4.5	Location table of rain gauge stations and data table showing the rainfall of Pattambi station	71
4.6	Delineated watershed showing outlet points and subbasins	72
4.7	Global sensitivity output showing ranking using t-stat and p-value	77
4.8	Dotty plot showing the most sensitive parameters	77-78

4.9	Observed and simulated discharge at Pulamanthole for calibration period	80
4.10	Observed and simulated discharge at Pulamanthole for validation period	80
4.11	Scatter plot of observed and simulated monthly discharges at Pulamanthole gauging station during calibration period	81
4.12	Scatter plot of observed and simulated monthly discharges at Pulamanthole gauging station during validation period	81
4.13	95 PPU plot obtained from SWAT-CUP and corresponding monthly rainfall	82
4.14	Observed and simulated streamflow at Pulamanthole during the entire simulation period	82
4.15	Water balance of Thuthapuzha watershed from 1992-1999	84
4.16	Water balance of Thuthapuzha watershed from 2000-2004	85
4.17	Water balance of Thuthapuzha watershed from 2005-2009	86
4.18	Annual streamflow and average annual rainfall of Thuthapuzha watershed	87
4.19	Comparison between observed precipitation and projected datasets without bias correction	88
4.20	Comparison between observed maximum temperature and projected datasets without bias correction	89
4.21	Comparison between observed minimum temperature and projected datasets without bias correction	89
4.22	Comparison of observed precipitation and bias corrected methods of CMIP5 precipitation datasets	91
4.23	Comparison of observed precipitation and bias corrected methods of CORDEX-SA precipitation datasets	91
4.24	Comparison of observed maximum temperature and bias corrected methods of CMIP5 maximum temperature datasets	92
4.25	Comparison of observed maximum temperature and bias corrected methods of CORDEX-SA maximum temperature datasets	93
4.26	Comparison of observed maximum temperature and bias corrected methods of CMIP5 maximum temperature datasets	94

4.27	Comparison of observed maximum temperature and bias corrected methods of CORDEX-SA maximum temperature datasets	94
4.28	Comparison of observed and bias corrected monthly precipitation under different scenarios	98
4.29	Percent change in monthly rainfall from observed data under different scenarios	98
4.30	Comparison of observed and bias corrected monthly maximum temperature under different scenarios	99
4.31	Comparison of observed and bias corrected monthly minimum temperature under different scenarios	100
4.32	Predicted annual streamflow under different scenario from 2021-40	103
4.33	Predicted annual streamflow under different scenario from 2041-70	103
4.34	Predicted monthly streamflow under different scenario from 2021-40	104
4.35	Predicted monthly streamflow under different scenario from 2041-70	104
4.36	Predicted monthly streamflow under different scenario in comparison with observed from 2021-70	105
4.37	Predicted water balance component for the entire simulation period	108
4.38	Predicted water balance component in RCP4.5 scenario from 2020-2070	108
4.39	Predicted water balance component in RCP6 scenario from 2020-2070	109
4.40	Predicted water balance component in RCP8.5 scenario from 2020-2070	110
4.41	SPI for the observed period from 1989 to 2017	112
4.42	RDI for the observed period from 1989 to 2017	113
4.43	Comparison between SPI and RDI for RCP4.5 scenario from 2021-2070	115
4.44	Comparison between SPI and RDI for RCP6 scenario from 2021-2070	115
4.45	Comparison between SPI and RDI for RCP8.5 scenario from 2021-2070	116
4.46	Regression analysis between SPI and RDI for RCP4.5 scenario	117
4.47	Regression analysis between SPI and RDI for RCP6 scenario	118
4.48	Regression analysis between SPI and RDI for RCP8.5 scenario	118
4.49	SPI under different scenarios for the projected period from 2021-2040	119
4.50	SPI under different scenarios for the projected period from 2041-2070	120
4.51	Map showing location of conservation practices of Thuthapuzha watershed	125
4.52	Predicted annual streamflow simulation with and without conservation structures	128

4.53	Predicted monthly streamflow simulation with and without conservation structures	129
4.54	Percentage change in streamflow with and without structure	129
4.55	Comparison between observed and simulated sediment yield with structure	131
4.56	Scatter plot between observed sediment yield and simulated sediment yield with structure	131
4.57	Predicted annual sediment yield with and without conservation structures	132
4.58	Predicted monthly sediment yield with and without conservation structures	133
4.59	Percentage change in sediment yield with and without structure	134

LIST OF APPENDICES

Appendix. No.	Title	Page No.
I	Monthly average Precipitation (mm) of Pattambi during 1989-2017	xxix
II	Monthly average Precipitation (mm) of Mannarkkad during 1989-2017	xxx
III	Monthly average Maximum temperature (°C) of Pattambi during 1989-2017	xxxi
IV	Monthly average Maximum temperature (°C) of Pulamanthole during 1989-2017	xxxii
V	Monthly average Minimum temperature (°C) of Pattambi during 1989-2017	xxxiii
VI	Monthly average Minimum temperature (°C) of Pulamanthole during 1989-2017	xxxiv
VII	Monthly average Relative humidity (%) of Pattambi during 1989-2017	xxxv
VIII	Monthly average Wind speed (m/s) of Pattambi during 1989-2017	xxxvi
IX	Monthly average Solar radiation (MJ/m²/day) of Pattambi during 1989-2017	xxxvii
X	Monthly average discharge (m³/s) of Pulamanthole gauging station during 1989-2017	xxxviii
XI	Annual Streamflow (Mm³) of Pulamanthole gauging station during 1989-2017	xxxix
XII	Bias corrected data of precipitation for different scenarios	xl
XIII	Bias corrected Maximum temperature (°C) data from 2021-70 under different scenarios	xl
XIV	Bias corrected Minimum temperature (°C) data from 2021-70 under different scenarios	xli
XV	Predicted annual streamflow under different scenario from 2021-40	xli
XVI	Predicted annual streamflow (Mm³) under different scenario from 2041-70	xlii
XVII	Predicted monthly streamflow (Mm³) under different scenario in comparison with observed from 2021-70	xliii
XVIII	Predicted annual streamflow simulation (Mm³) with and without conservation structures	xliv
XIX	Predicted monthly streamflow simulation (Mm³) with and without conservation structures	xlv
XX	Predicted annual sediment yield (t/h) with and without conservation structures	xlvi
XXI	Predicted monthly sediment yield (t/h) with and without conservation structures	xlvi

ABBREVIATIONS USED

AGCM	:	Atmospheric General Circulation Model
AOGCM	:	Atmospheric-Ocean Coupled General Circulation Model
ASABE	:	American Society of Agricultural and Biological Engineers
Assoc.	:	Association
BMP	:	Best Management Practice
CCAFS	:	Climate Change, Agriculture and Food Security
CCCR-IITM	:	Climate Change Research of Indian Institute of Tropical Meteorology
CIM	:	Climate Impact Model
CMhyd	:	Climate Model for Hydrological Modelling
CMIP5	:	Coupled Model Intercomparison Project Phase 5
CORDEX	:	Coordinated Regional Climate Downscaling Experiment
CREAMS	:	Chemicals, Runoff, and Erosion from Agricultural Management Systems
CWC	:	Central Water Commission
DCC	:	Delta change correction
DEM	:	Digital Elevation Model
DM	:	Distribution mapping
DrinC	:	Drought Indices Calculator
EPIC	:	Erosion Productivity Impact Calculator
ESGF	:	Earth System Grid Federation

ESRI	:	Environmental Systems Research Institute
et al.	:	and others
Fig.	:	Figure
GCM	:	General Circulation Model
GFDL	:	Geophysical Fluid Dynamics Laboratory
GIS	:	Geographic Information System
GLUE	:	Generalized Uncertainty Estimation
GSA	:	Global sensitivity analysis
GWLF	:	Generalized Watershed Loading Function
ha	:	Hectare
HRU	:	Hydrological Response Unit
HSPF	:	Hydrological Simulation Program-FORTRAN
IMD	:	India Meteorological Department
Int.	:	International
IPCC	:	Intergovernmental Panel on Climate Change
J.	:	Journal
km^2	:	Square kilometre
km^3	:	Cubic kilometre
LIS	:	Local Intensity Scaling
LS	:	Linear Scaling
LULC	:	Land use land cover
m^3	:	Cubic metre
MCMC	:	Markov Chain Monte Carlo
MIP	:	Model Intercomparison Projects
mm / year	:	Millimetre per year
mm	:	Millimetre
Mm^3	:	Million cubic metres

MSL	:	Mean sea level
MUSLE	:	Modified Universal Soil Loss Equation
NOAA	:	National Oceanic and Atmospheric Administration
NPS	:	Non-point source
NSE	:	Nash-Sutcliffe efficiency
OAT	:	One At a Time
OGCM	:	Ocean GCM
ParaSol	:	Parameter Solution
PBIAS	:	Percent bias
PDSI	:	Palmer Drought Severity Index
PET	:	Potential Evapotranspiration
PPU	:	Percent Prediction Uncertainty
Proc.	:	Proceedings
PSO	:	Particle Swarm Optimization
PT	:	Power transformation
R^2	:	Coefficient of Determination
RCD	:	Regional Climate Downscaling
RCM	:	Regional climate models
RCP	:	Representative Concentration Pathway
RD	:	Rainfall Deciles
RDI	:	Reconnaissance Drought Index
RDIn	:	Normalized RDI
RDIst	:	Standardized RDI
RMSE	:	Root Mean Square Error
Sci.	:	Science
SDI	:	Streamflow Drought Index
SHE	:	Systeme Hydrologique Europeen
Soc.	:	Society

SPI	:	Standardized Precipitation Index
SRES	:	Special Report on Emissions Scenarios
SRTM	:	Shuttle Radar Topography Mission
SUFI-2	:	Sequential Uncertainty Fitting Ver.2
SWAT CUP	:	SWAT Calibration and Uncertainty Procedures
SWAT	:	Soil and Water Assessment Tool
SWC	:	Soil and Water Conservation
t/ha	:	tonnes per hectare
TAR	:	Third Assessment Report
USGS	:	US Geological Survey
UTM	:	Universal Transverse Mercator
VCB	:	Vented Cross Bar
VIC	:	Variable Infiltration Capacity
Viz.	:	Namely
VS	:	Variance Scaling
W/m^2	:	Watts per square metre
WCRP	:	World Climate Research Programme
WEC-C	:	Water & Environmental Consultants – Catchment
WMO	:	World meteorological organization
WWDR	:	World Water Development Report
$\alpha 0$	:	Initial value

Introduction

CHAPTER I

INTRODUCTION

Land, water and vegetation are the three fundamental resources which support life on Earth. Even though water is the most widely distributed natural resource, its demand is increasingly challenging every day. Of all the water available on Earth, 97% exists as salt water, leaving just 3% as fresh water, of which only 1% is readily available for use. Freshwater resources are facing increased competition and its availability is limited in many parts of the world. There is competition within countries for available water, in and between economic sectors and there are more chances of struggle regarding this natural resource since the demand for various uses such as agriculture, industries, households etc. is increasing drastically. Currently, 47% of the world's population lives in areas suffering from water shortages at least for a period of one month in a year. The demand for water will increase by 2050 when world's population is expected to reach to the range 9.4 to 10.2 billion, an increase of 22 to 34% from the current population of 7.7 billion people (WWDR, 2018). This population growth is expected mainly in developing countries, first in Africa, and then in Asia, where water scarcity is already a serious problem. Significant factors influencing the rising global demand for water include demographic pressure, ongoing developments, urbanization, environmental changes, changing patterns of consumption etc. Most of the countries in the world are facing lack of water availability when compared to their growing demand. From the ever increasing population and security needs, it is clear that both land and water resources must be managed and used in an integrated and comprehensive manner. Sustainable development and efficient management are therefore of paramount importance, which is a complex as well as a challenging task.

In water-scarce areas, water management is a serious issue since it has a direct impact on people's livelihood and on land productivity. Watershed management involves land management by using the most suitable measures, whether engineering or biological, in such a way that the management work must be productive and socially acceptable. Understanding watershed hydrology is very important for effective water

resource management. Effective conservation as well as management of natural resources can be accomplished by adopting watershed as a basic unit of development. Watershed as a natural hydrological unit, responds very effectively to various conservation practices. In the past, the inhabitants of the dry lands have made use of water storage structures to overcome water scarcity. These structures have both positive as well as negative impacts on watershed hydrology. Positive impacts include enhancing water quality, ensuring proper water conservation, providing more sustainable water resources in the upstream reaches etc., and some negative impacts like erosion, water pollution, loss of homes and human lives due to flooding etc. may also occur. One of the main concerns relevant to watershed management is the inequitable benefits for downstream users.

The rate of degradation of soil and water resources is escalating throughout the world, influencing, directly or indirectly, all critical processes on the Earth's surface. It is largely due to improper land use planning, where land and water management must be the most important factor. Conservation practices are categorised as in-situ and ex-situ. In-situ management includes practices in agricultural fields like implementation of bunds, terraces and other soil and water conservation practices, whereas ex-situ management includes the construction of structures such as check dams, gully control structures, farm ponds, etc. which help to reduce peak discharge and capture a large amount of runoff resulting in increased groundwater recharge. Scientists are now focusing on the impact of these conservation practices on watershed hydrology including runoff, sediment, nutrient loss, quality of water etc.

Hydrological modelling is one of the most relevant methods used to evaluate the conservation structures impact on hydrology of a watershed. It is a difficult and time-consuming process to physically determine the efficiency and performance of conservation practices at the farm level. Modelling approaches are widely used to determine the efficiency of conservation practices in minimising nutrient runoff and sediment (Santhi *et al.,* 2006) and advancements in computer processing technology have indeed made it possible for scientists to use hydrological models to evaluate the

conservation practices impact on watershed hydrology. For watershed modelling studies, adequate knowledge of characteristics of the watershed, climate and conservation structures are needed.

According to Chow *et al.* (1988), the models represent the hydrological cycle as a system with various components such as inputs (e.g. rainfall, temperature) and outputs (e.g. discharge, sediment yield etc.) linking these components using a set of equations. Watershed models capable of representing such processes can be used to improve knowledge of the relationship between hydrological processes, erosion and management practices. Numerous models can predict runoff, nutrient loss, sediment yield, erosion etc. from a catchment including SWAT (Soil and Water Assessment Tool) (Arnold *et al.*, 1998). SWAT model has been commonly used for determining several environmental and water quality scenarios among the various available watershed models. Apart from being readily available, SWAT has the adaptability to simulate various conservation practices. The effectiveness of conservation practices in terms of water quality is also assessed using SWAT model (Arnold and Fohrer, 2005). The SWAT model has been successfully used by numerous researchers to predict sediment yield and streamflow from the watershed (Pisinaras *et al*., 2010; Nasrin *et al*., 2013).

Over the last few decades, studies related to climate change and its effects on both natural and man-made processes have gained significant attention. Climate change, accompanied by global warming, has become an important environmental concern in today's world. Many effects of climate change on the environment have already been reported. Its impact on hydrology and water resources is of great significance among the observed effects. Specifically, the effects of climate change on regional hydrology are significant, as the climate and hydrological cycle are physically interrelated. Climate change results in temperature rises, changes in precipitation patterns as well as snow cover, decreases water supply, rises water demand, brings about changes in groundwater recharge, results in severe events like floods and droughts, etc. which, in turn creates additional stress for the water managers and policy makers. Anthropogenic activities resulting in emissions of greenhouse gases and aerosols are the primary causes of

climate change. Impact assessment of climate change is unpredictable in nature. There is uncertainty at all stages in the methodology of a climate change impact assessment. Management and planning of water resources has become a challenging task as a result of climate change uncertainties. It will be difficult to adjust to these impacts in future without a drastic and appropriate plan of action immediately.

Several researchers have studied the impact of climate change on hydrology and water resources, analysis of variation trends in temperature and rainfall, watershed modelling approaches to assess the future impacts of climate change, assessment of extreme hydrological events under future climate change scenarios etc. Temperature and rainfall shifts due to global warming have already occurred in many parts of the world. According to independent reports by NASA and the National Oceanic and Atmospheric Administration (NOAA), global surface temperature in the year 2018 was the fourth warmest since 1880. As a result of global warming, atmospheric concentration of carbon dioxide and other trace gases are rising. These greenhouse gases will change the radiative balance of the atmosphere resulting in the alteration of climate variables. According to the NOAA Annual Greenhouse Gas Index, radiative greenhouse gas forcing increased by 41% from 1990 to 2017, with carbon dioxide responsible for a significant portion, about 82%. Greenhouse gas concentrations experienced a steady increase in carbon dioxide (CO_2) levels as well as other principal greenhouse gases in the atmosphere at a new peak from 2015-2019, with CO_2 growth rates close to 20% higher than in the previous five years, as reported by the WMO. Under these climate change conditions, hydrological modelling is the common method for evaluating the future impacts of climate change on water resources.

For simulating projected conditions of climate change, General Circulation Models (GCMs) are a reliable tool which gives us an idea of how the climate is going to change in future. There will be mismatch between regional variables and those simulated by GCMs. It is therefore mandatory to downscale GCM output for a specific area of interest in order to regionalize global climate data. Regional climate models (RCMs) which are applied for this purpose can be broadly categorised as physical-deterministic

and statistical RCMs (Varis *et al.*, 2004). Variations may exist within the RCM derived data as compared to reference period data. Therefore, the bias between the observations and the RCM output must be eliminated by some bias correction method prior to impact related studies. Bias corrected data are then fed to hydrological models for climate change impact assessment.

The Earth System Grid Federation (ESGF) is commonly used to assess climate data, which is a main tool of World Climate Research Programme (WCRP) for providing global and regional climate simulations along with observations and further study over the next decade. ESGF provided greater flexibility to generate large number of CORDEX RCM simulations developed by a number of modelling groups across the globe, and their GCMs derived from Coupled Model Intercomparison Project Phase 5 (CMIP5). CORDEX-SA is specifically designed for climate data projections in the South Asian zone. High-resolution simulations of 20^{th} century climatic change and future climate projections have been developed at Centre for Climate Change Research of Indian Institute of Tropical Meteorology (CCCR-IITM) in the South Asian region which is available on the CCCR-IITM data portal. The CGIAR Research Program on Climate Change, Agriculture and Food Security (CCAFS) data repository also provides high-resolution climate datasets for global and regional climate change impact assessment.

Several studies have explored the impact of climate change on extreme hydrological events. The majority of studies focused on flood events (Kobierska *et al.*, 2013). Few studies have focused on the relationship between drought and climate change (Muller, 2014). Drought would have an inevitable impact on water resources. This leads to further challenges for agriculture as well as food production. Future climate change is projected to analyse the impact of extreme events on the availability of water resources. Such projected condition seems to be of interest to water resource managers for sustainable resource planning and management. In fact, it provides local management authorities with a planning tool to establish sustainable adaptation options.

There are different hydrological models used for climate change impact assessment that may be process-based, semi-distributed, distributed etc. Most of the models were designed for flood forecasting, water yield estimation, erosion studies etc. Studies incorporating output from climate models into hydrological models have developed extensively throughout the world over the last two decades. Climate change studies have used standard hydrological models, such as the Soil and Water Assessment Tool (SWAT), the Hydrological Simulation Program-FORTRAN (HSPF), the Variable Infiltration Capacity (VIC) and the Generalized Watershed Loading Function (GWLF).

Generally, India has been extremely vulnerable to climate related severe events such as floods, droughts and cyclones. Extreme rainfall during monsoon and severe drought during summer has become a recent trend in India. Although the Kerala state in India has an average precipitation of 3000 mm per year, the state faces extreme water shortage during the summer months. Kerala was also hit by extreme floods in 2018 and 2019 due to heavy rainfall. In Kerala, all the rivers flow full during the monsoon, many of them eventually dry up in summer. Bharathappuzha, also known as the Nila, with a length of 209 km, is the second longest river in Kerala. Kalpathipuzha, Gayatripuzha, Thuthapuzha and Chitturpuzha are the four major tributaries of Bharathappuzha. The average annual discharge of Bharathapuzha is 3.94 km^3, of which Thuthapuzha contributes approximately 42% (1.6 km^3) (Raj and Azeez, 2009). The Bharathappuzha River is a source of water for both the Kerala and Tamilnadu states, covering the districts of Malappuram, Thrissur and Palakkad in Kerala and two districts, namely Coimbatore and Tiruppur in Tamilnadu. The river is now facing significant threats to its survival. Among them, sand mining is prominent as it deepens the river beds. Ecologists have predicted that extreme consequences will arise as a result of sand mining resulting in the death of the river in the near future. The river used to flow smoothly even in acute summers, until a few decades ago. Significant climate change has also modified the pattern of river flow. Extreme events due to climate change can be adjusted in the future by properly managing water resources through soil and water conservation. Therefore, a detailed study is needed to understand

the effects of climate change and conservation practices on the river basin. For this research, a modelling approach is used to analyse the impacts in the Thuthapuzha subbasin.

Modelling approach will help to simulate the long-term effects without the need for time-consuming and costly experiments. In addition, models can be used to answer the "if-then" questions that are often impossible to observe in the real world (Fu *et al.*, 2006). Since field observations cannot be extrapolated to the basin scale, the practice of using mathematical models is quite accepted these days (Verstraeten *et al.*, 2002), although it has been widely reported that insufficient good quality observations are a limiting factor for modelling applications (Bormann and Diekkruger, 2003). From this perspective, appropriate and flexible hydrological models are needed to address poor quality data in order to provide effective tools for water resource managers. Among the models available, the SWAT model used in this study can predict impacts and also evaluate best management practices in agriculture, specifically the soil and water conservation practices adopted in watersheds. Hence, this research work involves the setting up of a hydrological model SWAT for the area, and assessing the impacts of structural conservation measures and climate change on water yield and drought intensity in the watershed with the following objectives.

1.To set up a hydrological model (SWAT) for the area.
2. To assess the impact of conservation structures on monthly stream flow and sediment yield.
3. To predict the impact of climate change on water yield and drought intensity.

With this background, the impact of climate change and conservation structures on streamflow and sediment yield of the Thuthapuzha subbasin is evaluated and explained in the following chapters.

Review of Literature

CHAPTER II

REVIEW OF LITERATURE

This chapter includes a detailed review of the previous research work conducted in India and abroad in the field of hydrological modelling based on SWAT, steps involved in setting up of the SWAT model, impact assessment studies related to both climate change and conservation practices.

2.1 WATERSHED HYDROLOGY AND ITS IMPORTANCE

Watershed is defined as the basic unit of land that drains water to a common outlet for the water resource management (Edwards *et al.,* 2015). Hydrology, a study of the distribution and movement of water throughout the earth, describes both the hydrological cycle and water resources. As water is a renewable natural resource, it is recycled continuously and returned to the ecological system through the hydrological cycle. The hydrological cycle is the fundamental purification method for water on Earth as all components in water are left behind during the transition from liquid water to water vapour (Rast *et al.,* 2014). Precipitation, interception, depression storage, evapotranspiration, infiltration, percolation, ground water and runoff are the main components of the hydrological cycle.

Watershed hydrology lays the foundation for understanding hydrological processes and water resources management and planning. Understanding how water is used and recycled through a watershed is the basis for explaining the interaction between land and water. From a number of perspectives, water resource management has become an important issue, including the future development of water bodies, the protection of water bodies from pollution and over-exploitation, and the prevention of conflicts. In order to develop and protect water resources, detailed hydrological information prevailing in the chosen catchment area is needed.

2.2 HYDROLOGICAL MODELLING

Model is the simplification of reality and it is the representation of real world phenomena (Wheater *et al.,* 2008). A hydrological model is an approximation of complex realities through a system concept. A system consists of a group of interactive or interrelated components that form a complex whole. The ultimate aim of the hydrological system research is to study the function of the system and predict its output in order to understand different hydrological processes. The best model is the one that produces outputs that are close to the real world, using minimum number of parameters and model complexity. The model contains different parameters describing the characteristics of the model. Rainfall data and drainage area are the main inputs needed for almost all hydrological models. In addition to that, watershed features such as soil characteristics, vegetation, topography, characteristics of ground water aquifer, weather parameters like temperature, solar radiation etc. are also taken into consideration.

Water resource management in a single river basin system is the best way to address water-related issues. However, there are significant gaps in many areas where water balance planning requires basic knowledge of water resources. Among the resources available, hydrological models are generally used to gain adequate knowledge of the river basin characteristics in order to bridge these gaps. There are models that can evaluate the impact of natural and man-made changes on water resources and quantify the available water resources both spatially and temporally. The main challenges, however, are the selection and use of these models for a specific basin and management plan. Choosing a model depends on several factors such as the study purpose and the availability of the model (Ng and Marsalek, 1992). Several hydrological models have been developed world wide to determine the impact of climate and soil characteristics on hydrology and water resources. All these models can be used in large and very complex basins (Devi *et al.,* 2015). Each and every model has its own unique features. Monthly water balance models or rainfall-runoff models are effective in evaluating regional water resource management in order to determine the impact of climate change on watershed

hydrology (Arnell, 1992). Hydrological models are therefore now considered to be an important and vital tool for managing water and the environment.

2.2.1 Classification of models

Scientists have used a number of ways to categorise and separate models based on spatial and temporal resolution, input variables, model simplicity, physical concepts etc. Even though there are many ways to categorise models, not all models fall into a particular group as they have been designed for different applications (Singh, 1995).

The hydrological models were divided into two groups by Chow *et al.* (1988); physical and abstract. Physical models are again classified as scale models and analog models. Scale models are a scaled down or scaled up model of the real world, while analog models use another physical system with similar prototype properties. The mathematical form of a system that can be classified as stochastic and deterministic models based on how they handle the randomness of the hydrological process is demonstrated in the abstract model. Stochastic models allow a certain randomness that results in a single set of inputs with different output values and are based on the analysis of historical events, usually river discharge and rainfall (Ahmad *et al*., 2001; Tesfaye *et al.*, 2006). For a single set of input values, deterministic models generally produce the same output. Cunderlink (2003) divided the deterministic models into three; lumped models, where the variable or parameter is assumed to have an average value for the entire catchment area, semi-distributed, where the parameters are partially allowed to change in space by dividing the catchment area into several subbasins and distributed models, where all variables and parameters have different values. Empirical, conceptual and physically based models are another important classification of deterministic models. Empirical models are generally lumped models that are based on the analysis of parallel input-output time series. The Artificial Neural Network (ANN) model, which has the potential to successively learn from data, also known as the data-driven model, is one of the most recent approaches in this category (Govindaraju and Rao, 2000; Antar *et al*., 2006). The conceptual model, which can be lumped or distributed, portrays catchment as an integrated conceptual component and also integrates certain aspects

of the physical system. Examples of the conceptual models are TOPMODEL (Beven and Kirkby, 1979) and Soil and Water Assessment Tool (SWAT) (Arnold *et al*., 1998). Hydrological variables observed, usually river flow data, are needed for the calibration of both empirical and conceptual approaches in order to set up a model (Tessema, 2011). Physically based models are clearly based on the interpretation of physical processes through the application of fundamental hydrodynamic principles. The physical models can resolve several limitations of the other two models due to the physical interpretation of parameters. It can be used in ungauged watersheds, assuming that the parameters or variables required for the model can be observed. Moreover, physical models can provide substantial amount of data even beyond the boundary and can be applied for a broad range of applications. Water and Environmental Consultants – Catchment (WEC-C) (Croton and Barry, 2001), Systeme Hydrologique Europeen model (SHE) (Abbott *et al.,* 1986) are a few examples. Based on time factor, models are classified as static and dynamic models. Static model excludes time while dynamic model includes time. Another time based classification is by Wheater *et al.* (2008) as event-based and continuous models. Those models generate output over a specific time period, called event-based models, while continuous models produce continuous output.

2.3 SWAT (SOIL AND WATER ASSESSMENT TOOL) MODEL

Soil and Water Assessment Tool (SWAT) model developed by USDA Agricultural Research Service is a continuous-time, semi distributed, process based river basin or watershed scale model (Arnold *et al.,* 1998; Neitsch *et al.,* 2005). SWAT works on a daily basis and is designed to evaluate the effect of land use and management practices on runoff, sediment, and agricultural chemical yields in ungauged watersheds. It is also used to assess the environmental impact of best management practices (BMPs) and alternative management strategies for large catchments. The SWAT model contains subbasin, reservoir, and channel routing components. These components are modelled on the basis of scientific concepts and equations. In SWAT model, a watershed is divided into different subwatersheds, and thereafter subdivided into Hydrological Response Units (HRUs) consisting of homogeneous land use, management, topography, and soil

properties (Arnold *et al.,* 2012). The model enables users to model watersheds with less available data and use alternative input data such as climate and land use for runoff, sediment, water quality and other output parameters to determine predictive future scenarios (Venkatesh *et al.,* 2018).

The SWAT model includes built-in climate, soil, and plant growth datasets that can be used as data sources for running the model. Daily weather parameters like rainfall, maximum and minimum temperature, solar radiation, relative humidity and wind speed used in this model are capable of describing water and sediment yield, vegetation growth and nutrient cycle (Devi *et al.,* 2015). SWAT also contains the WXGEN (Sharpley and Williams, 1990) weather generator model for generating weather information or filling gaps in measured data. Three methods are used in the model for estimating the reference evapotranspiration (PET), namely Penman-Monteith (Monteith, 1977; Allen, 1986), Hargreaves (Hargreaves and Samani, 1985) and Priestley-Taylor (Priestley and Taylor, 1972). SWAT uses two options for determining surface runoff volume; the Green and Ampt (1911) infiltration method and the SCS curve number procedure. Channel routing in SWAT is done by variable storage routing method or the Muskingum River routing method. A simplified form of the EPIC crop model (Williams *et al.,* 1984) is used in the module for crop growth and biomass production. To estimate the possible accumulation of biomass (Monteith, 1977) along with variations in water, temperature and nutrient stress, the model uses the Monteith method. SWAT also simulates erosion and water quality processes.

2.3.1 Applications of SWAT Model

SWAT applications have experienced tremendous growth globally over the last few years. Modelling of the hydrologic balance of the watershed is the basis for almost all SWAT applications (Gassman *et al.,* 2007). Modelling hydrology of a watershed can be divided into two main categories, namely the land phase and the routing phase. The land phase regulates the quantity of water, sediment, nutrient and pesticide loads at the main channel of each subbasin, while the routing phase describes the flow of water, sediment, etc. to the outlet through the watershed channel network.

Runoff simulation is an essential aspect of hydrological modelling of a watershed and is the foundation for further research in hydrology related issues. The runoff simulation consists mainly of surface runoff, ET, groundwater and soil water. Arnold confirmed the applicability of the SWAT model to simulate runoff at national, basin and even smaller scales (Zhao *et al.*, 2013). With reference to a small watershed in the United Kingdom, Kannan *et al.* (2007) concluded that the flow output was more accurate using the curve number method. Van Liew and Garbrecht (2003) analysed the capability of the SWAT model in predicting streamflow under different climatic conditions and found that SWAT can accurately simulate streamflow under dry, average and wet climatic conditions. Yang *et al.* (2016) reported that in the large-scale Ru River Basin, the temporal resolution of precipitation inputs could have a significant impact on daily runoff simulations, and the sub-daily SWAT model was best suited to simulate peak flows during flood season. The results of various DEM resolution data on runoff simulation were analysed by Nagaveni *et al.* (2019), in the Krishna Basin of India and results showed that the simulation of runoff is sensitive to varying DEM resolution, with variations up to a maximum of 5 percent from different DEMs.

Several studies have demonstrated the applicability of SWAT model to predict sediment loads at different watershed scales. Chu *et al.* (2004) simulated the sediment load using SWAT in the Warner Creek watershed and found good correlation between the predicted and measured annual sediment load, but there was a poor correlation between the monthly sediment loads. In order to address snowmelt-induced problems in predicting sediment loss, sediment yield equation was modified by Tolston and Shoemaker (2007) and observed an enhanced sediment loss prediction. Sediment simulations using SWAT model have also been conducted in Asia, Europe, and North Africa. Based on daily observations of an agricultural watershed located in eastern India, Behera and Panda (2006) concluded that SWAT has the potential to effectively simulate sediment yield during the entire rainy season. Kaur *et al.* (2004) observed that the annual sediment yield simulated by SWAT model would be reasonably good for the sample watershed in Damodar-Barakar, India, the second most severely eroded area in the world.

In some studies, problems with temporal and/or spatial rainfall data were a possible cause of inconsistency in sediment yield results (Bieger *et al.*, 2014; Lu *et al.*, 2014). Bieger *et al.* (2014) also indicated that the low level of precision of the soil and land use data used, the poor resolution of the Digital Elevation Model (DEM), and problems related to the transferability of the Modified Universal Soil Loss Equation (MUSLE) (Williams and Berndt, 1977) may have contributed to further errors in the sediment yield output.

In addition, SWAT is also used to address water quality issues. Due to the lack of observed data for calibration and validation of the model, the application of SWAT for water quality simulations is comparatively poor. It is time-consuming and expensive to collect water quality parameters at the field level and due to this reason most SWAT users may not be able to perform water quality simulations without financial assistance from local government or international agencies. Watershed models are useful for determining contamination from different sources of pollutants, including faecal bacteria (Benham *et al.*, 2006). Non-point source (NPS) pollution is one of the most critical factors that have a negative impact on the global ecosystem. NPS pollution is mainly due to soil and water erosion in the river basin, the use of pesticides and fertilizers in agricultural land, the disposal of rural livestock and garbage, etc. Currently, NPS pollution researches using SWAT focus mainly on nitrogen and phosphorus (N&P). The SWAT model can also examine the contributing factors and the amount of NPS pollution related substances. Yazdi and Moridi (2017) used the SWAT model and concluded that the most significant pollution component of the Seimare reservoir is the waste water from Kermanshah city and the controlled waste water discharge resulted in the reduction of about 40-50 percent pollutants entering the reservoir under drought conditions. The application of SWAT to simulate nutrients has also been analysed in many countries. SWAT nitrogen and phosphorous simulations were verified in India with measured data from eastern Indian districts of Hazaribagh (Tripathi *et al.*, 2003) and Midnapore (Behera and Panda, 2006). Both authors reported that it is possible to effectively use the SWAT model to predict nutrient losses.

SWAT can also be used to predict the impact of land use changes, including different conservation practices on water quality and hydrological components. Mishra *et al.* (2007) reported that the impacts of three check dams on sediment loads in the Banha watershed in northeast India were accurately reproduced by the SWAT model. Singh and Gosain (2011) used the SWAT model to evaluate the impact of management practices on water availability by modelling nine reservoirs as impoundments structures in the Cauvery basin, India. Bracmort *et al.* (2006) reported an impact study on runoff, sediment and total phosphorous by using three SWAT scenario simulations in two small watersheds in Indiana. SWAT model application to evaluate the impact of land use and land cover on sustainable development and watershed hydrology is gaining attention globally as a result of immense human activities in the natural systems of river basins. The most appropriate land use management practice was identified by Sunandar *et al.* (2014) in the Indonesian Asaham watershed to reduce suspended sediment without affecting water yields. Tarigan *et al.* (2018) computed that about 30 percent of forest cover needs to be preserved in order to ensure sufficient ecosystem services to local water resources in Jambi province, Indonesia.

The impacts of climate change can be measured directly in SWAT, taking into account the implications of rising concentrations of CO_2 in the atmosphere and changes in climate data. Many SWAT studies provide valuable information on the impact of changes in CO_2 fertilization and/or changes in climate data's on runoff, plant growth etc (Stonefelt *et al*., 2000; Fontaine *et al*., 2001; Jha *et al*., 2006). Gosain *et al.* (2006) projected the impact of future climate change on runoff of the twelve major river basins in India. In Malaysia, in order to understand hydroclimatic impacts, Tan *et al.* (2017) and Dlamini *et al.* (2017) incorporated the CMIP5 GCM climate projections into the SWAT model. Researchers used the SWAT model to generate hydrological impacts under both historical and future climate change conditions. Zabaleta *et al.* (2014) proposed the evaluation of the impact of climate change on discharge and sediment yields using four climate change projections, integrating two general circulation models (GCMs) and two scenarios, from 2011 to 2100. Mishra and Lilhare (2016) projected rainfall and

temperature from two Representative Concentration Pathways (RCPs) 4.5 and 8.5 scenarios during 2010-2039, 2040-2069 and 2070-2099, and carried out a sensitivity analysis. Several researchers have used SWAT to address climate change impacts on both hydrology and pollution losses. Bouraoui *et al. (*2002) estimated that in six different climate change scenarios, the total phosphorus and nitrogen load increased by 5% to 34% and 6% to 27%, respectively, in the Ouse River watershed located in the United Kingdom.

Several scholars have examined the combined impacts of land use change and climate change. Jayakody *et al.* (2014) evaluated the future climate change impacts on sediment, nutrient transport and the performance of best management practices in the Pearl River basin of the Upper Mississippi River. Mekonnen *et al.* (2018) observed an increase of 16.9 percent in the average annual river flow from 1970 to 2000 in the Upper Blue Nile Basin as a result of the combined effects of LULC and climate change. Shrestha and Htut (2016) assessed the combined future impacts of land use and climate change in the Bago River basin, Myanmar. Future climate variables projected from six GCMs under RCP 4.5 and 8.5 for the 2020s, 2050s and 2070s were used for the study and found that combined impacts resulted in an increase of up to 68% in the annual river flow (Meinshausen *et al.,* 2011). Li *et al*. (2009, 2010) concluded that the combined impacts of changes in land use and climate variables could decrease runoff, soil moisture content and evapotranspiration.

2.3.2 Advantages and limitations

The main benefit of SWAT is its ability to run simulations for large catchments to predict hydrological variables under different management activities and physical environmental conditions without regular monitoring data (Gassman *et al.,* 2007; Daloglu *et al.,* 2014). The SWAT model has built-in inputs which allow the user to study the model. It is possible to model very large basins or a variety of management practices without excessive investment of time and money. The attractive factor is that the calibration, uncertainty and sensitivity analysis of the model can be performed using a separate program called the SWAT-CUP (SWAT-Calibration and Uncertainty

Procedures). SWAT model can be used in watersheds without any gauging stations and allows users to study long term impacts.

However, SWAT has some limitations. SWAT was developed by American scholars. Data used in the model, including soil types and land use types, are all based on the locations in the United States. Use of these variables as input will result in uncertainty about the accuracy of the simulation. It does not simulate sub-daily events, such as a single storm event, and cannot simulate detailed flood-based and sediment-based events. In the spring and winter months, the modelling of flood plain erosion and snow melt erosion is difficult (Hamlett and Peterson, 1998; Shoemaker *et al.*, 2005; Dai *et al.*, 2005). The existing SWAT model needs to use the latest data for calibration to make simulation more reliable when new data is added, which is a time-consuming and laborious process. Since the SWAT model divides watersheds into hundreds of HRUs, it is difficult to manage and modify input files when required.

2.4 SETTING UP OF SWAT MODEL

2.4.1 Datasets for SWAT model setup

Soil map, land use or land cover map and DEM are the basic maps used as input in the SWAT tool. Meteorological data like precipitation, maximum and minimum temperature, wind speed, solar radiation, and relative humidity of the study area are required for setting up of the model. For the analysis of the results, daily runoff volume, flow velocity and sediment yield, physical and chemical properties of soil etc. can be used depending on the study purpose. SWAT also has an option to incorporate reservoir details like surface area, volume, year of construction etc.

2.4.2 Sensitivity analysis, calibration and validation of SWAT

Sensitivity analysis is a method for quantifying the uncertainty in the output of a model with respect to the uncertainty in its inputs. Identification of the most sensitive parameters is the first step in the calibration and validation of the SWAT model. SWAT is a complex model with many parameters, making it difficult to calibrate manually (Abbaspour, 2012). Sensitivity analysis is as important as the calibration process, as it

gives an idea of which parameter needs to be calibrated in order to reduce model uncertainty. It helps to estimate the relative ranking of those parameters which mostly affect output variance due to input variability (Van Griensven *et al.,* 2002). Ranking results in a possible reduction in the number of parameters to be calibrated, thus reduce the computational time needed for model calibration and provide guidance on estimating the parameters for the calibration process. Sensitivity analysis can be divided into two categories, one at a time and global sensitivity analysis depending on the number of parameters analysed (Brouziyne *et al.,* 2017). Changing each model input parameter one at a time (OAT) is one of the simplest methods for conducting a sensitivity analysis, while other input parameters remain unchanged. The Global sensitivity analysis (GSA) considers changes in model outputs as input parameters can vary at the same time over specified ranges (Marino *et al.,* 2008; Saltelli *et al.,* 2008; Iooss and Lemaître, 2015). Global methods usually require more computational work than OAT methods and are mostly probabilistic in nature; they consider uncertainty as probability distributions in model inputs and outputs.

Calibration is the process in which the selected model parameters and variables are adjusted to match the model output to the results observed. Calibration is considered important because the model input can have uncertainties (Lenhart *et al.,* 2002). Calibration can be done manually or using SWAT auto calibration tool (Van Griensven and Bauwens, 2003; Van Liew *et al.,* 2005). Model validation is the process of re-running the model without altering any parameter values that may have been adjusted during calibration, using another time series of input data. Calibration and validation are generally carried out by dividing the observed data available into two datasets; one for calibration, and another for validation. The model is calibrated using the major portion of the data, and the remaining fraction of the record is used to validate the model. Graphical and statistical methods are generally used to check whether the model has been properly calibrated and validated. Calibration and validation are carried out in complex watersheds using multi-variable and multi-site approaches (Zhang *et al.,* 2008;

White and Chaubey, 2005). The multi-site approach uses data from multiple sites, while the multi-variable approach uses multiple variables for analysis.

2.4.2.1 SWAT-CUP (SWAT Calibration and Uncertainty Procedures)

SWAT-CUP is developed by Abbaspour *et al*. (2007) to make an interface with the SWAT model. SWAT-CUP is used to assess the prediction uncertainty of the calibration and validation results of the SWAT model. Within the SWAT-CUP it is possible to perform different sensitivity analysis, calibration, validation, and uncertainty analysis. The SWAT-CUP is a public domain program used to link five different uncertainty algorithms; Sequential Uncertainty Fitting Ver.2 (SUFI-2), Generalized Uncertainty Estimation (GLUE), Particle Swarm Optimization (PSO), Markov Chain Monte Carlo (MCMC) and Parameter Solution (ParaSol) to the SWAT model (Abbaspour, 2015). SWAT-CUP allows the user to select one of these algorithms and run the operation many times until the convergence between the simulated and the observed objectives has been reached.

The extent to which all uncertainties are contributed for can be quantified in SUFI-2 by using two factors, namely p-factor and r-factor. Calibration in SUFI-2 is accomplished when both factors are satisfied. The percentage of measured data bracketed by the 95% Prediction Uncertainty (95PPU) is the p-factor, which ranges between 0 percent and 100 percent whereas the average width of the 95PPU band divided by the standard deviation of the measured data is the r-factor, which ranges from 0 to infinity. The p-factor of 1 and the r-factor of zero is a simulation that corresponds exactly to the measured data.

The program SWAT-CUP couples various programs to SWAT model and the general concept is shown in Figure 2.1. Steps involved are as follows:

1. Model parameters are written to model by different calibration programs.
2. Swat edit.exe edits SWAT input files, inserts new parameter values and runs SWAT model
3. Finally, swat extract.exe extracts the desired variables from the output SWAT files and writes them to the output.

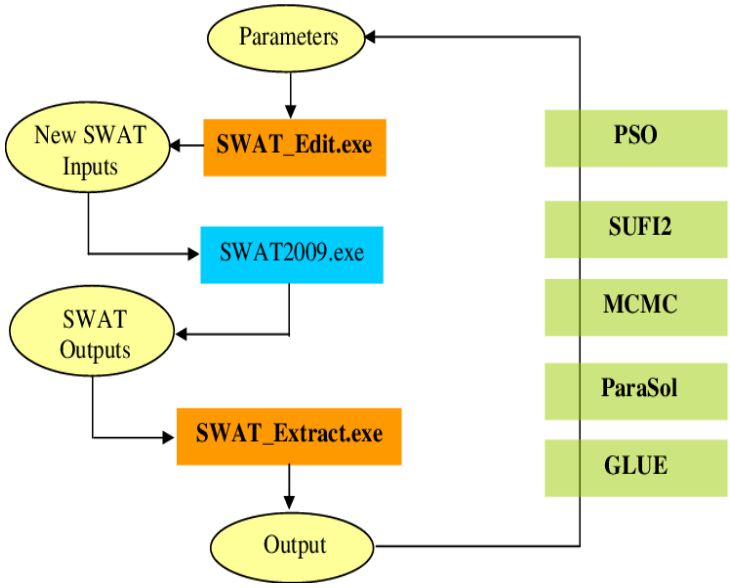

Fig. 2.1 Linkage between optimisation program and SWAT in SWAT-CUP

2.4.3 Model evaluation

The procedure for evaluating the model includes calibration and validation process. A number of test statistics and techniques may be used to evaluate the model and to test the model's fitness to simulate the reality. On the basis of test criteria and statistical indices, the performance of the model can be assessed, the most popular of which are Nash-Sutcliffe Efficiency (Nash and Sutcliffe, 1970), Coefficient of determination (R^2) (Moriasi *et al.*, 2007), Percent bias (PBIAS) (Gupta *et al.*, 1999) and Root Mean Square Error (RMSE).

2.5 IMPACT OF CONSERVATION PRACTICES ON WATERSHED HYDROLOGY

The runoff and suspended sediment process has changed significantly in many rivers due to the impacts of climate change, the rise in extreme precipitation events and human activities in recent decades (Panda *et al.*, 2011; Tang and Lettenmaie, 2012; Jiang *et al.*, 2017; Vaighan *et al.*, 2017). Hydrological impact of conservation practices is generally believed to minimise and delay surface runoff and thus reduce soil erosion (Sahin and Hall, 1996; Castillo *et al.*, 1997; Quinton *et al.*, 1997; Liu and Huang, 2001).

The implementation of integrated soil and water conservation measures in watersheds is one of the key factors responsible for reducing sediment discharges in the river basins. At the catchment level, these measures resulted in a decrease in flood peak discharges and volumes and increased base flows as a result of snowmelt impacts in winter and spring (Potter, 1991). Most of the catchment level studies have found that the dry season discharge from forest catchments is lower than that from natural grasslands (Edwards, 1979; Smith and Scott, 1992; Kramer *et al*., 1999; Best *et al*., 2003). However, other researchers indicate a rise in the base flow following afforestation in some semi-arid and humid regions (Bonell and Balek, 1993; Sandstrom, 1995). Soil and water conservation measures usually alter the topographical characteristics of the slope and have the potential to reduce raindrop kinetic energy, increase the roughness of the slope, and result in storage and retention of runoff and sediment. The most important role is to reduce erosion energy and thus reduce the level of pollutant migration (Han *et al.,* 2018).

Research suggests that physical, biological and agronomic interventions not only help to minimise runoff and soil erosion, but also increase soil fertility status (Mekuria *et al.,* 2007; Meshesha *et al.,* 2012; Jemberu *et al.,* 2018). Physical conservation practices have dramatically changed the hydrological regime by changing the runoff pathways as well as the spatial and temporal distribution of runoff generation (Huang and Zhang, 2004). Several studies have shown that the methods used to minimise soil loss and runoff to negligible levels are typically based on a combination of practices that help to maintain relatively high soil infiltration rates and efficient runoff of water (Herweg and Ludi, 1999). A number of agro-ecological zones and land use areas have been identified as having a positive impact of individual conservation practices on hydrology and soil loss (Descheemaeker *et al.,* 2006; Collick, 2008). However, the assessment of the overall impact of the various conservation practices at the watershed level appears to be more suitable for practical decision-making processes in order to further develop the practices (Mekonen and Tesfahuneg, 2011). In addition, conservation practices must be maintained in order to ensure the long-term sustainability of practices.

2.6 MODELLING OF CONSERVATION PRACTICES

Watershed models that simplify and predict complex processes in a watershed are useful tools for analysing best management practices and estimating their impact on soil erosion (Arabi *et al.,* 2008). In some studies, modelling soil and water conservation practices have been useful in determining the impacts of contour farming and vegetative filter strips, which, among others, comprise non-structural conservation practices (Brunner *et al.,* 2008; Parajuli *et al*., 2008; Kyalo *et al.,* 2014). Majority of research focused on the small-scale, on-site and in-situ impacts of conservation practices (Inbar and Llerena, 2000; Schiettecatte *et al.,* 2005; Nyssen *et al.,* 2007; Verbist *et al.,* 2009). Only a few scientists have focused on upscaling the impact of conservation practices at catchment level (Ngigi *et al.,* 2007; Andersson *et al.,* 2009; Ouessar *et al.,* 2009) and sometimes more spectacularly at global level(Wisser *et al.,* 2010). This can be easily achieved through a modelling approach. Modelling of hydrological processes has proven to be a very efficient tool for evaluating and predicting soil erosion processes for guiding soil and water conservation and management under very different soil, crop, climate, topography and management conditions (Pla, 2000). The lack of awareness of the impacts of conservation structures and inadequate economic assistance to implement them has also led to their low adoption rate (Gathagu *et al.,* 2017). Among the models available, SWAT (Soil and Water Assessment Tool) is found to be the most common in simulating conservation practices at watershed scale.

2.6.1 Simulation of Conservation Practices using SWAT Model

SWAT has already developed a method for modelling a number of agricultural practices, including changes in the application of fertilizers and pesticides, tillage, crop rotation, ponds, wetlands and dams. Conservation measures can be defined in the SWAT model by altering the SWAT parameters to represent the impact of the practices on the simulated processes (Bracmort *et al*., 2006). Arabi *et al.* (2008) proposed a method for representing conservation practice with SWAT model which includes a discussion on the specific parameters that need to be modified on the basis of the role of conservation practices. Different hydrological and water quality processes that have

been taken into account include: surface runoff (peak and volume); infiltration; upland nutrient and pesticide loading; upland erosion (sheet and rill erosion); gully and channel erosion; and within-channel process (Arabi *et al.*, 2008). After baseline simulation has been carried out using the SWAT model, sensitivity analysis, calibration and validation is performed. Thereafter, at the point-objective function such as R^2, NSE etc. satisfying the calibration, the final parameters calibrated value were modified in "edit SWAT input" and the parameters needed to be modified were altered and the SWAT model was run again to predict the impacts of conservation practices (Ayala *et al*., 2017). Examples of parameters involved in the representation of some of the conservation practices are shown in Table 2.1.

Parameter value obtained from a model calibration process or a 'suggested' value identified from the literature review, previous experience of the analyst or previous research in the study area can be used to select the baseline values as well as the values used to predict conservation practices for the input parameters (Arabi *et al.*, 2008). If the model is not sensitive to the chosen parameters, the process for representing conservation practices by changing the appropriate model parameters would be impaired. Therefore, sensitivity analysis should be carried out to evaluate that the parameters chosen for the representation of practices are not insensitive parameters (Arabi *et al.*, 2008). In general, in order to validate model simulation, advanced soil and water conservation impact assessments may be needed to satisfy the interaction between different conservation structures and heterogeneous landscape conditions in order to support appropriate future decision-making.

Table 2.1 Parameters used for the representation of conservation practices in SWAT (Arabi *et al.*, 2008).

Conservation practice	Function	Parameter (input file)
Grassed waterway	Increase channel cover Reduce channel erodibility Increasing channel roughness	CH_COV (.rch) CH_EROD (.rch) CH_N(2) (.rch)
Parallel terrace	Reduce overland flow Reduce sheet erosion Reduce slope length	CN(2) (.mgt) USLE_P (.mgt) SLSUBBSN (.hru)
Field border	Increase sediment trapping	FILTERW (.hru)
Grade stabilization structure	Reduce gully erosion Reduce slope steepness	CH_EROD (.rch) CH_S(2) (.rch)

SWAT has been used in a number of previous modelling studies to evaluate conservation practices impact around the world. The model was used by Vache *et al.* (2002) to determine the effects of crop rotation, strip-cropping and riparian buffer strips on water quality in two watersheds in central Iowa. Two segments of the Major Cypress Creek watershed were analysed by Santhi *et al.* (2003) to represent filter strips, riparian forest buffers, nutrient management plans, critical area planting, grade stabilization structures etc. using the SWAT model. However, in one of the reports, Bracmort *et al.* (2006) gives a detailed explanation of the way in which parallel terraces, field borders, grade stabilization structures and grassy waterways are represented. The lack of numerical guidelines for the representation of conservation practices is not limited solely to the SWAT model. And although researchers have suggested that the parameters of the model need to be modified, no numerical procedure has yet been published. Van Liew *et al.* (2003), who successfully modelled the impact of flood retarding structures in the Little Washita River in the south-west of Oklahoma, has reported as one of the few direct assessments of SWAT reservoirs. Abouabdillah *et al.* (2014) assessed

the impact of conservation measures using SWAT model in a semi-arid river basin in Tunisia. They modelled large dams as reservoirs, contour ridges as potholes filled with water and small dams as ponds.

2.7 IMPACT OF CLIMATE CHANGE ON WATERSHED HYDROLOGY

Climate change has been described as shifting the climate to a new balancing state with dramatically changed environmental components (Landsberg, 1975). Both natural and human factors contribute to climate change. Possible future climate change due to rising greenhouse gas emissions has gained the attention of scientists and policy makers in recent years. Climate change has a number of possible natural, social and economical impacts. As the global average temperature rises, the intensity of these impacts will increase. The water cycle is expected to accelerate with the rise in temperature (Oki and Kanae, 2006). Evapotranspiration, soil moisture and runoff are very sensitive to even slight changes in temperature and rainfall (Milly *et al.,* 2005; Seneviratne *et al.,* 2010).

The best way to assess the climate change impact on water resources is to simulate the hydrological conditions that will exist under the projected weather conditions in the area. The potential impacts of climate change on the hydrological processes include increased evaporation in summer, heavy rains due to increased convective precipitation during the summer season, increased tropical storm intensity and increased monsoon rainfall in the tropics. Assessment of the climate change impacts on regional watershed hydrology has an important role to play in the management of water resources. Evaluating the effects of climate change on water resources is very important for policy makers to minimise the effects and implement coping strategies (Delgado *et al.,* 2010; Fischer *et al.,* 2007). Impacts of climate change on watershed hydrology are generally determined by defining scenarios for climate change inputs to the hydrological model (Gosain *et al.,* 2006; Johnston and Smakhtin, 2014; Srinivasan *et al.,* 1998).

Sorg *et al.* (2012) suggested that the runoff is likely to remain constant or even increase significantly in the near future, but would decline for Central Asia by the end of the 21st century. Ficklin *et al.* (2009) assessed the climate change impacts on water resources in San Joaquin Watershed, California (USA) using the SWAT model and found that changes in carbon dioxide (CO_2) and climatic variables greatly affect water yield, evapotranspiration and other components of the hydrological cycle. A significant number of literature publications deal with a specific component of the hydrological cycle, like streamflow (Fu *et al.,* 2007), runoff (Nunes *et al.,* 2009), groundwater recharge (Jyrkama and Sykes, 2007), evapotranspiration (Calanca *et al.,* 2006) or a particular event in the year, e.g. peak flows (Cuo *et al.,* 2009), and extreme events (Xiong *et al.,* 2009). However, a very few researchers have studied the long-term assessment of the water balance of the basin due to the impact of climate change on hydrological processes.

2.8 CLIMATE MODELS

The main tool used to develop input data for climate change impact studies is climate models. Climate models are essential to improve our knowledge and predictability of climate behaviour in seasonal, annual, decadal and centennial timescales. Models analyse the extent to which observed changes in climate can be due to human activity, natural variability or both. Climate models provide essential information for decision-making of local, regional and national importance, like agriculture, water resource management, transport and urban planning. Climate models rely on well known physical processes that represent the energy transfer and material transfer through the climate system. Various types of climate models have been developed for specific applications, ranging from simple energy balance models to three-dimensional Global Circulation Models (GCMs) and Regional Climate Models (RCMs). Hydrological, general circulation or regional climate model simulations are popular methods for analysing the climate change impact on water resources. Climate models divide the Earth's surface into a three-dimensional grid of cells. In order to model the exchange of energy and matter over time, the outputs of the processes modelled in each cell are

transferred on to neighbouring cells. The size of the grid cell describes the resolution of the model, the smaller the size of the grid cells, the higher the information of the model.

2.8.1 General Circulation Models (GCMs)

General circulation models (GCMs), also known as global climate models, simulate climate change resulting from slow changes in certain boundary conditions (like the solar constant) or physical parameters (like the concentration of greenhouse gases). GCM is a complex mathematical representation of significant components of the climate system, such as atmosphere, land surface, ocean, etc., and their interactions. There are both atmospheric GCMs (AGCMs) and ocean GCMs (OGCMs). Atmospheric GCMs (AGCMs) model the atmosphere and apply sea surface temperatures as boundary conditions. The OGCMs characterize the physics and dynamics of oceans and sea ice and have been independently developed. The AGCM and the OGCM can be combined together to develop an atmospheric-ocean coupled general circulation model (AOGCM). At the end of the 1960s, the NOAA Geophysical Fluid Dynamics Laboratory developed the first general circulation climate model that combined oceanic and atmospheric processes.

Some of the climate model equations are based on the laws of physics, including the Newton's laws of motion and the first thermodynamic law, and the model has key processes that are approximate rather than physical laws. GCMs will divide land, atmosphere, and oceans into a three-dimensional grid system to solve these equations on a computer. The equations for each cell in the grid are then repeatedly calculated for each time-step of the simulation period (Curry, 2016). Common resolutions for GCMs are approximately 100–200 km in horizontal direction, 1 km vertically and generally 30 min in time-stepping resolution. GCMs produce large uncertainties and the IPCC (2007) recommends that climate change studies should take into account the outputs of different models and scenarios.

2.8.2 Regional Climate Models (RCMs)

Coarse horizontal resolution is a key limitation of Global Climate Models (GCMs). Regional Climate Models (RCMs) operate by increasing GCM resolution in a

small, restricted area of interest. Since RCMs only cover a limited domain, the values at their boundary must be explicitly specified as boundary conditions by the results of a coarser GCM or re-analysis. RCMs are used not only for downscaling GCMs, but also to obtain useful regional climate data for seasonal climate predictions with similar objectives. RCMs have also been effective in enhancing our understanding of climate processes, like cloud-radiation, cumulus convection and land surface processes (Sen *et al.,* 2004).

2.8.3 Downscaling methods for climate change projections

The downscaling of climate models is the process by which large-scale climate models are used to make climate predictions at finer spatial and temporal scales to fit the purpose of local level research and analysis. Very high-resolution GCMs will enhance regional and local simulations, but remain inaccessible due to the enormous cost of computing (Fowler *et al.,* 2007), which results in the adaptation of the downscaling techniques (Rummukainen, 2010). There is no special classification system to be used to fully understand and summarise downscaling methods. Methods are categorised into two groups in a number of studies (Fowler *et al.,* 2007; Trzaska and Schnarr, 2014), namely dynamic downscaling and statistical downscaling. Downscaling can be done on both spatial and temporal aspects of climate projections. The method used to extract finer-resolution spatial climate data from the coarser-resolution GCM output referred to as spatial downscaling, whereas the extraction of finer-scale temporal data from the coarser-scale temporal GCM output is referred to as temporal downscaling.

2.8.3.1 Statistical downscaling

Statistical downscaling involves establishing an empirical relationship between historical and/or present large-scale local and atmospheric climatic parameters. Once a relationship is established and validated, future atmospheric parameters used by the GCM will be used to predict the future local climate parameters. This method is based on the critical assumption that under different scenarios of potential future climates, the relationship between current large-scale circulation and local climate remains valid

(Zorita and von Storch, 1999). Statistical downscaling allows the simulation of multiple outputs at the same time, such as precipitation, maximum and minimum temperatures, solar radiation, relative humidity and wind speed (Parlange and Katz, 2000), which is of great significance for impact studies in particular (Wilby *et al.,* 2004).

2.8.3.2 Dynamic downscaling

Dynamic downscaling is a method for obtaining regional climate information based on large-scale climate conditions using high-resolution RCMs. RCMs take advantage of the large-scale atmospheric information of the GCM outputs at the lateral boundaries and integrate more complex topography, land-sea contrast, surface heterogeneity, and detailed physical process information to generate realistic climate information at a spatial resolution of about 20-50 km. As the RCM is encased in the GCM, the overall quality of dynamically reduced RCM output depends on the accuracy and bias of the GCM scenarios (Seaby *et al.,* 2013). Dynamic models address GCM equivalent data and physical processes, but on finer scales, and only deliver results to selected limited regions of the globe (Trzaska and Schnarr, 2014).

2.9 EMISSION SCENARIOS

The emission scenarios are possible future pathways of human development of greenhouse gas and aerosol emissions. In order to project future climate, climate change will be determined according to a possible future scenario. Scenarios are alternative representations of the future and are an appropriate tool to evaluate how driving forces can affect the future emission outputs and evaluate the uncertainties associated with them. They help in the analysis of climate change, including climate modelling and impact assessment, adaptation, and mitigation. Future anthropogenic emissions level largely depends on political decision making, population growth and technological advancements.

Emission scenarios are an important part of the IPCC assessment and are part of a long process and do not describe a single occurrence. The first set of three scenarios was developed in 1990 and used as input to climate models. The second series, completed in

1992, comprised a broader range of driving forces and emissions, the so-called IS92 set of six scenarios (Leggett *et al.*, 1992). The IPCC thoroughly assessed the IS92 scenarios in 1995 and found that they were innovative in their coverage of the full range of GHG emissions at the time they were published and were effective in driving atmospheric and climate models (Alcamo *et al.*, 1995). In 2000, IPCC published a Special Report on Emissions Scenarios (SRES) which discuss four scenario families characterising a set of possible future conditions, namely A1, A2, B1 and B2, based on a complex relationship between the socio-economic forces driving greenhouse gas and aerosol emissions and the levels to which those emissions would rise in the 21st century. The A1 scenario is classified into three groups that characterise alternative directions for technological change in the energy system, which include A1FI (fossil fuel intensive), A1B (balanced) and A1T (predominantly non-fossil fuel). These were used in two consecutive reports, the Third Assessment Report (TAR) and the Fourth Assessment Report (AR4), and have provided common reference points over the last decade for a large portion of climate change research. In 2007, the IPCC reacted to calls for advancement of the SRES by facilitating the process that generated the Representative Concentration Pathways (RCPs). In 2013, the Fifth Climate Assessment Report (AR5) of the IPCC identified feasible future climate scenarios; the RCPs for the evaluation of radiative forcing changes caused by global warming and suggested the use of potential global changes for future projections (Moss *et al.*, 2008). The amount of radiative force expressed in W/m² that will arise from greenhouse gases by the year 2100 is represented by each RCP. The rate and trajectory of the radiative forcing is the pathway. There are four pathways: RCP8.5, RCP6, RCP4.5 and RCP2.6 (Fig. 2.2). The RCP2.6 scenario peaks at 3.0 W/m² before falling to 2.6 W/m² in 2100, requiring a strong reduction in greenhouse gas concentrations in the 21st century. After 2100, the scenarios RCP4.5 and RCP6.0 stabilize at 4.2 W/m² and 6.0 W/m² respectively. The scenarios RCP4.5 and SRES B1 are comparable; RCP6.0 is between the scenarios SRES B1 and A1B. The RCP8.5 scenario has comparable radiative forcing as that of SRES A2. Representative international intercomparison projects, the Coupled Models Intercomparison Project

Phase 5 (CMIP5) and the Coordinated Regional Climate Downscaling Experiment (CORDEX), have produced a number of global and regional climate information under the RCP scenarios (Giorgi *et al.*, 2012; Taylor *et al.*, 2012; Lee *et al.*, 2013).

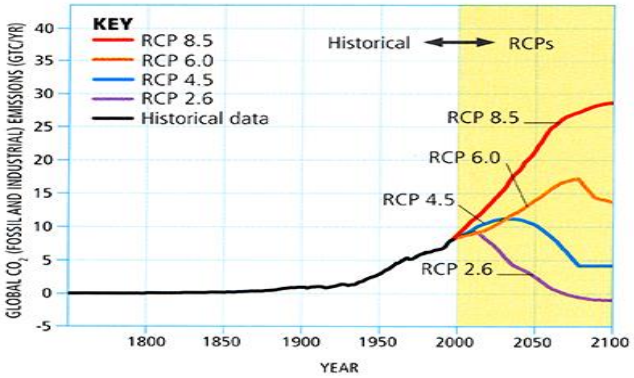

Fig. 2.2 RCP CO_2 Emission Scenarios

(Source: Mann and Kump, 2015)

2.9.1 Coordinated Regional Climate Downscaling Experiment (CORDEX)

The Coordinated Regional Downscaling Experiment (CORDEX) initiative is a key project of the World Climate Research Program (WCRP) (Giorgi and Gutowski, 2015), through which regional climate downscaling (RCD) techniques (Hewitson and Crane, 1996) were coordinated, promoting the availability of regional climate information across continental regions of the world. CORDEX is a platform for the generation of regional climate projections for impact assessment and adaptation studies globally. In fourteen geographical areas, covering the world's main continental regions, various research groups have contributed to the production of climate outputs based on different RCMs. The Earth System Grid Federation (ESGF) web portals are the main source of CORDEX data. CORDEX outputs consist of multivariable time - series data with spatial and temporal resolution and climate scenarios. A set of simulations is available for each CORDEX domain based on the combination of GCMs and RCMs.

2.9.2 Coupled Models Intercomparison Project phase 5 (CMIP5)

The Coupled Model Intercomparison Project Phase 5 (CMIP5) is a collaborative climate modelling framework, coordinated by the World Climate Research Program (WCRP), involving 20 climate modelling groups from all over the world; the Coupled Modelling Working Group (WGCM). The Fifth Assessment Report (AR5) of the IPCC relies heavily on CMIP5. CMIP5 has generated a multi-model data set aimed at enhancing knowledge of climate, its variability and change through the application of global climate system models (Taylor *et al.,* 2012). Two types of climate change modelling experiments are included in the CMIP5 framework (Hibbard *et al.,* 2007; Meehl and Hibbard 2007), near-term simulations (10–30 yr) and long-term (century-time) simulations (Meehl *et al.,* 2009). Both the experiments are carried out using AOGCMs, the standard models used in previous phases of CMIP. CMIP3 was extensively evaluated in IPCC AR4 (IPCC 2007a; Meehl *et al.,* 2007). GFDL-CM3 was found to be the best performing model for the Indian conditions.

2.10 UNCERTAINITY IN CLIMATE PROJECTION AND BIAS CORRECTION

Characterising and quantifying the uncertainty of climate change projections is of great importance for the purpose of detection and substantiation. One of the limitations to the political agreement on adaptation and mitigation policy is the great uncertainty associated with future climate change projections. Forcing, model response and internal variability are the three main factors that lead to uncertainty in future climate change projections (Hawkins and Sutton, 2009; Tebaldi and Knutti, 2007). Forced uncertainty arises from incomplete understanding of external factors affecting the climate system. Uncertainty of the model arises because different models will respond differently to the same external force. Internal variability is the natural variability of the climate system, including processes inherent in the atmosphere, ocean, and ocean-atmosphere systems, arising in the absence of external force. Uncertainties arise from a variety of climate projection sources (structural model differences, initial conditions, scenarios, parameters and resolution / bias-correction), climate impact models (CIMs), and observations (Osborne *et al.,* 2013). Model Intercomparison Projects (MIPs) and Multi-member

model ensembles (Collins *et al.,* 2010) are used to evaluate uncertainties regarding projected climate data and climate impacts. The use of a number of climate scenarios to describe future climate uncertainty has now become a standard procedure (Arnell *et al.,* 2004).

GCM outputs are rarely used directly in impact studies because climate models show systematic errors due to limited spatial resolution, simplified physics and thermodynamic processes, numerical schemes, or inconsistent climate system information. Errors in GCM simulations are significant in relation to historical observations. Therefore, to produce climate projections that are better suited to agricultural modelling, it is essential to bias-correct raw climate model outputs. A number of bias correction methods have been developed, ranging from simple scaling techniques to more sophisticated distribution mapping techniques, to correct bias RCM outputs (Teutschbein *et al.,* 2012). Selecting an appropriate bias correction method is important in order to provide reliable input for the regional impact analysis. Precipitation and temperature projections provided by climate models during the monitoring period generally do not fit the observations at the same time period from a statistical perspective. The problem with the direct use of regional climate model output for hydrological purposes is that the calculated precipitation and temperature are significantly different from the precipitation and temperature observed (Frie *et al.,* 2003). Consequently, the biases in output have an impact on other hydrological processes (Hurkmans *et al.,* 2010). To remove bias present in the computed climate output results, some form of pre-processing is important before they are used for impact assessment studies (Christensen *et al.,* 2008).

2.11 CLIMATE CHANGE IMPACT ON DROUGHT

Drought is an extreme climate event that, as it develops slowly, is dangerous in nature (Mishra and Singh, 2010). It can have significant implications as it increases in intensity and duration gradually. Drought has numerous socio-economic and environmental impacts including increased risk of wild fire, water scarcity, crop and livestock loss, high food price, migration, and indirect health effects. Various forms of

droughts, including meteorological, agricultural, hydrological and socio-economic droughts, are being studied. However, a lack of a consensus on the concept complicates the study of droughts.

Global climate change affects a variety of drought-related factors. In the future, the effect of drought on global warming is likely to intensify (Trenberth *et al.,* 2014; Dai, 2011). With the rising climate change impacts, the frequency and intensity of extreme weather events such as drought is growing drastically and have negative impacts on the fragile environment and human society. Droughts occur naturally, but the hydrological processes have typically been accelerated by climate change, making it faster and more intense, with many consequences, including an increased risk of wildfire. Variation of sea surface temperature discrepancies may cause global drought (Seager *et al.,* 2008). In addition, regional climate change may be responsible for improving the land-atmosphere feedback processes, such as slow-moving anticyclones that change the environment of the region by disrupting the development of synoptic weather systems (Trenberth and Shea, 2005). Land-atmosphere feedback processes complicate the situation by increasing atmospheric temperatures and thus increasing atmospheric demand for moisture due to the absence of available moisture in these regimes, leading to increased drying and heating of the land surface. Drought is a natural hazard and its impacts can only be mitigated by taking prior measures to adapt to climate variability.

2.11.1 Drought Indices

In order to control hydrological processes, drought indicators and drought indices have been developed and are used interchangeably in the drought analysis. Drought indicators are used in a wider context, with overall variables like rainfall, temperature, stream flow, reservoir levels, groundwater levels, snow packs and soil moisture levels. Drought indices, on the other hand, are single numerical values that affect drought and thus have a strong advantage in the quantification of drought characteristics over mere raw data (Hayes *et al.,* 2012). PDSI (Palmer Drought Severity Index) is the oldest and most well-known drought index, and the SPI is the most extensively used one for

understanding the extent and duration of drought events. The two most commonly used drought indices are explained below.

2.11.1.1 Standardised Precipitation Index (SPI)

The SPI (Mckee *et al.,* 1993) is one of the widely used indices to measure meteorological drought. SPI estimation requires only precipitation data that is based on a probabilistic approach and is relatively easy to calculate. The absence of wind speed, temperature, PET and soil moisture data as input parameters, however, is a major constraint on the generation of accurate drought information. Positive SPI values indicate greater than median precipitation, and negative values indicate less than median precipitation.

2.11.1.2 Reconnaissance Drought Index (RDI)

An improved index over the SPI is RDI (Tsakiris *et al.,* 2007) and requires PET as one of the key variables. However, PET evaluates the atmospheric water demands, but does not generally relate to evapotranspiration since it also needs to evaluate the availability of water. RDI has been used to monitor drought and analyse the effects of climate change on water resources (Tigkas *et al.,* 2013). RDI is estimated as the ratio between accumulated precipitation and PET over a given time period. However, in terms of temperature change, the RDI lacks the ability to effectively capture drought variability. Wet periods are indicated by positive RDI values, while dry periods are indicated by negative values when compared to normal conditions in the region. When RDI values become extremely negative, the severity of drought events increases.

Materials and Methods

CHAPTER III

MATERIALS AND METHODS

This chapter details the materials used, including data collection and analysis, the software used, and the methodology adopted to achieve the research objectives. The description of the study area including location, physiography, climate, etc., is also covered. Based on the review, the SWAT model was found to be well suited to both climate change impact studies and study of conservation practices and hence the model was used for the study. The methodologies used to get the climate data and the procedures for setting up the model are also detailed.

3.1 DESCRIPTION OF THE STUDY AREA

3.1.1 Location of the watershed

Thuthapuzha, a sixth-order subbasin, covers an area of 905 km². It lies between latitude 10°50'N to 11°15'N, and longitude 76°05' to 76°40' E. Of the total area, 75% is in the Palakkad district and 25% is in the Malappuram district. Thuthapuzha is approximately 63 km long with four tributaries, including Nellipuzha, Kanjirapuzha, Karimbuzha and Kunthipuzha (Unnikrishnan Warrier and Manjula, 2014). Thuthapuzha watershed is located in the north-eastern part of the Bharathapuzha River and is the main tributary that supplies water to Bharathapuzha, particularly during the summer. The annual average discharge of Thuthapuzha sub basin is about 1750 MCM (CWC, 2012). Other than the reservoir built across Kanjirapuzha, which serves as a source of water for irrigation, there are no other major structures in the watershed. In the north-east corner of the subbasin, the Silent Valley Reserve Forest is situated. The location map of study area is shown in Figure 3.1.

3.1.2 Physiography

Physiographically, the land of Kerala is divided into three natural regions, namely lowlands, midlands, and highlands. The study area lies within the midland

(7.5–75 m above MSL) and highland (> 75 m above MSL) regions of Kerala and experiences a humid tropical climate. The elevation of the study area ranges from 20 meters above sea level in the western side of the basin to 2308 meters above sea level in the northern side of the Silent Valley Reserve Forest. A number of small, cultivated watersheds characterise the midland belt with laterite soil. The highland region is characterised by crystalline rocks. The reserve forest in the study area falls within the highland region. In a watershed, general land use differs as per local physiography. The main crops in the midlands are rice, banana, tapioca, seasonal vegetables and coconut, while rubber plantations and coconut grooves dominate in the high land region and some of the midland region.

3.1.3 Climate

The average annual precipitation in the Thuthapuzha subbasin is 3830 mm (Manjula and Unnikrishnan Warrier, 2019). This is greater than the average annual precipitation of the whole Bharathapuzha River Basin which is about 1822 mm (Raj and Azeez, 2012) and the average annual precipitation of Kerala state (2817 mm) (Krishnakumar *et al.,* 2009). The area also has two distinct monsoons, like the other parts of Kerala, namely the south-west (June-September) and the north-east (October-December) monsoon. The south west monsoon contributes for around 65 percent of the annual precipitation, the north east monsoon and the summer showers contribute to the remaining total annual rainfall in the subbasin. There are wide spatial variations in precipitation ranging from 2020 mm to over 5000 mm / year, with heavy precipitation in the direction of the Silent Valley Reserve Forest (Manjula and Unnikrishnan Warrier, 2019). The average temperature in the area is 27.3 °C (Tejaswini and Sathian, 2018). Variations in general precipitation (Raj and Azeez, 2009) and surface temperature in the region have been observed over the last few years. In recent years, severe water scarcity and drought conditions have also been reported in the river basin.

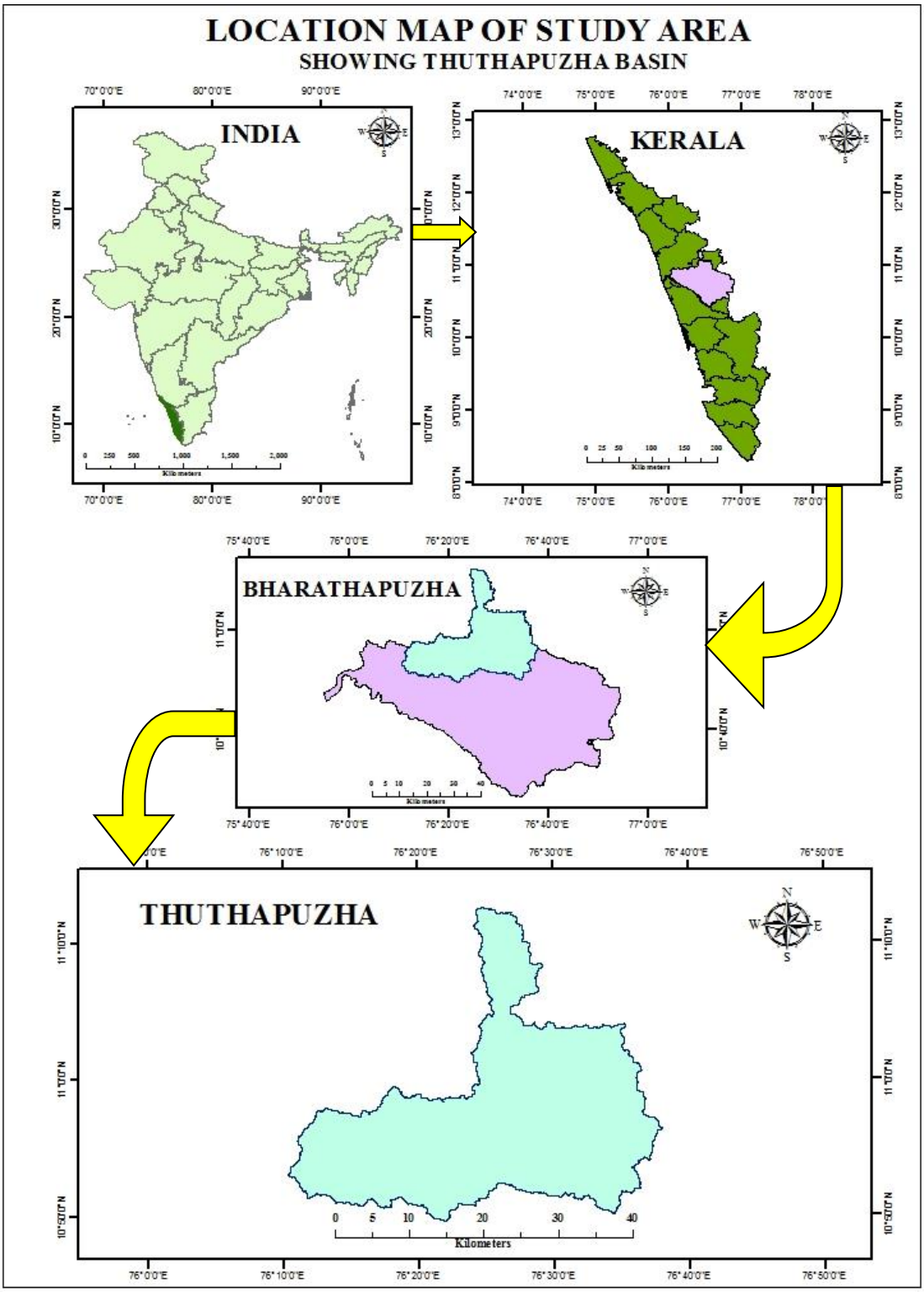

Fig. 3.1 Location map of study area

3.2 MATERIALS USED

3.2.1 Input data for SWAT model setup

3.2.1.1 Digital Elevation Model (DEM)

Digital Elevation Models (DEM) is a gridded digital terrain representation, with each pixel value corresponding to an elevation above a datum. DEM of the study area was taken from NASA SRTM (Shuttle Radar Topography Mission) Version 3.0 Global 1 arc second (about 30 meters) resolution dataset (SRTMGL1). This is the third release in the series that provides access to various NASA SRTM data that coincides with areas released by the USGS (US Geological Survey) and was downloaded via the USGS Earth Explorer with additional login to the EARTHDATA website (https:/urs.earthdata.nasa.gov). To setup the SWAT model, the DEM in the projected coordinate system WGS_1984_UTM_Zone_43N was used. Slope map of the study area has been obtained from DEM in ArcSWAT.

3.2.1.2 Land use map

Land use map of Thuthapuzha was prepared through supervised classification using the 2008 image data of Landsat 4-5 TM (Thematic Mapper). The areal imagery was downloaded from the USGS Earth Explorer and the supervised classification was carried out using ERDAS IMAGINE 2014 developed by Intergraph, USA. Landsat 4-5 TM image data files are made up of seven spectral bands. The resolution for bands 1 to 7 is 30 meters. Electromagnetic spectral bands 3, 2 and 1 have been used to prepare the imagery for classification. The supervised classification is based on the concept that "the user can select a sample of pixels in an image that is representative of a specific class and then direct the image processing software to use these training sites as references for the classification of all other pixels in the image". The pixels have been analysed by means of Google Earth, aerial photos, ground truthing, previous literature, etc. The classified image along with the lookup table, including the information of each class, was entered as an input into the SWAT model.

3.2.1.3 Soil map

The soil properties for the basin are one of the main inputs required by the model. They have a significant role to play in determining the movement of water and air within the HRU. The soil map and attribute information on the soil properties were collected from the Soil Survey and Soil Conservation Directorate of Kerala state. The soil map was digitised and converted into the raster format in ArcGIS 10.4 for input into the SWAT model. In addition, the lookup table, including the information for each class, was also given as input along with the soil map.

3.2.1.4 Meteorological data

Meteorological data include precipitation, minimum and maximum temperature, wind speed, relative humidity and solar radiation on a daily basis. Historical precipitation data for 28 years (1989-2017) were collected from RARS (Regional Agricultural Research Station), Pattambi and IMD (India Meteorological Department), Mannarkkad station. The observed temperature data for the same period were obtained from RARS, Pattambi and Pulamanthole gauging station of Central Water Commission (CWC). Other meteorological data, including solar radiation, relative humidity and sunshine hours, were collected from RARS, Pattambi. Sunshine hours were then converted into solar radiation for further use in SWAT model. The monthly average of all the meteorological data collected are given from Appendix I to X.

3.2.1.5 River discharge data

River discharge data (daily basis) were collected from the Central Water Commission (CWC) at the outlet of the Pulamanthole gauging site (1989–2017). The catchment area of the Pulamanthole gauging station (10° 53' 50" N, 76° 11' 50" E) is 822 km². SWAT model calibration and validation was performed using the discharge data obtained from CWC. The location of meteorological stations and river gauge station is shown in Figure 3.2.

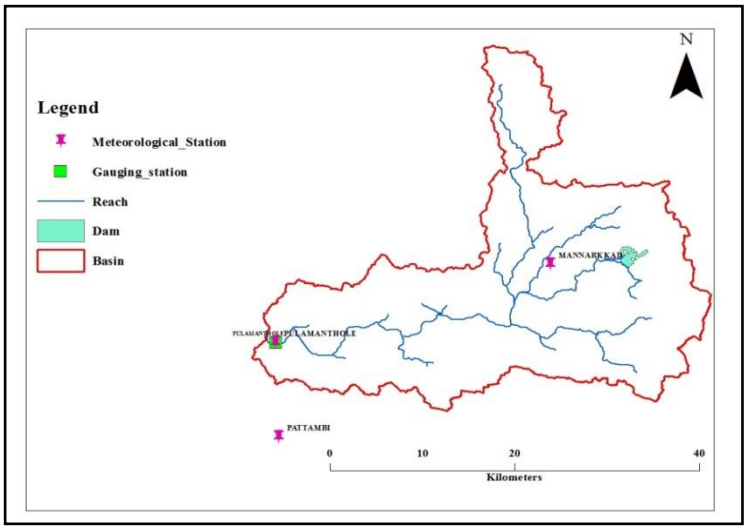

Fig. 3.2 Location map of meteorological and rain gauge stations of Thuthapuzha

3.2.2 Climate change data and analysis

One of the main input sets for modelling future watershed conditions in SWAT is data on climate change. Major climatic parameters, such as precipitation, maximum temperature and minimum temperature, are changed in order to achieve future climatic conditions. The most basic method of generating climate projections is based on a climate model concept and scenarios for future emissions of greenhouse gases. Global Climate Models (GCMs) are tools for conducting climate change experiments that can be used to construct climate change scenarios. GCMs can only be used on a rather coarse horizontal and vertical resolution. This is a source of error in simulating regional climate. In addition, the lack of regional information makes the GCM output unsuitable for a number of impact studies requiring regional information. The downscaling process in which a high-resolution (usually 10-50 km) RCM is nested into a GCM is a more systematic approach to address this scale discrepancy. This can significantly improve regional climate simulations and projections due to higher resolution and a more complete representation of physical processes in RCMs (Maraun *et al.*, 2010). However, there are problems related to the nesting approach of the RCMs and the choice of integration domains. In many assessment studies there is a further need for even better

resolution than that provided by the RCMs. It may also be desirable to remove systematic errors in the RCM / GCM output.

The Earth System Grid Federation (ESGF) portal provides access to a wide variety of data sets, including the Coupled Model Intercomparison Project Phase 5 (CMIP5) model data that serves as the basis for IPCC AR5. ESGF also have provision for downloading numerous CORDEX RCM simulations produced by a number of modelling groups around the globe, similar to the CMIP5. CORDEX simulation over the South Asian domain (CORDEX-SA) was available in the Centre for Climate Change Research Indian Institute of Tropical Meteorology regional data portal.

Moreover, it is not yet clear that if dynamically downscaled precipitation from regional climate models improves the ability of GCMs to simulate extreme precipitation events (Racherla *et al.*, 2012; Laprise, 2014). In general, there was a lack of thorough evaluation for GCMs and RCMs in simulating the observed characteristics of daily precipitation extremes across the Indian region and specifically Kerala. This is also true in the case of temperature simulation. In addition, it was found from the literature review that the GFDL-CM3 model provides better simulation of the Indian condition. The GFDL-CM3 model was developed by the National Oceanic and Atmospheric Administration (NOAA) Geophysical Fluid Dynamics Laboratory. Climate change data of the GFDL-CM3 model (precipitation, maximum temperature and minimum temperature) was downloaded from the ESGF-CMIP5 dataset and the CORDEX-SA FTP server. In the CMIP5 download, all four RCP scenarios, namely RCP2.6, RCP4.5, RCP6.0 and RCP8.5, were available for the period 2006-2100, while in the CORDEX-SA GFDL-CM3 download data, only RCP4.5 and RCP8.5 were available for the period 2006-2070. For historical data comparison, the 1989-2005 data was downloaded from both datasets. These data were used to evaluate the GFDL-CM3 GCM data from CMIP5 and the RCM data from the CORDEX-SA.

3.2.2.1 Bias correction

Although significant progress has been made in recent years, the output of both GCMs and RCMs continues to be affected by bias to an extent that prevents their direct use, particularly in climate change impact studies. Bias correction, i.e. "the correction of model output for its subsequent application in climate change impact studies", has now become standard practice to address this issue. Prior to the evaluation of both CMIP5 and CORDEX-SA data, bias correction was performed to determine which bias correction method is best suited for further analysis separately for precipitation, maximum temperature and minimum temperature. Statistical parameters such as standard deviation, correlation coefficient and coefficient of variation were used to select the best method. Several bias correction methods for precipitation and temperature data are available separately. There are many tools and many approaches in literature for bias correction. Various software are now available to correct climate data for bias. The CMhyd tool was used in this study to extract and bias correct data from the climate model. The tool compares the output of the raw climate model with the data observed, calculates the difference between the data observed and the simulated climate model, and applies methods of statistical bias correction to correct the output of the historical and future climate model. In order to correct the bias of the future climate model simulation, bias correction algorithms derived from the observed data and the historical climate model simulation were used. The CMhyd is designed to prepare simulated climate data for climate change impact studies using the SWAT model. The tool provides several methods of bias correction, including linear scaling, non-linear scaling and distribution mapping. Bias correction methods used for the study are shown in Table 3.1.

Table 3.1 Bias correction methods used for precipitation and temperature

Bias correction for precipitation	Bias correction for temperature
Linear Scaling (LS)	Linear Scaling (LS)
Local Intensity Scaling (LIS)	Variance Scaling (VS)
Delta change correction (DCC)	Delta change correction (DCC)
Distribution mapping (DM)	Distribution mapping (DM)
Power transformation (PT)	

3.2.2.2 Comparison of CMIP5 and CORDEX-SA dataset

The comparison of model output from CMIP5 and CORDEX-SA was made after the bias correction. Historical data from 1989 to 2005 was used for comparison purposes. These historical data was compared with the observed data and the model with a high correlation with the observed data was selected using statistical parameters (standard deviation, correlation coefficient and coefficient of variation) for further analysis.

3.2.3 Details of conservation practices in the watershed

Details of the reservoirs and conservation structures in the study area are needed to study the impact of conservation practices on watershed hydrology. The necessary details include area, volume, year of construction of the structure, etc. Several conservation structures were present in the study area such as check dam, vented cross bars, brushwood dam etc. The Kanjirapuzha dam is the only reservoir in the Thuthapuzha subbasin. The Kanjirapuzha reservoir is built across the Kanjirapuzha River in Mannarkkad, Palakkad District. The nearest town is Palakkad, which is 46 km from the dam site. The reservoir has latitude of 10°59’8.515”N and a longitude of 76°32’18.955”E. Details of the reservoir have been collected from previous literature and the annual report on the Kanjirapuzha Irrigation Project. Details of the conservation practices have been collected from the Regional Office, Kerala State Land Use Board,

Thrissur. Details were collected as five subwatersheds in the study area, namely Thuthapuzha, Nellipuzha, Kunthipuzha, Karimpuzha and Kanjirapuzha.

3.2.4 Softwares used

The study was carried out using different softwares and models to analyse the input data and to achieve the research objectives. The description of the models and software used for the study is given below.

3.2.4.1 ArcGIS 10.4

ArcGIS is a geographic information system developed by the Environmental Systems Research Institute (ESRI) to work with maps and geographic information and was released in New York on 27 December 1999. ArcGIS Server is a complete, integrated GIS server, which supports spatial data management, mapping and spatial analysis across distributed systems. ArcGIS consists of four key components including a geographic information model for the modelling of real-world aspects, components for the storage and management of geographic information in files and databases, a set of applications for creating, editing, mapping, manipulating, analysing and interpreting geographic informations; and a collection of web services that provides content and capabilities. In general, the ArcGIS Desktop software module includes ArcMap, ArcCatalog, ArcToolbox and ArcGlobe. ArcMap is an application that allows users to create and modify maps and analyse (2D) spatial data (Fig. 3.3). There are three other modules within ArcMap; ArcView level install for basic level application; ArcEditor for data editing and ArcInfo for advanced editing and analysis features. The ArcCatalog module is a tool for viewing and managing spatial data files (windows explorer analogue). ArcToolbox contains a set of tools and functions used for converting data formats, managing map projections, analysing and modifying data. The ArcGlobe application is designed for displaying large, global 3D datasets.

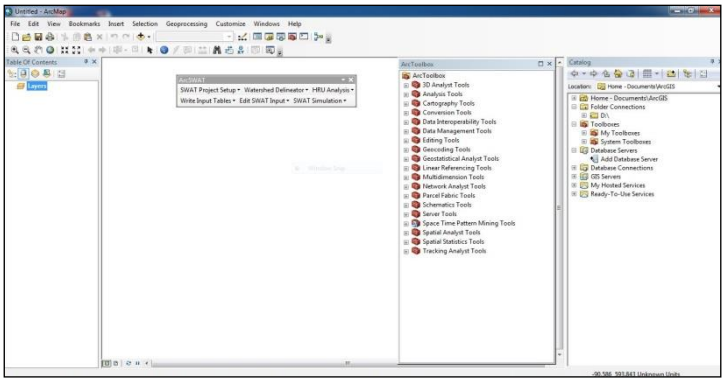

Fig. 3.3 ArcMap interface showing ArcSWAT menu

The latest version of ArcGIS is 10.8, which was released in 2020 and ArcGIS 10.4, released in 2016, was used for the study. In this research, ArcGIS 10.4 is used to make a shape file for the study area, to clip input maps, to set projections, raster conversions, to digitise soil maps, and to prepare different layout maps for results.

3.2.4.2 ERDAS IMAGINE 2014

A number of image processing software is available in both paid and free source categories. ERDAS Imagine is an image processing software that was previously supported by Leica Geosystems Inc. but is now being provided by Hexagon Geospatial. It is raster-based software specifically designed to extract image information. Import, view, modify and analyse both raster and vector data sets are built-in software functions. This software can handle an unlimited number of image data bands within a single file. These bands are often treated as layers in the ERDAS IMAGINE software. Additional layers can be created and added to the existing image file. It enables users to import a wide range of remotely sensed images from satellite and aerial platforms.

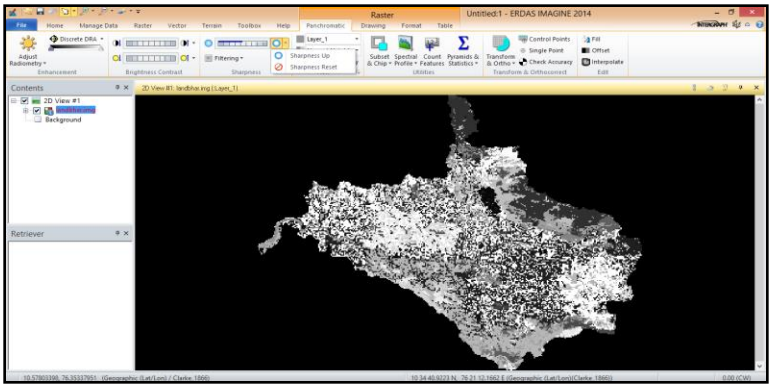

Fig. 3.4 ERDAS IMAGINE 2014 interface

Image processing and supervised image classification helps in extracting data from imagery. In this study, the ERDAS IMAGINE 2014 software was used for image processing. The layers were stacked and subset to delineate the catchment area for classification. Layer stacking option of this software was used to convert three bands; 3, 2, 1 of Landsat 4-5 TM to a single layer. From the layer file, land use map of the study area was classified. To geocode the imported image, the UTM Zone 30N Coordinate on WGS 84 was used. Interface of ERDAS IMAGINE 2014 is shown in Figure 3.4.

3.2.4.3 SWAT-CUP

SWAT-CUP (Calibration and Uncertainty Programs) is an automated calibration tool for SWAT model developed by Eawag, a Switzerland-based aquatic research institute (Abbaspour, 2015). The SWAT-CUP is a public domain program using a generic interface. Within the SWAT-CUP it is possible to perform different sensitivity analysis, calibration, validation, and uncertainty analysis. There are five different uncertainty algorithms (SUFI-2, MCMC, PSO, GLUE and ParaSol) available in the SWAT-CUP software (Abbaspour, 2015). The SWAT-CUP systematically modifies the uncertain model parameters and runs the model. The outputs required are then extracted and compared with the observed data. For this study, version 5.2.1 of SWAT-CUP 2019 was used (Fig. 3.5).

SUFI-2 (Sequential Uncertainty Fitting) algorithm was chosen to calibrate the SWAT model for this research work. SUFI-2 is a semi-automatic program in which the

user manually performs some of the steps during calibration. For this purpose, the user must be familiar with the SWAT model parameters and also the hydrological features of the watershed being modelled. SUFI-2 contains all uncertainties, such as input data (e.g. precipitation), the conceptual model, the parameters and the observed data. To generate an independent set of parameters, SUFI-2 uses Latin hypercube sampling (Abbaspour *et al.*, 2007). The uncertainty of the parameter is described by a multivariate uniform distribution in the hypercube parameter. When all types of uncertainty are included in the measured variables (e.g. discharge), the 95PPU (95 percent prediction uncertainty) produced by the parameter uncertainty defines all uncertainties. The 95PPU accounts for 2.5 and 97.5 percent of the cumulative distribution of the output variable derived from the Latin hypercube sampling (Abbaspour *et al.*, 2007).

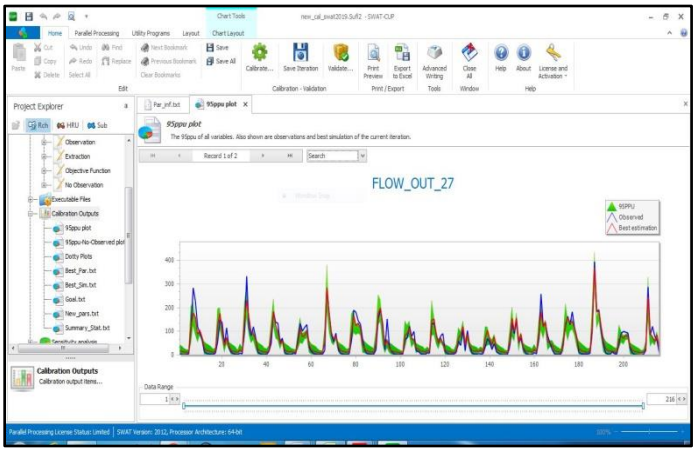

Fig. 3.5 SWAT-CUP interface

3.2.4.4 CMhyd

CMhyd is a tool that can be used to extract and correct the data generated from global and regional climate models. In order to reduce the mismatch between simulated and observed climate parameters on a daily time step, bias correction methods are used so that hydrological simulations driven by the bias corrected climate data coincide reasonably well with simulations using observed climate data. Climate Model for Hydrological Modelling (CMhyd) was developed by Rathjens *et al.* (2016) to perform bias correction of precipitation and temperature data from several climate models.

CMhyd tool includes eight bias correction methods, including power transformation, linear scaling, local intensity scaling, delta change, distribution mapping and variance scaling. CMhyd was developed to provide projected climate data that could be considered indicative of the gauge locations used in the SWAT model setup. For each gauge locations, the climate model data should therefore be extracted and bias corrected. The CMhyd software interface is shown in Figure 3.6.

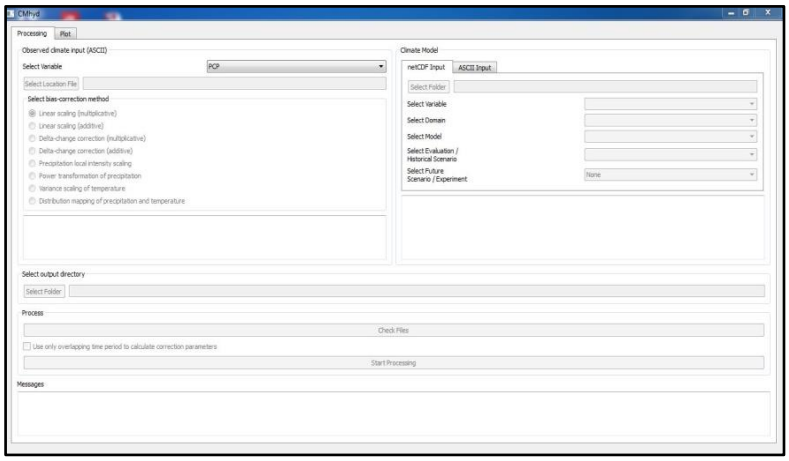

Fig. 3.6 CMhyd interface

This research used the CMhyd tool for the extraction and correction of climatic parameters derived from GCMs and RCMs. CMhyd was written in Python 2.7 using several Python packages mainly NetCDF, SciPy (Oliphant, 2007; Millman and Aivazis, 2011), PyQt4 and the NumPy (Van der Walt *et al.,* 2011) application framework. To adjust the output of the climate model, bias correction methods use a transformation function. The basic method was to identify biases between simulated and observed historical climate parameters in order to develop a bias correction algorithm to correct simulated historical climate parameters. The ASCII format is used by CMhyd for the data observed as well as for the corrected output bias. The ASCII format is also used by the ArcSWAT Interface which promotes the use of projected climate data in the SWAT model (Winchell *et al.,* 2010). The tool was checked using both CORDEX and CMIP data. For simulated climate data, CMhyd supports two data formats; netCDF (*.nc) files and ASCII input. Time series of climate model are usually given in a netCDF

(Network Common Data Form) format. CMhyd uses the information in the netCDF file to locate the climate model grid cells that overlay the gauge positions and convert temperature and precipitation data to degrees Celsius and millimetres, respectively. CMhyd eventually uses netCDF data for extracting the time series of the related grid cells. For each gauge location files, the Plot tab in the software can be used to plot an annual and monthly time series and a monthly summary of the outputs generated.

3.2.4.5 DrinC

DrinC (Drought Indices Calculator) is a software package designed to provide a basic but adaptable interface for the computation of drought indices. The DrinC software package was developed by the Centre for the Assessment of Natural Hazards and Proactive Planning and the Laboratory for the Management of Reclamation Works and Water Resources of the National Technical University of Athens (Fig. 3.7). Maximum possible application for different types of drought (hydrological, meteorological, agricultural) and different locations has been the main objective in its design. DrinC software was developed with the aim of providing a simple interface for calculating four different drought indices including the Standardised Precipitation Index (SPI), the Reconnaissance Drought Index (RDI), the Streamflow Drought Index (SDI), and the Rainfall Deciles (RD). In addition, DrinC also contains a module for temperature-based methods (Blaney-Criddle, Hargreaves and Thornthwaite) to estimate potential evapotranspiration (PET) that can be used to calculate RDI. Using a window-based interface, the user can choose from a number of options that may be best suited to the specific requirements of each study.

Meteorological drought can be analysed using RDI, SPI and RD indices which require precipitation as the main component for calculation (additionally PET is required for RDI calculation). Reconnaissance Drought Index can also be used to analyse agricultural droughts, as the water balance can be adequately described and is especially useful when selecting reference periods related to crop growth (Tsakiris *et al.,* 2010). SDI, on the other hand, refers to the hydrological drought and uses the streamflow as a

major component of the calculation. In DrinC, the hydrological year (October-September) is the main reference base, so the default calculation period starts in October and the main time steps are yearly, monthly, three months, and six months. However, starting months (e.g. January) or other time periods (e.g. 5 months) can be specified. This adaptability may be useful for a wide range of real-world applications. Two distributions are available in the drought index analysis of CMhyd software *viz.*, gamma and log-normal distribution.

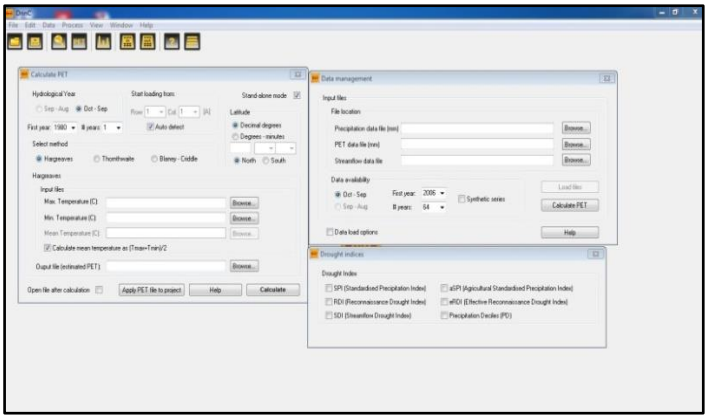

Fig. 3.7 DrinC software interface

In this study, two indicators of drought intensity analysis, SPI and RDI, were used for both historical and future time periods using climate model bias corrected data for different RCP scenarios.

3.2.4.6 SWAT

The SWAT (Soil and Water Assessment Tool) model is a public domain software developed jointly by Texas A&M AgriLife Research, part of the Texas A&M University System and the USDA Agricultural Research Service. Though SWAT was developed in the early 1990s, it has undergone extensive evaluation and its functions have been continuously improved. The Green and Amp infiltration method and the improved weather generator are important to note, enabling the generation of data for daily relative humidity, solar radiation and wind speed in SWAT2000 (Neitsch *et al.*, 2011). SWAT is a spatially-distributed, physically-based watershed model capable of simulating the

impact of land, topography and vegetation on water movements on and near the soil surface (Arnold, 2010). SWAT is free software and is coupled to the GIS platform via ArcSWAT interface that facilitates data processing and modelling easier. In order to simulate flows and direct subbasin routing, SWAT requires information about land use, soil, and elevation. SWAT2012 (latest version) (Neitsch *et al.,* 2011) was used for this research and the ArcSWAT 2012 extension of GIS was used as an interface for SWAT modelling. The SWAT model software is freely available for download from the SWAT website (swat.tamu.edu).

Main components of SWAT are weather, hydrology, soil properties, plant growth, nutrients, pesticides, bacteria and land management (Arnold *et al.,* 2012). The watershed is divided into different subwatersheds, depending upon the topography. Each subwatershed has been further subdivided into Hydrological Response Units (HRUs) which are combinations of homogeneous land use, soil and slope (Arnold *et al.,* 2012). Many inputs, including DEM, soil type, land use and slope, affect the size of the HRU. The HRU distribution is defined by user-defined thresholds in the current SWAT model. Although the size of the HRU varies depending on the requirements of the user, the normal area of the HRU in the SWAT varies from approximately 50 to 500 ha.

Hydrology can be divided into two main components in the SWAT model, including the land phase and the routing phase (Neitsch *et al.,* 2011). The land phase controls the amount of water, sediment and nutrient loads to the main channel in each subbasin, whereas the flow of water, sediment, etc. to the outlet through the watershed channel network is described by the routing phase (Neitsch *et al.,* 2011). Based on the equation of the water balance, SWAT calculates the land phase hydrological cycle (Neitsch *et al.,* 2011) as follows:

$$\Delta SW = P - (QSURF + ET + WSEEP + QGW) \quad (1)$$

Where, ΔSW is the change in soil water content, P is the precipitation, QSURF is the surface runoff out of the watershed, ET is the evapotranspiration, WSEEP is the percolation from the soil profile and QGW represent the transmission losses from the

streams. All parameters are expressed in (mm) over the watershed area. A schematic representation of the hydrologic cycle is shown in Figure 3.8.

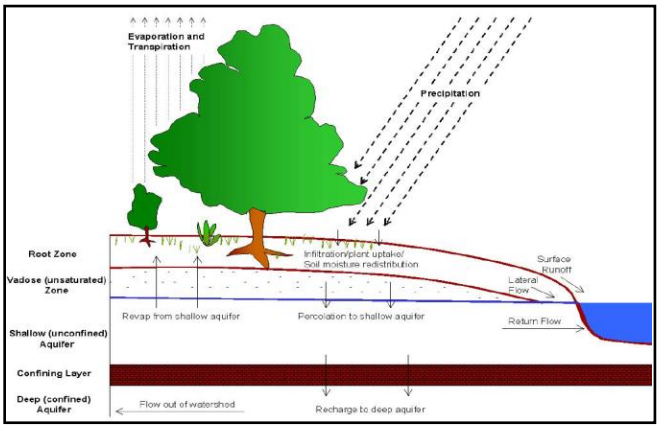

Fig. 3.8 Schematic representation of the hydrologic cycle in SWAT (Neitsch *et al*., 2011)

3.2.4.7 Additional software used

In addition to all of the above mentioned software, MS Excel was used for the model performance analysis and all graph preparations for results.

3.3 REASERCH METHODOLOGY

3.3.1 SWAT Model setup

SWAT hydrological model was chosen for this project. The development of the SWAT model is the basis for achieving the remaining research objective. A toolbar has been added to ArcGIS to develop the SWAT model once the ArcSWAT programme has been downloaded, displaying the main procedures for the modelling process. These include SWAT Project Setup, Watershed Delineation, HRU Analysis, Write Input Tables, Edit SWAT Input and SWAT Simulation process. After each step is completed, the following step in the model will be enabled. After the model is run, the sensitivity analysis, calibration, validation and performance of the model need to be done to develop the model for the study area.

3.3.1.1 SWAT Project Setup

To start with, the "New SWAT Project" button in the SWAT Project Setup menu was selected. The "Project Setup" menu will open. The input data's for SWAT model setup described in this chapter were placed in a particular folder on the computer. In the "Project Setup" menu, the "Project Directory" button was pressed, and the input data folder on the computer was chosen. This folder will be the only option that the user selects to allow ArcSWAT software to access all required input data during the setup process. The toolbar is shown in Fig. 3.9.

3.3.1.2 Watershed delineation

The next step to be followed in the ArcSWAT program was the watershed delineation (Fig. 3.10). The first step was to load the DEM file and press the "DEM projection setup" button. It was then necessary to define the streams in the watershed. The program provided two options for defining streams; a predefined stream and a watershed option that can be used if the stream location in the watershed is known, and a DEM-based stream definition option which can be used if the exact stream location in the watershed is not known. Based on the elevation values of individual cells in the DEM, the model estimated flow paths. The selected option in this study was DEM-based stream definition. The program creates outlets in the subbasins which could however, be modified. This is useful if a streamflow gauge has a known location within the catchment area. During the model setup process, by pressing the 'Add' button under the 'Outlet and Inlet Definition' option in the watershed delineation submenu, the position of the Pulamanthole streamflow gauging station was added manually. A whole watershed outlet was selected to define the overall area being modelled. The watershed was then successfully delineated. SWAT model finally generates a report explaining the distribution of discrete land elevations and summary statistics in each subwatersheds and watersheds. There is an option to add the reservoir component of the watershed within this watershed delineation menu.

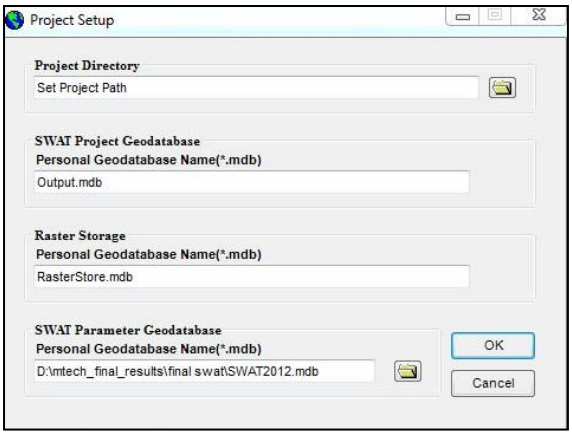

Fig. 3.9 Project setup menu in SWAT

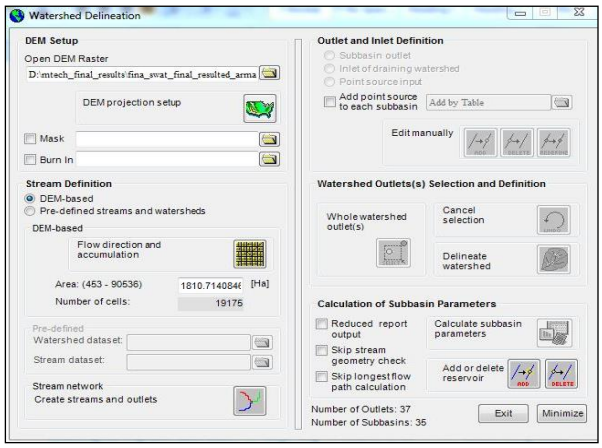

Fig. 3.10 Watershed delineation sub menu in ArcSWAT

3.2.1.3. Soil, land use, slope definition and overlay

The definition and overlaying process divides subbasins into areas, referred to as hydrological response units (HRUs), of similar soil, land use and slope. This is where the user begins making options on the basis of information about their study area. The overlaying process required land use and soil data. There is an option that enables users to add new classes to the SWAT database manually. Thus, users can add classes that are specific to their study area. For land use and soil data, a lookup table is also required to specify the code of each category to be modelled. After entering the maps and the lookup table, each class has been reclassified to SWAT defined classes. The definition and

reclassification of slope classes is the final step before the overlay operation to determine the hydrological response units (HRUs). Slope map is defined using DEM in the SWAT model. The SWAT model generates a report detailing the distribution of land use, soil and slope classes in the watershed after completion of the overlay process. Fig. 3.11 shows the overlay menu.

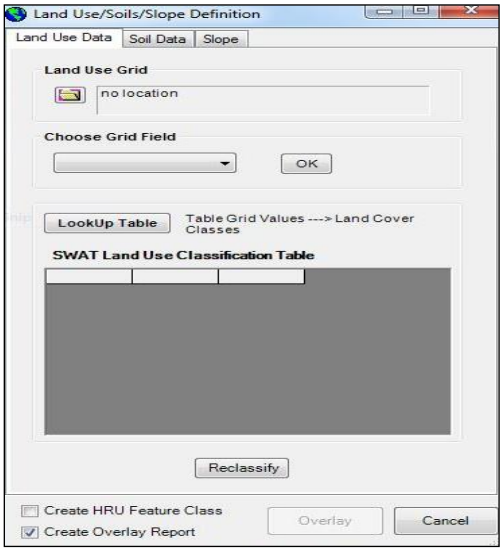

Fig. 3.11 Overlay menu in ArcSWAT

3.2.1.4. Hydrological Response Unit (HRU) definition

The HRUs must be determined after importing and overlaying the land use, soil and slope data layers into the model. HRU refers to homogeneous areas that constitute unique soil, land use and slope combinations. Each subwatershed can be assigned a single HRU or multiple HRUs. The model will determine the HRU by the dominant category of land use, soil type and slope class if a single HRU is selected for each subwatershed. The user-specified sensitivity for land use, soil and slope data determines multiple HRUs. Multiple HRUs option was selected for this study. The threshold value used for each class was 10 percent. This refers to "the percentage of subbasin areas with a unique land use, soil or slope class under which that class is considered to be negligible and excluded from the analysis". HRU definition menu is shown in Fig. 3.12.

3.2.1.5. Weather data definition

Loading the weather data to the model was the next step. The first tab was the data tab of the weather generator. This is an important part of the process if there are gaps in the weather data used. Rather than any weather generator options, the WGEN user option was chosen for this research. In order to add weather data of the study area, the following five tabs (Fig. 3.13) were used. This was accomplished by successively specifying the precipitation, temperature, relative humidity, solar radiation and wind speed for the Thuthapuzha watershed. For inputting the data, the "Location Table" of each gauge is required.

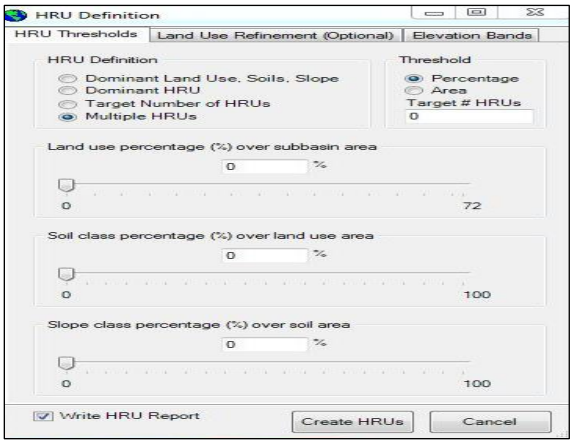

Fig. 3.12 HRU Definition menu in ArcSWAT

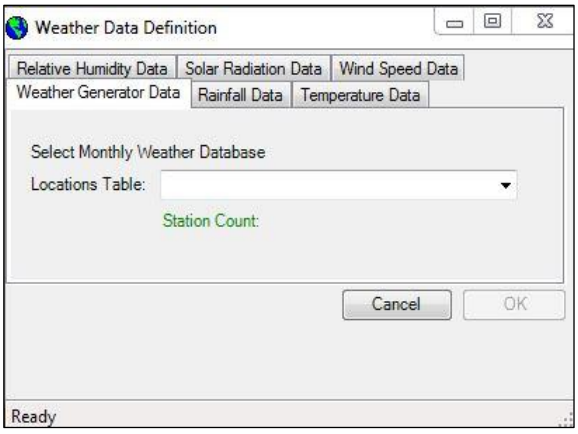

Fig. 3.13 Weather data definition menu in ArcSWAT

3.2.1.6. Write SWAT input tables

Database files constructed by the ArcSWAT program contain informations required to generate the default input files for running the model (Arnold *et al.*, 1998). The "Select All" button was pressed, followed by the "Create Tables" button to create and populate the SWAT model default input tables. The tick in the box and the "completed" next to the name of each SWAT table were the indication that the process was completed. Write SWAT input tables menu in SWAT model is shown in Fig. 3.14.

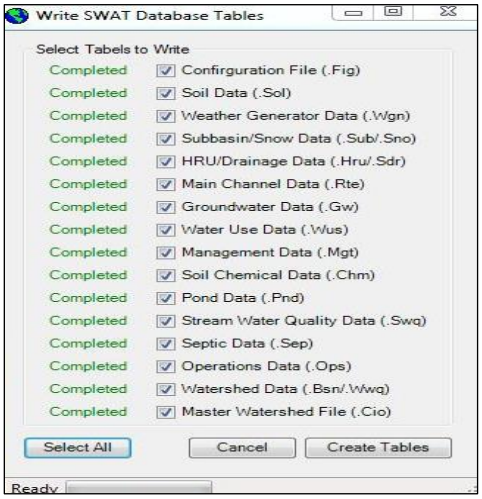

Fig. 3.14 Write SWAT input tables menu in SWAT model

3.2.1.7. Running the SWAT model

There was an 'Edit SWAT input' option to edit the ArcSWAT input before the SWAT model run option, and this tab is useful if the user wishes to use the model to study future climate change or land use scenarios. The input for this project has been modified for the impact assessment of conservation practices. The simulation period needed to be specified before the model run. For this study, the simulation period was from 01/01/1989 to 31/12/2009 for the calibration period and 01/01/2010 to 31/12/2017 for the validation period with daily time intervals. The NYSKIP specified a three-year warm-up period. The "Setup SWAT Run" button was started. After the model had completed the SWAT model setup, the "Run SWAT" button was enabled. The model

was individually executed for each year and notified when the specified period was successfully modelled. The output files to be imported into the database were selected and imported as output files, and the simulation with a specific name is saved. Using the SWAT check option, users can check whether there are any aspects of the results that cause a problem. Setup menu for the process of running SWAT model in ArcSWAT is shown in Fig. 3.15.

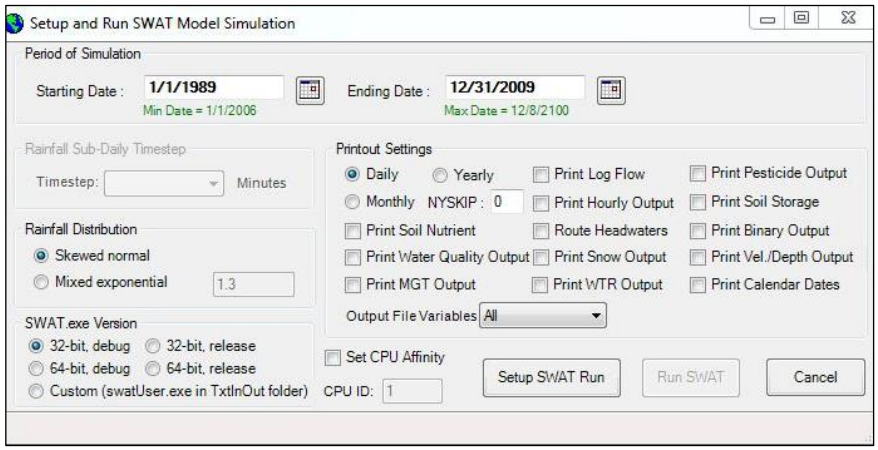

Fig. 3.15 Setup menu for the process of running SWAT model in ArcSWAT

3.2.1.8 Sensitivity Analysis and Calibration

The first step in the process of calibration and validation is the sensitivity analysis. Sensitivity analysis can be described as the process of determining the rate of change in the parameters of the model output relative to changes in the parameters of the model input. There are two types of sensitivity analysis; one-at-a-time and global analysis. This study carried out a global sensitivity analysis using the Sequential Uncertainty Fitting (SUFI-2) algorithm. SUFI-2 is a program connected to SWAT in the Calibration Uncertainty Programs known as SWAT- CUP (Abbaspour, 2008). The selected 13 parameters were ranked using Global sensitivity analysis tool by varying them over defined range of values and comparing those parameters with output discharge variations. A sensitivity measure was given by the t-stat value while the p-value calculated the significance of the sensitivity. SUFI-2 evaluates to what degree uncertainties are compensated for, and provides a range of outputs. In SUFI-2, the

uncertainty parameter accounts for all sources of uncertainty. The SUFI-2 algorithm used 500 simulations with a 3-year warm-up period from 1989 to 2009 using 13 parameters. After iteration, each parameter was adjusted based on the parameter ranges indicated by SUFI-2. For SWAT model calibration, a total of three model iterations were used. The accuracy of the calibration was assessed on the basis of the proximity of the p-factor to 100 percent and the prediction uncertainty on the basis of the proximity of the r-factor to 1. The Nash Sutcliffe Efficiency Value (NSE) and the coefficient of determination (R^2) were also used as fitness measurements between observed simulated discharges generated in the SWAT-CUP. After calibration in the SWAT-CUP, the parameters needed to be changed in the SWAT model were adjusted and the calibrated model was run.

3.2.1.9 Model Validation

Once the model was calibrated, model validation was performed via the SWAT-CUP interface. Validation of the model was carried out by running the model with calibrated parameters without any further modification and comparing the simulated and observed daily discharge values. The SWAT model has been run from 2010 to 2017 without any further adjustment of the calibrated parameters. The p-factor and r-factor were used to measure the prediction uncertainty and NSE, R^2 and PBIAS were used to evaluate the model performance.

3.2.1.10 Model performance

Commonly used statistical measure for hydrological modelling is the NSE value which can be used as a measure of goodness of fit. Generally, when assessing the performance of the hydrological model, NSE and R^2 are evaluated together (Zhou *et al.,* 2012). In this research, in addition to NSE and R^2 efficiency, percent bias (PBIAS) was also used to evaluate model performance. The general performance rating for the statistical measures are given in Table 3.2.

3.2.1.10.1 Nash-Sutcliffe efficiency (NSE)

It is generally defined as "the absolute difference between observed and predicted, which is then normalized by the variance of the observed discharge in order to eliminate

any bias". The range lies between 1 and -∞, with 1 being the perfect fit (Krause *et al.,* 2005).

$$NSE = 1 - \frac{\sum_{i=1}^{n}(O_i - P_i)^2}{\sum_{i=1}^{n}(O_i - \tilde{O})^2} \quad \text{---------} \quad (2)$$

Where, O_i is the observed discharge, P_i is the Predicted discharge, $\tilde{O}$ is the Mean of observed discharge and n is the number of simulations. The main drawback of the Nash-Sutcliffe efficiency is that the differences between the observed and the predicted values are computed as squared values. Therefore, in a time series, larger values are strongly overestimated whereas lower values are neglected (Legates and McCabe, 1999).

3.2.1.10.2 Coefficient of Determination (R^2)

Coefficient of Determination (R^2) can be expressed as "the squared ratio between the covariance and the multiplied standard deviations of the observed and predicted values". The range of R^2 lies between 0 and 1. A zero value means absolutely no correlation; while a value of one means that the distribution of the prediction is the same as the observation. Since only the linear relationship between the variables is measured, the coefficient of determination has many drawbacks. It is calculated as:

$$R^2 = \left(\frac{\left(\sum_{i=1}^{n}(O_i - \tilde{O})(P_i - P)\right)}{\sqrt{\sum_{i=1}^{n}(O_i - \tilde{O})^2}\sqrt{\left(\sum_{i=1}^{n}(P_i - P)^2\right)}} \right)^2 \quad \text{---------} \quad (3)$$

Where, P is the mean of simulated discharge.

3.2.1.10.3 Root Mean Square Error (RMSE)

RMSE indicates a perfect match between the observed and the predicted values when it is equal to zero, with increasing RMSE values indicating an increasingly poor match. Singh *et al*. (2004) stated that "RMSE values of less than half the standard deviation of the measured data could be considered low and will indicate a good model prediction". It is calculated as:

$$RMSE = \sqrt{\frac{\sum_{i=1}^{n}(P_i - O_i)^2}{n}} \quad \text{---------} \quad (4)$$

3.2.1.10.4 Percent bias (PBIAS)

It measures the average negative dispersion of the predicted data from the observed data with an optimum value of zero percent, which means no deviation. The optimum value for PBIAS is zero, with low magnitude values indicating accurate model simulation. PBIAS positive values denote under estimation bias and negative values denote overestimation bias (Gupta *et al.,* 1999). It is calculated as follows:

$$\text{PBIAS} = \left[\frac{\sum_{i=1}^{n}(O_i - P_i)*100}{\sum_{i=1}^{n}(O_i)}\right] \quad \text{---------} \quad (5)$$

Table 3.2 General performance rating of statistical measures

Performance rating	R^2	NSE	PBIAS
Very good	R^2>0.85	0.75<NSE<1.0	PBIAS<±10
Good	0.75< R^2<0.85	0.65<NSE<0.75	±10<PBIAS<±15
Satisfactory	0.6< R^2<0.75	0.50<NSE<0.65	±15<PBIAS<±25
Unsatisfactory	R^2<0.60	NSE<0.50	PBIAS>±25

3.3.2 Climate change impact analysis

3.3.2.1 Climate change impact on wateryield

Climate change is expected to have an impact on hydrology of a watershed due to changes in precipitation, temperature, and evapotranspiration. The impact of water resources on the global water supply may be the most profound and undoubtedly important. Water resources and climate change have been extensively studied and reported around the world. For example, the Intergovernmental Panel on Climate Change (IPCC) reviewed and referenced several studies on water resources and climate change

on a wide range of physiographical conditions, ranging from local to continental scales (IPCC, 1996). Accurate determination of the hydrological effects of climate change will help in understanding possible future problems with water resources and result in better decision making. With economic growth and population growth, the conflict between water use and water supply will become even more serious issue in the future.

It is of paramount importance to identify the potential impacts of climate change on water resources in order to achieve their proper management and utilisation. An appropriate hydrological model (SWAT) was identified for this purpose and the climate model projections were used as inputs in addition to the watershed parameters. The model was initially calibrated and subsequently validated during the period 1989-2010 using the observed streamflow data at the Pulamanthole gauging station. The temperature and precipitation scenarios for climate change (RCPs) were then projected using the GFDL-CM3 model. The projected climate scenarios were bias corrected and then used as input into the SWAT model to calculate water yield during the future period. Few studies have focused on climate change impacts on watersheds in humid tropical areas even though the use of climate model outputs in a hydrological model is not a new concept. For each climate change scenarios considered, the water yield generated by the SWAT model was compared to evaluate the impact of each RCP scenario.

3.3.2.2 Climate change impact on drought intensity

Drought is a complex phenomenon that can be characterised primarily by its duration, severity and areal extent. Drought severity is a major element among these three dimensions that can be used for drought analysis. Drought indices are widely used in a meaningful way to evaluate the severity of the drought. Among the various drought indices, SPI and RDI have been selected for analysing the climate change impacts on drought intensity.

The SPI is defined as “the number of standard deviations from the mean at which an event occurs”. The long-term record of precipitation for the chosen period of time is fitted to a probability distribution for the SPI calculation, which is then converted into a

normal distribution so that the mean SPI for the location and desired period is zero (McKee *et al.*, 1993). Positive SPI values indicate greater than median precipitation, and negative values indicate less than median precipitation. Thom (1958) found that the gamma distribution fits well with the time series of climatological precipitation. The magnitude of drought is calculated as the positive sum for each month SPI during the drought event (Hayes *et al.*, 2007). Drought classification based on SPI value (Tigkas and Tsakiris, 2004) is shown in Table 3.3. The ability of SPI to calculate at different time periods allows multiple applications. The SPI values for 3 months or less could be useful for basic drought monitoring, values for 6 months or less for monitoring agricultural impacts, and values for 12 months or longer for hydrological impacts, depending on the study purpose. The use of different timescales enables assessment of the effects of a precipitation deficit on different components of the water resource including groundwater, reservoir storage, soil moisture, streamflow etc.

Table 3.3 Classification of drought based on SPI values

SPI values	Classification
2.0 or more	Extremely Wet
1.5 to 1.99	Very Wet
1.0 to 1.49	Moderately Wet
-.99 to .99	Near Normal
-1.0 to -1.49	Moderately Dry
-1.5 to -1.99	Severely Dry
-2 or less	Extremely Dry

In order to analyse the impact of climate change on drought intensity, the bias corrected precipitation, the maximum temperature and the minimum temperature data derived from the climate model were given as input into DrinC software and the drought indices, namely SPI and RDIst, were calculated. The number of drought occurrences was then analysed to determine the intensity of the drought. For each RCP scenario, PET was calculated separately using the Hargreaves method in the software module. Since both

SPI and RDI fit well with the gamma distribution, it was selected for the calculation of drought indices. In order to analyse the long-term effects of drought, the time-scale was set at 12 months.

3.3.3 Conservation practices impact analysis

For watershed management, it is necessary to quantify the changes in the water balance and soil erosion over a long period of time which is a challenging task. The SWAT model was used here to analyse the impact of conservation practices on hydrological processes. Water management from farmland to basin level will need to improve in the future, to meet water resource requirements in different sectors. It is therefore essential to analyse the impacts of conservation practices. The SWAT model itself is capable of simulating a number of management practices such as tillage, fertiliser application, crop rotation, dams, ponds, etc. But fewer researchers analysed the impact of conservation practices on watersheds using SWAT. In addition, there is no standard procedure to simulate conservation practices to date.

For this research, the collected details of conservation practices were analysed. The three main conservation practices; Vented Cross Bar (VCB), check dam and brushwood dam in the study area were selected for further analysis. The SWAT models divide the area of simulation into subwatersheds connected following the river network in a cascade structure. From the literature, it was found that check dams could be modelled as ponds in the SWAT model. Since the conservation practices chosen have a similar function as the check dams, all three have been modelled as ponds. Thus, for each subbasin, the storage area and the volume of all three conservation practices were summed up and given as a single pond at the outlet of subbasins in which it is located. The SWAT model already has the option to simulate the reservoir. As a result, the Kanjirapuzha Dam was modelled as a reservoir. Following the modelling of ponds and reservoirs, the SWAT model was run to simulate the impact of conservation practices on stream flow and sediment yield. In general, the impacts of conservation practices on streamflow and sediment yield were evaluated by running the model with and without conservation practices and comparing streamflow and sediment yield in both cases.

Results and Discussion

CHAPTER IV

RESULTS AND DISCUSSION

The present study was conducted to assess the impact of conservation practices and climate change on watershed hydrology. The bias correction methods, as well as the comparison of CMPI5 and CORDEX-SA data, have been detailed in this chapter. The hydrological model SWAT and the climate model GFDL-CM3 were used for the study. The research findings are analysed for each objective and discussed under separate sections in this chapter.

4.1 MODEL DEVELOPMENT

4.1.1 Preparation of data inputs

The primary datasets required for the SWAT model are DEM, land use map, soil map and meteorological data.

4.1.1.1 Digital Elevation Model (DEM)

DEM data was used to delineate the watershed boundary corresponding to the outlet at the Pulamanthole gauging station in the SWAT model. NASA SRTM DEM has been used with a resolution of 30 m. The SRTM DEM used for this study is shown in Fig. 4.1. The properties of the DEM are shown in Table 4.1.

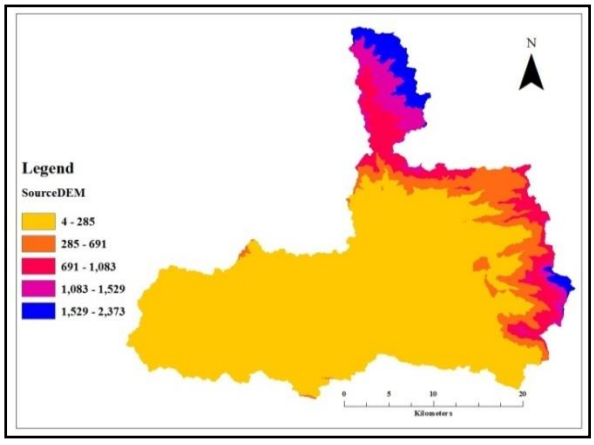

Fig. 4.1 Digital Elevation Model of Thuthapuzha watershed

Table 4.1 DEM properties

Metadata parameter	Value/Description
Projection	Universal Transverse Mercator (UTM)
False Northing	0
False Easting	500000
Central Meridian	75
Scale factor	0.996
Reference Latitude	0
Geographic coordination system	WGS_1984_43 N
Column/Row count	1636/1381
Cell size (X/Y)(m/m)	30/30

4.1.1.2 Land use map

ERDAS IMAGINE 2014 software was used to prepare the Land use map. Using the ArcSWAT project, the classified image was clipped and reprojected. Land use map was projected in WGS_1984_UTM_Zone_43N projection. Prepared land use was given as input into the model (Fig. 4.2 A). In order to link the land use layer to the SWAT land use database, a lookup table (Fig. 4.2 B) containing different SWAT land use class codes was used.

Land use resolution is 30x30 m. In the study area, there are 14 land use classes for land use (Table 4.2). Agricultural Land Row Crops, which cover 20.30 percent of the watershed area, is the most dominant land use class. Rubber and forest are the other dominant land use classes in the study area.

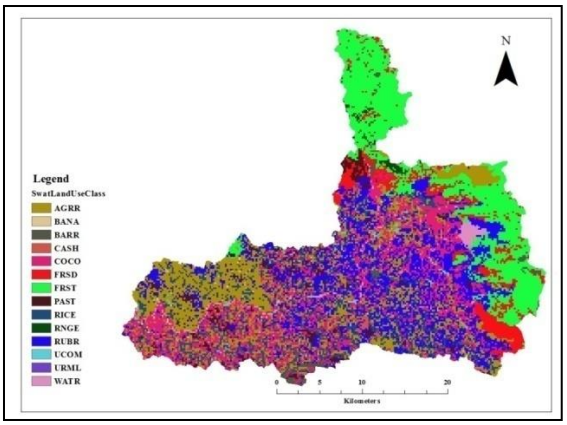

Fig 4.2 (A) Land use map

VALUE	LandUseSwat
2	AGRR
3	URML
5	UCOM
6	FRST
7	FRSD
12	PAST
15	RNGE
18	WATR
33	RICE
101	RUBR

Fig.4.2 (B) Lookup table of land use map

Table 4.2 Land use distribution in the study area

SWAT Land use class	Land use type	% Area
AGRR	Agricultural Land-Row Crops	20.30
URML	Urban Medium Density	0.21
UCOM	Urban- commercial	0.52
FRST	Forest-Mixed	18.91
FRSD	Forest-Deciduous	5.78
PAST	Pasture	3.32
RNGE	Degraded	0.61
WATR	Water bodies	1.72
RICE	Rice	8.47
RUBR	rubber	19.94
BANA	Banana	0.21
COCO	Coconut	18.00
CASH	Cashew	0.44
BARR	Barren	1.58

4.1.1.3 Soil map

The characteristics of the soil and the vegetation cover influence the movement of the water. The soil layer was digitised in ArcGIS and converted to the raster format prior to input to the SWAT model. Using the ArcSWAT project database, soil map data was clipped and reprojected. It was also projected in the same projected coordinated system as that of land use. Soil properties have been entered in the SWAT soil user database. The database was linked to the soil map by means of a lookup table, which was given to the SWAT model as an input. The soil map and corresponding lookup table are shown in Fig. 4.3 A and 4.3 B respectively.

In the study area, there are 14 soil classes. The major soil series are Karinganthodu and Mannursree, which contribute approximately 21.79% and 20.02% of the watershed area respectively.

4.1.1.4 Slope map

The characterisation of the slope depends on the DEM provided in the watershed delineation process. Slope was calculated from the DEM and reclassified into four slope classes, the class units were in percent (%). The slope map and the slope distribution of the study area are shown in Fig. 4.4 and Table 4.3 respectively.

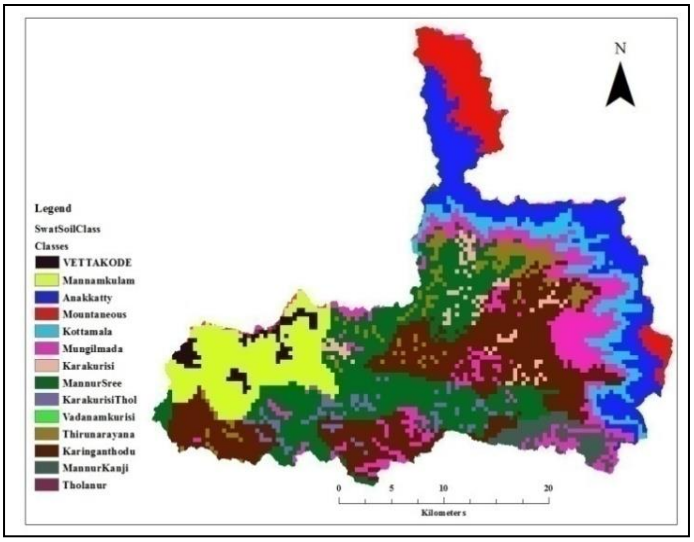

Fig. 4.3 (A) Soil map of the study area

VALUE	Area(%)	Name
3	1.60	VETTAKODE
4	9.89	Mannamkulam
7	13.00	Anakkatty
8	5.89	Mountaneous
9	5.87	Kottamala
10	11.53	Mungilmada
11	1.93	Karakurisi
14	20.02	MannurSree
15	1.94	KarakurisiThol
16	0.00	Vadanamkurisi
16	0.00	Vadanamkurisi
17	3.64	Thirunarayana
18	21.79	Karinganthodu
19	2.79	MannurKanji
20	0.09	Tholanur

Fig. 4.3 (B) Lookup table showing area and soil series

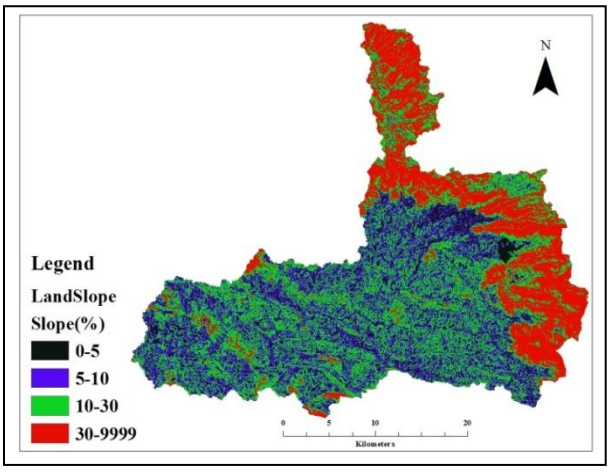

Fig. 4.4 Slope map of the study area

Table 4.3 Slope class distribution

Slope (%)	% Watershed Area
0-5	14.27
5-10	23.51
10-30	38.82
30-9999	23.40

4.1.1.5 Meteorological data

For the modelling of various physical processes, daily precipitation, maximum and minimum temperature, relative humidity, wind speed and solar radiation are needed for the SWAT model as meteorological input, with daily precipitation being the most important. Rain gauge location (RARAS, Pattambi and IMD, Mannarkkad) text file containing the location details were provided, and these location file were linked to the

rainfall data file containing the daily precipitation values in mm. Both these files should be in the .txt (.text) extension and in a single folder. Fig. 4.5 shows the link between location file and rainfall data file. In the same way, the maximum and minimum temperature values of two stations (RARS, Pattambi and CWC, Pulamnthole) were given as location files which were linked to a data file containing the maximum and minimum temperatures in Degree Celsius. Similarly, the remaining parameters including relative humidity, wind speed and solar radiation collected from RARS, Pattambi were also given to the model in units percentage fraction, m/s and MJ/m²/day respectively.

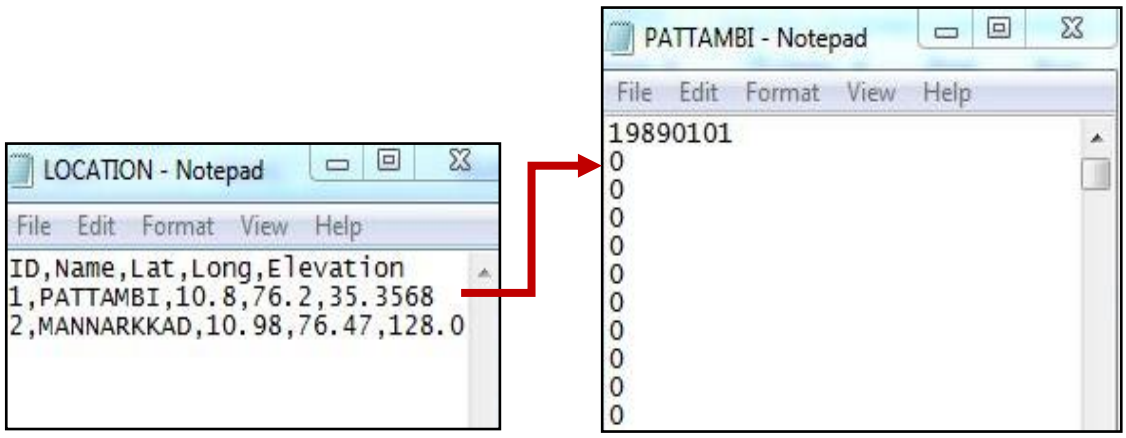

Fig.4.5 Location table of rain gauge stations and data table showing the rainfall of Pattambi station

4.1.2 SWAT model setup

Model setup includes watershed delineation, HRU analysis, input table writing and SWAT simulation. The outputs obtained during each step are discussed briefly in this section.

4.1.2.1 Watershed Delineation

A procedure using the DEM (Winchell *et al*., 2013) is used to delineate subbasins. In order to avoid potential problems in the routing process in subbasin inlets / outlets, a uniform distribution of subbasins in size within the model area should be achieved by delineating the watershed in the SWAT model (Winchell *et al*. 2013). Watershed definition includes three steps to be completed; DEM setup, stream definition and inlet outlet definition. To delineate the watershed, NASA SRTM DEM with a resolution of

30 m was used. After loading the DEM on the model, change the DEM projection to WGS_1984_UTM_Zone_43N. The DEM projection set up has been completed. The streams and outlets were then defined by SWAT. DEM based stream definition was made by specifying a threshold limit of 1810 ha and manually adding one outlet at the Pulamanthole gauging station to delineate the watershed based on the outlet location. Selection of the output helps to compare model results and observation data. For improved hydrographic segmentation and subbasin delineation, the model was provided with drainage lines (Neitsch *et al.*, 2005a). As a result, the Thuthapuzha watershed was divided into 35 subbasins (Fig. 4.6). Calculation of subbasin parameters, including relative stream reach and geomorphic parameters was the final step in the watershed delineation. Thus, a topographic report was generated by the SWAT model showing the calculated maximum, minimum, mean and standard deviations of the elevation values for each subbasin separately.

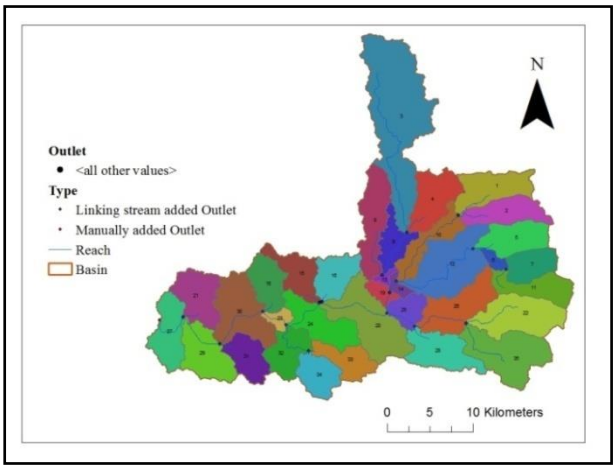

Fig. 4.6 Delineated watershed showing outlet points and subbasins

4.1.2.2 HRU analysis

HRU analysis includes two steps; Landuse/soils/slope definition and HRU definition. Land use and soil data were defined for each subbasin for the modelling of different hydrological and other physical processes. The prepared land use and soil map, along with the lookup table, was provided as input to the model. Four slope classes have been selected, and the slope map has been prepared and added to the model. The soil,

land use and slope data were then overlapped together to generate unique combinations of land use, soil type and slope known as hydrological response units (HRUs). The model is capable of assessing changes in evapotranspiration and other hydrological conditions for various land use and soils by subdividing watersheds into HRUs. There are two methods for creating HRUs, one of which was dominant land use and soil, in which one HRU for each subbasin is defined by the dominant land use type and soil type. The second method considers multiple HRUs for each subbasin; the number of HRUs may differ depending on the requirements of the user. In this study, the second method was chosen and the threshold value was set at 10 percent for all three classes. Threshold levels of soil, land use and slope types were determined below which unique soil, land use and slope areas are not considered in subbasins (Winchell *et al*., 2013). The use of threshold values decreases the number of HRUs in the SWAT model and optimises both the SWAT model and the demand for computing (Winchell *et al*., 2013). A total of 841 HRUs were thus created for the Thuthapuzha watershed. For each subbasin, a detailed report on HRUs, land use classes, and soil types were generated.

4.1.2.3 Writing Input Tables

It includes two steps; weather stations and write input tables. Precipitation, minimum and maximum temperature, wind speed, relative humidity and solar radiation from the available meteorological locations were entered into the SWAT model. The location file in the text format is imported into the model. After importing all the required data, the initial watershed input values must be defined using the write input table option. SWAT generates default input values for each HRU and subbasin in the ArcGIS Geodatabase using the information already given for soil, land use, topography and meteorological data to the model. All the spatial data used in ArcSWAT were projected to WGS_1984_UTM_Zone_43N. The metric unit system was used for all SWAT tabular inputs.

4.1.2.4 SWAT simulation

This includes running the SWAT model and reading the outputs. The start and end dates of the simulation were selected and the SWAT simulation was completed. The rainfall distribution was set us skewed normal. The simulation period was fixed between 1989 and 2009 (21 years) for calibration and 2010-2017 (8 years) for validation; the warm-up period is three years. For climate change studies, simulations were conducted between 2021-2040 and 2041-2170. The selected output files were exported to the database, and the simulation was saved with a proper name. SWAT error check option enables the user to check whether any result contains an error.

4.1.3 Sensitivity Analysis and calibration using SWAT- CUP

The choice of parameters for the calibration process depends up on their significance to the simulated output. Parameter sensitivity was evaluated using the built-in SWAT-CUP sensitivity analysis tool using the SUFI-2 algorithm linked to the SWAT. SWAT-CUP uses t-stat and p-value to determine the sensitivity of the parameter. The parameter will be more sensitive if the t-stat value is higher and the p-value is smaller (Abbaspour, 2015). There are two indicators in the SUFI-2 algorithm to quantify the calibration strength and model uncertainty, namely the p-factor and the r-factor.

As suggested in the calibration procedure developed by Abbaspour *et al.* (2015), the sequential calibration process has been carried out. A new project was created in SWAT- CUP after setting up the ArcSWAT model using the best parameter estimates based on the available data, analyst expertise and literature. All files in SWAT TxtInOut were copied to the project directory in the SWAT-CUP project setup. The calibration process was done after the calibration inputs were modified as per the research requirement. In the calibration parameter input, a total of thirteen parameters were given for sensitivity analysis. Initial calibration ranges were assigned to parameters based on the previously identified parameters. It is also possible to define additional, user-defined parameter ranges. The model was run 500 times (great time savings can be made by using the parallel processing option in SWAT-CUP). The most sensitive

parameters were determined after iteration using the Global Sensitivity Analysis Tool. Post-processing options are calculated after iteration, where 95 percent prediction uncertainty and the objective function for all observed variables were calculated, a new set of parameter ranges is generated. Iteration with changed parameter ranges was conducted again, based on new suggested parameter range sets. The procedure was continued until satisfactory NSE and R^2 model results were achieved. A total of three iterations have been made. SUFI-2s Global Sensitivity ranked the 13 selected parameters by changing them over a defined range of values and comparing those parameters with output discharge variations. Discharge was taken as the observed variable for analysis. Out of the thirteen parameters, eight of the most sensitive parameters were chosen for calibration. During calibration, the input values of the model were adjusted to match the simulated and observed discharge. The calibration period was set at 21 years from 1989 to 2009. The parameters ranking after sensitivity analysis and the global sensitivity output are shown in Table 4.4 and Fig. 4.7 respectively. The dotty plot of the most sensitive parameter in SWAT-CUP (Fig. 4.8) shows the objective function values as a function of the parameters. It also indicates whether or not the objective function is sensitive to the parameter. When points are scattered and haphazard, it indicates the sensitivity is small and the sensitivity is higher when there is a trend.

Table 4.4 Parameters raking after sensitivity analysis and fitted range of values

Rank	Parameter	SWAT-CUP initial range	Range after calibration
1	r__CN2.mgt	-0.2 to 0.2	-0.16 to 0.08
2	v__ALPHA_BF.gw	0 to 1	-0.43 to 0.52
3	v__GW_DELAY.gw	30 to 450	-117.67 to 260.83
4	v__GWQMN.gw	0 to 2	0.78 to 2.35
5	r__SOL_AWC().sol	-0.2 to 0.4	0.09 to 0.66
6	v__ESCO.hru	0.8 to 1	0.90 to 1.10
7	v__CH_K2.rte	5 to 130	57.80 to 163.45
8	r__SOL_K().sol	0 to 100	30.04 to 90.16
9	r__SOL_BD().sol	0.9 to 3	1.64 to 3.13
10	v__CH_N2.rte	-0.01 to 0.3	-0.13 to 0.16
11	a__SURLAG.bsn	0.05 to 24	11.53 to 34.50
12	v__GW_REVAP.gw	0.02 to 0.2	0.10 to 0.26
13	r__EPCO.hru	0 to 1	0.14 to 0.71

In the above table, v-represents the default value is replaced by the value, r-represents that the existing value is multiplied by the default value, and a-represents the default values is added by the value.

Parameter Name	t-Stat	P-Value
9:R__SOL_BD(..).sol	-0.112212408	0.910701322
13:R__EPCO.hru	-0.319791264	0.749263996
10:V__CH_N2.rte	-0.533773726	0.593742135
4:V__GWQMN.gw	-0.860293775	0.390051308
6:V__ESCO.hru	0.986912983	0.324176373
12:V__GW_REVAP.gw	1.062508529	0.288532557
11:A__SURLAG.bsn	-1.091144141	0.275750115
2:V__ALPHA_BF.gw	-2.025391621	0.043373181
3:V__GW_DELAY.gw	-2.037130505	0.042178250
1:R__CN2.mgt	-2.203682022	0.028014935
5:R__SOL_AWC(..).sol	3.340224565	0.000901516
7:V__CH_K2.rte	3.753230520	0.000195671
8:R__SOL_K(..).sol	-4.286492996	0.000021897

Fig. 4.7 Global sensitivity output showing ranking using t-stat and p-value

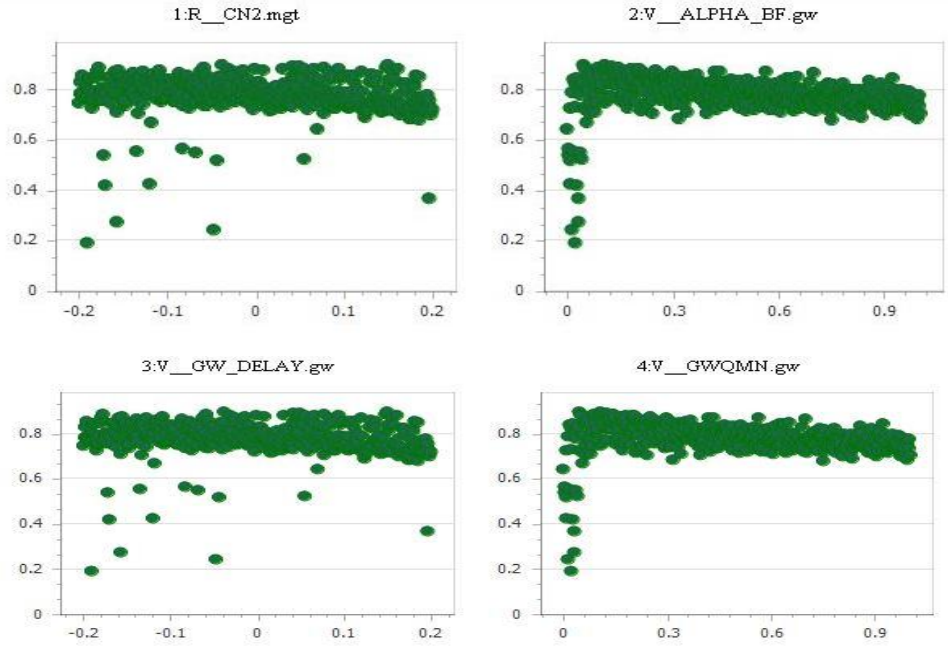

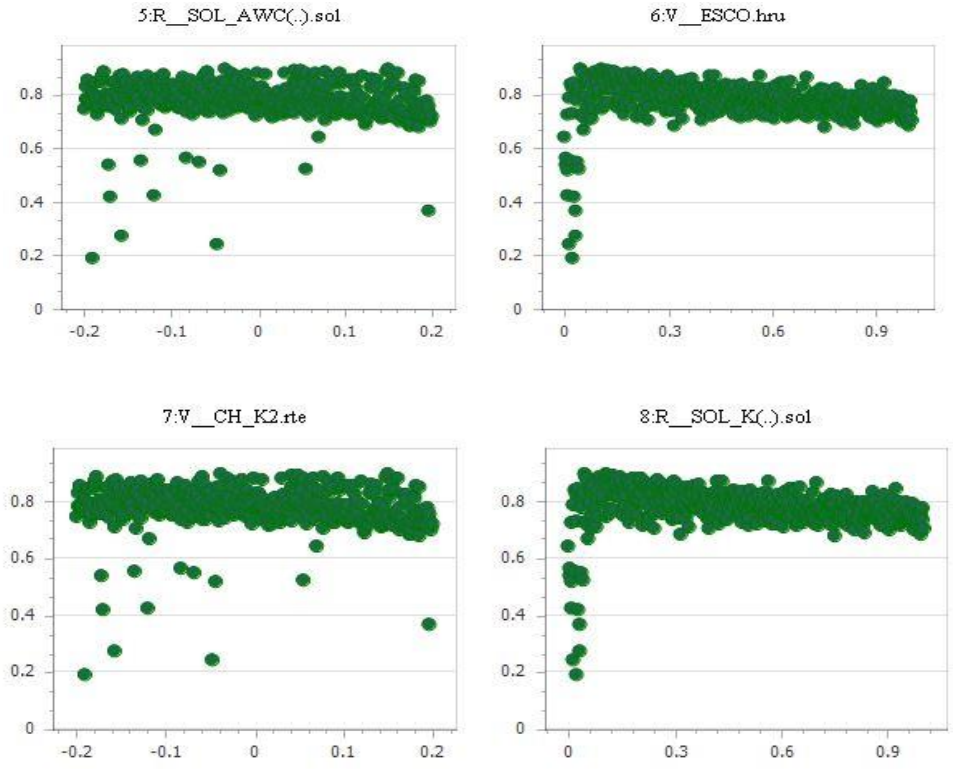

Fig. 4.8 Dotty plot showing the most sensitive parameters

4.1.5 Model performance evaluation

Model performance was evaluated on the basis of three statistical parameters, namely NSE (Nash-Sutcliffe Efficiency), R^2 (Coefficient of Determination) and PBIAS. As per the performance rating as discussed in the previous chapter, the performance of the model was analysed for both the calibration and the validation period using discharge as the parameter. It was concluded from the values that the model performed well in both periods. Model evaluation statistics for monthly discharge of Pulamanthole gauging station is shown in Table 4.5. The performance evaluation based on scattered plot and time series graph for both calibration and validation is shown in Fig. 4.9 to Fig. 4.12.

Table 4.5 Model evaluation statistics

Statistical parameter	Calibration period	Validation period
NSE	0.88	0.8
R^2	0.88	0.8
PBIAS (%)	-1.4	5.4

4.1.6 Model Validation

Following satisfactory calibration of the hydrological model (by achieving very good performance statistics), the validation process was carried out. The validation period consists of the remaining eight years (2010 – 2017). The model was validated using the SWAT-CUP interface following the calibration of the model. Validation of the model refers to running the model without further changes in the calibration parameters and comparing the observed and simulated discharges. From 2010 to 2017, the SWAT model was run with eight calibrated parameters without any further parameter changes. The NSE, R^2 and PBIAS were used to measure the model performance and the p-factor and r-factor were used to quantify the uncertainty of the prediction. During calibration, the p-factor and the r-factor were 0.77 and 0.64, and during validation, the p-factor and the r-factor were 0.85 and 0.56, respectively. Overall statistics shows that the model can be successfully used to simulate outputs in the Thuthapuzha watershed. The 95PPU plot obtained from SWAT-CUP and the corresponding rainfall distribution for both the calibration and the validation period are shown in Fig. 4.13. The developed model was further used to achieve the remaining objectives of the study. Streamflow simulated by the developed model for calibration and validation period was compared with the observed as shown in Fig. 4.14 and annual observed streamflow (Mm^3) of Pulamanthole gauging station during 1989-2017 are given in Appendix XI.

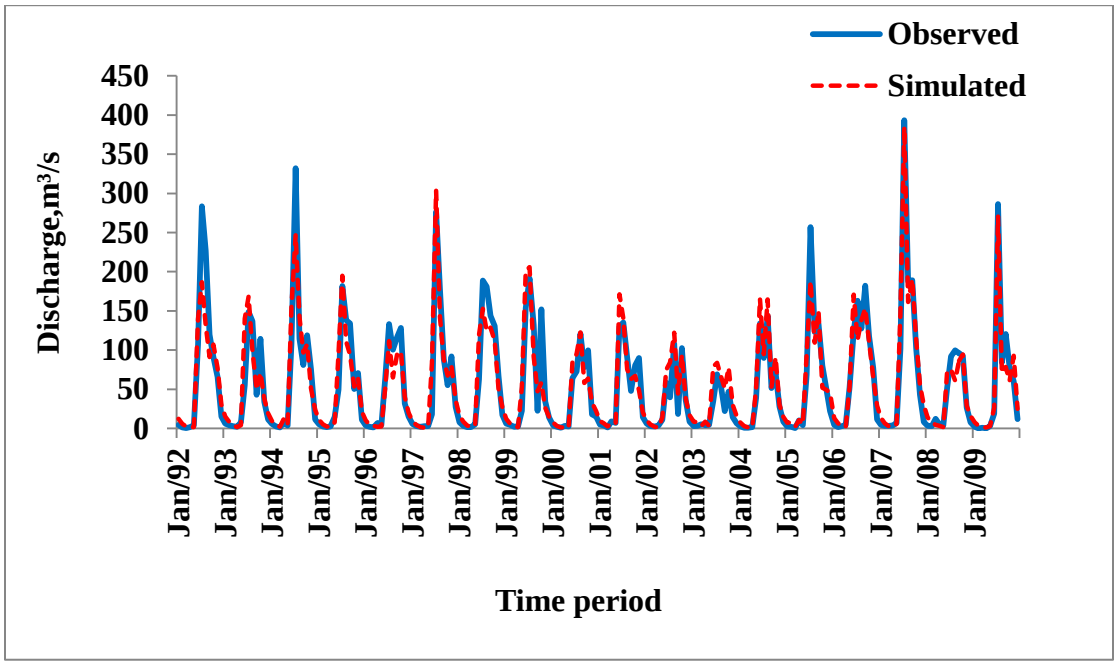

Fig. 4.9 Observed and simulated discharge at Pulamanthole for calibration period

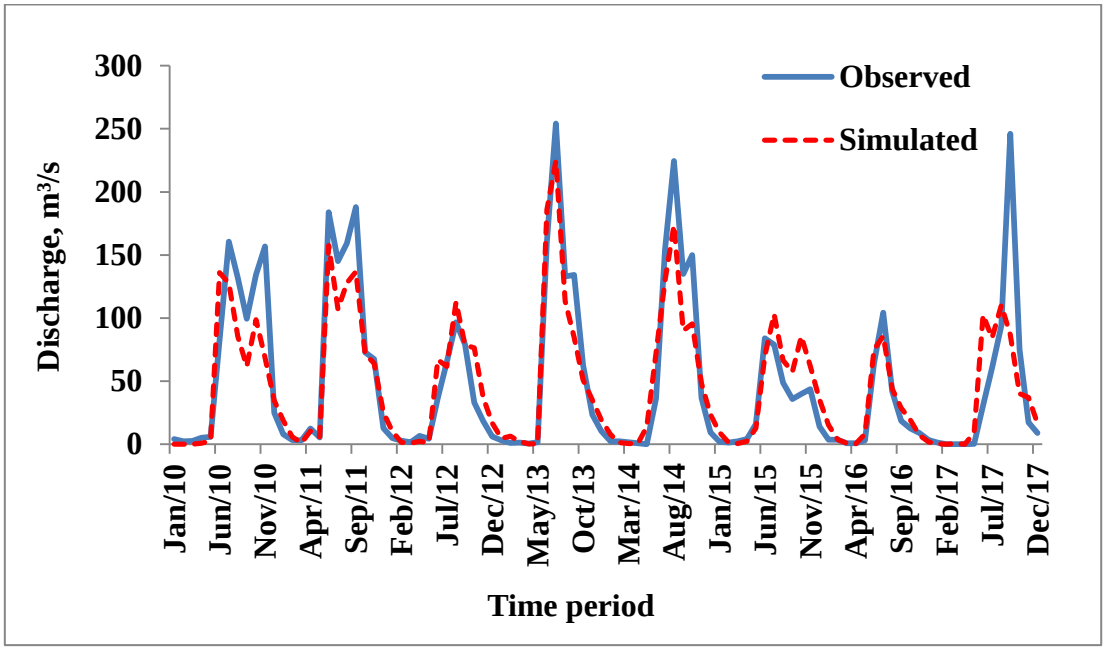

Fig. 4.10 Observed and simulated discharge at Pulamanthole for validation period

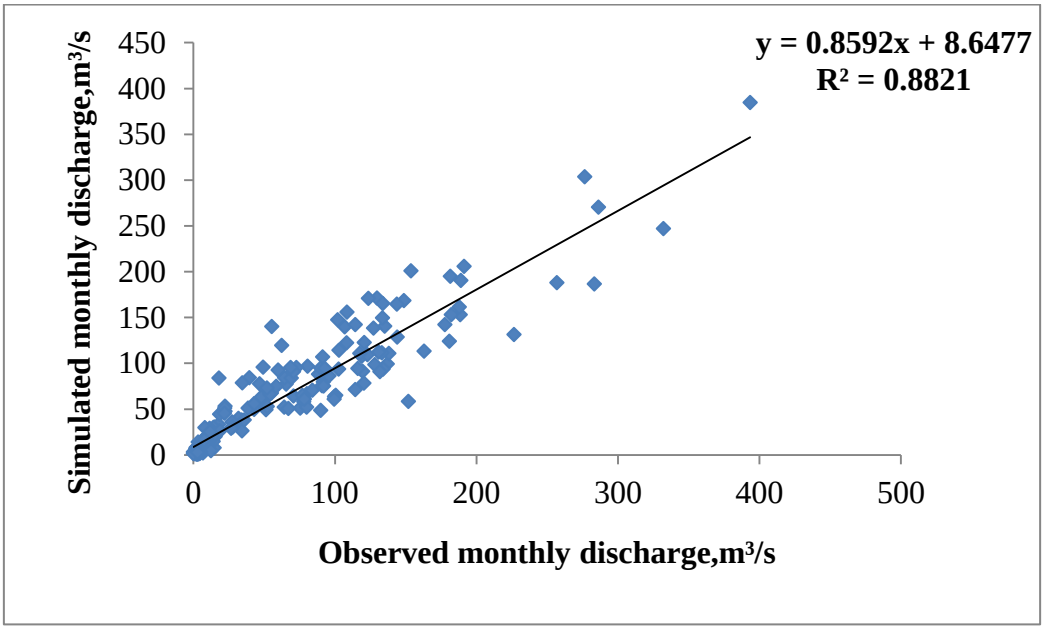

Fig. 4.11 Scatter plot of observed and simulated monthly discharges at Pulamanthole gauging station during calibration period

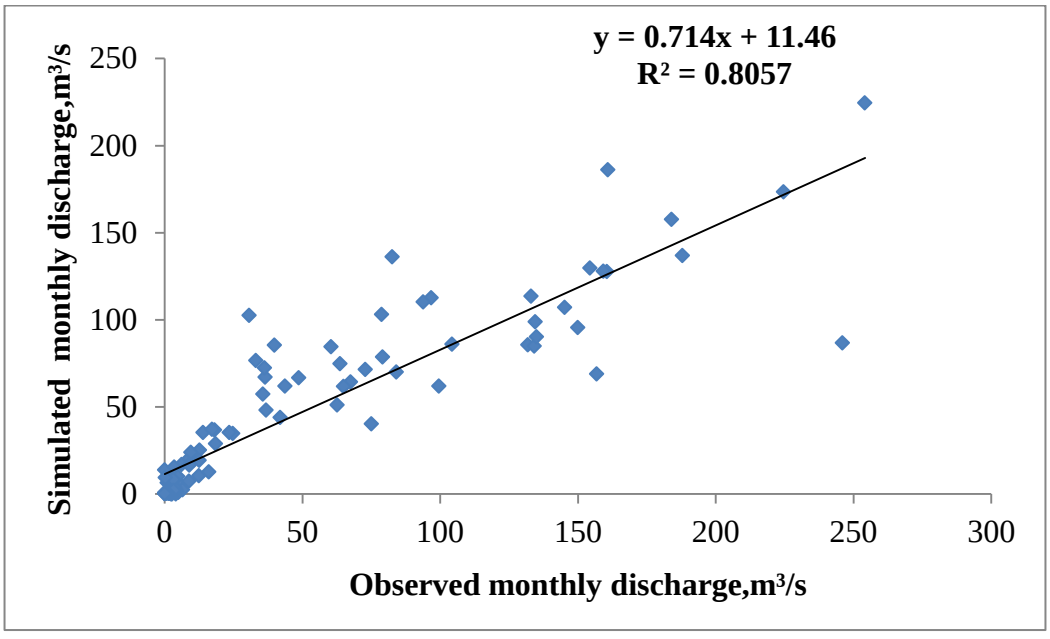

Fig. 4.12 Scatter plot of observed and simulated monthly discharges at Pulamanthole gauging station during validation period

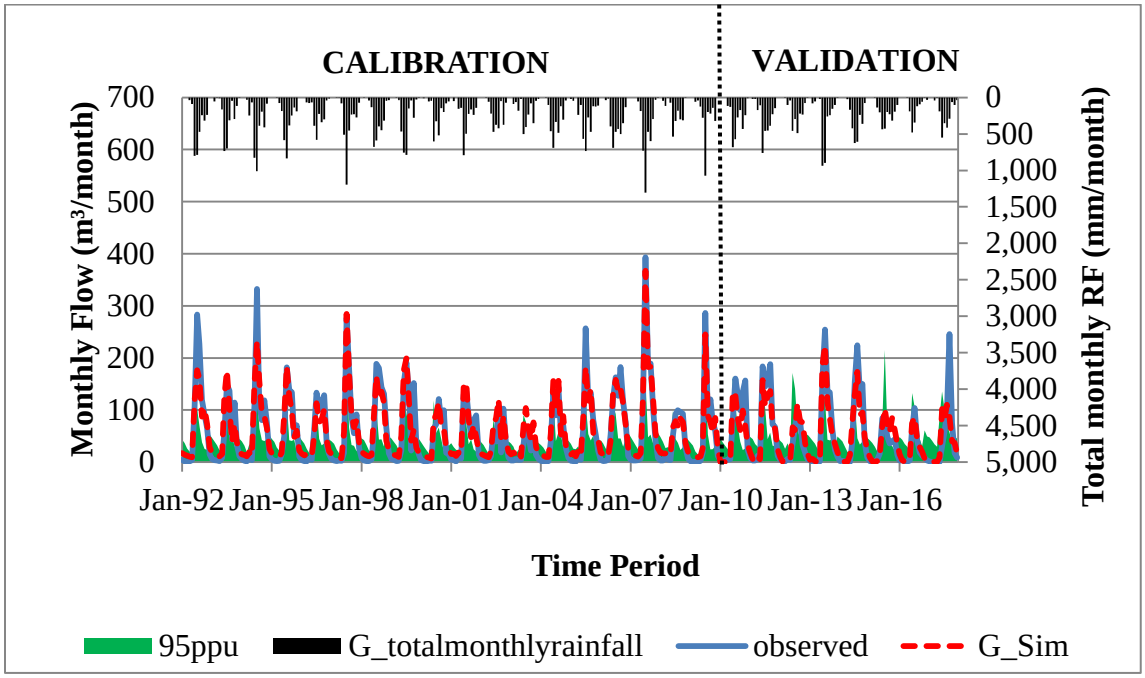

Fig. 4.13 95PPU plot obtained from SWAT-CUP and corresponding monthly rainfall

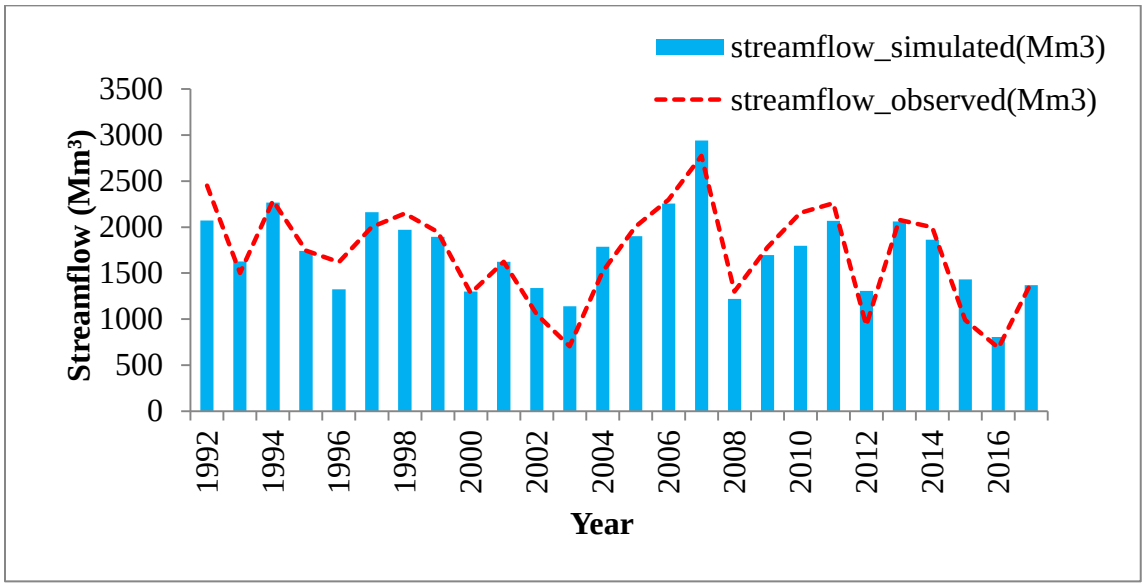

Fig. 4.14 Observed and simulated streamflow at Pulamanthole during the entire simulation period

4.1.7 Water balance of Thuthapuzha watershed

The water balance components of the Thuthapuzha watershed were predicted by the developed model. From the output reach file, the water balance components including surface runoff, lateral flow, evapotranspiration and ground water flow were represented as the percentage of rainfall for the calibration period from 1992-2009. The percentage of each components were plotted as pie diagram as shown in Fig. 4.15, Fig. 4.16 and Fig. 4.17. From the pie diagram, it is clear that the outflow from the watershed is mainly in the form of surface runoff (ranges between 29 to 51%) followed by ground water flow (23 to 31%). Evapotranspiration varied from 15 to 38% and lateral flow from 6 to 8% during 1992-2009. Thus it is concluded that the major portion of river flow is in the form of surface runoff and groundwater flow. Groundwater component is significant during summer season since the summer river flow is mainly contributed by the ground water. Conservation practices are playing an important role in conserving the water during rainy season and contribute a major part as ground water. This highlights the need to analyse the conservation practices impact on river flow of the watershed.

A relationship between the rainfall and runoff was also analysed to know the trend of streamflow in the watershed from 1992-2017. For that, a time series representation of streamflow and rainfall was made as shown in Fig. 4.18. A decreasing trend in the streamflow was observed from 1992 to 2017 with the observed rainfall. This shows that there is a need for evaluating the impact of climate change on streamflow.

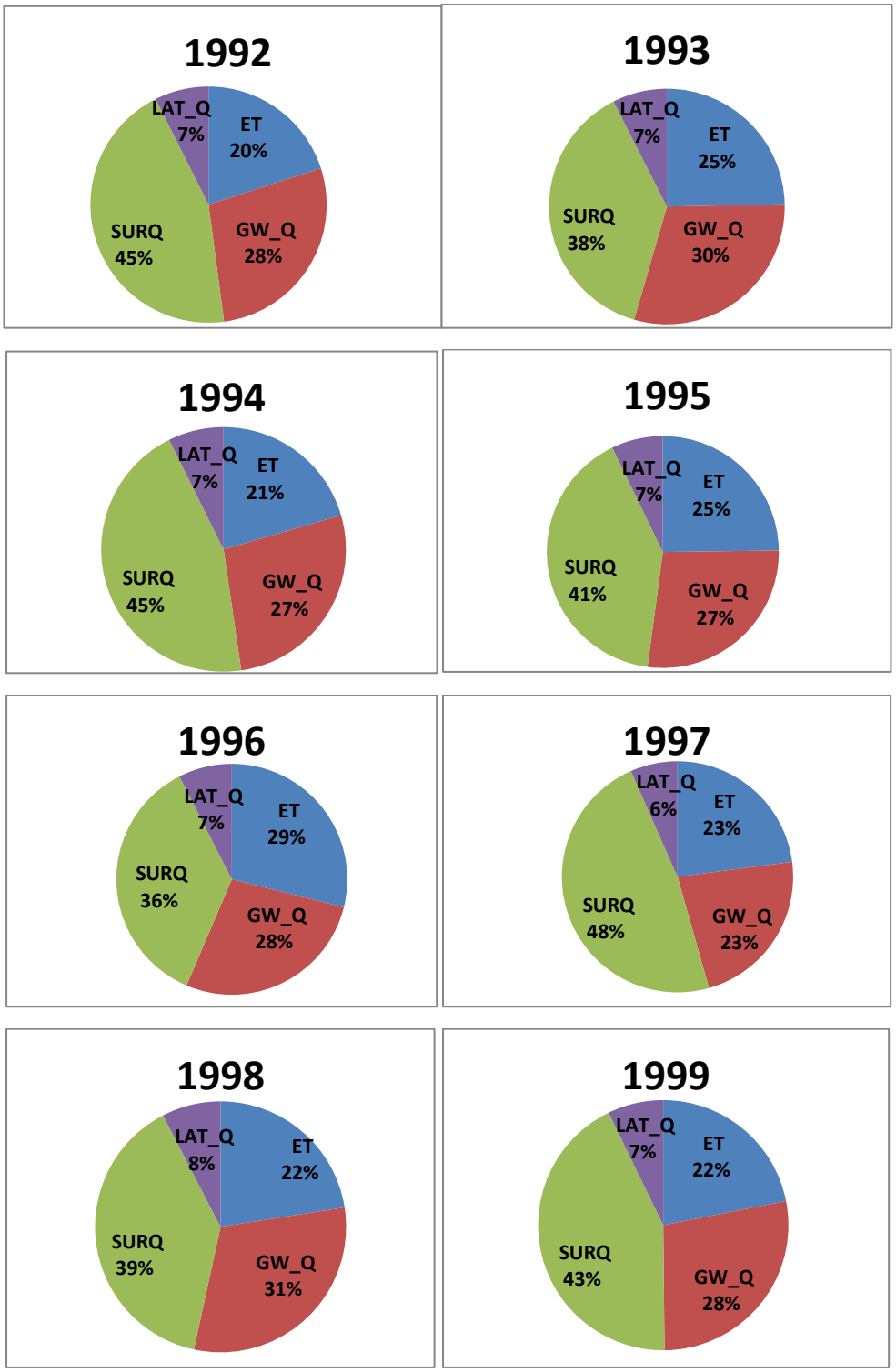

Fig. 4.15 Water balance of Thuthapuzha watershed from 1992-1999

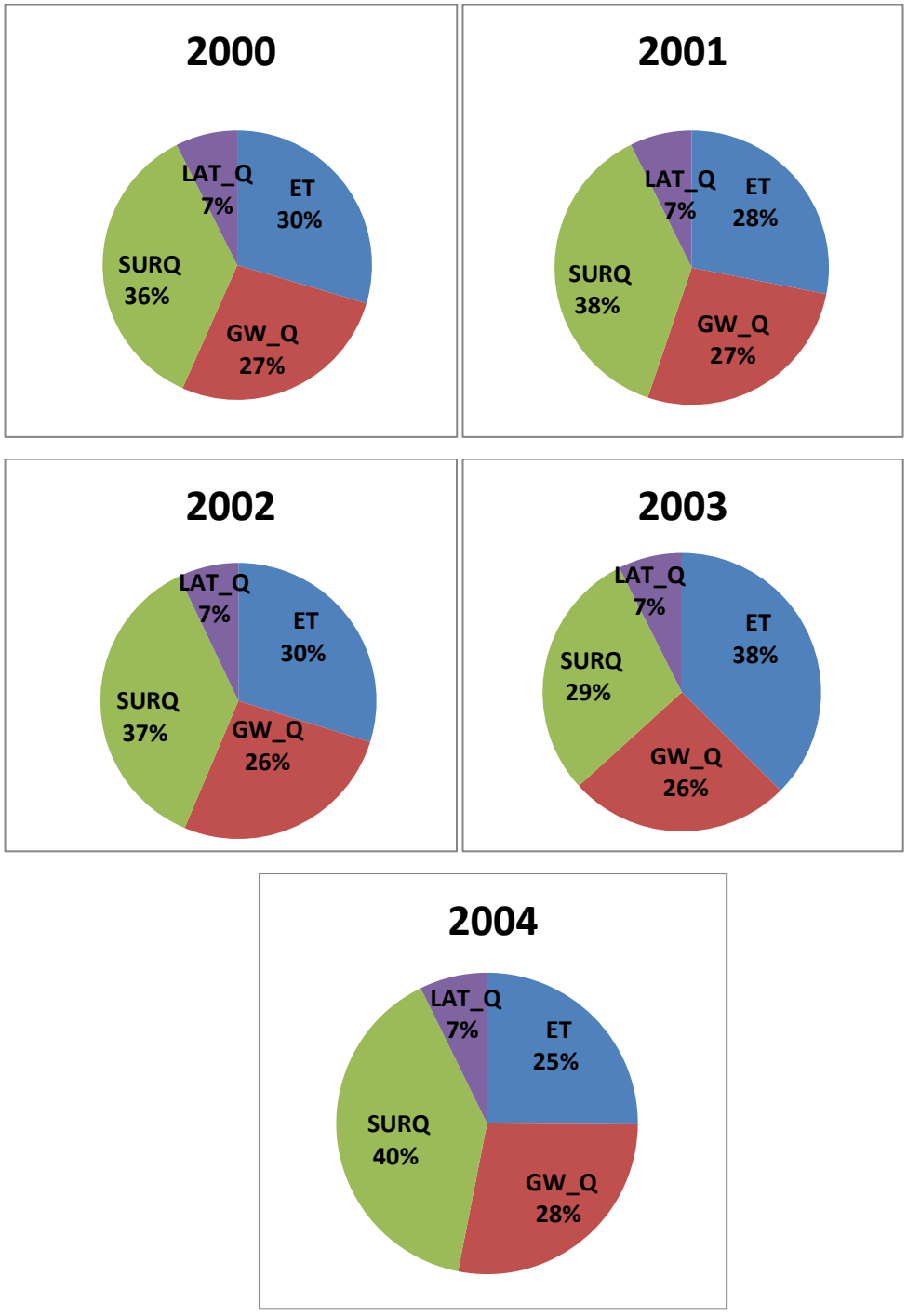

Fig. 4.16 Water balance of Thuthapuzha watershed from 2000-2004

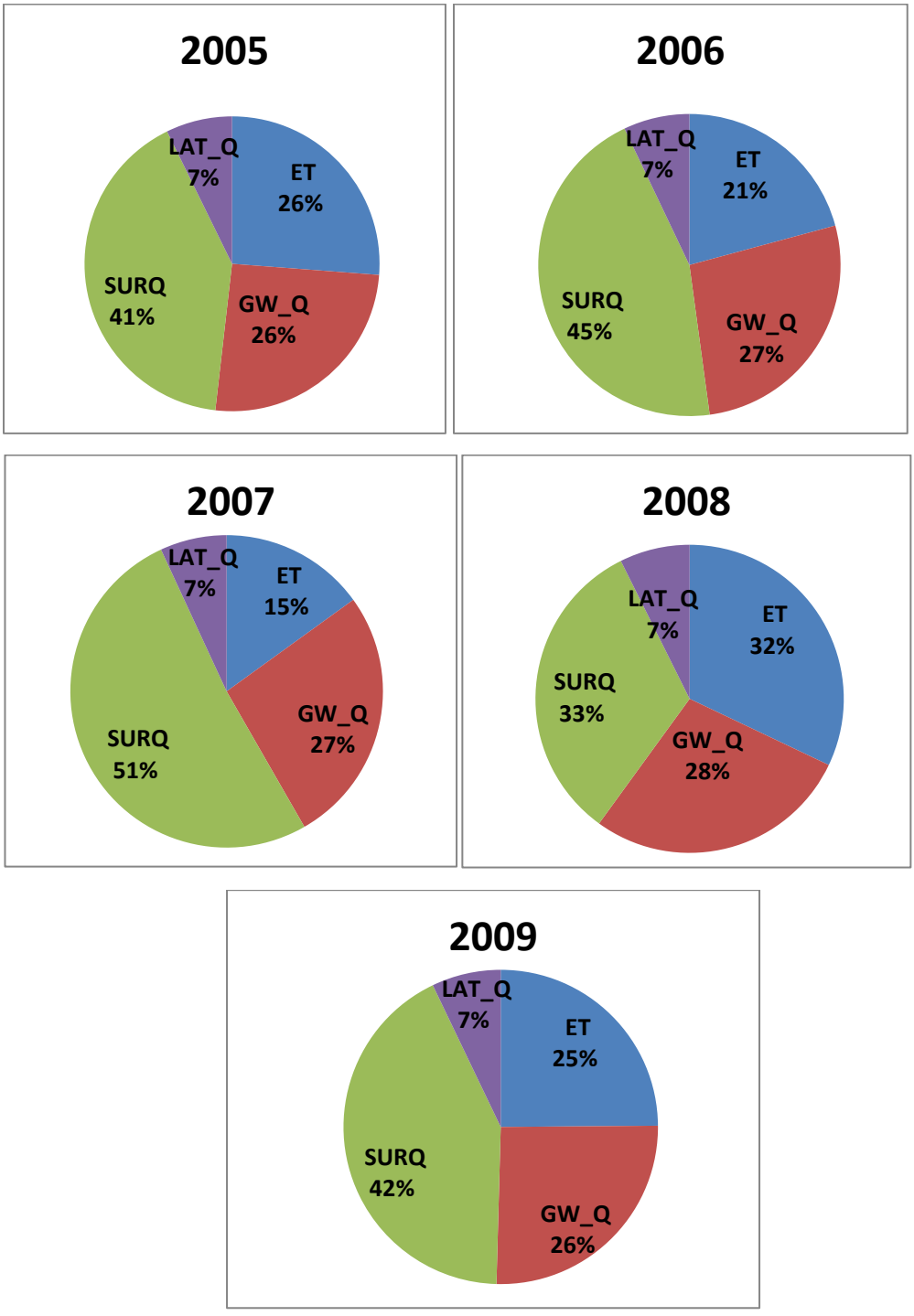

Fig. 4.17 Water balance of Thuthapuzha watershed from 2005-2009

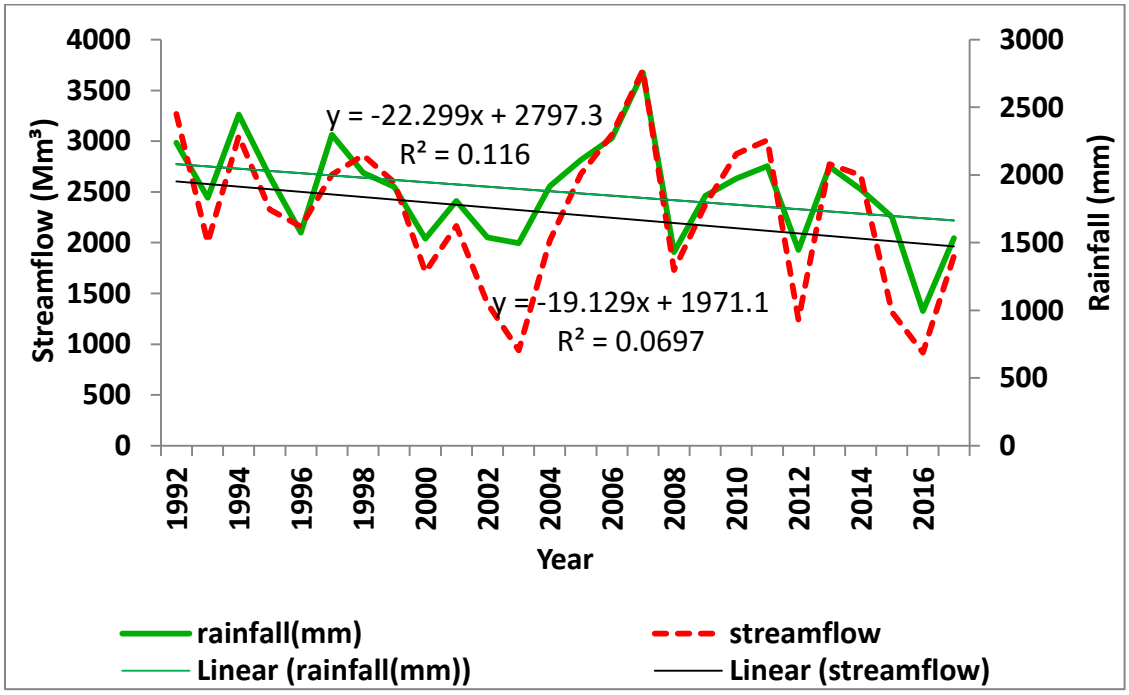

Fig. 4.18 Annual streamflow and average annual rainfall of Thuthapuzha watershed

4.2 IMPACT OF CLIMATE CHANGE ON WATERYIELD AND DROUGHT INTENSITY

The developed model was used to study the impact of climate change on Thuthapuzha watershed. Projected climate change is the basis for doing climate change analysis. From the literature review, GFDL-CM3 model was selected for projecting climate change data's of Thuthapuzha river basin. The model data from CMIP5 dataset and CORDEX-SA dataset was taken and the following procedures were adopted to select the input data for SWAT model to simulate the future impact of climate change on streamflow and drought intensity.

4.2.1 Selection of bias correction method

Uncertainties associated with the climate model datasets need to be corrected before impact related studies since there will be a great mismatch between observed and

predicted datasets. In order to analyse the datasets from CMIP5 and CORDEX-SA, bias correction was done to eliminate the uncertainties associated with the future climate change. Graphical representation of observed data's which are not bias corrected (precipitation, maximum temperature and minimum temperature) from CMIP5 and CORDEX-SA datasets (Fig. 4.19 to Fig. 4.21) shows that there exists a great mismatch between observed and projected datasets. Thus, different bias correction methods were performed to determine which bias correction method is best suited for further analysis separately for precipitation, maximum temperature and minimum temperature for both the datasets. To compare the bias corrected data with the observed data, the historical data from 1989-2005 was taken. Bias corrected methods were statistically as well as graphically compared to establish the results. Bias correction was performed using CMhyd software.

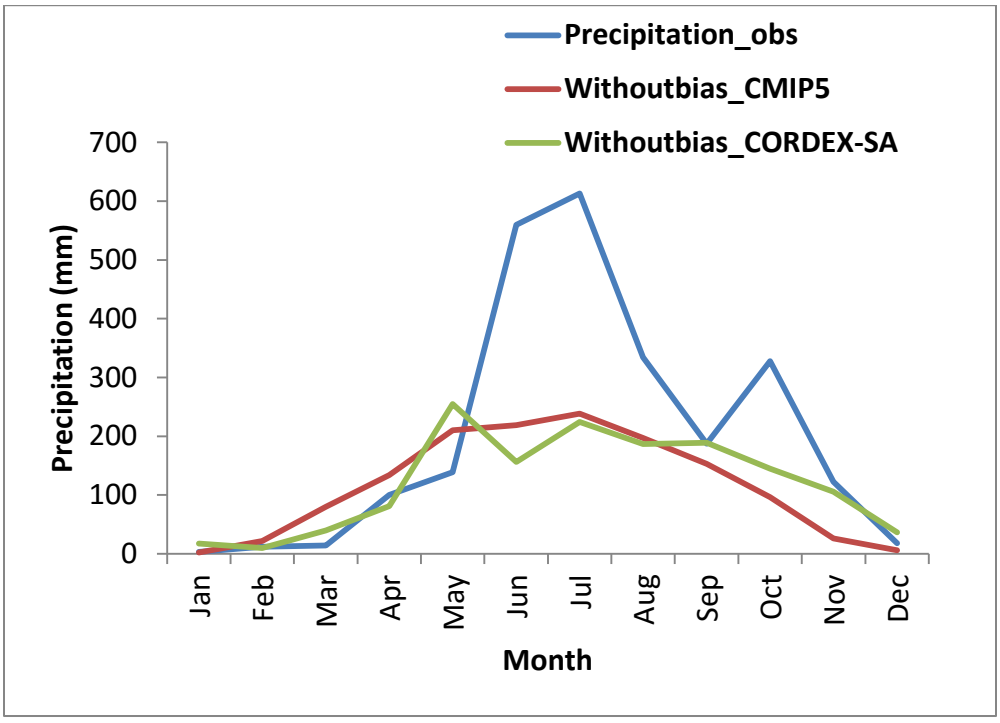

Fig. 4.19 Comparison between observed precipitation and projected datasets without bias correction

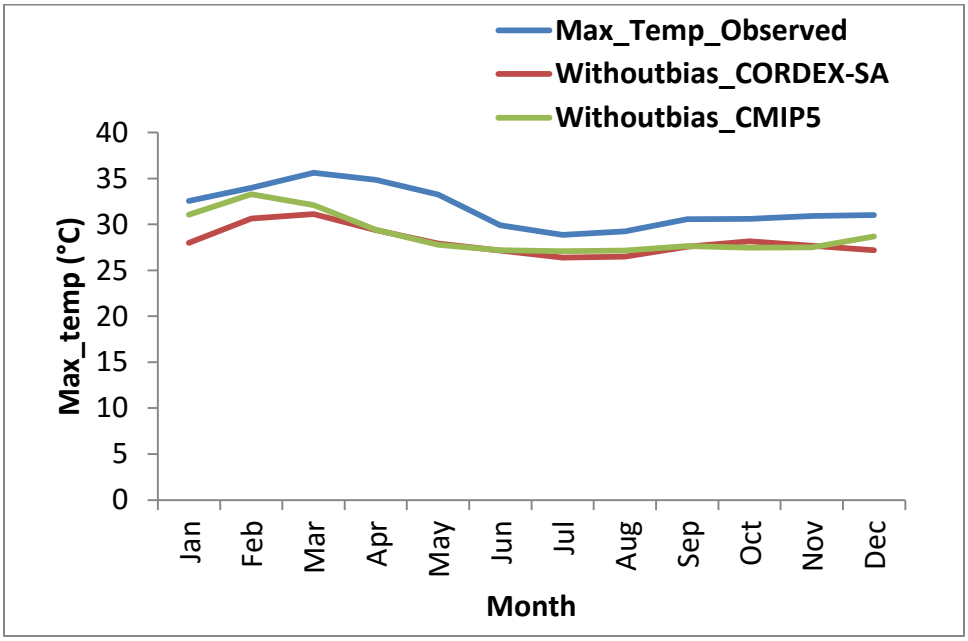

Fig. 4.20 Comparison between observed maximum temperature and projected datasets without bias correction

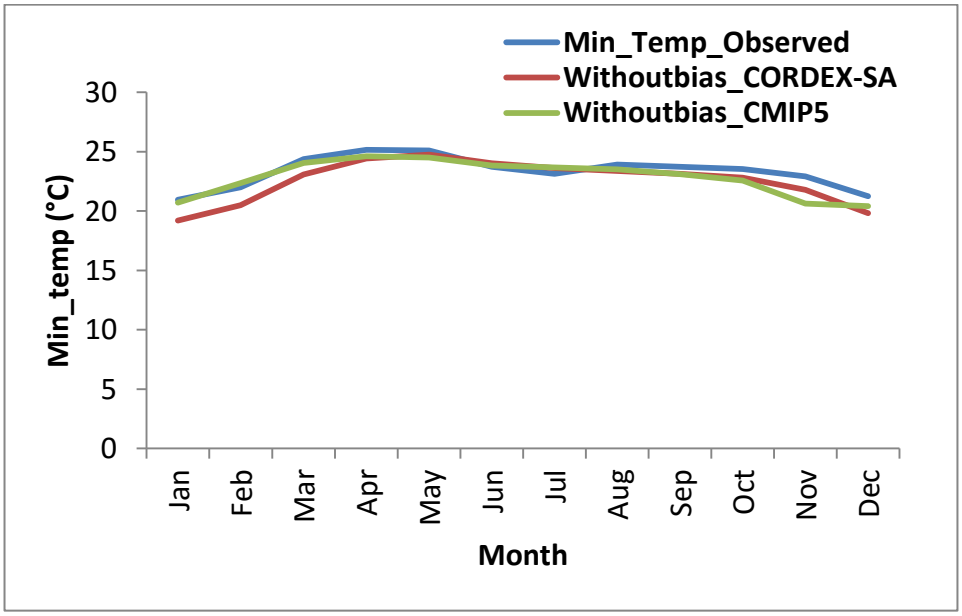

Fig. 4.21 Comparison between observed minimum temperature and projected datasets without bias correction

4.2.1.1 Bias correction of precipitation data

For precipitation data, five different bias correction methods were used separately for the CMIP5 and CORDEX-SA datasets. They are Linear Scaling (LS), Local Intensity Scaling (LIS), Delta change correction (DCC), Distribution mapping (DM) and Power transformation (PT). Statistical comparison of the precipitation data (Table. 4.6) was done using three statistical parameter; standard deviation, coefficient of variation and correlation coefficient. Graphical comparison of CMIP5 and CORDEX-SA data is shown in Fig. 4.22 and Fig. 4.23 respectively. Power transformation method is found to be the best correlated one among others when comparing CMIP5 dataset with observed data while linear scaling showed a good correlation with observed data when comparing CORDEX-SA dataset.

Table 4.6 Statistical comparison of different bias correction methods of future climate datasets (CMIP5 and CORDEX-SA) with observed precipitation

	Observed	LS	LIS	DCC	DM	PT
Precipitation_CMIP5_GFDLCM3						
Standard deviation	213.34	214.57	151.66	212.03	194.25	214.56
Coefficient of variation	1.04	1.04	1.06	1.03	1.09	1.04
Correlation coefficient		1.00	0.99	1.00	0.99	1.00
Precipitation_CORDEX-SA_GFDLCM3						
Standard deviation	213.34	212.93	212.94	211.82	215.35	212.94
Coefficient of variation	1.04	1.04	1.04	1.04	1.03	1.04
Correlation coefficient		1.00	1.00	1.00	1.00	1.00

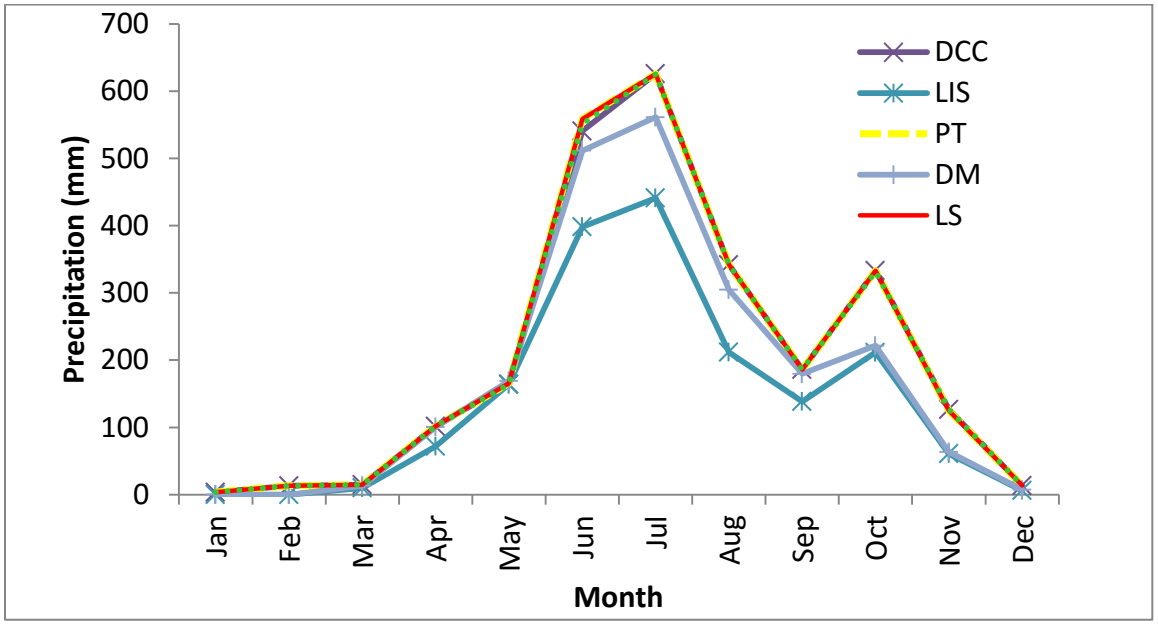

Fig. 4.22 Comparison of observed precipitation and bias corrected methods of CMIP5 precipitation datasets

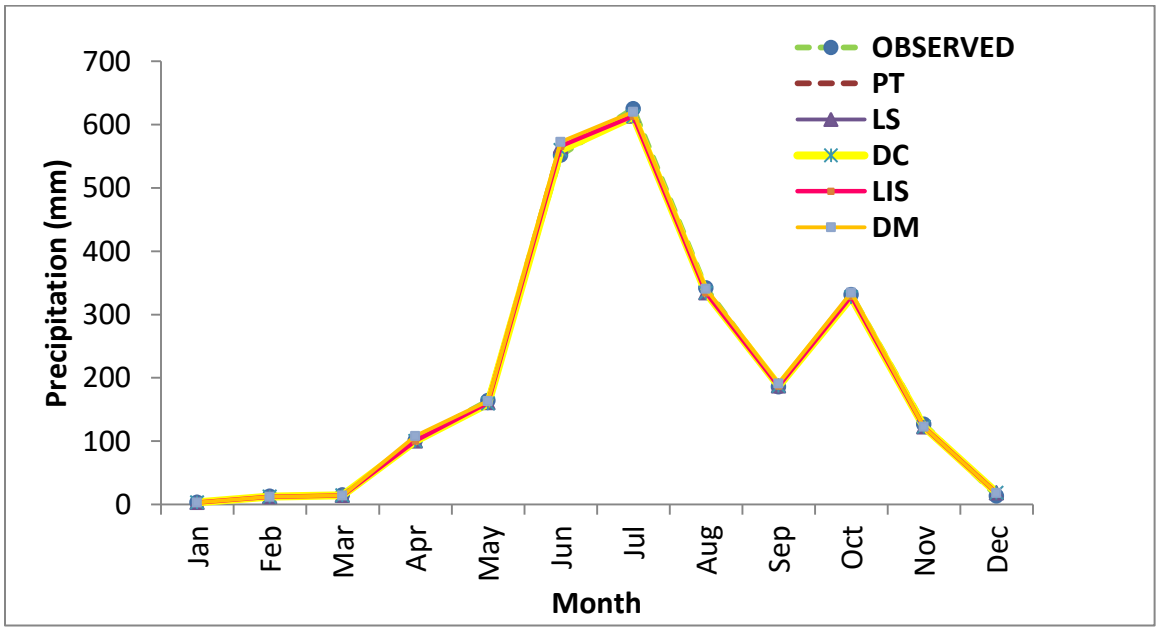

Fig. 4.23 Comparison of observed precipitation and bias corrected methods of CORDEX-SA precipitation datasets

4.2.1.2 Bias correction of temperature data

For temperature data correction (maximum temperature and minimum temperature), four different bias correction methods were used, separately for CMIP5 and CORDEX-SA datasets. They are Linear Scaling (LS), Variance Scaling (VS), Delta change correction (DCC) and Distribution mapping (DM). Statistical comparison of the maximum temperature data (Table 4.7) and minimum temperature data (Table 4.8) was done using three statistical parameters; standard deviation, coefficient of variation and correlation coefficient. Graphical comparison of CMIP5 and CORDEX-SA temperature data separately for maximum and minimum temperature is shown in Fig. 4.24, Fig. 4.25, Fig. 4.26 and Fig. 4.27. For maximum temperature as well as minimum temperature data, linear scaling is found to be the best correlated one among others when comparing CMIP5 dataset with observed data while variance scaling showed a good correlation with observed data when comparing CORDEX-SA dataset. Zhang *et al.*, 2018 used CMhyd software to bias correct the CanRCM4 model data and found that DM performed the best for both precipitation and temperature. Thus, the selection of bias correction method primarily depends on the model used in the study.

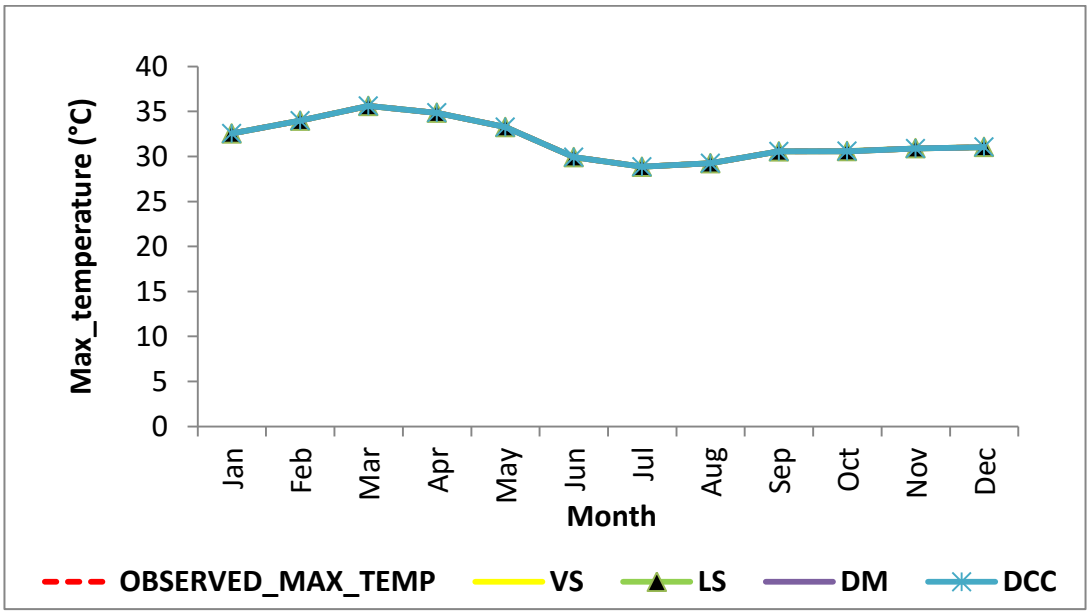

Fig. 4.24 Comparison of observed maximum temperature and bias corrected methods of CMIP5 maximum temperature datasets

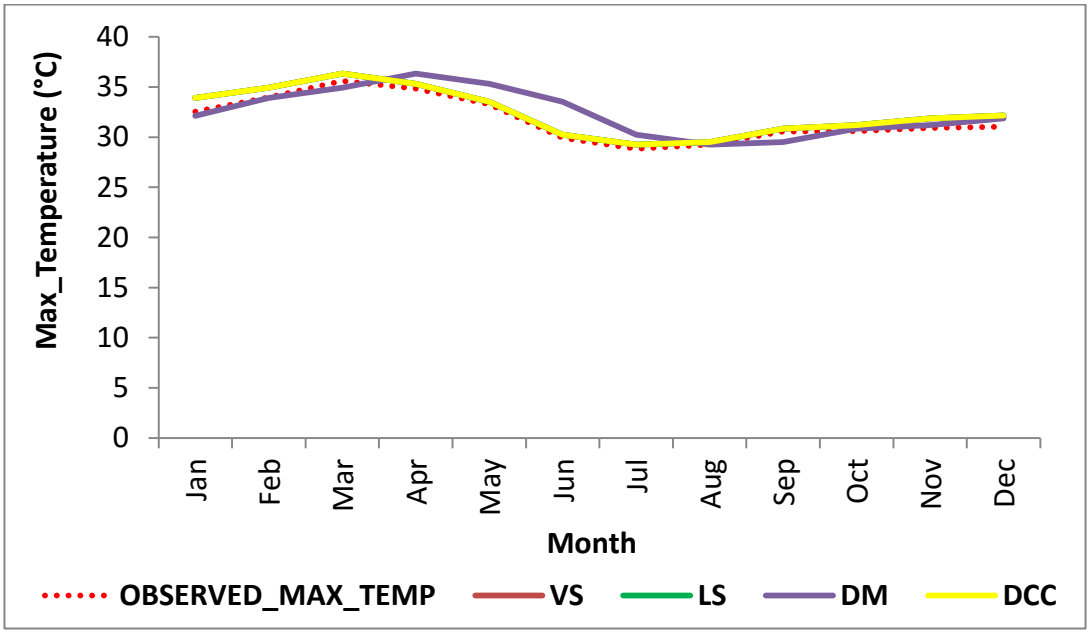

Fig. 4.25 Comparison of observed maximum temperature and bias corrected methods of CORDEX-SA maximum temperature datasets

Table 4.7 Statistical comparison of different bias correction methods of future climate datasets (CMIP5 and CORDEX-SA) with observed maximum temperature

	Observed	LS	VS	DCC	DM
Maximum Temperature_CMIP5_GFDLCM3					
Standard deviation	2.222348	2.222348	2.222336	2.222778	2.221779
Coefficient of variation	0.069928	0.069928	0.069926	0.069943	0.069909
Correlation coefficient		1.00	0.99999967	0.99999728	0.99999966
Maximum Temperature _CORDEX-SA_GFDLCM3					
Standard deviation	2.222348	2.358041	2.357347	2.357287	2.357535
Coefficient of variation	0.069928	0.072719	0.072698	0.072696	0.072708
Correlation coefficient		0.988373	0.988400	0.988373	0.837175

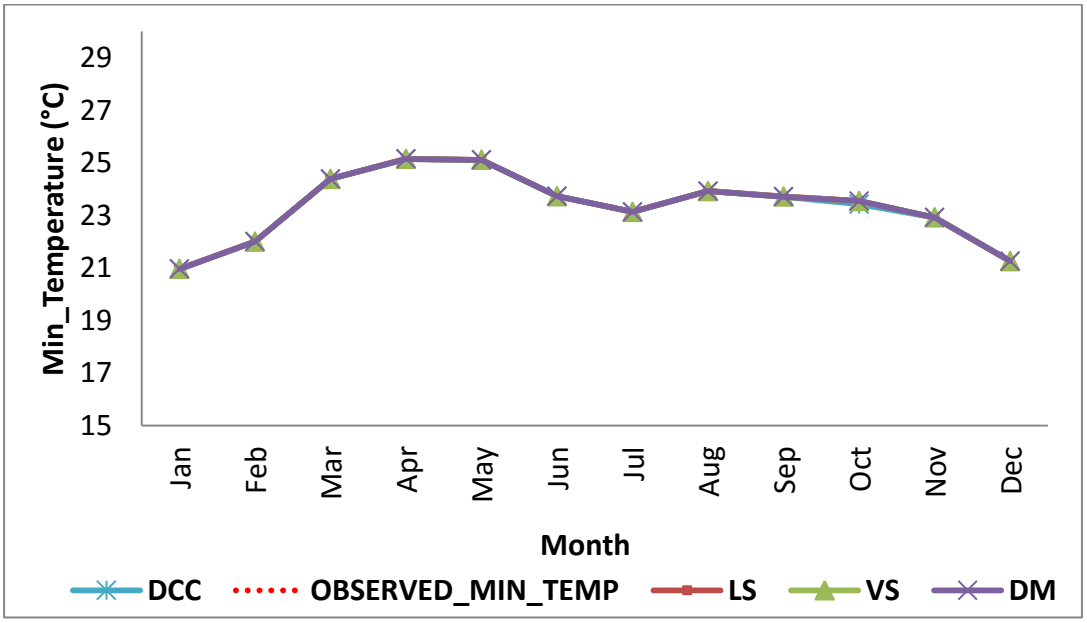

Fig. 4.26 Comparison of observed minimum temperature and bias corrected methods of CMIP5 minimum temperature datasets

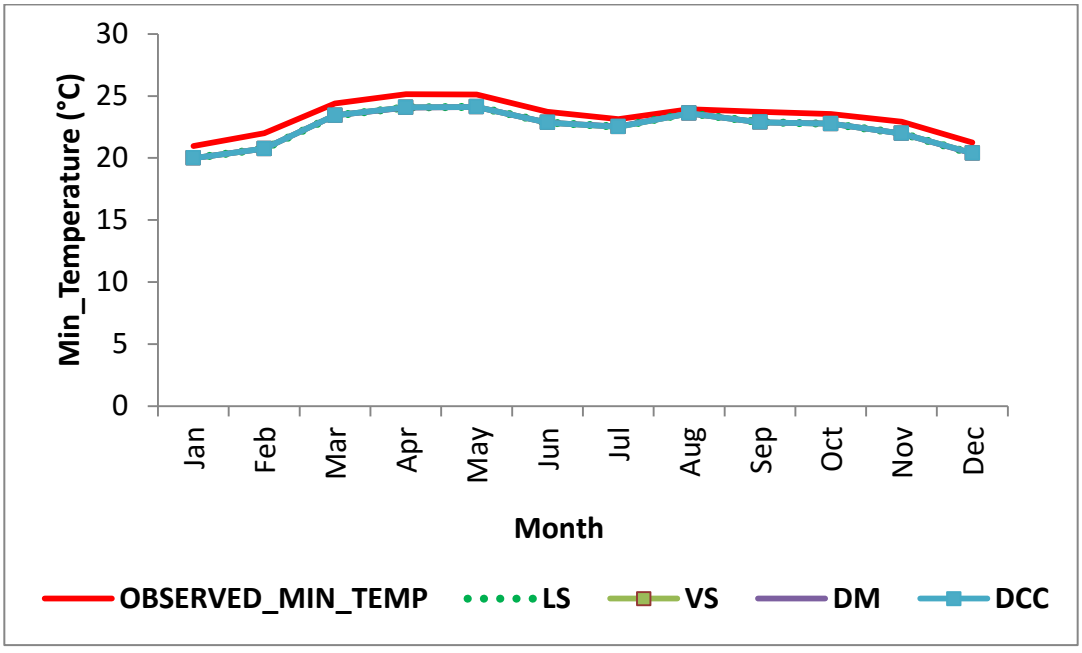

Fig. 4.27 Comparison of observed minimum temperature and bias corrected methods of CORDEX-SA minimum temperature datasets

Table 4.8 Statistical comparison of different bias correction methods of future climate datasets (CMIP5 and CORDEX-SA) with observed minimum temperature

	Observed	LS	VS	DCC	DM
Minimum Temperature_CMIP5_GFDLCM3					
Standard deviation	1.353914	1.354081	1.354255	1.352858	1.353748
Coefficient of variation	0.058053	0.058060	0.058068	0.058035	0.058046
Correlation coefficient		0.999999	0.999999	0.999664	0.999999
Minimum Temperature _CORDEX-SA_GFDLCM3					
Standard deviation	1.353914	1.403428	1.402229	1.401649	1.404167
Coefficient of variation	0.058053	0.062520	0.062464	0.062437	0.062554
Correlation coefficient		0.985930	0.986041	0.985959	0.986126

4.2.2 Comparison of CMPI5 and CORDEX-SA bias corrected outputs

In order to make choice between CMPI5 and CORDEX-SA datasets, the bias corrected outputs of both the datasets were compared among each other statistically using the above tables. From the tables, it was found that precipitation datasets are showing a good correlation with the observed data when using CORDEX-SA datasets whereas temperature datasets (minimum and maximum temperature) are showing good correlation with observed data when using CMIP5 datasets. In general, both the datasets are almost showing excellent correlation with the observed one with only a small decimal point variation.

4.2.3 Criteria for selecting climate change data input

CMIP5 datasets provides the global climate data whereas CORDEX-SA datasets is specifically for South Asian domain and provides regional data. The lack of regional information makes the GCM output unsuitable for a number of impact studies requiring regional information. RCMs have not only been used for downscaling GCM climate

change simulations, but also for seasonal climate predictions with similar objectives to obtain useful regional climate data. A strong conclusion cannot be drawn for selecting bias corrected GCM and RCM due to the different ways of controlling the atmospheric circulation in the RCM and the GCM simulations. Thus by considering the above aspects as well as the results obtained, CORDEX- SA dataset was selected. CORDEX- SA is providing data for two RCP scenarios, RCP4.5 and RCP8.5 which represents low and high scenario respectively. A medium scenario related study is not possible using CORDEX-SA datasets. Since CMIP5 datasets provides medium scenario datasets, RCP6 data from CMIP5 dataset was also taken for the study purpose. In general, RCP4.5 (low) and RCP8.5 (high) scenarios from CORDEX-SA bias corrected dataset and RCP6 (medium) scenarios from CMIP5 bias corrected dataset from 2021-2070 were selected for further impact related analysis.

4.2.4 Predicted future precipitation and temperature for different scenarios

Monthly variation of the bias corrected data including precipitation and temperature data for different scenario selected (RCP4.5, RCP6 and RCP8.5) from 2021-70 were compared with the observed data from 1989-2017. Precipitation data variation under different scenarios for two time periods, 2021-40 and 2041-70 with the observed data is shown in Fig. 4.28 and the average monthly precipitation values under different scenarios is given in Appendix XII. There is a significant decrease in precipitation during June to December for RCP 4.5 and increase in precipitation from January to May except February for 2021-40. During 2041-70 for RCP 4.5, increase in precipitation was found for all months except June, July, September and October. Significant increase in precipitation was observed for RCP6 for almost all months except February, July and October during 2021-40 whereas from 2041-70, increase in precipitation was observed for all months except February and October. For RCP 8.5, decrease in precipitation was found for all the months except January, March and December from 2021-40 whereas from 2041-70 decrease is precipitation is found for the months of June, July, September, October and November. When comparing between scenarios, precipitation is increasing for RCP6 whereas decreasing for both RCP8.5 and

RCP4.5. Chong-Hai and Ying (2012) projected precipitation over China under RCP Scenarios using a CMIP5 multi-model ensemble and found that precipitation will tend to decrease especially under RCP 8.5. Rajczak and Schar (2017) projected precipitation and its extremes over the European continent using EURO-CORDEX Regional Climate Models (RCMs) under RCP4.5 and RCP 8.5 and found that precipitation decreases under both RCP scenarios but predicted extreme rainfalls. The percent change in monthly rainfall from the observed monthly values is plotted in Fig. 4.29. The percent decrease in precipitation is found to be higher for RCP8.5 followed by RCP4.5 whereas percent increase in precipitation is higher for RCP6. In RCP4.5, emissions are starting to decline by around 2045 to reach approximately half of the 2050 levels by 2100. Emissions continue to rise in RCP8.5 throughout the 21st century (Riahi *et al.*, 2011). Based on the annual average precipitation predicted for the entire period (2021-70), a decrease of about 13 and 16 percent was found for RCP4.5 and RCP8.5 respectively and an increase of 33 percent was observed for RCP6 from the observed annual average precipitation. Unlike temperature, there exist large uncertainties in the precipitation obtained from GCM than RCM. Since RCP6 scenario data was collected from CMIP5 GCM datasets, precipitation data is showing an increase in trend than the observed period of time. Moreover, in RCP6 scenarios, emission peaks around mid century (2080s) and then stabilises by 2100. Since the time period taken for the study purpose is from 2021-2070 where peak emission occurs, may result in the increased precipitation. This change in precipitation pattern may affect the streamflow of the Thuthapuzha watershed in future, thus proper planning and conservation of soil and water should be taken in advance.

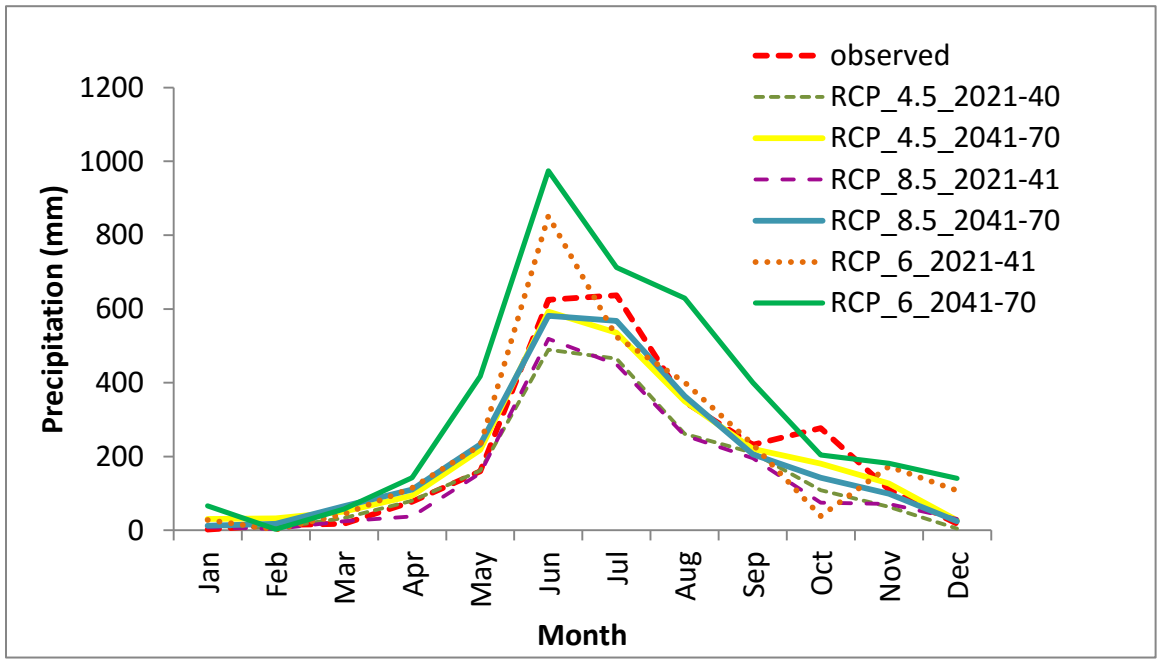

Fig. 4.28 Comparison of observed and bias corrected monthly precipitation under different scenarios

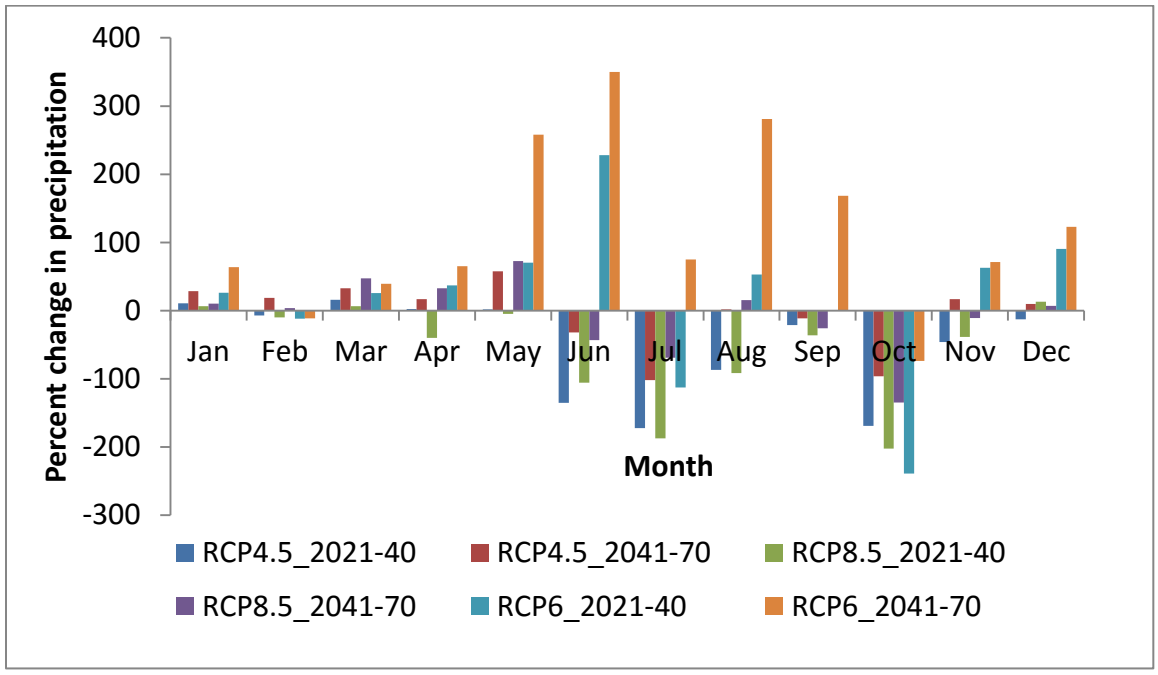

Fig. 4.29 Percent change in monthly rainfall from observed data under different scenarios

Monthly variation of bias corrected maximum and minimum temperature data for different RCP scenario from 2021-70 in comparison with observed maximum and minimum temperature is shown in Fig. 4.30 and Fig. 4.31 respectively and the average monthly values are given in Appendix XIII and XIV respectively. Maximum temperature shows an increase in the trend for all months in the RCP4.5 and RCP8.5 scenarios compared to the observed data, while the RCP6 scenario shows a decrease in the trend for January, February and December. Maximum temperature projected for the entire India showed an increase within the range 2.5°C to 4.4°C by end of the century (Bal *et al.*, 2016). When comparing minimum temperature data, it is found that minimum temperature is almost in the same range as that of the observed minimum temperature for RCP4.5 and RCP8.5 scenarios. A similar increasing trend in minimum temperature was also noted in case of RCP6 scenario. These results were used for studying the climate change impact using SWAT model.

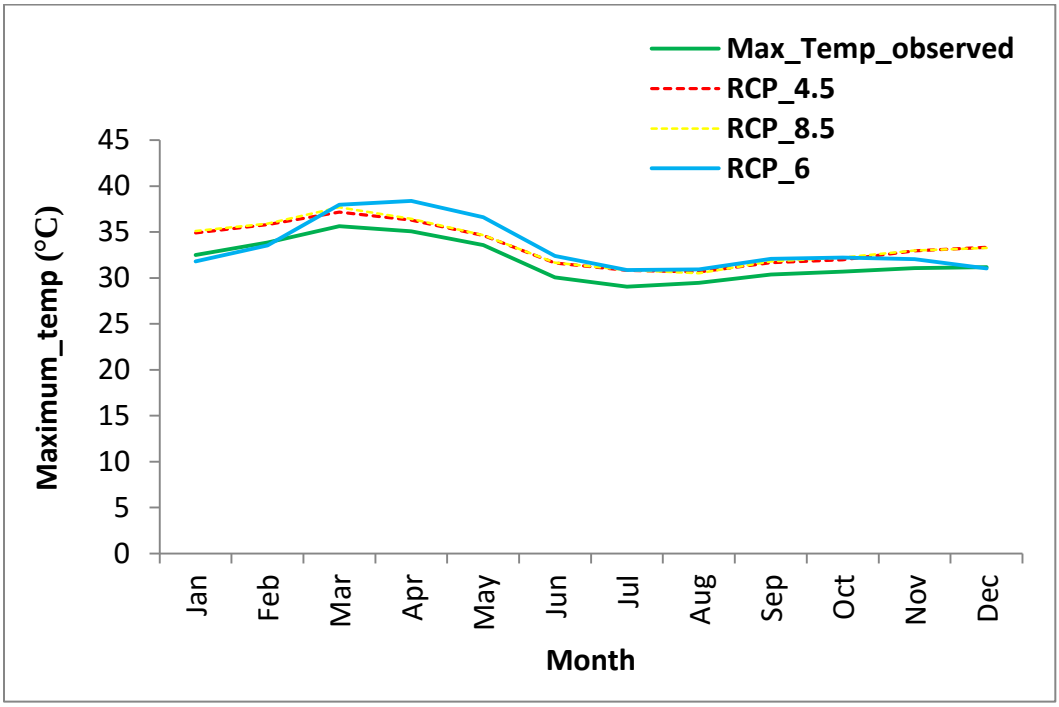

Fig. 4.30 Comparison of observed and bias corrected monthly maximum temperature under different scenarios

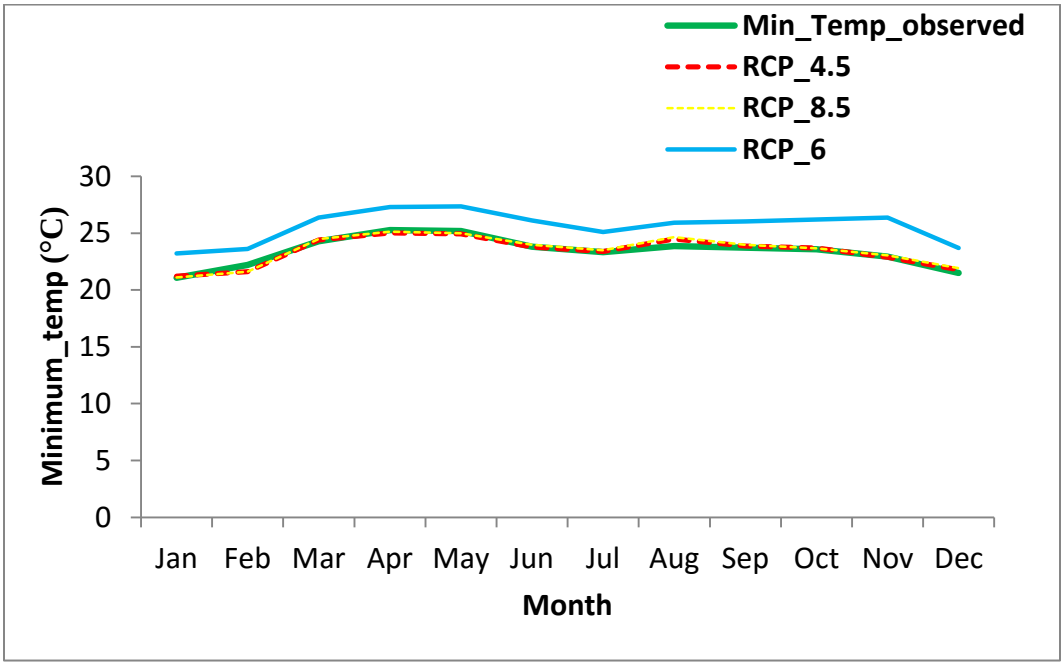

Fig. 4.31 Comparison of observed and bias corrected monthly minimum temperature under different scenarios

4.2.5 Impact of climate change on streamflow under different scenarios

The developed model was used to study the climate change impact on streamflow of the watershed. Climate model GFDL-CM3 data corresponding to three RCP scenarios; RCP4.5, RCP6 and RCP8.5 from 2021-2070 were used for the study. For convenience of the study, the entire projected period of simulation was divided into two time periods; 2021-2040 and 2041-2070. Although it is not a new concept to use climate model outputs in a hydrological model, few studies have focused on the impact of climate change on watersheds in humid tropical areas. The bias corrected precipitation and temperature data were given as weather inputs to the SWAT model. The streamflow generated by the SWAT model was compared for each of the climate change scenarios considered in the study to assess the impact of each RCP scenario. The streamflow simulated by the projected data was compared with the observed flow to analyse the trend of streamflow in future periods.

Annual and monthly streamflow under different scenarios (RCP4.5, RCP6, and RCP8.5) was studied. The total streamflow at Pulamanthole gauging station is based on the combined features of all the upstream subbasins of Thuthapuzha watershed. The annual observed streamflow of Pulamanthole gauging station was compared with the simulated future annual streamflow values. Predicted annual streamflow under different scenarios in comparison with observed streamflow for time period 2021-40 and 2041-70 is shown in Fig. 4.32 and Fig. 4.33 respectively and the annual average values are given in Appendix XV and XVI respectively. From the figure, it is found that the annual river flow under all the scenarios selected for the projected period is higher than the present annual river flow. When comparing between scenarios, increase in annual streamflow is found to be higher in RCP6 scenario (37-60%) followed by RCP4.5 (13-16%) and RCP8.5 (9-16%) during the entire period of simulation. Sathya and Thampi (2020) studied the impact of projected climate change on streamflow of the Chaliyar river basin of Kerala and reported that the annual streamflow is likely to increase by about 27.27% under RCP 4.5 and 42.44% under RCP 8.5. The increase in streamflow may be due to the changes in the projected precipitation pattern. Githui *et al.,* 2009 reported an increase in streamflow due to increased rainfall in western Kenya. Anthropogenic activities have already changed the river flow patterns in several river basins. Moreover, there are chances of increased population, land use changes, increased demand for irrigation can also add to this streamflow change. Decrease in streamflow is also observed in some years between 2021-40 and 2041-70 due to increase in temperature during the predicted period. Overall annual average streamflow for the entire simulation is showing an increase in streamflow under all RCP scenarios. Predominant increase in streamflow was found in RCP6 scenario may be due to changes in the precipitation patterns observed from the projected CMIP5 datasets. The simulated streamflow using projected dataset from CORDEX-SA for RCP4.5 and RCP8.5 shows that annual average streamflow under RCP8.5 is less than that of RCP4.5. In both the periods from 2021-40 and 2041-70, it is observed that the increase in streamflow is more significant at the end periods of the simulation.

Predicted monthly streamflow under different scenarios in comparison with observed streamflow for the time period 2021-40 and 2041-70 is shown in Fig. 4.34 and Fig. 4.35 respectively. For almost all the months in both the periods and all the scenarios, the streamflow was observed to be higher than the one observed. In case of rainfall also, an increase in rainfall is found for all the months this might have caused increased streamflow for the predicted periods. Predicted monthly streamflow under different scenario in comparison with observed from 2021-70 is shown in Fig. 4.36 and the average monthly values are given in Appendix XVII. During 2021-70, the streamflow in RCP4.5 showed almost similar trend in variation as that of observed with a slight increase in streamflow for all the months except July and October during 2041-70. In RCP8.5 from 2021-70, the streamflow is found to be increasing from January to July and decreasing afterwards. But the peak flow is found to be higher than that of RCP4.5 from June to August. Thus, in RCP8.5 it is found that during peak flows the climate will become wetter than that of current scenario. Moreover, during 2021-70 in RCP6 scenario, increase in streamflow is observed in all months except during December in the period from 2021-40. The observed and simulated data is showing similar trend in variation except in case of RCP6 scenario during the months of June and July, where there is peak flow in the catchment. Scientists have reported this uncertainty in predicting the peak flows when using SWAT model. The streamflow increase is found to be significant during the end period of simulation for all the scenarios taken for the study purpose. Thus, necessary steps should be taken to mitigate the extreme events due to streamflow increase during future periods.

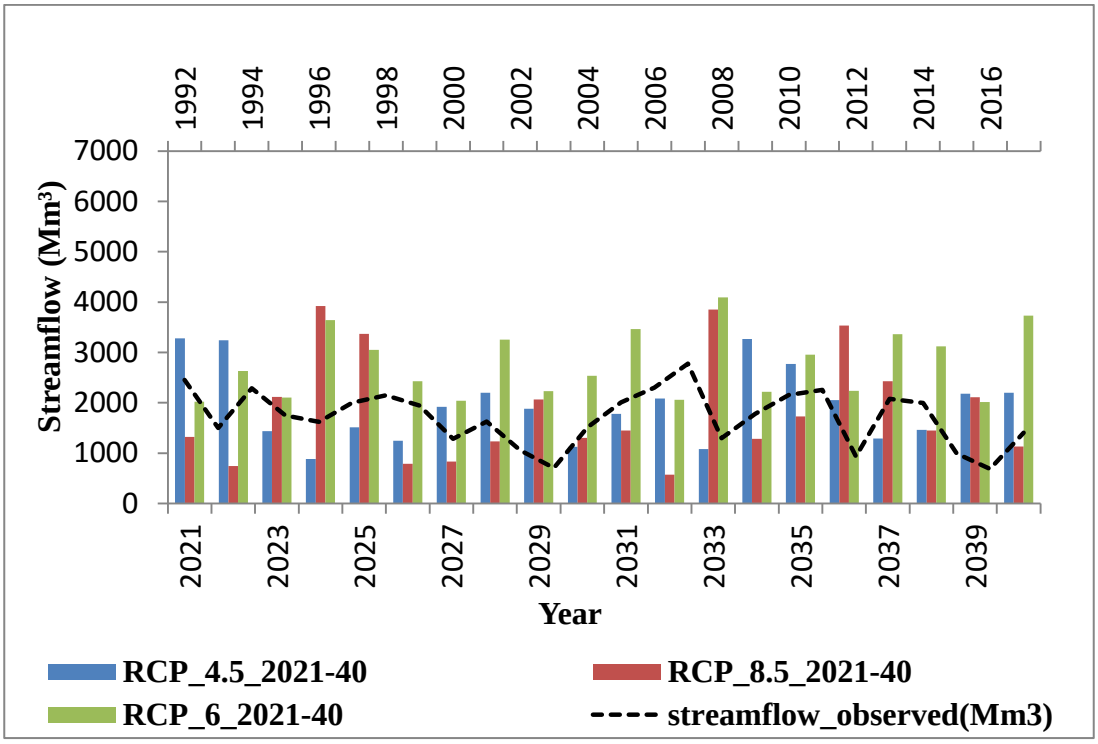

Fig. 4.32 Predicted annual streamflow under different scenario from 2021-40

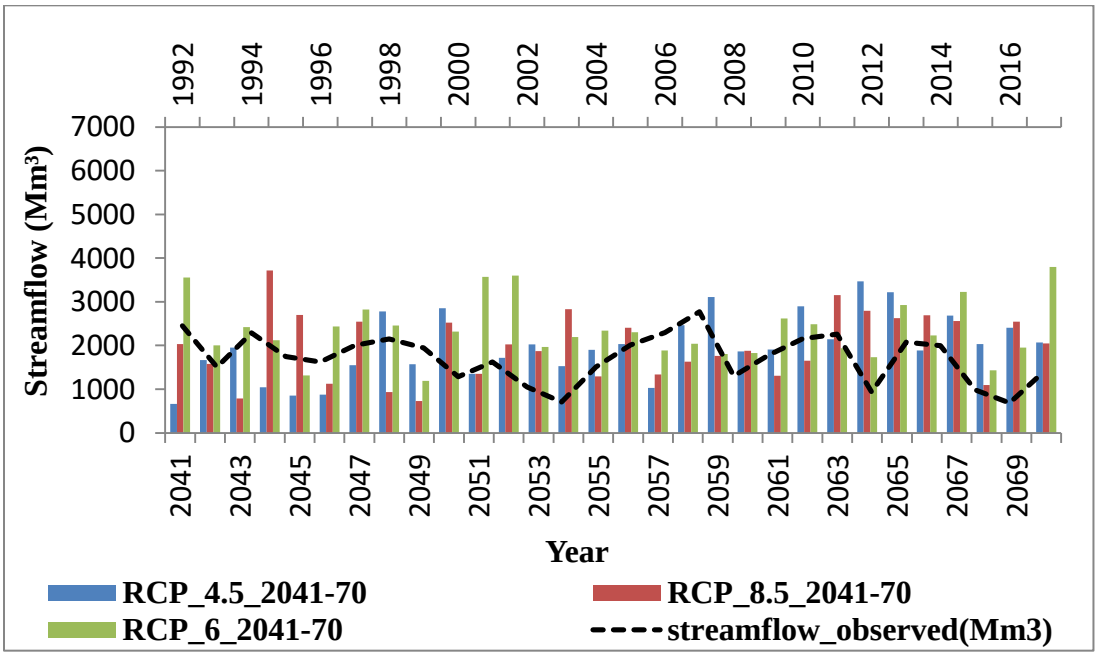

Fig. 4.33 Predicted annual streamflow under different scenario from 2041-70

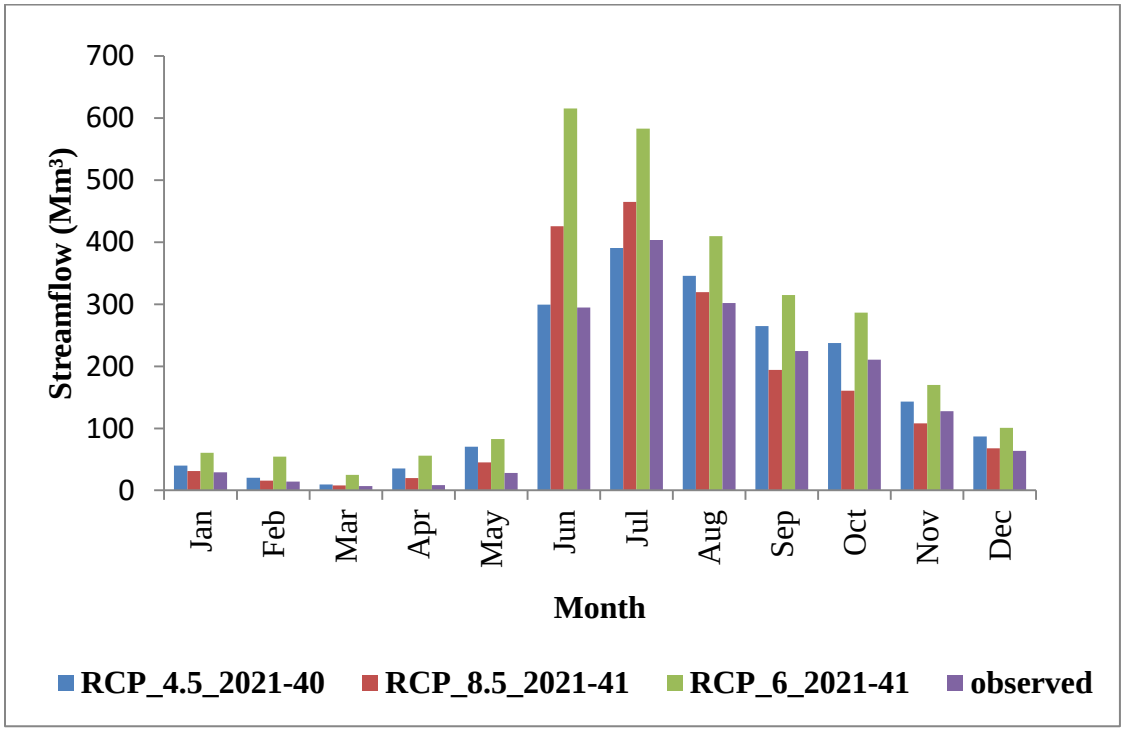

Fig. 4.34 Predicted monthly streamflow under different scenario from 2021-40

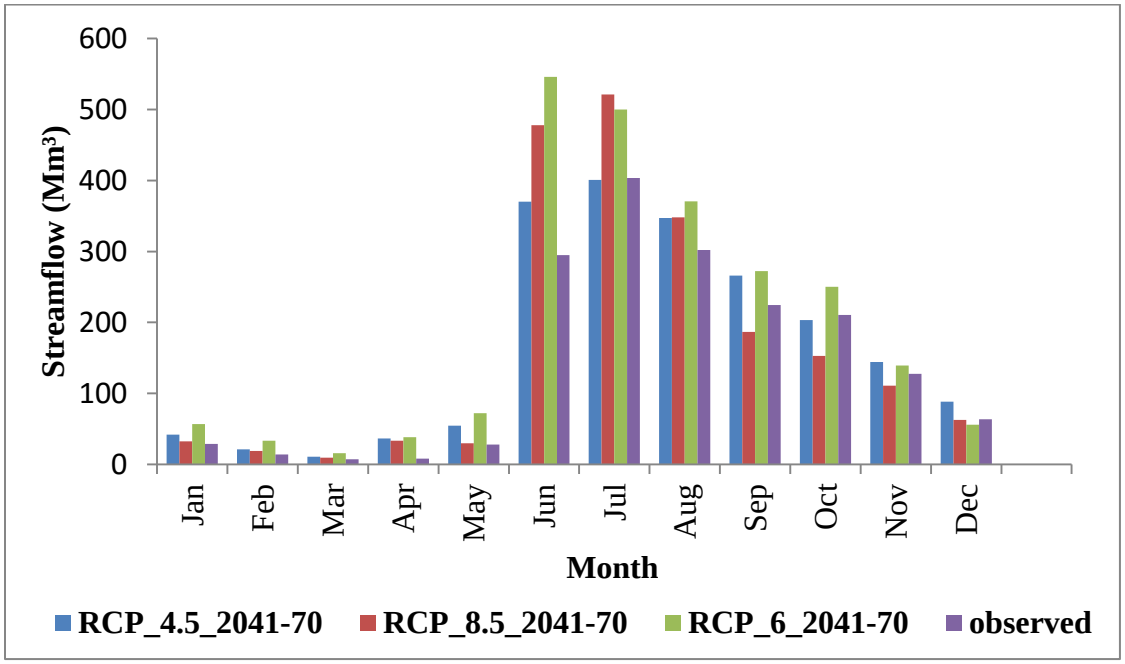

Fig. 4.35 Predicted monthly streamflow under different scenario from 2041-70

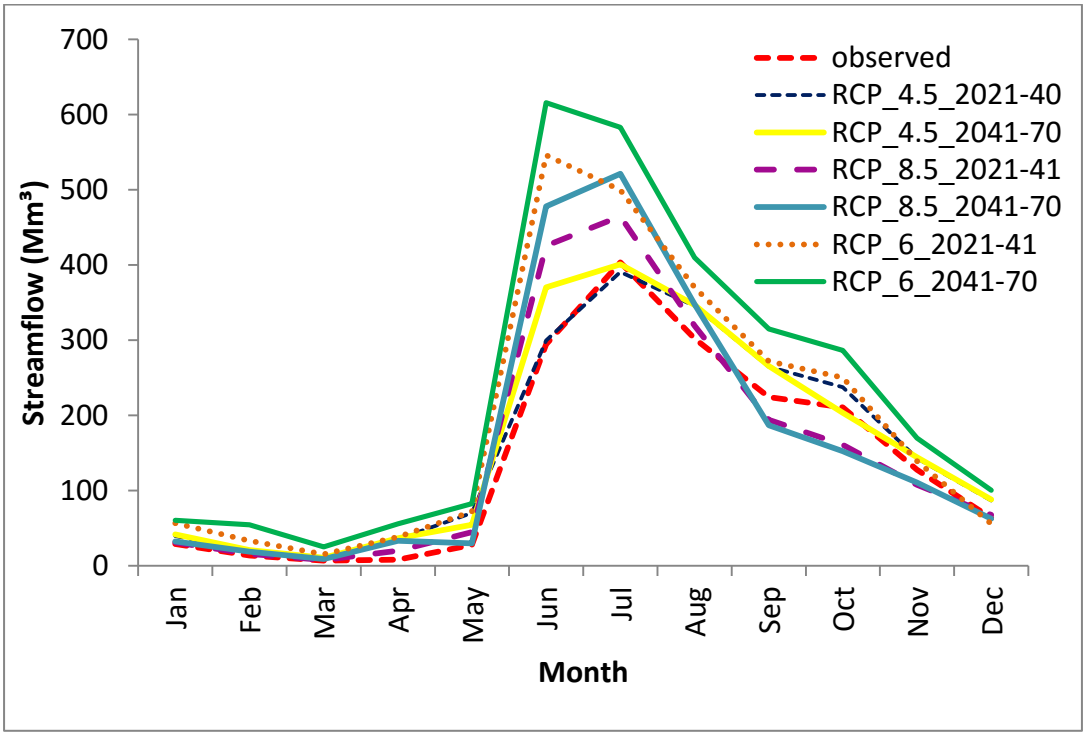

Fig. 4.36 Predicted monthly streamflow under different scenario in comparison with observed from 2021-70

4.2.6 Water balance component under different scenarios

Water balance components of the basin for future predicted climate under different RCP scenarios from 2021-70 in comparison with the observed period of 1992-2017 is shown in Table 4.9. The water balance component is also affected by change in precipitation pattern and decrease in temperature predicted for future on account of climate change. From the table, it is found that the precipitation increase is significant at the end period of simulations when compared to observed period. From the trend analysis of rainfall, a decreasing trend was observed from 1992-2017 whereas the predicted climate shows a reverse trend during the end period which might be due to the effect of rainfall patterns predicted from the model. But this research is based on a single model and a more detailed research based on multiple models and the use of multiple

ensembles is necessary since researchers have already reported some uncertainty regarding impact studies using single model for projecting climate data's.

Water balance components including surface runoff, ground water flow, evapotranspiration and lateral flow were represented as the percentage of rainfall for the entire simulation period (Fig. 4.37) and for the future RCP scenarios *viz.*, RCP4.5, RCP6 and RCP8.5 is shown in Fig. 4.38, Fig. 4.39 and Fig. 4.40 respectively. The percentage of each component was plotted as pie diagram. From the pie diagram, it is clear that the outflow from the watershed is mainly in the form of surface runoff, followed by ground water flow, evapotranspiration and lateral flow under all RCP scenarios similar to the observed period of time. The percent contribution of rainfall to all these components is changing under different scenarios. Analysis of the results showed that in case of RCP4.5, the contribution of surface runoff is about 43-51% followed by groundwater flow which is about 24-28% where as in case of RCP8.5 scenario, the contribution of surface runoff is about 39-46% followed by groundwater component which is about 26-29%. In case of RCP6, the major fraction of rainfall is contributed by surface runoff (43-53%) followed by groundwater component (27-33%). In all the scenarios, surface runoff and groundwater component range is higher than that of observed period with surface runoff about 40% and groundwater flow in the range of 28-29%. Significant contribution is observed in RCP6 followed by RCP4.5 and RCP8.5. ET ranges from 24-25% of the annual rainfall for the observed period and a similar variation in the range of 20-24% in RCP4.5 and 20-25% in RCP8.5 is observed for future climate change. A decrease of 14-19% of ET is observed in the analysis of RCP6 might be due to higher fractional contribution of rainfall as surface runoff. Lateral flow component is lowest comprising only 7% of the total precipitation and there is no significant variation between the scenarios for the lateral component. From this analysis, it is clear that the streamflow changes in the basin is due to the high contribution of surface runoff in all the scenarios and this analysis can be taken as a justification regarding the streamflow changes predicted during climate change conditions.

Table 4.9 Water balance components under different climate scenarios

Period	Precipitation (mm)	ET (mm)	SURQ (mm)	LAT_Q (mm)	GW_Q (mm)
1992-2004	2733.97	679.90	1080.22	196.01	736.54
2005-2017	2456.81	581.46	961.78	180.06	695.61
RCP_4.5_2021-30	2132.01	501.94	945.39	121.29	523.83
RCP_4.5_2031-40	2268.34	495.09	953.92	145.21	621.97
RCP_4.5_2041-50	2250.06	443.74	1113.45	119.92	529.44
RCP_4.5_2051-60	2450.32	552.62	1038.27	152.18	659.60
RCP_4.5_2061-70	2619.75	515.18	1242.19	152.84	656.27
RCP_6_2021-30	2830.10	449.77	1189.38	215.12	908.89
RCP_6_2031-40	3371.50	453.24	1756.22	212.13	894.31
RCP_6_2041-50	2458.25	447.89	963.04	188.63	793.25
RCP_6_2051-60	2695.96	455.63	1220.92	185.08	790.18
RCP_6_2061-70	2703.93	464.71	1140.67	199.65	836.01
RCP_8.5_2021-30	2140.83	490.75	929.25	131.06	553.37
RCP_8.5_2031-40	2250.73	476.56	1023.61	135.34	573.24
RCP_8.5_2041-50	2026.06	491.40	773.88	131.75	577.12
RCP_8.5_2051-60	2269.50	503.66	924.80	146.43	647.44
RCP_8.5_2061-70	2742.89	530.35	1237.16	170.25	747.86

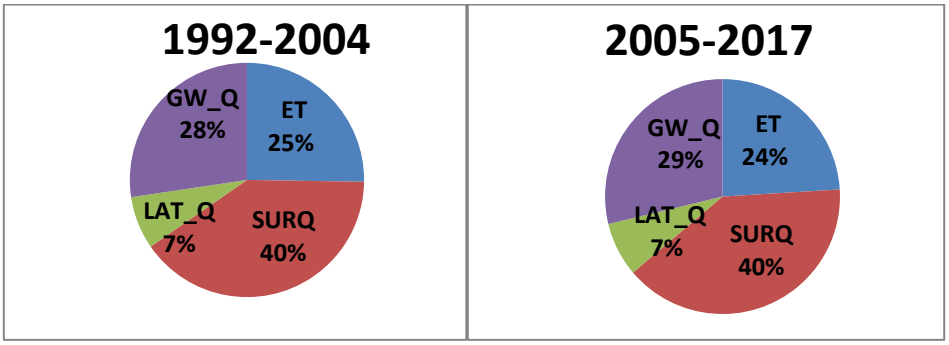

Fig. 4.37 Predicted water balance component for the entire simulation period

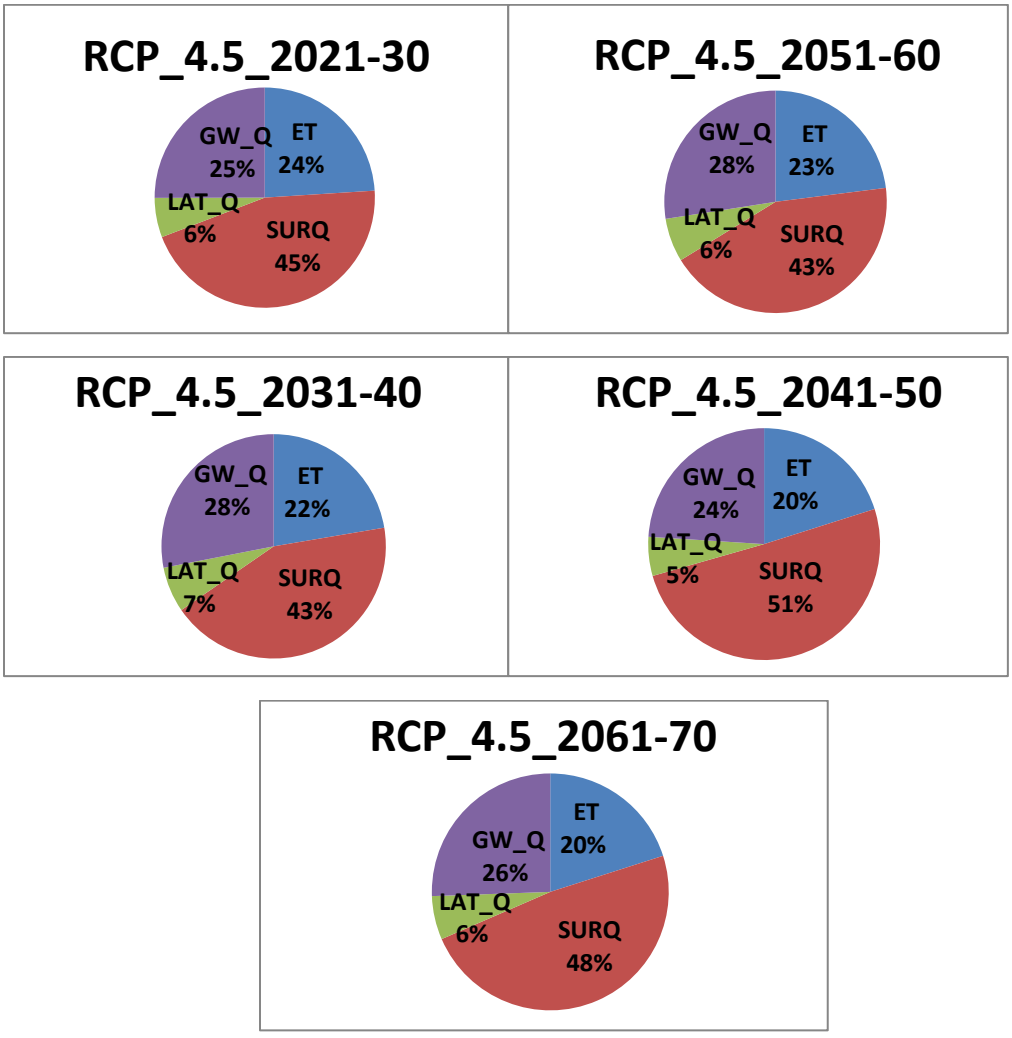

Fig. 4.38 Predicted water balance component in RCP4.5 scenario from 2020-2070

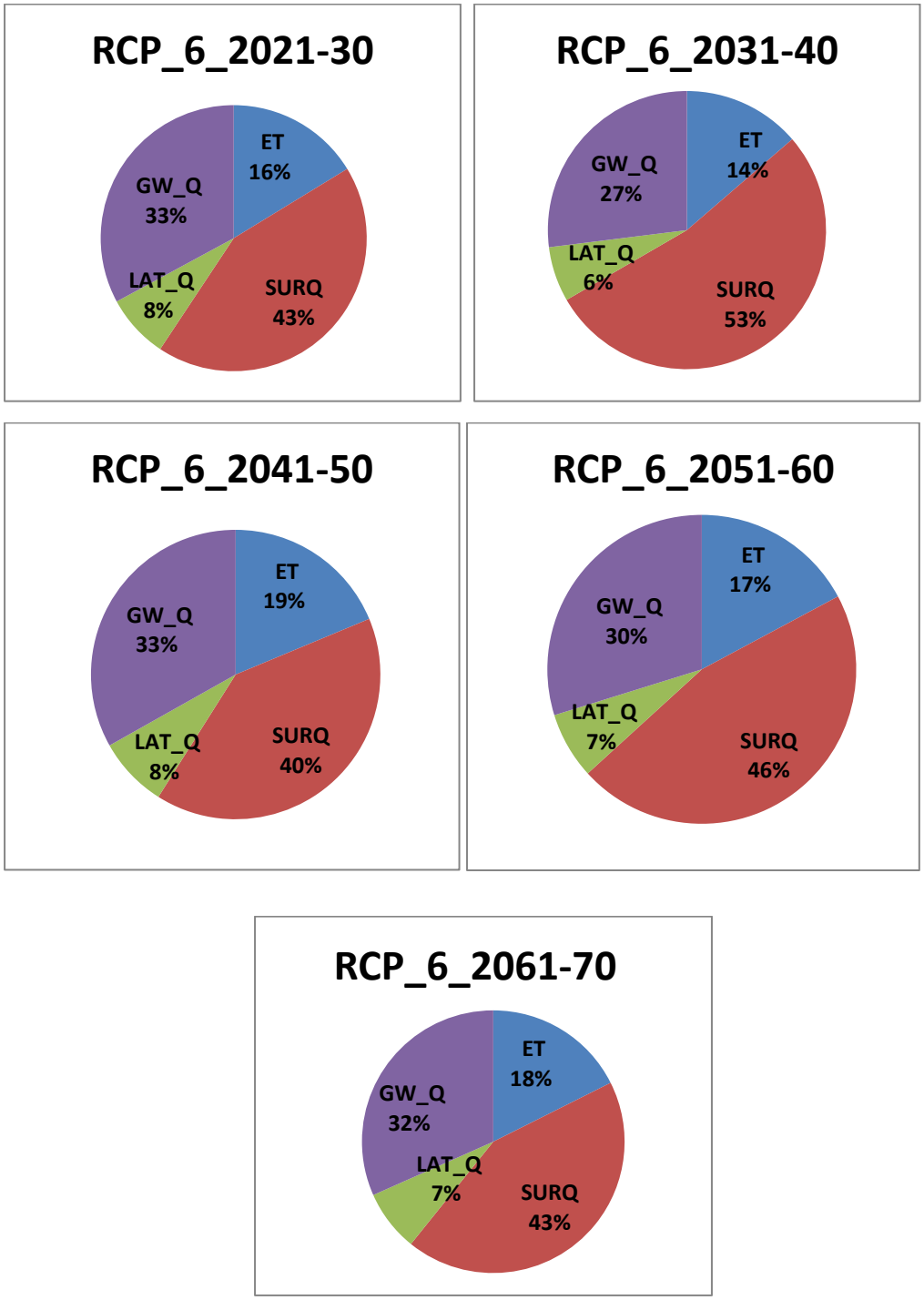

Fig. 4.39 Predicted water balance component in RCP6 scenario from 2020-2070

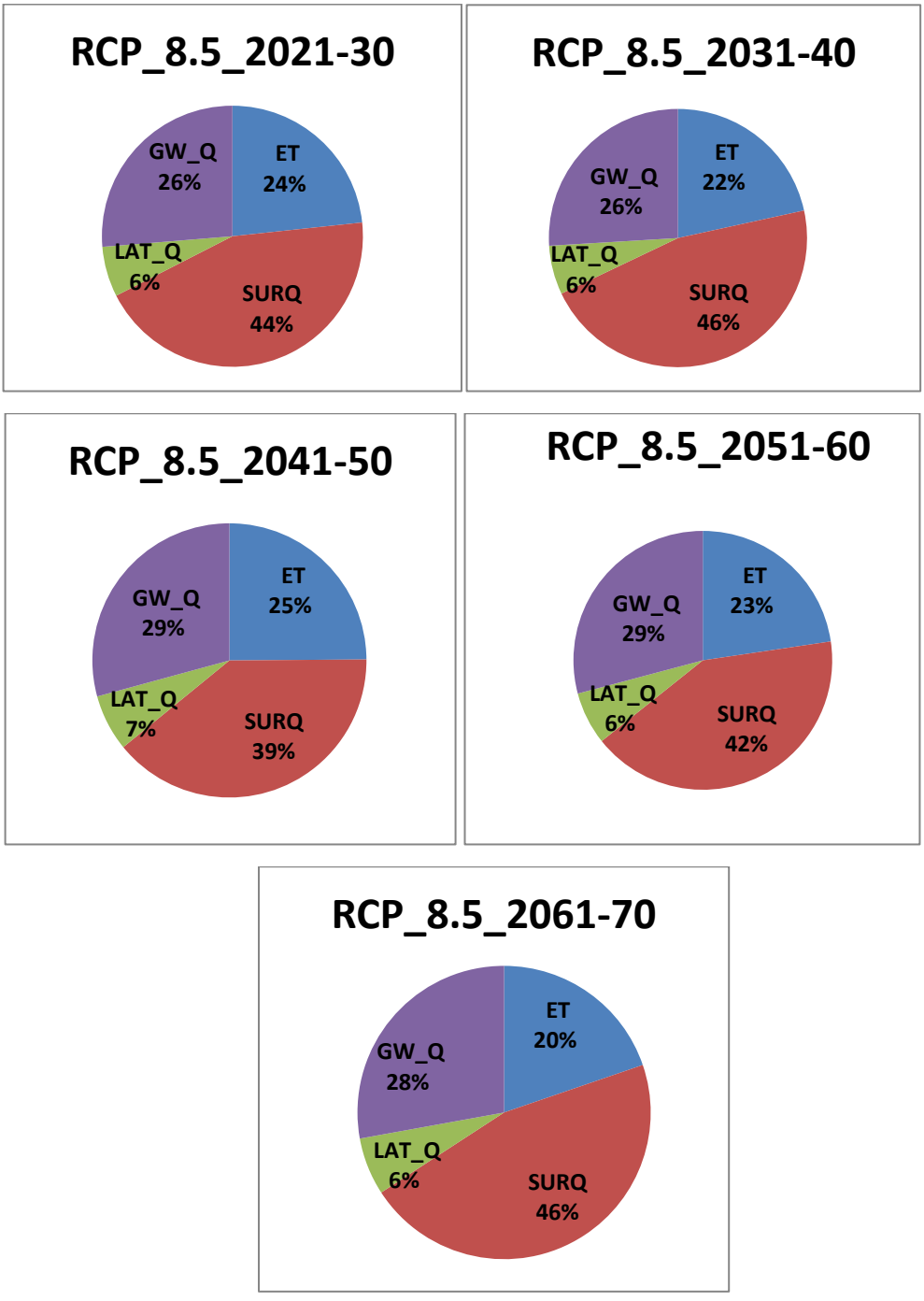

Fig. 4.40 Predicted water balance component in RCP8.5 scenario from 2020-2070

4.2.7 Drought intensity calculation for the observed period

Precipitation and temperature based drought indices were taken for analysing drought for observed as well as for future climate scenarios. SPI index based on precipitation and RDI index based on precipitation and potential evapotranspiration is taken for the drought intensity analysis. The DrinC software was used to calculate both SPI and RDI indices based on gamma distribution method with a 12 month period.

Drought in the Thuthapuzha watershed for the observed period from 1989-2017 was analysed using both SPI and RDI index. SPI and RDI drought index calculation for the observed period is shown in Fig. 4.41 and Fig. 4.42 respectively. A functional and quantitative definition of drought can be created using SPI as an indicator. The calculated annual SPI index showed that droughts were quite frequent during the 1999-2000, 2001-2003, 2007-2008, 2011-2012, and 2016-2017. However, a severe dry period was observed from 2015-2016. The duration of drought for the entire historical period from 1989-2017 and the corresponding number of dry and wet years and are shown in Table 4.10. Because the SPI is normalised, it is possible to represent drier and wetter climates in the same way. The number of dry years (Moderately dry, severely dry and extremely dry) observed is about seven years from 1989-2017. Moderately dry events have occurred 6 times from 1989-2017 whereas severely dry events have occurred once during 2015-16. An important point to note was that during the period 1989-2017, no extremely dry events were observed when using SPI as drought indicator.

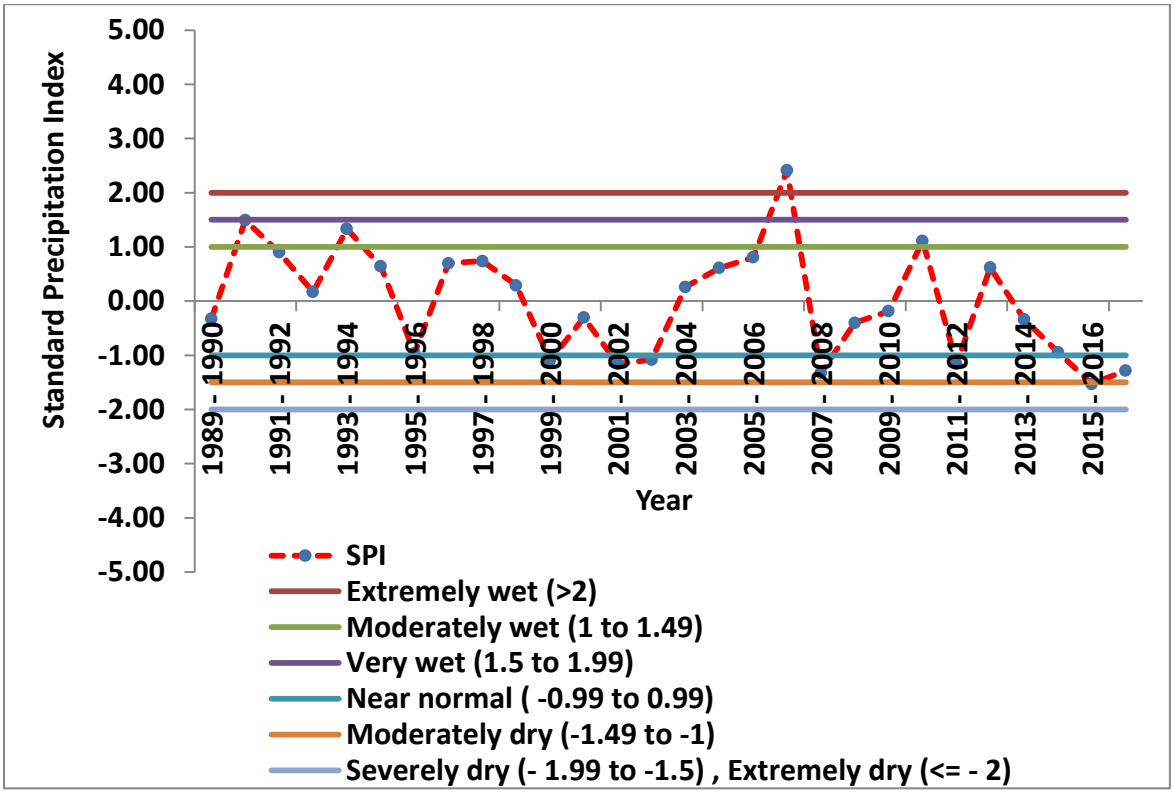

Fig. 4.41 SPI for the observed period from 1989 to 2017

Table 4.10 SPI analysis of observed period

SPI	Number of drought	Duration
Extremely wet (>2)	1	2006-2007
Very wet (1.5 to 1.99)	0	-
Moderately wet (1 to 1.49)	2	1993-1994, 2010-2011
Near normal (-0.99 to 0.99)	17	1989-1993, 1994-1999, 2000-2001, 2003-2006, 2008-2010, 2012-2015
Moderately dry (-1.49 to -1)	6	1999-2000, 2001-2003, 2007-2008, 2011 2012, 2016-2017
Severely dry (= 1.99 to -1.5)	1	2015-2016
Extreamly dry (<= - 2)	0	-

The standardised RDI (RDIst) followed the same method used to calculate the SPI. Apart from rainfall data, the RDIst calculation requires PET and therefore gives a better interpretation than the SPI. Twelve month RDIst calculated for the entire historical period between 1989-2017 showed that droughts were quite frequent during 1995-1996, 1999-2000, 2001-2002, 2007-2008, 2011-2012, and 2015-2017. All the drought periods observed using RDI were under moderate dry period. Similar to SPI calculation, no extreme drought years were observed during 1989-2017. The duration of the drought for the entire historical period and the corresponding number of dry years are shown in Table 4.11. The total number of dry years (Moderate, severe and extreme) observed are seven years similar to SPI from 1989-2017 but having only moderate dry periods and no severe and extreme dry periods. When comparing both the indices, it is found that both indices are showing similar trend with little variation in the drought period but the overall number of drought occurrence is same.

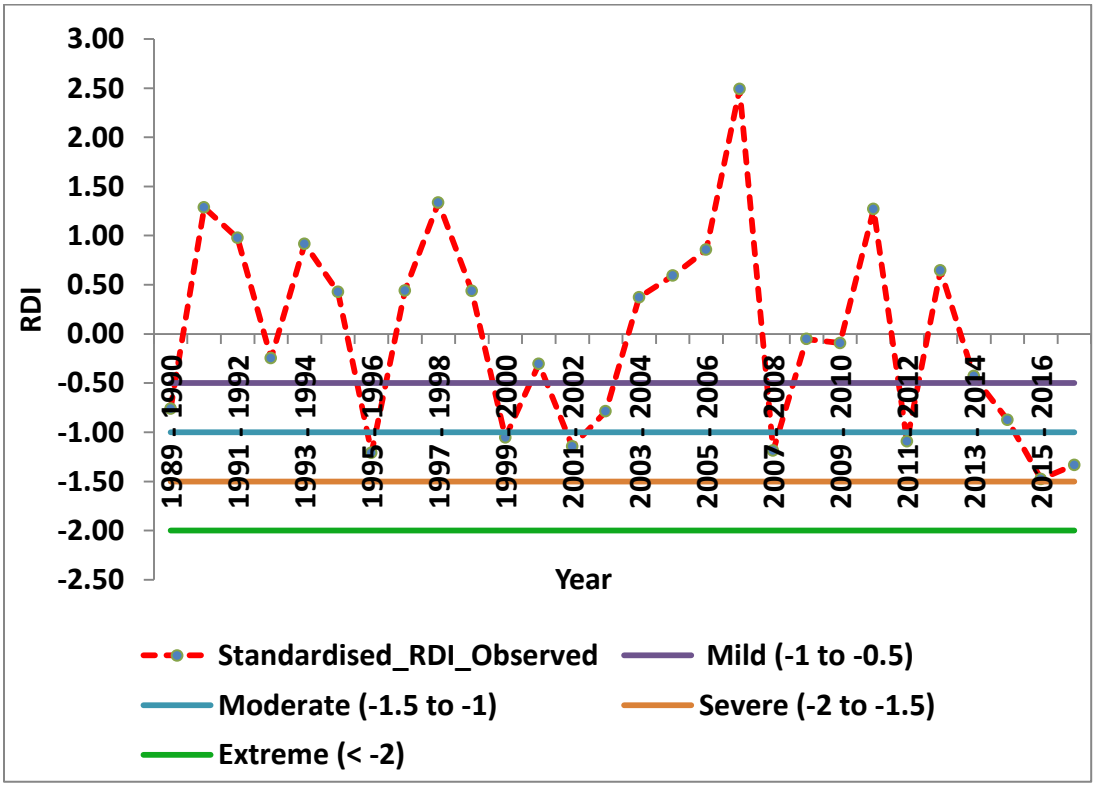

Fig. 4.42 RDI for the observed period from 1989 to 2017

Table 4.11 RDIst analysis of observed period

RDIst	Number of drought	Duration
Mild (-1 to -0.5)	3	1989-1990, 2002-2003, 2014-2015
Moderate (-1.5 to -1)	7	1995-1996, 1999-2000, 2001-2002, 2007-2008, 2011-2012, 2015-2017
Severe (-2 to -1.5)	0	-
Extreme (< -2)	0	-

4.2.8 Comparison and regression analysis between SPI and RDIst under different scenarios

In order to determine the drought occurrence for the projected climate scenarios, the projected precipitation and temperature data's were given as input to the DrinC software and the SPI index as well as RDIst was calculated. But from the analysis of drought intensity for the observed period of time, it is found that both the indices are showing similar trend. To select the index for further analysis of drought intensity for the future period, a comparative study between SPI and RDIst under different RCP scenarios were done from 2021-2070. Predicted temperature and precipitation for projected period was already studied and found that temperature is almost in the same range as that of observed period whereas precipitation is increasing under all the RCP emission scenarios. The severity of the drought will be affected by changes in precipitation and temperature caused by climate change. Thus, both drought indices were compared to select the index for analysing climate change impact on drought intensity. Comparison between SPI and RDIst under different RCP scenarios, RCP4.5, RCP6 and RCP8.5 is shown in Fig. 4.43, Fig. 4.44 and Fig. 4.45 respectively. From the graphical representation, it is clear that both SPI and RDIst is showing similar trend under all the RCP scenarios considered. The number of drought events was also analysed between SPI and RDIst from 2021-70 which is shown in Table.4.12. When using both the index, SPI and RDIst, it is found that drought events will occur 8 times during RCP4.5 and 6 times during RCP6 scenario. In case of RCP8.5, it is found that drought events will occur 10 times when using SPI and

13 times when using RDIst. Thus, it is concluded that SPI and RDI are showing similar trend in both RCP4.5 and RCP6 scenario and a little variation in RCP8.5 scenario with almost similar duration in all the cases.

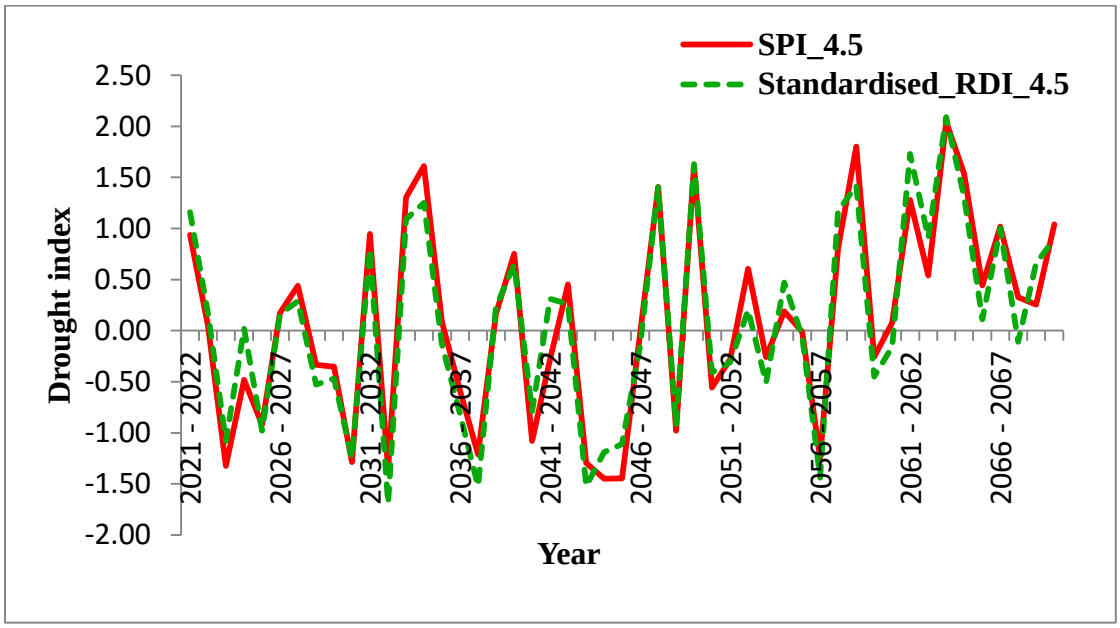

Fig. 4.43 Comparison between SPI and RDI for RCP4.5 scenario from 2021-2070

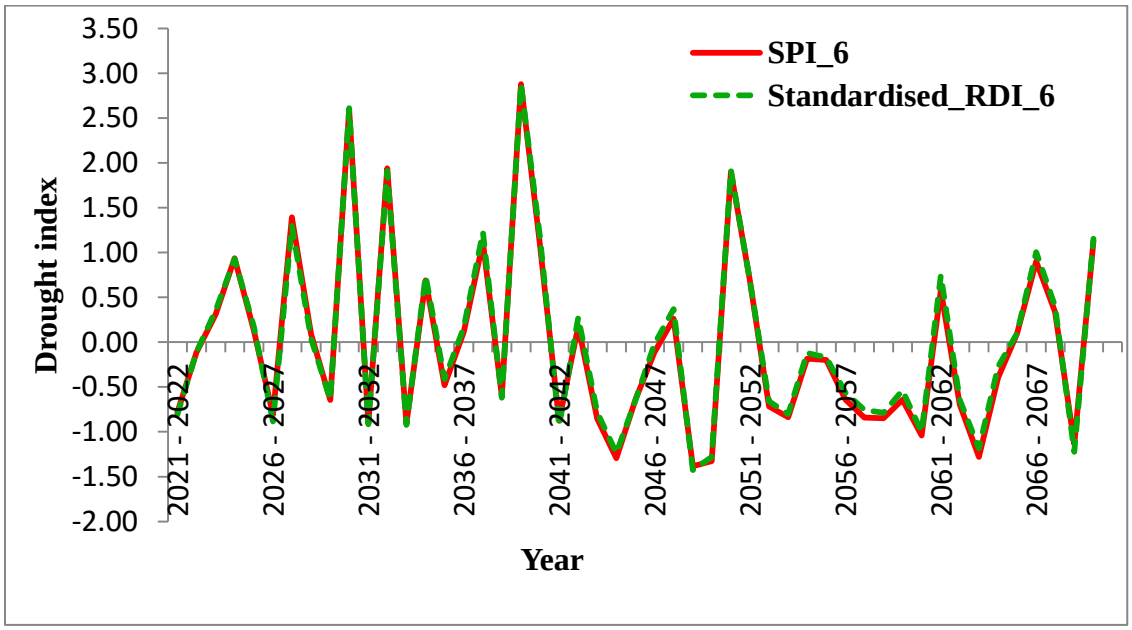

Fig. 4.44 Comparison between SPI and RDI for RCP6 scenario from 2021-2070

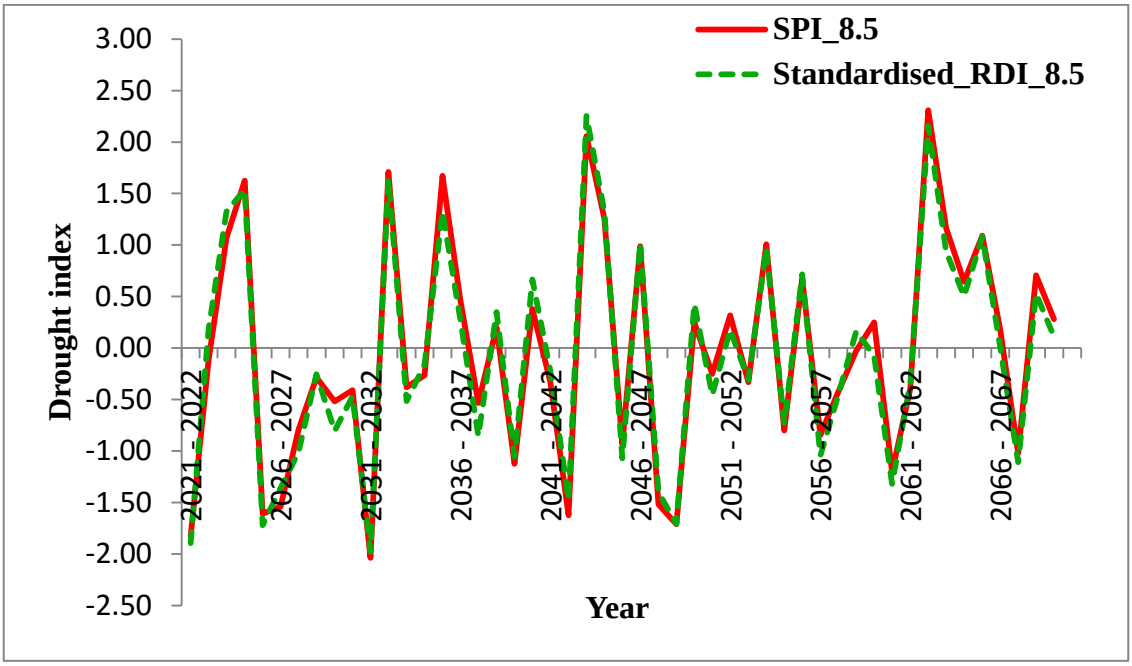

Fig. 4.45 Comparison between SPI and RDI for RCP8.5 scenario from 2021-2070

Table 4.12 Number of drought events using SPI index and RDI index

Drought index	4.5	6	8.5
SPI_2021-70	**8** (2023-24, 30-31, 32-33, 37-38, 43-46, 56-57)	**6** (2044-45, 48-50, 60-61, 63-64, 68-69)	**10** (2021-22, 25-27, 31-32, 39-40, 42-43, 47-49, 60-61, 67-68)
RDI_2021-70	**8** (2023-24, 30-31, 32-33, 37-38, 43-44, 44-46, 56-57)	**6** (2044-45, 48-50, 60-61, 63-64, 68-69)	**13** (2021-22, 25-26, 26-28, 31-32, 39-40, 42-43, 45-46, 47-49, 56-57, 60-61, 67-68

A regression analysis was also performed between SPI and RDI under different scenarios which are shown from Fig. 4.46 to Fig. 4.48. For the regression analysis, twelve month SPI values were compared with the annual RDI values. The results

showed that SPI and RDI were well correlated in all the RCP scenarios. The R^2 value for RCP4.5, RCP6 and RCP8.5 were found to be 0.931, 0.996 and 0.975 respectively. From the R^2 value, it is concluded that both SPI and RDI index were well correlated and the drought intensity calculation using SPI and RDI were almost the same under all the RCP scenarios. Significant correlation between SPI and RDI was also reported by Surendran *et al.* (2017) using DrinC software in Madurai district of Tamil Nadu. In this study, RDI calculation was done using Hargreaves method to find PET due to limited data availability. But SPI was calculated using the precipitation data. SPI is the most widely used indicator which is a suitable index for agricultural as well as hydrological purposes. Since this research mainly focus on the hydrological behaviour of the watershed, SPI indicator was selected for further analysis in the impact of climate change on drought intensity.

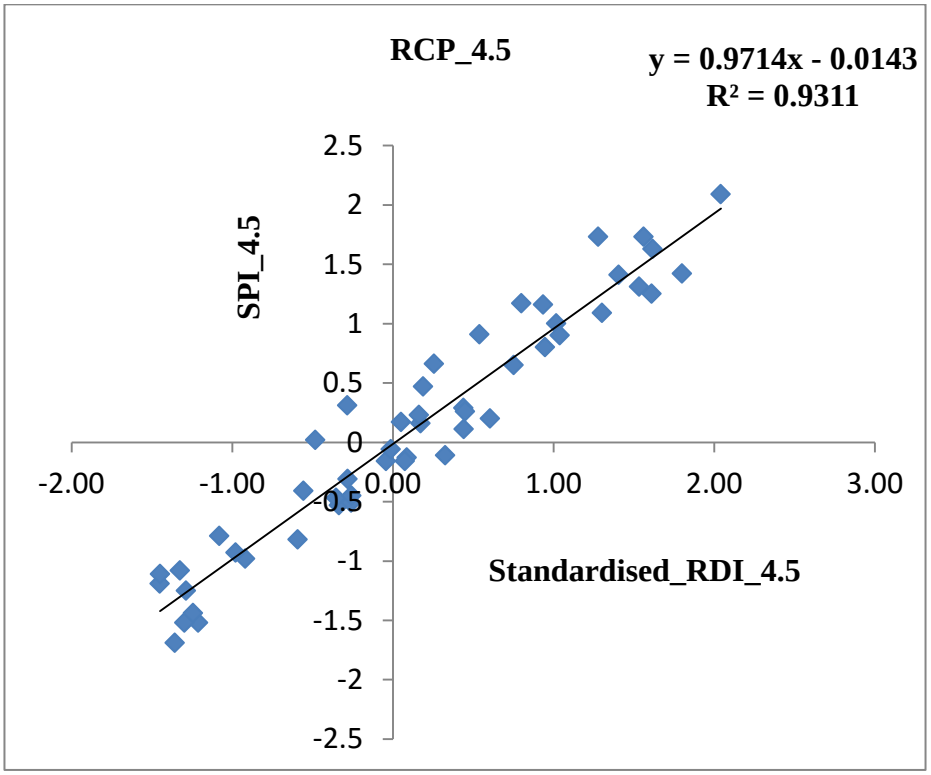

Fig. 4.46 Regression analysis between SPI and RDI for RCP4.5 scenario

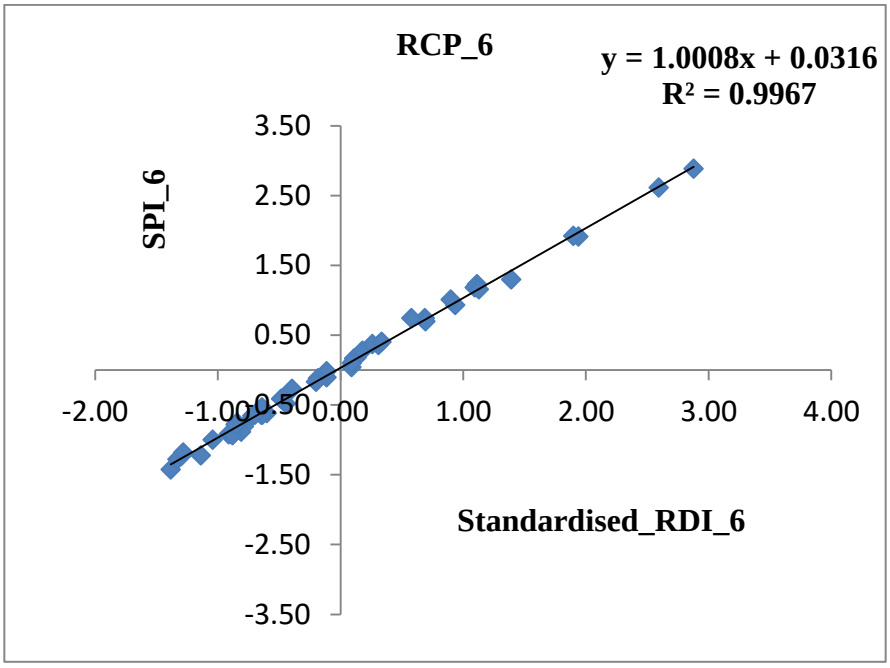

Fig. 4.47 Regression analysis between SPI and RDI for RCP6 scenario

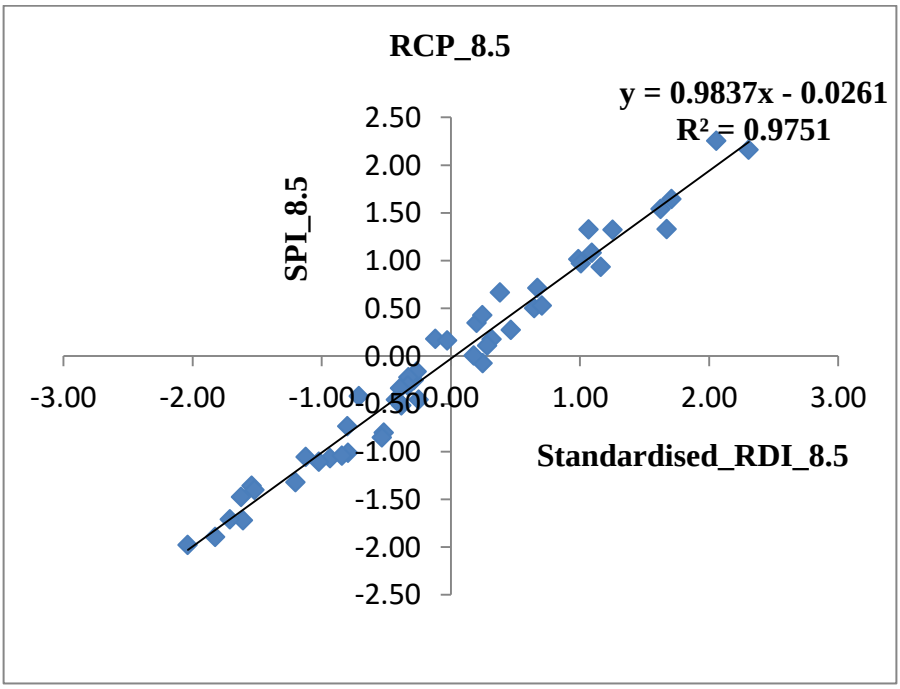

Fig. 4.48 Regression analysis between SPI and RDI for RCP8.5 scenario

4.2.9 Impact of climate change on drought intensity

Future drought condition under different RCP scenarios was assessed by SPI from 2021-2070. Temperature and precipitation are the important factors expected to change as a result of global warming, and therefore an assessment of the possible impact of these changing climate conditions on drought is needed. The bias corrected GFDLCM3 model data were used in this study to calculate the drought intensity under RCP4.5, RCP6 and RCP8.5 from 2021 to 2070. For the convenience of the study purpose, the entire period of simulation was divided into two, 2021-40 and 2041-70. The graphical representation of SPI under different scenarios from 2021-40 and 2041-70 is shown in Fig. 4.49 and Fig. 4.50 respectively. From the graph, it is found that the wet years are more than drought years for all the RCP scenarios for both the periods. When comparing between scenarios, RCP 8.5 shows more drought period followed by RCP4.5.

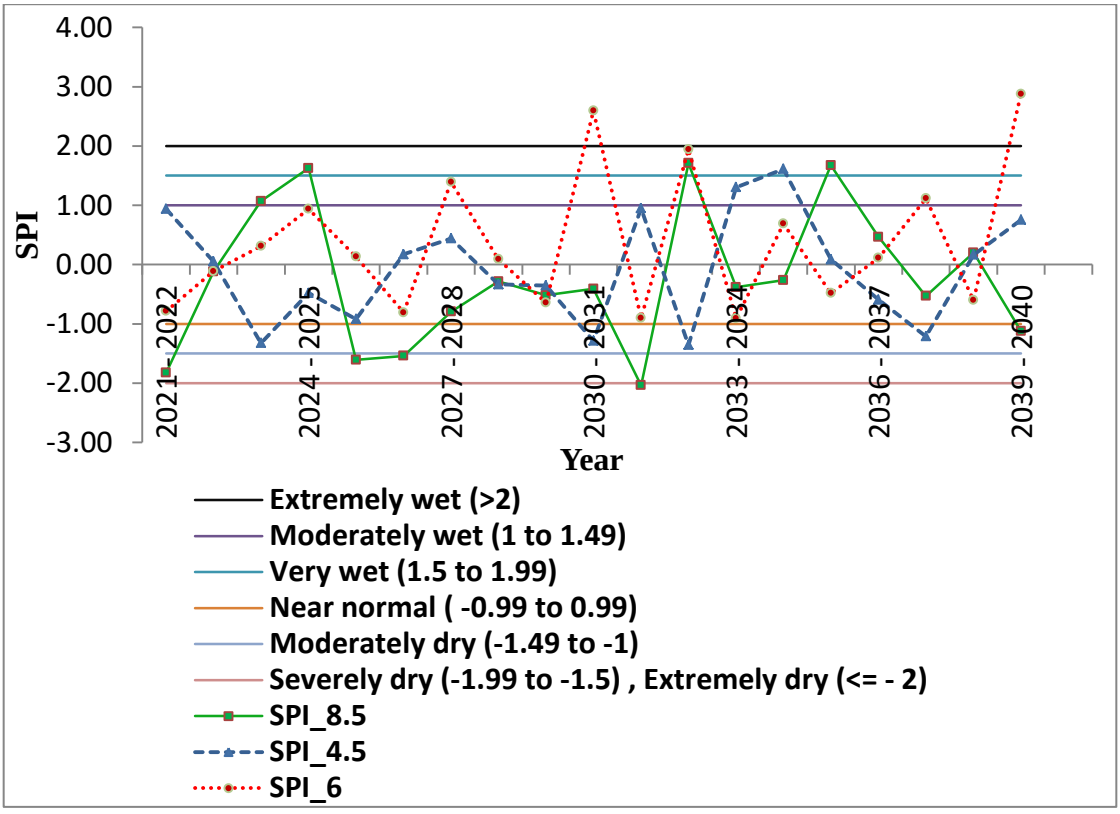

Fig. 4.49 SPI under different scenarios for the projected period from 2021-2040

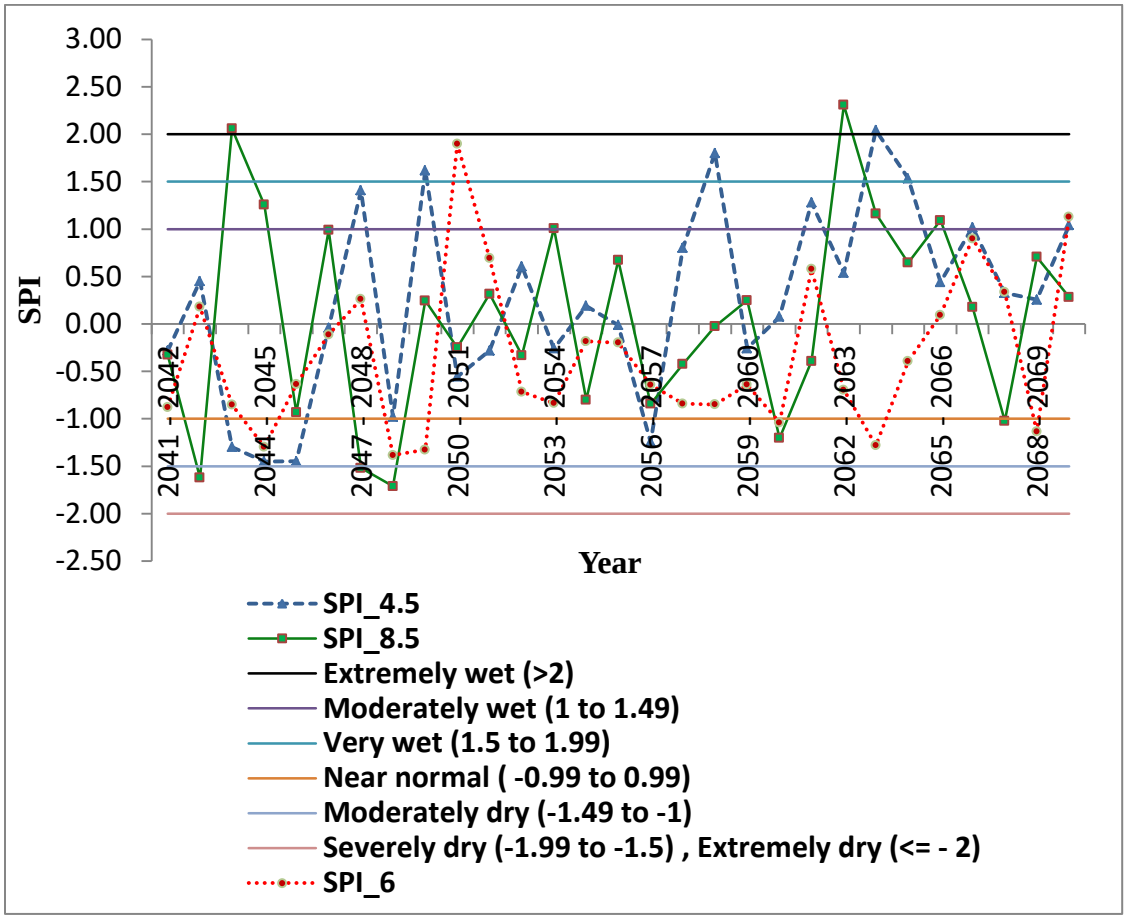

Fig. 4.50 SPI under different scenarios for the projected period from 2041-2070

To analyse the drought intensity and duration, number of drought occurrence under both the periods was studied separately which is shown in Table.4.13 and Table.4.14. In all the scenarios from 2021-70, moderate droughts have a longer duration than the other drought categories, while extreme droughts have a shorter duration. On the other hand, duration of moderate drought is less in RCP6 followed by RCP8.5 and RCP4.5. Lesser duration for RCP6 scenario might be due to the increase in precipitation in the projected data. Normal condition occurs with a longer duration with higher number for RCP6 followed by RCP4.5 and RCP8.5. In this case also, the highest value for RCP6 scenario is due to the precipitation increase in the projected climate data.

From 2021-40, number of drought events under different scenarios were analysed and found that in case of RCP8.5 scenario, extreme drought condition will occur only once during the period 2031-32 and severe drought condition will occur three times for the periods 2021-22, 2025-26 and 2026-27. No drought events were found under extreme and severe drought condition for both RCP4.5 and RCP6 scenarios. It is found that, moderate drought condition will occur 4 times from 2023-28 for RCP4.5 scenario and once from 2039-40 for RCP8.5 scenario. But in case of RCP6 scenario, no moderate drought condition was found since the projected precipitation data is higher than the observed period for RCP6 scenario.

Table 4.13 Number of drought events and duration from 2021-40 under different scenarios using SPI

SPI	4.5	6	8.5
Extremely wet (>2)	**0**	**2** (2030-31, 39-40)	**0**
Very wet (1.5 to 1.99)	**1** (2034-35)	**1** (2032-33)	**3** (2024-25, 32-33, 35-36)
Moderately wet (1 to 1.49)	**1** (2033-34)	**2** (2027-28, 37-38)	**1** (2023-24)
Near normal (-0.99 to 0.99)	**13** (2021-22, 22-23, 24-32, 35-37, 38-40)	**14** (2021-27, 28-30, 31-32, 32-37, 38-39)	**10** (2022-23, 27-31, 33-35, 36-39)
Moderately dry (-1.49 to -1)	**4** (2023-24, 30-31, 32-33, 37-38)	**0**	**1** (2039-40)
Severely dry (-1.99 to -1.5)	**0**	**0**	**3** (2021-22, 25-27)
Extremely dry (<= - 2)	**0**	**0**	**1** (2031-32)

Table 4.14 Number of drought events and duration from 2041-70 under different scenarios using SPI

SPI	4.5	6	8.5
Extremely wet (>2)	**1** (2063-64)	**0**	**2** (2043-44, 62-63)
Very wet (1.5 to 1.99)	**3** (2049-50, 58-59, 64-65)	**1** (2050-51)	**0**
Moderately wet (1 to 1.49)	**4** (2047-48, 61-62, 66-67, 69-70)	**1** (2069-70)	**4** (2044-45, 53-54, 63-64, 65-66)
Near normal (-0.99 to 0.99)	**17** (2041-43, 46-47, 48-49, 50-56, 57-58, 59-61, 62-63, 65-66, 67-69)	**21** (2041-44, 45-48, 51-60, 61-63, 64-68)	**18** (2041-42, 45-47, 49-53, 54-60, 61-62, 64-65, 66-67, 68-70)
Moderately dry (-1.49 to -1)	**4** (2043-46, 56-57)	**6** (2044-45, 48-50, 60-61, 63-64, 68-69)	**2** (2060-61, 67-68)
Severely dry (-1.99 to -1.5)	**0**	**0**	**3** (2042-43, 47-49)
Extremely dry (<= - 2)	**0**	**0**	**0**

Number of drought events under different scenarios were analysed for 2041-70 and found that there will be no extreme drought condition for all the RCP scenarios considered. Severe drought events will occur three times during 2042-43, 2047-48 and 2048-49 for RCP8.5 scenario whereas no severe drought condition was found for both RCP4.5 and RCP6 scenarios. Moderate drought condition will occur 4 times from 2043-57 for RCP4.5 scenario and twice from 2060-68 for RCP8.5 scenario. Moderate drought events are higher in case of RCP6 scenario and found that it will occur six times from 2044-69. When comparing the time periods, it is clear that the severe and extreme drought events will decrease towards the end of simulation periods for all the RCP scenarios whereas moderate dry events will increase in case of RCP6 and RCP8.5 scenario with a higher value for RCP6 scenario. This increase is also found in case of

projected precipitation data for RCP6 scenario. From these results, it can be concluded that the drought events is found to occur in periods where decrease in precipitation and increase in temperature is significant. The extreme drought condition is high for RCP8.5 scenario where temperature increase is higher than other scenarios. But the number of drought occurrence will decrease towards the end periods of simulation since the increase in precipitation become more significant at the ends. Chun *et al.* (2012) studied the drought characteristics in six catchments of UK and reported that the drought pattern in the future period will be less certain than the observed period of time. This result provides insight into the possible droughts conditions in the future due climate change, which can be used to protect and manage water resources. Sustainable measures for water management should therefore be planned to mitigate the future impacts of droughts.

4.3 IMPACT OF CONSERVATION PRACTICES IN THE WATERSHED

Watershed management, specifically Soil and Water Conservation (SWC), promotes sustainable livelihoods by reducing environmental degradation and increasing crop production since it increases infiltration and reduces erosion and at the same time maintains soil fertility. Conservation practices are implemented in Kerala for augmenting surface as well as groundwater resources. In order to conserve water resources and reduce soil erosion, studies on the conservation practices impact on river hydrology, particularly streamflow and sediment yield, are important. Among the available models, SWAT (Soil and Water Assessment Tool) is found to be most common in simulating conservation practices at watershed scale. The developed SWAT model was used in this research to study the impact of conservation practices on streamflow and sediment yield of Thuthapuzha watershed. The conservation practices selected for the study were Vented Cross Bar (VCB), check dam and brushwood dam. All these structures were modelled as ponds separately for each subbasin and the model was run and the results were analysed to find the impact of conservation practices. Other than these structures, Kanjirapuzha reservoir located within the watershed was also considered. In general, the impacts of conservation practices on streamflow and sediment yield were evaluated by running the

model with and without conservation practices and comparing streamflow and sediment yield in both cases.

4.3.1 Impact of conservation practices on streamflow of Thuthapuzha watershed

Generally, impact of conservation practices on hydrology is to delay or reduce the surface runoff thereby increasing the groundwater recharge. In order to analyse the impact of conservation practices on streamflow of the watershed, the SWAT model was run by incorporating the effects of conservation practices and the results were compared with the model results without adding conservation practices. The SWAT model defines reservoirs as water bodies located on the stream network, which receive loadings from all upstream subbasin at the subbasin outlet, whereas ponds and wetlands as water bodies located off the stream network, and do not receive loadings from other subbasins (Neitsch *et al.,* 2002). SWAT allows for one reservoir, one pond, and one wetland for each subbasin (Neitsch *et al.,* 2002). If there is a defined pond, wetland, and reservoir in a subbasin, the predicted runoff from each HRU shall be aggregated by first routing the runoff into ponds and wetlands followed by channel reach, and finally into the reservoir, irrespective of the location of the impoundments in the subbasin.

For this study, the conservation practices considered were Vented Cross Bar (VCB), check dam, brushwood dam and a reservoir located at Kanjirapuzha. Here, SWAT was used to model the Kanjirapuzha dam as reservoir component and the remaining structures as ponds. The required input parameters for the pond and reservoir are volume of water and surface area at both the principal spillway and the emergency spillway. The amount of water entering the water body throughout the day is estimated for the ponds as a fraction of the runoff provided by the user from all the HRUs within the subbasin, irrespective of their location in the subbasin. Data needed for the conservation practices simulation was collected and summed up for each subbasin. The structures in the study area were collected separately for each tributary. The location of the structures considered for the study separately for each tributary is shown in Fig. 4.51.

The details of conservation practices at each subbasin are given in Table. 4.15. The inputs used for reservoir component was also collected which is shown in Table. 4.16.

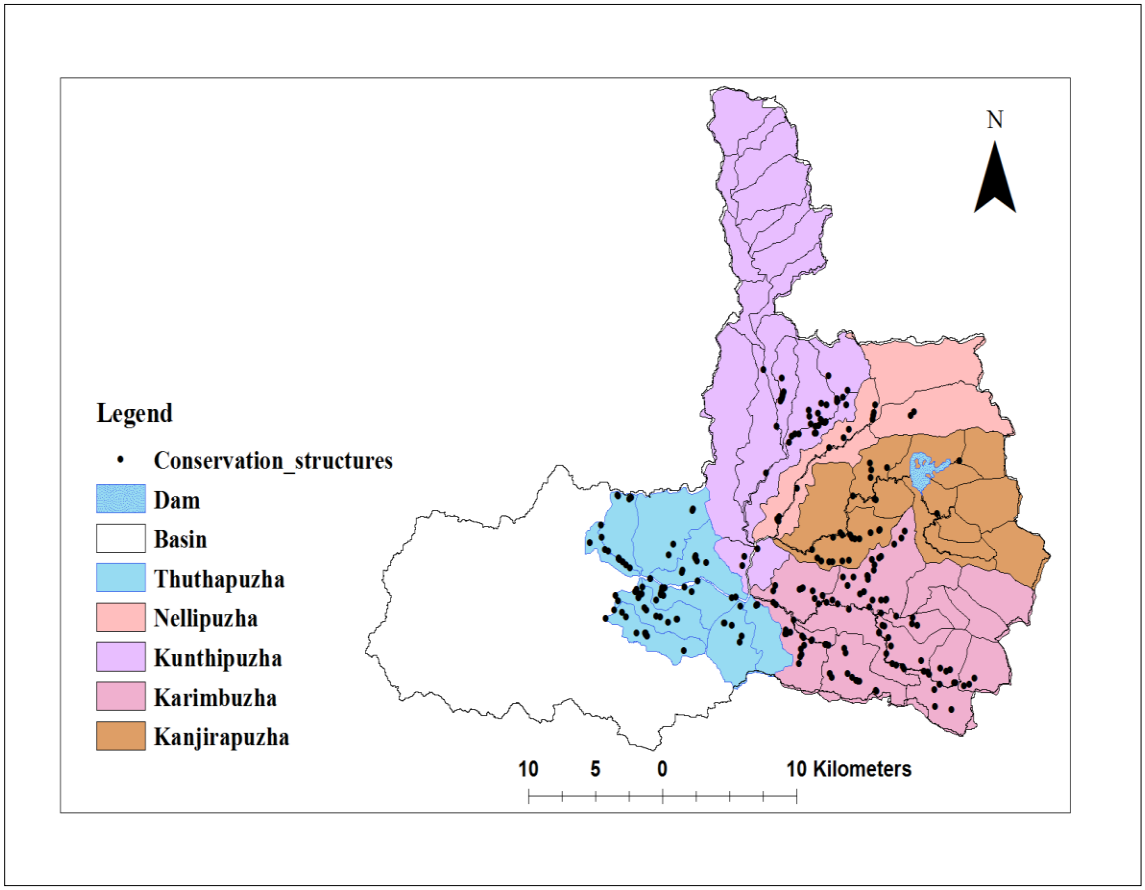

Fig. 4.51 Map showing location of conservation practices of Thuthapuzha watershed

Table 4.15 Surface area and volume of conservation practices summed up at each subbasin outlet

Subbasin	Surface_area (ha)	Volume (10^4 m^3)
1	0.0001	0.0001
2	0.0165	0.0465
3	0.0478	0.0591
4	0.0373	0.0624
5	0.0035	0.0014
6	0.0002	0.0001
7	0	0
8	0	0
9	0.004	0.004
10	0.0058	0.0066
11	0	0
12	0.0161	0.0442
13	0	0
14	0	0
15	0.0112	0.0203
16	0.0018	0.0028
17	0	0
18	0	0
19	0.0004	0.0003
20	0.0245	0.032
21	0	0
22	0.0172	0.0335
23	0	0
24	0.0097	0.0097
25	0.0309	0.1515
26	0.031	0.0706
27	0	0
28	0.0277	0.0686
29	0	0
30	0	0
31	0	0
32	0	0
33	0	0
34	0	0
35	0.0314	0.0713

Table 4.16 Details of Kanjirapuzha dam needed as input to SWAT

IYRES	Year the reservoir become operational	1980
RES_ESA	Reservoir surface area when filled to emergency spillway (ha)	505
RES_EVOL	Volume of water needed to fill the reservoir to emergency spillway(10^4 m^3)	18135
RES_PSA	Reservoir surface area when filled to principal spillway(ha)	401
RES_PVOL	Volume of water needed to fill the reservoir to principal spillway(10^4 m^3)	17205

In the developed SWAT model, the inputs for ponds and reservoir are given and the SWAT model was run. Annual and monthly streamflow outputs were analysed. In order to study the impact of conservation practices on streamflow, the streamflow values were compared with the results of SWAT model run without considering conservation practices. Comparison of annual and monthly streamflow simulated with and without structures for the period 1992-2017 is shown in Fig. 4.52 and Fig. 4.53 respectively and the average values are given in Appendix XVIII and XIX respectively. Predicted annual streamflow simulation is showing an average decrease of 55 Mm^3 in streamflow in all the years when conservation practices was added. The annual streamflow is found to be decreasing with the implementation of conservation structures from 1992-2017. Though there is a small decrease in the annual streamflow, the peak flow redistribution to summer months is of great importance.

Monthly streamflow simulated with and without structures was compared and found that the streamflow value increased largely during summer season with the effect of conservation structures from January to May whereas decreased slightly during rainy months. Large increase in the streamflow value with the implementation of conservation structures helps in maintaining a better environmental flow regime. Percent increase in monthly streamflow with the addition of conservation practices was calculated and is shown in Fig. 4.54. From the graph, it is clear that percent increase in streamflow is high in the range of 9 to 17 percent from January to April and a small decrease of about

0.5 to 7 percent in flow was observed from June to October. This redistribution of peak flow to summer months helps in increasing the groundwater recharge. During summer season, generally very lean river flow occurs in the watershed which results in water scarcity especially for the downstream water users. Such a situation can be avoided with the implementation of conservation practices. Moreover, the conservation practices will delay or reduce the surface runoff thereby recharge to groundwater also increases. Thus it is concluded that considering conservation practices in the watershed will be helpful for supporting the flow regime during summer season and decreases the flow regime during rainy season thereby a sustainable environment can be developed.

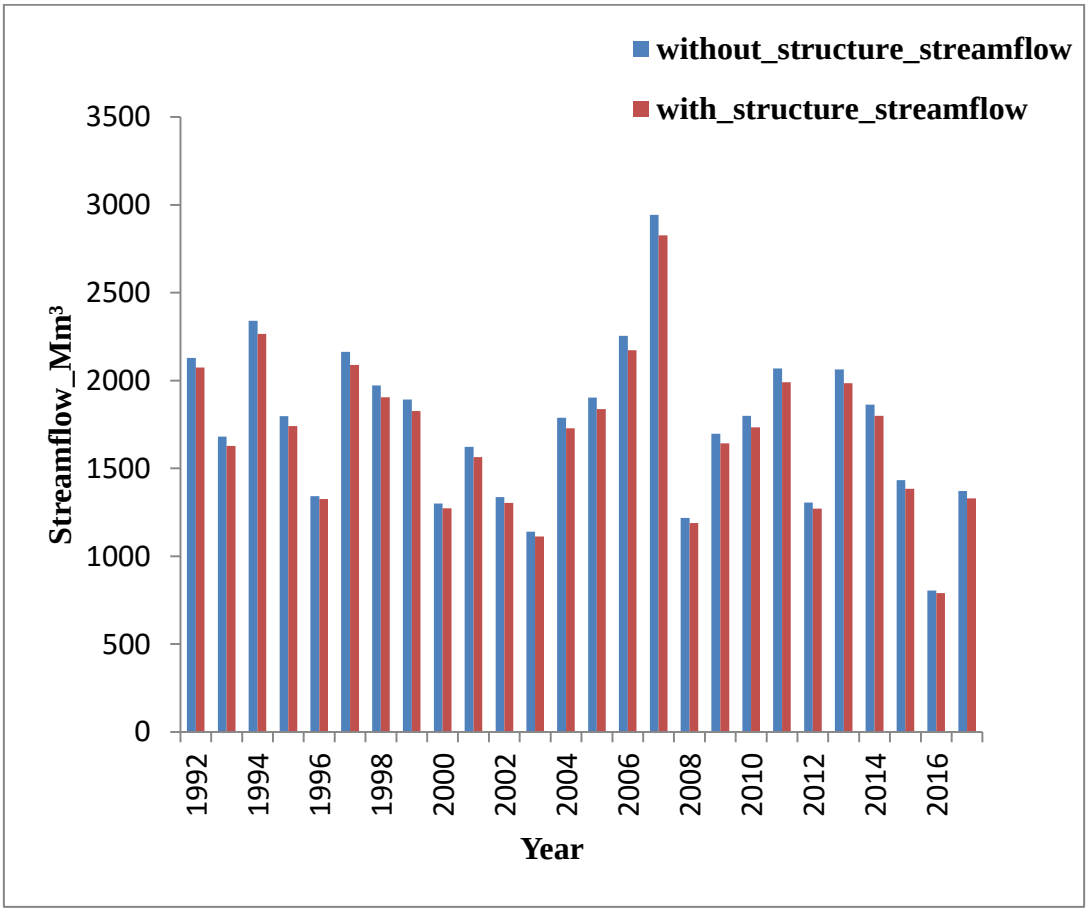

Fig. 4.52 Predicted annual streamflow simulation with and without conservation structures

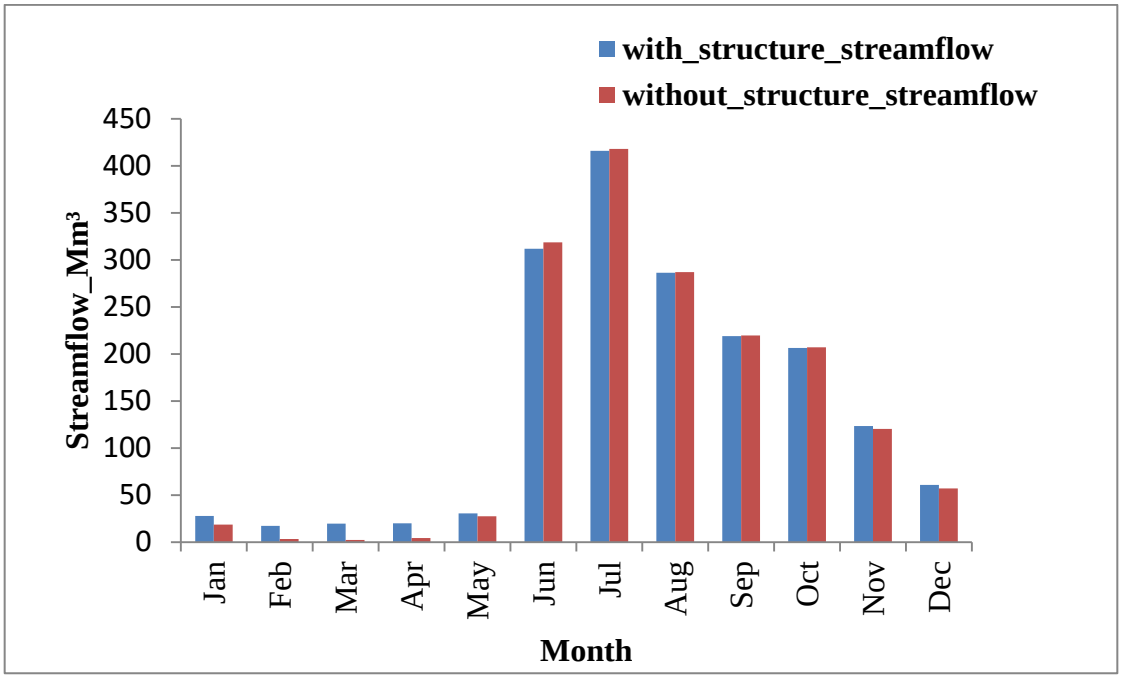

Fig. 4.53 Predicted monthly streamflow simulation with and without conservation structures

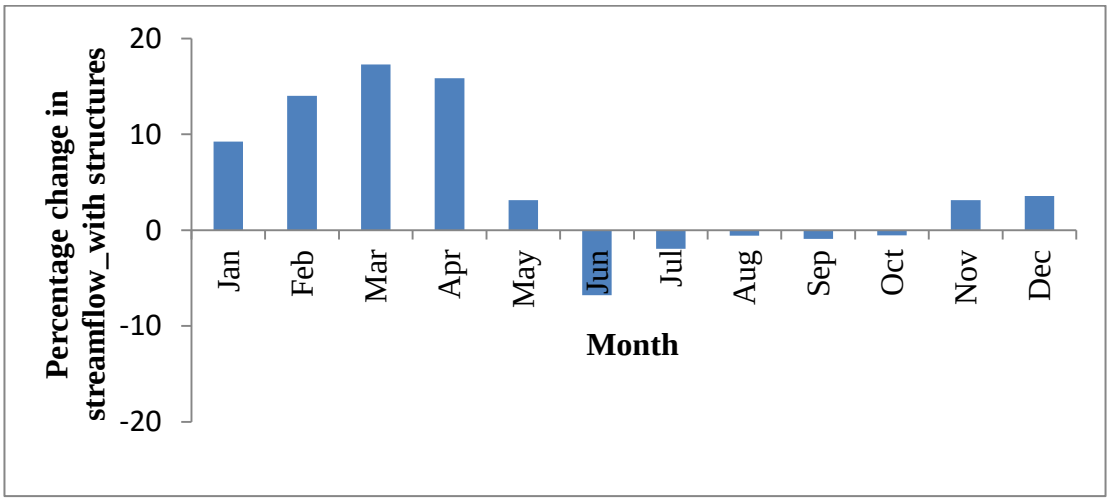

Fig. 4.54 Percentage change in streamflow with and without structure

4.3.2 Impact of conservation practices on sediment yield of Thuthapuzha watershed

The impact of conservation practices is to delay or reduce the surface runoff which results in decreased soil erosion. Worldwide research shows that 80-90 percent of all sediments eroded per year from watersheds are trapped within river channels and impoundments, before it reaches the oceans, with a large percentage trapped within the reservoirs (Kondolf *et al.*, 2014). The conservation practices thus play a major role in yielding the sediments at the watershed outlet. Thus, studying the impacts of conservation practices on sediment yield is of great significance. Similar to the impact study of streamflow on conservation practices, SWAT model was run with and without the conservation practices and the sediment yield results were analysed.

Sediment routing through the impoundment is calculated on the basis of the sediment mass balance equation in the SWAT model. An important part of the sediment mass balance is the sediment removal by settling which depends on the volume of the impoundment and the amount of sediment delivered to the impoundment, which is calculated as a function of the sediment concentration in the impoundment. Settling occurs when the concentration of sediment in the water body exceeds the concentration of equilibrium sediment defined by the user. A thorough calibration is required for the estimation of equilibrium sediment concentration as it is very difficult to calculate (Jalowska and Yuan, 2018). Impoundments will not discharge enough sediment if the value is set too low and the impoundments will become a source of sediment if the value is set too high (Neitsch *et al.*, 2002). Data related to sediment concentration is not available from any of the department for the study area. Thus, the sediment concentration values were estimated by calibration process. The calibrated model was run and the sediment concentration values of conservation practices and reservoir were changed accordingly and the simulated sediment yield was compared with the observed sediment yield at Pulamanthole gauging station of the watershed. Comparison of calibrated output and observed output is shown in Fig. 4.55. Scatter plot between observed sediment yield and simulated sediment yield is shown in Fig. 4.56. From the graph it is clear that simulated and observed sediment yield are in good correlation. Due

to the limitation of data availability, the calibrated model output was taken as the sediment yield of the Thuthapuzha watershed with the implementation of conservation practices.

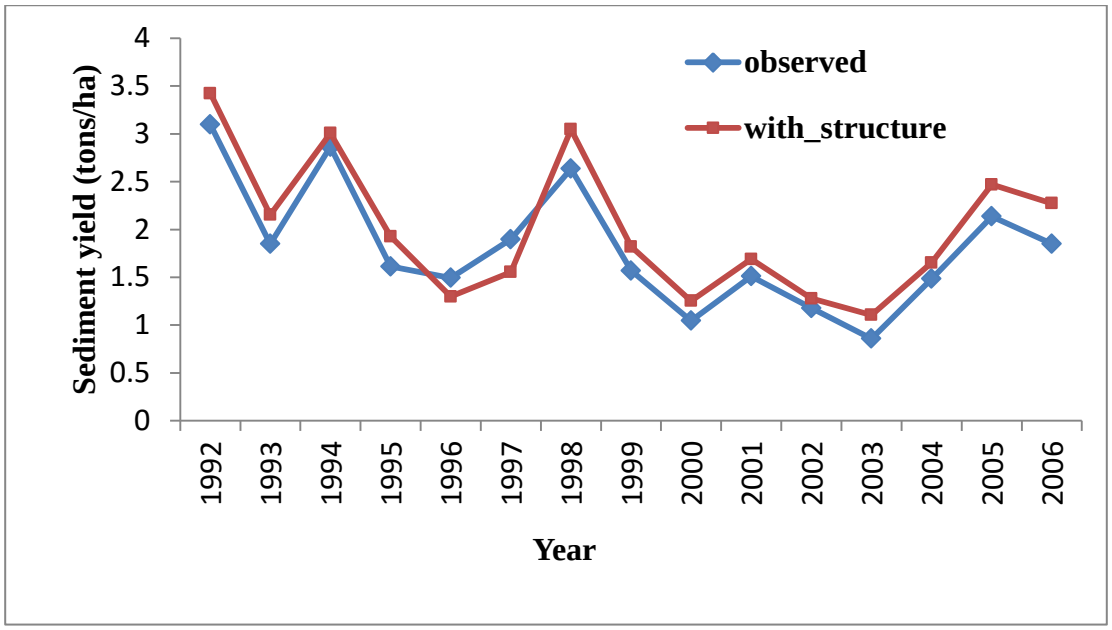

Fig.4.55 Comparison between observed and simulated sediment yield with structure

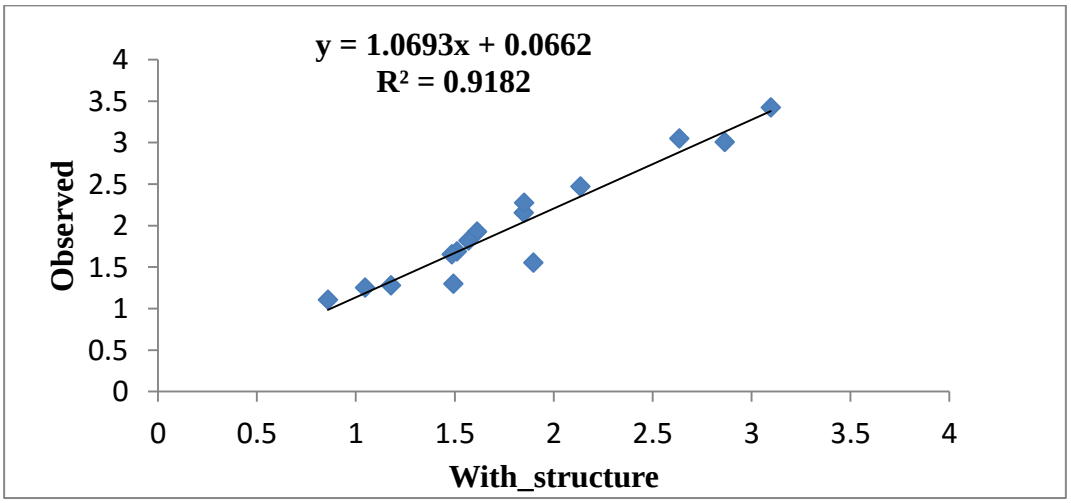

Fig. 4.56 Scatter plot between observed sediment yield and simulated sediment yield with structure

In order to study the impact of conservation practices on sediment yield, SWAT model was run with and without considering the conservation practices and the results were analysed. Comparison of annual and monthly sediment yield simulated with and without structures for the period 1992-2017 is shown in Fig. 4.57 and Fig. 4.58 respectively and the average values are given in Appendix XX and XXI respectively. Predicted annual sediment yield simulation is showing a decrease in sediment yield for all the years goes up to 1 to 5 t/ha with conservation practices from 1992-2017. With the addition of conservation practices, the sediment trapping occurs thus the sediment yielding at the outlet of the watershed decreases.

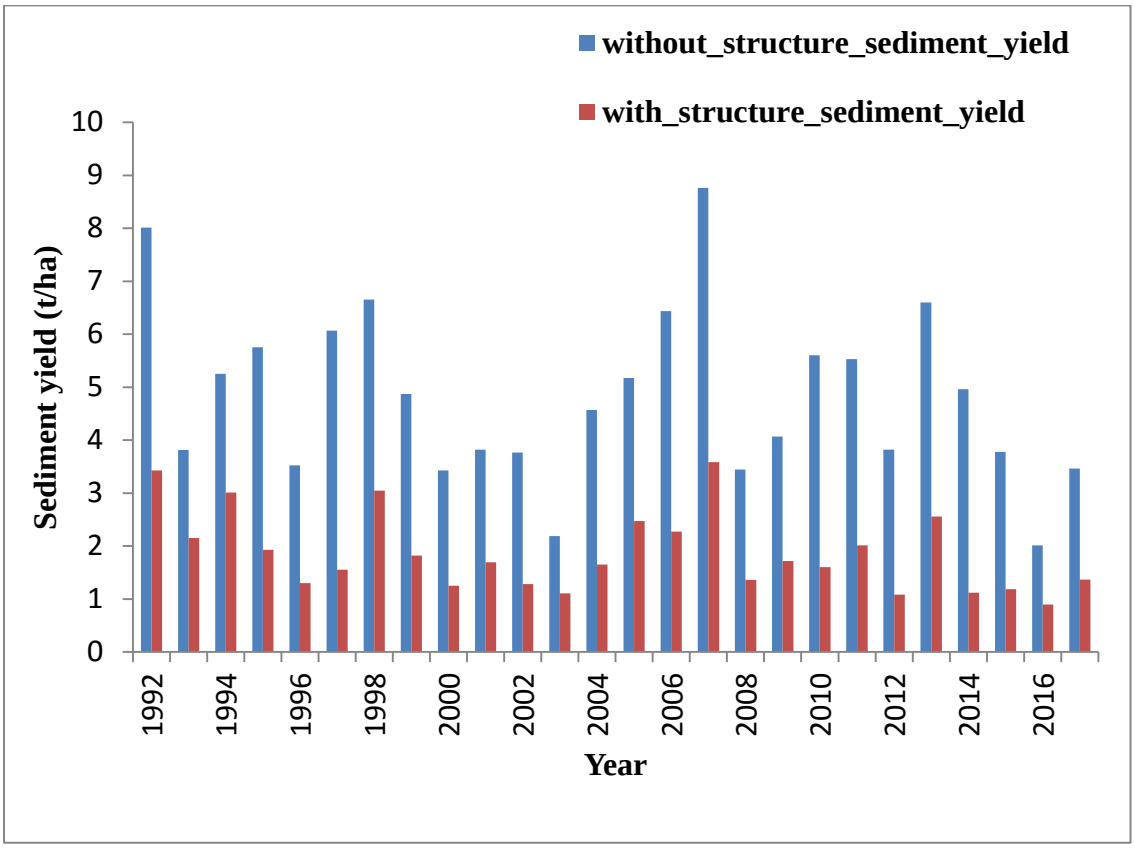

Fig. 4.57 Predicted annual sediment yield with and without conservation structures

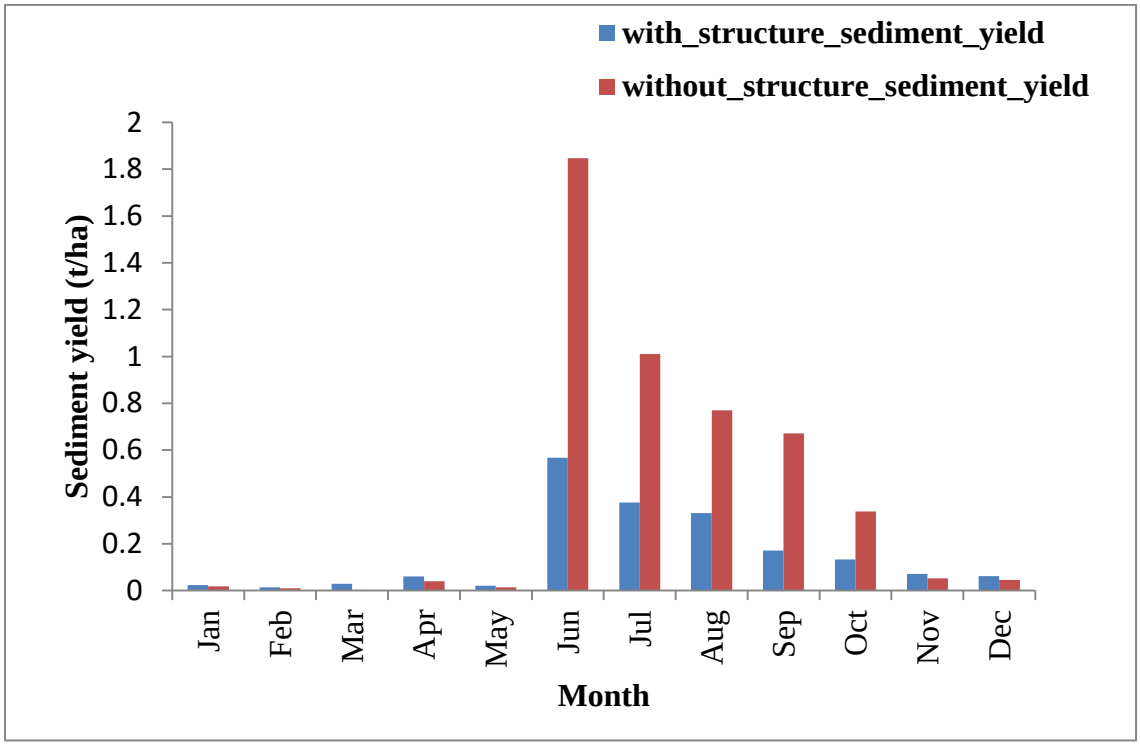

Fig. 4.58 Predicted monthly sediment yield with and without conservation structures

Monthly sediment yield at the outlet was compared with and without considering the conservation practices which is shown in Fig. 4.58. Sediment yield is found to be increasing slightly during the summer months (0.001 to 0.04%) from January to May with the addition of conservation practices. Similar trend is also found in the streamflow simulation also and the sediment yield increase might be due to the increase in streamflow during summer months. During peak flows, sediment yield is showing large decrease (0.2 to 1.3%) with the addition of conservation practices. This decrease might be due to the sediment trapping of impoundments in the watershed resulting in less sediment yield at the outlet when compared to sediment yield without conservation practices. The graph is showing similar trend as that of streamflow but the percent increase is different. Percent change in sediment yield is shown in Fig. 4.59. From the graph, the percent change in sediment yield is found to be high during peak flows and a

slight increase was observed for the summer months. It is therefore concluded that, in order to reduce the sediment loss of fertile soil by erosion during the peak periods, proper mitigation measures including conservation practices as well as its maintenance need to be adopted in time. Moreover, it is found that conservation practices are playing an important role in conserving soil and water in a watershed.

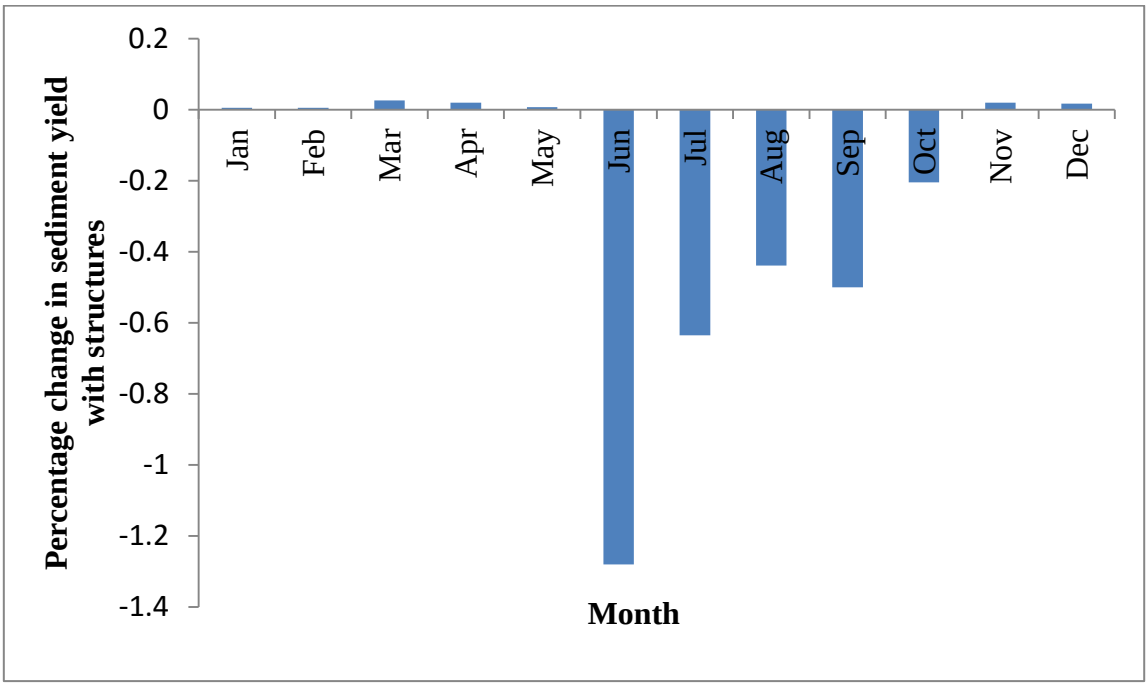

Fig. 4.59 Percentage change in sediment yield with and without structure

With the use of a properly calibrated model, the objectives of the entire research work were accomplished. The calibrated SWAT model was used to study both the streamflow and the sediment yield of the watershed. The overall results have shown that the SWAT model can very well be used in studying the climate change impacts. The capability of a well calibrated SWAT model in simulating conservation practices was also analysed and concluded that the SWAT model can be used effectively in conservation practice impact studies. The results of the entire research work will give an insight to the hydrologists in arriving solutions for problems regarding climate change as well as watershed development activities in the study area.

Summary and Conclusion

CHAPTER V

SUMMARY AND CONCLUSIONS

Efficient land and water resources management is essential for the sustainable development of a watershed. Water resource management is very important from a number of perspectives, such as developing and preserving water bodies for the future, protecting water bodies against pollution and over exploitation and preventing disputes. Water resource management and planning are becoming increasingly challenging every day as result of the uncertainties arising from climate change. Alterations in the hydrological processes, in turn, will affect the availability and runoff of water and may therefore affect river flows. Conservation measures can significantly modify the hydrological regime by altering the runoff pathways, as well as the temporal and spatial distribution of water availability. Detailed hydrological information on the watershed and its subsequent management using conservation structures is needed for the future development and protection of water resources.

Bharathapuzha, the second longest river in the state of Kerala is now facing significant threats to its survival due to many natural and man-made reasons. Climate change effects have modified the river flow pattern resulting in extreme rainfall during monsoon and severe drought during summer. It is necessary to analyse the reasons for this river flow pattern. Thus, a detailed study was carried out to understand the impacts of climate change and conservation practices on the Thuthapuzha subbasin of Bharathapuzha using the SWAT hydrological model. In order to analyse the impacts of climate change and conservation practices, SWAT based hydrological model was developed for the study area. A well calibrated and validated model will be able to reproduce or predict different hydrological variables for the future scenarios. The calibration of the model for the Thuthapuzha region was done taking care of the different parameters affecting the hydrology of the region. The simulation period for calibration was 1989 to 2009 and for validation 2010 to 2017 data was used and the simulation was done on daily basis. The initial period of three years (1989-1991) is taken as a warm-up

period. In the SWAT-CUP uncertainty analysis, two indices, p-factor and r-factor, were considered. During calibration, the p-factor and the r-factor were 0.77 and 0.64, and during validation, the p-factor and the r-factor were 0.85 and 0.56, respectively. Nash – Sutcliffe efficiency (NSE), coefficient of determination (R^2), and Percent bias (PBIAS) were used to assess the model performance. The R^2, NSE and PBIAS values were 0.88, 0.88 and-1.4 for the calibration period and 0.8, 0.8 and 5.4 for the validation period. Overall model statistics have shown that streamflow simulation can be successfully performed in the Thuthapuzha watershed using the developed model. Water balance components predicted by the model from 1992-2009 reveal that the major portion of the river flow is in the form of surface runoff (ranges between 29 to 51%) followed by ground water flow (23 to 31%). A relationship between the rainfall and runoff was also analysed and a decreased trend was observed.

Modelling of hydrological processes has proved to be an efficient tool for evaluating and predicting soil erosion to guide soil and water conservation practices under very different climatic, topographical, soil and management conditions (Pla, 2000). The lack of awareness of the impacts of conservation structures and insufficient economic assistance to implement them has also led to their low adoption rate (Gathagu *et al.*, 2017). A method for modelling a number of agricultural practices has already been developed by SWAT model, including changes in the application of fertilizers and pesticides, tillage, crop rotation, wetlands, ponds and dams. But fewer researchers focused on the impact of conservation practices on watersheds using SWAT. In addition, there is no standard procedure to simulate conservation practices to date.

Three main conservation structures in the study area *viz.*, Vented Cross Bar (VCB), check dam and brushwood dam and Kanjirapuzha reservoir were selected for impact analysis. From the literature review, it was found that check dams and VCB's can be modelled as ponds and the reservoir can be modelled as dam in the SWAT model. Since the conservation practices chosen have similar functions as that of check dams, all three were modelled as ponds. Thus, for each subbasin, the storage area and the volume

of all three conservation practices were summed up and given as a single pond at the outlet of subbasins in which it is located. After modelling ponds and reservoir, the SWAT model output was compared with the output without considering structures and the impact of conservation practices on streamflow was studied. Monthly streamflow simulated showed a large increase (9- 17%) during summer season from January to May when the river has a very lean flow whereas simulated annual streamflow decreased about 55Mm^3 for all the years from 1992-2017 with the addition of conservation structures. Large increase in the summer flows is due to the redistribution of peak flows with the addition of structures which helps in maintaining a better environmental flow regime.

Conservation structures impact on sediment yield was also studied by comparing the outputs with and without the addition of structures. Equilibrium sediment concentration is needed to study the sediment routing which is hard to calculate and requires thorough calibration (Jalowska and Yuan, 2018). Thus, the sediment concentration values were estimated by calibration process. The calibrated output was assumed as the sediment yield with the addition of conservation structures. Monthly sediment yield showed a slight increase (0.001-0.04%) during the summer months from January to May whereas sediment yield showed comparatively higher decrease (0.2-1.3%) during peak flows with the addition of conservation structures. Predicted annual sediment yield simulation is showing a decrease in sediment yield for all the years goes up to 1 to 5 t/ha with conservation practices from 1992-2017. In order to decrease the sediment loss of fertile soil by erosion during the peak periods, proper mitigation measures including conservation practices as well as its maintenance need to be adopted in time.

The developed model was used to study the impacts of climate change on Thuthapuzha watershed. Climate models are the basis for studying the impacts of climate change. GFDL-CM3 climate model was selected which provides better simulation for the Indian condition. The model data from CMIP5 dataset and CORDEX-SA dataset was collected and both the datasets were bias corrected and compared each other to select the

datasets for the climate change impact study. Extraction and bias correction of data was done using CMhyd software. Both the datasets were compared graphically and statistically and found that both datasets showed excellent correlation with the observed one with only a small decimal point variation. Thus, RCP4.5 (low) and RCP8.5 (high) scenarios from bias corrected CORDEX-SA dataset and RCP6 (medium) scenarios from CMIP5 bias corrected dataset from 2021-2070 were selected. Projected precipitation and temperature data were analysed and found that percentage increase in precipitation is predominant in RCP6 whereas as decrease in precipitation was found for RCP4.5 and RCP8.5 and the projected temperature showed an increase in trend for all the months from the observed data for RCP4.5 and RCP8.5 scenarios where as a decrease in trend was observed for RCP6 scenario.

The climate model output was given to the developed SWAT model and the results were analysed to study the climate change impacts on streamflow. Overall annual average streamflow for the entire simulation showed an increase under all RCP scenarios with predominant increase in RCP6 scenario (37-60%) followed by RCP4.5 (13-16%) and RCP8.5 (9-16%). Monthly streamflow predicted during 2021-70 was compared with observed and it was found that the streamflow in RCP 4.5 showed almost similar trend in variation as that of observed with a slight increase in streamflow for all the months except July and October during 2041-70. From 2021-70, the streamflow is found to be increasing from January to July and decreasing afterwards in RCP8.5. But the peak flow is found to be higher than that of RCP4.5 from June to August. Thus, in RCP8.5 it was found that during peak flows the climate will become wetter than that of current scenario. Moreover, during 2021-70 in RCP6 scenario, increase in streamflow was observed in all months except during December in the period from 2021-40. Significant increase in streamflow was found during the end periods of simulation for all the scenarios taken for the study purpose. Thus, necessary steps to be taken to mitigate the extreme events due to streamflow increase during future periods. Predicted water balance component under different scenarios reveal that the outflow from the watershed is mainly in the form of

surface runoff, followed by ground water flow, evapotranspiration and lateral flow under all RCP scenarios similar to the observed period of time.

Drought indices are widely used to evaluate the severity of the drought in a meaningful way. Among the various drought indices, SPI and RDI were selected for the impact analysis of climate change on drought intensity using DrinC software. Drought in the Thuthapuzha watershed for the observed period from 1989-2017 was analysed using both SPI and RDI index. Twelve month SPI values for the historical period from 1989-2017 showed that droughts were quite frequent during the 1999-2000, 2001-2003, 2007-2008, 2011-2012 and 2016-2017 whereas annual RDIst value showed that droughts were quite frequent during 1995-1996, 1999-2000, 2001-2002, 2007-2008, 2011-2012 and 2015-2017. Predicted drought intensity using both the SPI and RDI index for the period 1989-2017 showed that severely dry events have occurred once during 2015-16 when using SPI index. Comparison between both the indices showed a similar trend with little variation in the drought period, and the overall number of drought occurrence was same. To select the index for analysing drought intensity for the future period, a comparative study and regression analysis between SPI and RDIst under different RCP scenarios were done from 2021-2070 and found that both indices are well correlated and the drought intensity calculation using SPI and RDI were almost the same under all the RCP scenarios.

Future drought condition under different RCP scenarios was assessed by SPI from 2021-2070 and found that the wet years are more than drought years for all the RCP scenarios. When comparing between scenarios, RCP8.5 shows more drought period followed by RCP4.5. In all the scenarios from 2021-70, the duration of moderate droughts is longer than that of the other categories of drought, while extreme droughts are shorter. On the other hand, moderate drought duration is less in RCP6 followed by RCP8.5 and RCP4.5. In case of RCP8.5 scenario, extreme drought condition will occur only once during the period 2031-32 and severe drought condition will occur six times for the periods 2021-22, 2025-26, 2026-27, 2042-43, 2047-48 and 2048-49 whereas no

extreme and severe drought conditions were observed for RCP4.5 and RCP6. This result provides insight into the possible drought conditions in the future due to climate change, which can be used to protect and manage water resources. Sustainable measures for water management should therefore be planned to mitigate the future impacts of droughts.

The research findings could be useful for water resource planning and management by providing a planning tool for local management authorities to establish sustainable adaptation options. Climate change impact results were based on only one model. The results can be more accurately obtained with multiple models using multiple ensembles. Thus, the studies should be done in a site specific manner following the same procedures and appropriate mitigation measures and management practices need to be taken. The developed model can be used in the same area for further studies including management impact analysis, land use change impact assessment etc. The capability of a well calibrated SWAT model in simulating conservation practices was also analysed and concluded that SWAT model can be used effectively in conservation practices impact related studies. Since, sediment yield impact analysis was done through calibration using sediment concentration; the results may not be fully reliable. Thus, if there is good availability of data regarding sediment concentration or by physical measurements, further studies can be done in accurately simulating sediment yield. The results of the entire research work will give an insight to the hydrologists in arriving solutions for problems regarding climate change as well as watershed development activities specifically in the adoption of more conservation structures in the area.

References

REFERENCES

Abbaspour, K. 2008. SWAT-CUP: SWAT Calibration and Uncertainty Programs - A User Manual. Department of Systems Analysis, Integrated Assessment and Modelling (SIAM), Eawag, Swiss Federal Institute of Aquatic Science and Technology, Duebendorf, Switzerland.

Abbaspour, K. C. 2015. SWAT-CUP. SWAT Calibration and Uncertainty Programs. A User Manual. Swiss Federal Institute of Aquatic Science and Technology.

Abbaspour, K. C., Rouholahnejad, E., Vaghefi, S., Srinivasan, R., Yang, H., and Kløve, B. 2015. A continental-scale hydrology and water quality model for Europe. Calibration and uncertainty of a high-resolution large-scale SWAT model. *J. Hydrol.* 524:733-752.

Abbaspour, K.C. 2012. SWAT-CUP-2012.SWAT Calibration and Uncertainty program-A User Manual. Swiss Federal Institute of Aquatic Science and Technology, Dübendorf.

Abbaspour, K.C., Yang J., Maximov I., Siber R., Bogner K, Mieleitner J., Zobrist J., and Srinivasan R. 2007. Spatially-distributed modelling of hydrology and water quality in the prealpine/alpine Thur watershed using SWAT. *J. Hydrol.* 333:413-430.

Abbott, M.B., Bathurst, J.C., Cunge, J.A., O'Connel, P.E., and Rasmussen, J. 1986. An introduction to the European hydrological system- Systeme Hydrologique Europeen, SHE.2: Structure of a physically based, distributed modelling system. *J. Hydrol.* 87:61-77.

Abouabdillah, A., White, M., Arnold, J.G., De Girolamo, A.M., Oueslati, O., Maataoui, A., and Lo Porto, A. 2014. Evaluation of soil and water conservation measures in a semi-arid river basin in Tunisia using SWAT. *Soil Use Manag*. 30:1-12.

Ahmad, S., Khan, I.H., and Parida, B.P. 2001. Performance of stochastic approaches for forecasting river water quality. *Water Res.* 35(18):4261-4266.

Alcamo, J., Bouwman, A., Edmonds, J., Griibler, A., Morita, T., and Sugandhy, A. 1995. An evaluation of the IPCC 1S92 emission scenarios. Houghton, J.T. *et al.,* (eds.). In: Climate Change 1994, Radiative Forcing of Climate Change and An Evaluation of the IPCC IS92 Emission Scenarios, Cambridge University Press, Cambridge, pp. 233-304.

Allen, R. G. 1986. A Penman for all seasons. *J. Irrig. Drain. Eng*. 112(4):348-368.

Andersson, J., Zehnder, A., Jewitt, G., and Yang, H. 2009. Water availability, demand and reliability of in situ water harvesting in smallholder rain-fed agriculture in the Thukela River Basin, South Africa. *Hydrol. Earth System Sciences*. 13 (12):2329-2347.

Antar, M.A., Elassiouti, I., and Allam, M.N. 2006. Rainfall-runoff modelling using artificial neural net-works technique: a Blue Nile catchment case study. *Hydrological Processes.* 20:1201-1216.

Arabi, M., Frankenberger, J.R., Engel, B.A., and Arnold, J.G. 2008. Representation of agricultural conservation practices with SWAT. *Hydrological Processes.* 22:3042-3055.

Arnell, N. W., Livermore, M. J. L., Kovats, S., Levy, P. E., Nicholls, R., Parry, M. L., and Gaffin, S. R. 2004. Climate and socio-economic scenarios for global-scale climate change impacts assessments: Characterising the SRES storylines. *Glob. Environ. Change.* 14:3-20.

Arnell, N.W. 1992. Factors controlling the effects of climate change on river flow regimes in a humid temperate environment. *J. Hydrol*. 132:321-342.

Arnold, J. G. 2010. SWAT: model use, calibration, and validation. *Trans. ASABE.* 55(4):1491-1508.

Arnold, J. G., Moriasi, D. N., Gassman, P. W., Abbaspour, K. C., White, M. J., Srinivasan, R., Santhi, C., Harmel, R. D., van Griensven, A., van Liew, M. W., Kannan, N., and Jha, M. K. 2012. Swat: Model use, calibration, and validation. *Trans. ASABE*. 55(4):1491-1508.

Arnold, J.G. and Fohrer, N. 2005. SWAT2000: Current capabilities and researchopportunities in applied watershed modelling. *Hydrological Processes*. 19(3):563-572.

Arnold, J.G., Sirinivasan, R., Muttiah, R.S., and William, J.R. 1998. Large area hydrologic modeling and assessment.Part 1, model development. *J. Am. Water Resources Assoc.* 34(1):73-89.

Ayala, G., Berhanu, S., and Tolesa, O. 2017. Assessing the Effect of Soil and Water Conservation Practices on Runoff and Sediment Yield on HundeLafto watershed of Upper Wabi Shebelle Basin. *Civil Environ. Res.* 9(9):36-49.

Bal, P. K., Ramachandran, A., Palanivelu, K., Perumal, T., Rajadurai, G., and Bhaskaran, B. 2016. Climate change projections over India by a downscaling approach using PRECIS. *Asia-Pac. J. Atmos. Sciences*. 52:353-369.

Behera, S. and Panda, R. K. 2006. Evaluation of management alternatives for an agricultural watershed in a sub-humid subtropical region using a physical process model. *Agric. Ecosys. Environ.* 113(1-4):62-72.

Benham, B. L., Baffaut, C., Zeckoski, R. W., Mankin, K. R., Pachepsky, Y. A., Sadeghi, A. M., Brannan, K. M., Soupir, M. L., and Habersack, M. J. 2006. Modeling bacteria fate and transport in watersheds to support TMDLs. *Trans. ASABE.* 49(4):987-1002.

Best, A., Zhang , L., McMahon, T., Western, A., and Vertessy, R. 2003. *A critical review of paired catchment studies with reference to the seasonal flows and climate variability*. Technical Report No. 03/4, Cooperative Research Centre for Catchment Hydrology.

Beven, K.J. and Kirkby, M.J. 1979. A physically based variable contributing area model of basin hydrology. *Hydrological Sciences Bull.* 24 (1):43-69.

Bieger, K., Hörmann, G., and Fohrer, N. 2014. Simulation of streamflow and sediment with the Soil and Water Assessment Tool model in a data scarce catchment in the Three Gorges Region, China. *J. Environ. Qual*. 43:37-45. doi:10.2134/jeq2011.0383.

Bonell, M. and Balek, J. 1993. Recent and scientific developments and research needs in hydrological processes of the humid tropics. In: *Hydrology and Water Managment in the Humid Tropics*, Bonell M, Hufschmidt MM, Gladwell JS (eds). UNESCO, Paris, pp. 167-260.

Bormann, H. and Diekkreuger, B. 2003. Possibilities and limitations of regional hydrological models applied within an environmental change study in Benin West Africa. *Phys. Chem. Earth.* 28:1323-1332.

Bouraoui, F., Galbiati, L., and Bidoglio, G. 2002. Climate change impacts on nutrient loads in the Yorkshire Ouse catchment (UK). *Hydrol. Earth System Sci.* 6(2): 197-209.

Bracmort, K. S., Arabi, M., Frankenberger, J. R., Engel, B. A., and Arnold, J. G. 2006. Modeling long-term water quality impact of structural BMPs. *Trans. ASABE.* 49(2): 367-374.

Brouziyne, Y., Abouabdillah, A., Bouabid, R., Benaabidate, L., and Oueslati, O. 2017. SWAT manual calibration and parameters sensitivity analysis in a semi-arid watershed in North-western Morocco. *Arabian J. Geosciences*. 10:1-13.

Brunner, A.C., Park, S.J., Ruecker, G.R., and Vlek, P.L.G. 2008. Erosion modelling approach to simulate the effect of land management options on soil loss by considering catenary soil development and farmers perception. *Land Degradation Dev.* 19(1):242-256.

Calanca, P., Roesch, A., Jasper, K., and Wild, M. 2006. Global warming and the summertime evapotranspiration regime of the Alpine region. *Clim. Change*. 79(1–2):65-78. doi:10.1007/s10584-006-9103-9.

Castillo,V.M., Martinez-Mena, M., and Albaladejo, J. 1997. Runoff and soil loss response to vegetation removal in a semiarid environment. *Soil Sci. Soc. Am. J.* 61:1116-1121.

Chong-Hai, X. and Ying, X. 2012. The Projection of Temperature and Precipitation over China under RCP Scenarios using a CMIP5 Multi-Model Ensemble. *Atmos. Ocean. Sci. Letters*. 5(6):527-533.

Chow, V.T., Maidment, D.R., and Mays, L.W. 1988. *Applied Hydrology*. McGraw-Hill: New York. 572 p.

Christensen, J. H., Boberg, F., Christensen, O.B., and Lucas-Picher, P. 2008. On the need for bias correction of regional climate change projections of temperature and precipitation. *Geophys. Res. Lett*. 35: L20-709.

Chu, T. W., Shirmohammadi, A., Montas, H., and Sadeghi, A. 2004. Evaluation of the SWAT model's sediment and nutrient components in the Piedmont physiographic region of Maryland. *Trans. ASAE*. 47(5): 1523-1538.

Chun, K. P., Wheater, H., and Onof, C. 2012. Prediction of the impact of climate change on drought: an evaluation of six UK catchments using two stochastic approaches. *Hydrological Processes.* 27(11):1600-1614.

Collick, A.S. 2008. Community water use in the Yeku watershed and hydrological modelling in watersheds of the upper Nile basin, northern Ethiopia. PhD Thesis, Cornell University, USA.

Collins, M., Booth, B. B. B., Bhaskaran, B., Harris, G. R., Murphy, J. M., Sexton, D. M. H., and Webb, M.J. 2010. Climate model errors, feedbacks and forcings: a comparison of perturbed physics and multi-model ensembles. *Clim. Dyn*. 36:1737-1766. doi: 10.1007/s00382-010-0808-0.

Croton, J.T. and Barry, D.A. 2001. WEC-C: a distributed, deterministic catchment model-theory, formulation and testing. *Environ. Modelling Software.* 16:583-599.

Cunderlik, M.J. 2003. Hydrologic Model Selection For The CFCAS Project:Assessment Of Water Resource Risk And Vulnerability To Changing Climate Conditions. *Project Report I.* University Of Western Ontario, Canada.

Cuo, L., Lettenmaier, D. P., Alberti, M., and. Richey, J. E. 2009. Effects of a century of land cover and climate change on the hydrology of the Puget Sound basin. *Hydrological Processes.* 23(6):907-933.

Curry, J. 2016. Schematic of a global climate model [online]. Available: https://upload.wikimedia.org/wikipedia/commons/thumb/7/73/AtmosphericModelSchematic.png/350pxAtmosphericModelSchematic.png.

CWC. 2012. Integrated hydrological data book (Non classified river basins), Central Water Commission, p 675.

Dai, A. 2011. Drought under global warming: a review. *Wiley Interdiscip. Rev. Clim. Change*. 2:45-65.

Dai, T., Koenig, J., Shoemaker, L., Tech, T., and Hantush, M. 2005. TMDL model evaluation and research needs. EPA/600/R-05/149. National Risk Management Research Laboratory, Office of Research and Development.

Daloglu, I., Nassauer, J.I., Riolo, R., and Scavia. D. 2014. An integrated social and ecological modeling framework—impacts of agricultural conservation practices on water quality. *Ecol. Soc.* 19 (3):12.

Delgado, J.M., Apel, H., and Merz, B. 2010. Flood trends and variability in the Mekong river. *Hydrol. Earth Syst. Sciences.* 14(3):407-418.

Descheemaeker, K., Nyssen, J., Rossi, J., Poesen,J., Haile, M., Raes,D., Muys,B., Moeyersons, J., and Deckers, J. 2006. Sediment deposition and pedogenesis in exclosures in the Tigray Highlands, Ethiopia. *Geoderma.* 132(3):291-314.

Devi, G. K., Ganasri, B. P., and Dwarakish, G. S. 2015. A Review on Hydrological Models. *Aquatic Procedia.* 4:1001-1007.

Dlamini, N.S., Kamal, M.R., Soom, M.A.B., Bin Mohd, M.S.F., Bin Abdullah, A.F., and Hin, L.S. 2017. Modeling potential impacts of climate change on streamflow using projections of the 5th assessment report for the Bernam River basin, Malaysia. *Water.* 9:226.

Edwards, K.A. 1979. The water balance of the Mbeya experimental catchments. *E. Afr. Agric. For. J.* 43:231-247.

Edwards, P.J., Williard, K.W., and Schoonover, J.E. 2015. Fundamentals of watershed hydrology. *J. Contemp. Water Res. Educ.* 154:3-20.

Ficklin, D.L., Luo, Y., Luedeling, E., and Zhang, M. 2009. Climate change sensitivity assessment of a highly agricultural watershed using SWAT. *J. Hydrol*. 374(1):16-29.

Fischer, E.M., Seneviratne, S.I., Lu thi, D., and Schar, C. 2007. Contribution of land-atmosphere coupling to recent European summer heat waves. *Geophys. Res. Letters.* 34(6):L06707.

Fontaine, T. A., Klassen, J. F., Cruickshank, T. S., and Hotchkiss, R. H. 2001. Hydrological response to climate change in the Black Hills of South Dakota, USA. *Hydrol. Sci. J.* 46(1):27-40.

Fowler, H. J., Blenkinsop, S., and Tebaldi, C. 2007. Linking climate change modelling to impacts studies: Recent advances in downscaling techniques for hydrological modelling. *Int. J. Climatol*. 27(12):1547-1578.

Frei, C., Christense, J.H., Deque, M., Jacob, D., Jones, R.G., and Vidale, P.L. 2003. Daily precipitation statistics in regional climate models: Evaluation and intercomparison for the European Alps. *J. Geophys. Res.* 108:4124.

Fu, G., Charles, S. P., Viney, N. R., Chen, S. L., and Wu, J. Q. 2007. Impacts of climate variability on stream-flow in Yellow River. *Hydrological Processes*. 21(25):3431-3439. doi:10.1002/hyp.6574.

Fu, G., Chen, S., and McCool, D. 2006. Modelling the impacts of no-till practice on soil erosion and sediment yield with RUSLE, SEDD, and ArcView GIS. *Soil Tillage Res*. 85:38-49.

Gassman, P. W., Reyes, M. R., Green, C. H., and Arnold, J. G. 2007. The soil and water assessment tool: historical development, applications, and future research directions. *Trans. ASABE*. 50 (4):1211-1250.

Gathagu, J.N., Isiah, M.J., Oduor, B.O., and Mourad, K. 2017. Soil and water conservation in Thika-Chania catchment, Kenya. *Int. J. of Sustain. Water Environ. Syst.* 9(10):59-65.

Giorgi, F. and Gutowski, J. 2015. Regional dynamical downscaling and the CORDEX initiative. *Annu. Rev. Environ. Resources.* 40:467-490. https://doi.org/10.1146/annurev-environ102014-021217.

Giorgi, F., Coppola, E ., Solmon, F., Mariotti, L., Sylla, M.B., Bi, X., Elguindi, N., Diro, G. T., Nair, V.S., Giuliani, G., Turuncoglu, U.U., Cozzini, S., Güttler, I., O'Brien, T.A., Tawfik, A.B., Shalaby, A., Zakey, S., Steiner, A.L., Stordal, F., and Branković, Č. 2011. RegCM4: Model description and preliminary tests over multiple CORDEX domains. *Clim. Res.* 52:7-29.

Githui, F., Gitau, W., Mutua, F., and Bauwens, W. 2009. Climate Change Impact on SWAT Simulated Streamflow in Western Kenya. *Int. J. Climatol*. 29:1823-1834.

Gosain, A., Rao, S., and Basuray, D. 2006. Climate change impact assessment on hydrology of Indian river basins. *Curr. Sci.* 90(3):346-353.

Govindaraju, R.S. and Rao, A.R. 2000. *Artificial Neural Networks in Hydrology*. Kluwer Academic Pub, Netherlands. 348 p.

Green, W. H. and Ampt, G. A. 1911. Studies on soil physics, 1.The flow of air and water through soils. *J. Agric. Sciences*. 4:11-24.

Gupta, H., Sorooshian, S., and Yapo, P. 1999. Status of Automatic Calibration for Hydrologic Models: Comparison with Multilevel Expert Calibration. *Int. J. Hydrologic Eng.* 4(2):135-143.

Hamlett, J.M. and Peterson, J. R. 1998. Hydrologic calibration of the SWAT model in a watershed containing fragipan soils. *J. Am. Water Resources Assoc*. 34(3):531-544.

Han, Y., Feng, G., and Ouyang, Y. 2018. Effects of Soil and Water Conservation Practices on Runoff, Sediment and Nutrient Losses. *Water*. 10(10):1333.

Hargreaves, G. H. and Samani, Z. A. 1985. Reference crop evapotranspiration from temperature. *Appl. Eng. Agric.* 1:96-99.

Hawkins, E. and Sutton, R. 2009. The potential to narrow uncertainty in regional climate predictions. *Bull. Am. Meteorol. Soc*. 90:1095.

Hayes, M. J., Svoboda, M. D., Wardlow, B. D., Anderson, M. C., and Kogan, F. 2012. Drought Monitoring: Historical and Current Perspectives. *Drought Mitigation Center Faculty Publications.* 94.

Hayes, M.J., Alvord, C., and Lowrey, J. 2007. Drought Indices. *Intermountain West Clim. Summary.* 3(6):2-6.

Herweg, K. and Ludi, E. 1999. The performance of selected soil and water conservation measures – Case studies from Ethiopia and Eritrea. *Catena*. 36(1):99-114.

Hewitson, B. C. and Crane, R. G. 1996. Climate downscaling: Techniques and application. *Clim. Res.* 7:85-95. https:// doi.org/10.3354/cr007085.

Hibbard, K.H., Meehl, G., Cox, P., and Friedlingstein, P. 2007. A strategy for climate change stabilization experiments. *EOS*. 88(20):217-219.

Huang, M. and Zhang, L. 2004. Hydrological responses to conservation practices in a catchment of the Loess Plateau, China. *Hydrological Processes*. 18:1885-1898.

Hurkmans, R., Terink, W., Uijlenhoet, R., Torfs, P., and Jacob, D. 2010. Changes in Streamflow Dynamics in the Rhine Basin under Three High-Resolution Regional Climate Scenarios. *J. Clim.* 23:679-699.

Inbar, M. and Llerena C.A. 2000. Erosion processes in high mountain agricultural terraces in Peru. *Mountain Res. Dev*. 20(1):72-79.

Iooss, B. and Lemaître, P. 2015. A review on global sensitivity analysis methods. In: *Uncertainty Management in Simulation-Optimization of Complex Systems.* Springer, Boston, MA, pp. 101-122.

IPCC (Intergovernmental Panel on Climate Change). 1996. *Climate Change 1995: Impacts, Adaptations, and Mitigation of Climate Change: Scientific -Technical Analyses*, Watson, R. T., Zinyowera, M. C., and Moss, R. H. (eds.). Cambridge University Press, New York, pp. 879.

IPCC (Intergovernmental Panel on Climate Change). 2007. *Climate Change 2007: Impacts, Adaptation, and Vulnerability—Contribution of Working Group II to the Third Assessment Report of the Intergovernmental Panel on Climate Change*, Parry, M. L. *et al.*, (eds). In: IPCC Fourth Assessment Report, Cambridge Univ. Press, Cambridge, U. K.

IPCC. 2007a. *Climate Change 2007: The Physical Science Basis. Contribution of Working Group I to the Fourth Assessment Report of the Intergovernmental Panel on Climate Change*, Solomon, S. *et al.* (eds.), Cambridge University Press, Cambridge, United Kingdom and New York, NY, USA, pp. 996.

Jalowska, A.M. and Yuan, Y. 2018. Evaluation of SWAT Impoundment Modeling Methods in Water and Sediment Simulations. *J. Am. Water Resources Assoc.* 55 (1):209-227.

Jayakody, P., Parajuli, P.B., and Cathcart, T.P. 2014. Impacts of climate variability on water quality with best management practices in sub-tropical climate of USA. *Hydrological Processes*. 28:5776-5790.

Jemberu, W., Baartman, J.E., Fleskens, L., and Ritsema, C.J. 2018. Participatory assessment of soil erosion severity and performance of mitigation measures using stakeholder workshops in Koga catchment, Ethiopia. *J. Environ. Manag*. 207:230-242.

Jha, M., Arnold, J. G., Gassman, P. W., Giorgi, F., and Gu, R. 2006. Climate change sensitivity assessment on upper Mississippi river basin streamflows using SWAT. *J. Am. Water Resour. Assoc.* 42(4):997-1015.

Jiang, C., Zhang, L., and Tang, Z. 2017. Multi-temporal scale changes of streamflow and sediment discharge in the headwaters of Yellow River and Yangtze River on the Tibetan Plateau, China. *Ecological Eng*. 102:24-54.

Johnston, R. and Smakhtin, V. 2014. Hydrological modeling of large river basins: how much is enough?. *Water Resources Manag*. 28(10):2695-2730.

Jyrkama, M. I. and Sykes, J. F. 2007. The impact of climate change on spatially varying groundwater recharge in the Grand River watershed (Ontario). *J. Hydrol*. 338(3-4):237-250. doi:10.1016/j.jhydrol. 2007.02.036.

Kannan, N., White, S. M., Worrall, F., and Whelan, M. J. 2007. Sensitivity analysis and identification of the best evapotranspiration and runoff options for hydrological modeling in SWAT-2000. *J. Hydrol.* 332(3-4):456-466.

Kaur, R., Singh, O., Srinivasan, R., Das, S. N., and Mishra, K. 2004. Comparison of a subjective and a physical approach for identification of priority areas for soil and water management in a watershed: A case study of Nagwan watershed in Hazaribagh District of Jharkhand, India. *Environ. Model. Assess.* 9(2):115-127.

Kobierska, F., Jonas, T., Zappa, M., Bavay, M., Magnusson, J., and Bernasconi, S.M. 2013. Future runoff from a partly glacierized watershed in Central Switzerland: A two-model approach. *Adv Water Resour.* 55:204-214.

Kondolf, G., Rubin, Z., and Minear, J. 2014. Dams on the Mekong, Cumulative Sediment Starvation. *Water Resources Res.* 50(6):5158-69.

Kramer, L.A., Bukart, M.R., Meek, D.W., Jaquis, R.J., and James, D.E. 1999. Field-scale watershed evaluations on deep-loess soils: II. Hydrologic responses to different agricultural land management systems. *J. Soil Water Conserv.* 54:705-710.

Krause, P., Boyle, D.P., and Bäse, F. 2005. Comparison of different efficiency criteria for hydrological model assessment. *Adv. Geosciences*. 5:89-97.

Krishnakumar, K. N., Rao, G.S.L.H.V.P., and Gopakumar, C.S. 2009. Rainfall trends in twentieth century over Kerala, India. *Atmos. Environ.* 43:1940-1944.

Kyalo, D., Zhunusova, E., and Holm-müller, K. 2014. Estimating the joint effect of multiple soil conservation practices: A case study of small holder farmers in the Lake Naivasha basin,Kenya. *Land Use Policy*. 39:177-187.

Landsberg, H.E. 1975. Sahel drought: Change of climate or part of climate?. *Arch. Met. Geoph. Biokl. B.* 23:193-200. https://doi.org/10.1007/BF02246775.

Laprise, R. 2014. Comment on "The added value to global model projections of climate change by dynamical downscaling: A case study over the continental U.S. using the GISS-ModelE2 and WRF models" by Racherla *et al. J. Geophys. Res. Atmos.* 119:3877-3881.

Lee, J.W., Hong, S.Y., Chang, E.C., Suh, M.S., and Kang, H.S. 2013. Assessment of future climate change over East Asia due to the RCP scenarios downscaled by GRIMs-RMP. *Clim. Dyn.* 42:733-747.

Legates, D.R. and McCabe, G.J. 1999. Evaluating the use of ‘‘goodness-of-fit” measures in hydrologic and hydro climatic model evaluation. *Water Resources Res.* 35:233-241.

Leggett, J., Pepper, W. J., and Swart, R. J. 1992. Emissions scenarios for IPCC: An update, Houghton J. T. *et al.*, (eds). In: Climate Change 1992: The Supplementary Report to the IPCC Scientific Assessment, Cambridge University Press, New York, pp. 69-95.

Lenhart, T., Eckhardt, K., Fohrer, N., and Frede, H. G. 2002. Comparison of two different approaches of sensitivity analysis. *Phys. Chem. Earth.* 27:645-654.

Li, Z., Liu, W. Z., Zhang, X. C., and Zheng, F.L. 2010. Assessing and regulating the impacts of climate change on water resources in the Heihe watershed on the Loess Plateau of China. *Sci. China Earth Sciences.* 53:710-720.

Li, Z., Liu, W.Z., Zhang, X.C., and Zheng, F.L. 2009. Impacts of land use change and climate variability on hydrology in an agricultural catchment on the Loess Plateau of China. *J. Hydrol.* 377:35-42.

Liu, X. and Huang, M. B. 2001. Analysis on benefits of water reduction by soil and water conservation in different physiognomy type areas of big watershed scale. *Bull. Soil Water Conserv.* 1:36-41.

Lu, S., Kayastha, N., Thodsen, H., Van Griensven, A., and Andersen. H.E. 2014. Multiobjective calibration for comparing channel sediment routing models in the Soil and Water Assessment Tool. *J. Environ. Qual.* 43:110-120. doi:10.2134/jeq2011.0364.

Manjula, P. and Unnikrishnan Warrier, C. 2019. Evaluation of water quality of Thuthapuzha Sub-basin of Bharathapuzha, Kerala, India. *Appl.Water Sci.* 9:70.

Mann, M. E. and Kump, L. R. 2015. *Dire Predictions: Understanding Climate Change, 2nd Edition.*

Maraun, D., Wetterhall, F., Ireson, A. M., Chandler, R. E., Kendon, E. J., Widmann, M., Brienen, S., Rust, H. W., Sauter, T., Themessl, M., Venema, V. K. C., Chun, K. P., Goodess, C. M., Jones, R. G., Onof, C., Vrac, M., and Thiele-Eich, I. 2010. Precipitation downscaling under climate change: recent developments to bridge the gap between dynamical models and the end user. *Rev. Geophys*. 48:Rg3003.

Marino, S., Hogue, I.B., Ray, C.J., and Kirschner, D.E. 2008. A methodology for performing global uncertainty and sensitivity analysis in systems biology. *J. Theor Biol*. 254(1):178-196.

McKee, T.B., Doesken, N.J., and Kleist, J. 1993. The relationship of drought frequency and duration to time scale. In: *Proceedings of the Eighth Conference on Applied Climatology*, American Meteorological Society. Anaheim (CA), 17-22 January 1993, AMS, pp. 179-184.

Meehl, G. A. and K. A. Hibbard. 2007. *A strategy for climate change stabilization experiments with AOGCMS and ESMS.* WCRP Informal Rep. 3/2007, ICPO Publ. 112, IGBP Rep. 57. pp35.

Meehl, G. A., Goddard, L., Murphy, J., Stouffer, R.J., Boer, G., Danabasoglu, G., Dixon, K., Giorgetta, M.A., Greene, A.M., Hawkins, E., Hegerl, G., Karoly, D., Keenlyside, N., Kimoto, M., Kirtman, B., Navarra, A., Pulwarty, R., Smith, D., Stammer, D., and Stockdale, T. 2009. Decadal prediction: Can it be skillful?. *Bull. Amer. Meteor. Soc*. 90:1467-1485. doi:10.1175/2009BAMS2778.1.

Meehl, G.A., Covey, C., Delworth, T., Latif, M., McAvaney, B., Mitchell, J.F.B., Stouffer, R.J., and Taylor, K.E. 2007. The WCRP CMIP3 multimodel dataset: A new era in climate change research. *Bull. Amer. Meteor. Soc.* 88:1383-1394. doi: 10.1175/BAMS-88-9-1383.

Meinshausen, M., Smith, S.J., Calvin, K., Daniel, J.S., Kainuma, M.L.T., Lamarque, J.F., Matsumoto, K., Montzka, S.A., Raper, S.C.B., and Riahi, K. 2011. The RCP greenhouse gas concentrations and their extensions from 1765 to 2300. *Clim. Change.* 109:213-241.

Mekonnen, D.F., Duan, Z., Rientjes, T., and Disse, M. 2018. Analysis of combined and isolated effects of land-use and land-cover changes and climate change on the upper Blue Nile River basin's streamflow. *Hydrol. Earth System Sci.* 22(12):6187-6207.

Mekonnen, K. and Tesfahunegn, G. 2011. Impact assessment of soil and water conservation measures at Medego watershed in Tigray, northern Ethiopia. *Maejo Int. J. Sci. Technol.* 5(03):312-330.

Mekuria, W., Vedcamp, E., Haile, M., Nyssen, J., Muys, B., and Gebirehiwot, K. 2007. Effectiveness of exclosures to restore degraded soils as a result of overgrazing in Tigray, Ethiopia. *J. Arid Environments*. 69:270-284.

Meshesha, D., Tsunekawa, A., Tsubu, M., and Haregeweyn, N. 2012. Dynamics and hotspots of soil erosion and management Scenario of the Central Rift valley of Ethiopia. *Int. J. Sediment Res.* 27:84-99.

Millman, K.J. and Aivazis, M. 2011. Python for scientists and engineers. *Computing Sci. Eng.* 13:9-12.

Milly, P.C.D., Dunne, K., and Vecchia, V. 2005. Global pattern of trends in streamflow and water availability in a changing climate. *Nat.* 438:347-350. https://doi.org/10.1038/nature04312.

Mishra, A. K. and Singh, V.P. 2010. A review of drought concepts. *J. Hydrol.* 391:202-16.

Mishra, A., Froebrich, J., and Gassman, P. W. 2007. Evaluation of the SWAT model for assessing sediment control structures in a small watershed in India. *Trans. ASABE.* 50(2):469-478.

Mishra, V. and Lilhare, R. 2016. Hydrologic sensitivity of Indian sub-continental river basins to climate change. *Glob. Planetary Change*. 139:78-96.

Monteith, J. L. 1977.Climate and the efficiency of crop production in Britain.*Philosophical Trans. R. Soc. Lond*. 281:277-329.

Moriasi, D. N., Arnold, J. G., Van Liew, M. W., Bingner, R. L., Harmel, R. D., and Veith T. L. 2007. Model evaluation guidelines for systematic quantification of accuracy in watershed simulations. *Am. Soc. Agric. Biol. Eng.* 50(3):885-900.

Moss, R., Babiker, M., Brinkman, S., Calvo, E., Carter, T., Edmonds, J., Elgizouli, I., Emori, S., Lin, E., Hibbard, K., Jones, R., Kainuma, M., Kelleher, J., Lamarque, J. F., Manning, M., Matthews, B., Meehl, J., Meyer, L., Mitchell, J., and Zurek, M. 2008. *Towards new scenarios for analysis of emissions, climate change, impacts, and response strategies*. Intergovernmental Panel on Climate Change, Geneva, 25 pp.

Muller, J.C.Y. 2014. Adapting to climate change and addressing drought – learning from the Red Cross Red Crescent experiences in the Horn of Africa. *Weather Clim. Extremes.* 3:31-36.

Nagaveni, C., Kumar, K.P., and Ravibabu, M.V. 2019. Evaluation of TanDEMx and SRTM DEM on watershed simulated runoff estimation. *J. Earth System Sci*. 128 (1):2.

Nash, J. E. and Sutcliffe, J. V. 1970. River flow forecasting through conceptual models: Part-I A discussion of principles. *J. Hydrol*. 10(3):282-290.

Nasrin, Z., Gholamabbas, S., and Ebrahim, H.S. 2013. Hydrological and Sediment Transport Modelling in Maroon Dam Catchment Using Soil and Water Assessment Tool (SWAT). *Int. J. Agron. Plant Prod.* 4(10):2791-2795.

Neitsch, S. L., Arnold, J. G., Kiniry, J. R., and Williams, J. R. 2005. Soil and Water Assessment Tool Theoretical Documentation. Ver. 2005. Temple, Tex.: USDA-ARS Grassland Soil and Water Research Laboratory, and Texas A.M University, Blackland Research and Extension Center.

Neitsch, S. L., Arnold, J. G., Kiniry, J. R., and Williams, J. R. 2011. Soil and Water Assessment Tool Theoretical Documentation Version 2009. (No. Technical Report No. 406). Texas Water Resources Institute, Temple. Texas.

Neitsch, S.L., Arnold, J.G., Kiniry, J.R., Srinivasan, R., and Williams, J.R. 2002. Soil and Water Assessment Tool User's Manual, Version, 2000. College Station, TX: Texas Water Resources Institute.

Neitsch, S.L., Arnold, J.G., Kiniry, J.R., Williams, J.R., and King, K.W. 2005a. Soil and Water Assessment Tool Theoretical Documentation Grassland, Soil and Water Research Laboratory, Temple ,Texas, pp. 506.

Ng, H.Y.F. and Marsalek, J. 1992. Sensitivity of streamflow simulation to changes in climatic inputs. *Nord Hydrol*. 23:257-272.

Ngigi, S.N., Savenije, H.H., and Gichuki, F.N. 2007. Land use changes and hydrological impacts related to up-scaling of rainwater harvesting and management in upper Ewaso Ng'iro river basin, Kenya. *Land Use Policy*. 24(1):129-140.

Nunes, J. P., Seixas, J., Keizer, J. J., and Ferreira, A. J. D. 2009. Sensitivity of runoff and soil erosion to climate change in two Mediterranean watersheds: Part I. Model parameterization and evaluation. *Hydrological Processes*. 23(8):1202-1211. doi:10.1002/hyp.7247.

Nyssen, J., Poesen, J., Gebremichael, D., Vancampenhout, K., Daes, M., Yihdego, G., Govers, G., Leirs, H., Moeyersons, J., and Naudts, J. 2007. Interdisciplinary on-site evaluation of stone bunds to control soil erosion on cropland in Northern Ethiopia. *Soil Tillage Res*. 94(1):151-163.

Oki, T. and Kanae, S. 2006. Global hydrological cycles and world water resources. *Sci.* 313:1068-1072.

Oliphant, T.E. 2007. Python for scientific computing. *Computing Sci. Eng*. 9:10-20.

Osborne, T., Rose, G., and Wheeler, T. 2013. Variation in the global-scale impacts of climate change on crop productivity due to climate model uncertainty and adaptation. *Agric. For. Meteorol*. 170:183-194.

Ouessar, M., Bruggeman, A., Abdelli, F., Mohtar, R., Gabriels, D., and Cornelis, W. 2009. Modelling water-harvesting systems in the arid south of Tunisia using SWAT. *Hydrol. Earth System Sciences.* 13(10):2003-2021.

Panda, D. K., Kumar, A., and Mohanty S. 2011. Recent trends in sediment load of the tropical (Peninsular) river basins of India. *Glob. Planetary Change (GLOB. PLANET CHANGE).* 75(3):108-118.

Parajuli, P. B., Mankin, K. R., and Barnes, P. L. 2008. Applicability of targeting vegetative filter strips to abate fecal bacteria and sediment yield using SWAT. *Agric. Water Manag.* 95:1189-1200.

Parlange, M. B., and Katz, R. W. 2000. An extended version of the Richardson model for simulating daily weather variables. *J. Appl. Meteorol.* 39(5):610-622.

Pisinaras, V., Petalas, C., Gikas, G.D., Gemitzi, A., and Tsihrintzis, V.A. 2010. Hydrological andwater quality modelling in a medium- sized basin using the Soil and Water Assessment Tool (SWAT). *Desalination*. 250:274-286.

Pla, I. 2000. Hydrological approach to soil and water conservation, *In* Keynotes-ESSC Third International Congress. Valencia, Spain. pp. 45-69.

Potter, K.W. 1991. Hydrological impacts of changing land management practices in a moderate-sized agricultural catchment. *Water Resources Res.* 27(5):845-855.

Priestley, C. H. B. and Taylor, R. J. 1972. On the assessment of surface heat flux and evaporation using large-scale parameters. *Mon. Weather Rev.* 100:81-92.

Quinton, J.N., Edwards, G.M., and Morgan, R.P.C. 1997. The influence of vegetation species and plant properties on runoff and soil erosion: results from a rainfall simulation study in south east Spain. *Soil Use Manag.* 13:143-148.

Racherla, P. N., Shindell, D. T., and Faluvegi, G. S. 2012. The added value to global model projections of climate change by dynamical downscaling: A case study over the continental U.S. using the GISS-ModelE2 and WRF models. *J. Geophys. Res.* 117:D20118. doi:10.1029/2012JD018091.

Raj, N.P.P. and Azeez, P.A. 2009. Historical Analysis of the First Rain Event and the Number of Rain Days in the Western Part of Palakkad Gap, South India, Climate Change: Global Risks, Challenges and Decisions. *IOP Conf. Ser. Earth Environ. Sci.* 6(7).

Raj, N.P.P. and Azeez, P.A. 2012. Trend analysis of rainfall in Bharathapuzha river basin, Kerala, India. *Int. J. Climatol*. 32:533-539.

Raj, N.P.P. and Azeez, P.A. 2009. Spatial and temporal variation in surface water chemistry of a tropical river, the river Bharathapuzha, India. *Curr Sci*. 96(2):245-251.

Rajczak, J. and Schar, C. 2017. Projections of future precipitation extremes over Europe: A multimodel assessment of climate simulations. *J. Geophys. Res.: Atmospheres*. 122(10):773-800.

Rast, M., Johannessen, J., and Mauser, W. 2014. Review of Understanding of Earth's Hydrological Cycle: Observations, Theory and Modelling. *Surveys Geophys.* 35(3):491-513. doi:10.1007/s10712-014-9279-x.

Rathjens, H., Bieger, K., Srinivasan, R., Chaubey, I., and Arnold, J.G. 2016. CMhyd User Manual. Available online: http://swat.tamu.edu/software/cmhyd/

Riahi, K., Rao, S., Krey, V., Cho, C., Chirkov, V., Fischer, G., Kindermann, G., Nakicenovic, N., and Rafaj, P. 2011. RCP 8.5 - A scenario of comparatively high greenhouse gasemissions. *Climatic Change*. 109:33-57.

Rummukainen, M. 2010. State-of-the-art with regional climate models. *Wiley Interdisciplinary Reviews: Clim. Change.* 1(1):82-96.

Sahin,V. and Hall, M.J. 1996. The effects of afforestation and deforestation on water yields. *J. Hydrol.* 178(1/4):293-309.

Saltelli, A., Ratto, M., Andres, T., Campolongo, F., Cariboni, J., and Gatelli, D. 2008. *Global sensitivity analysis: the primer*. John Wiley., Sons Ltd, England, 5p.

Sandstrom, K. 1995. Modelling the effects of rainfall variability on groundwater recharge in semi-arid Tanzania. *Nordic Hydrol*. 26:313-330.

Santhi, C., Srinivasan, R., Arnold, J. G., and Williams, J. R. 2006. A modelling approach toevaluate the impacts of water quality management plans implemented in a watershed in Texas. *Environ. Modelling Software*. 21(8):1141-1157.

Santhi, C., Srinivasan, R., Arnold, J.G., and Williams, J.R. 2003. A modelling approach to evaluate the impacts of water quality management plans implemented in the Big Cypress Creek watershed. In : Saleh A (ed). ASAE: St Joseph, *Total Maximum Daily Load (TMDL) Environmental Regulations-II.* Proceedings of the 8-12 November 2003 Conference. Albuquerque, New Mexico USA, pp 384-394.

Sathya, A. and Thampi, S.G. 2020. Impact of Projected Climate Change on Streamflow and Sediment Yield – A Case Study of the Chaliyar River Basin, Kerala. In: *Roorkee Water Conclave;* 26-28, February, 2020. Indian Institute of Technology, Roorkee and National Institute of Hydrology, Roorkee.

Schiettecatte, W., Ouessar, M., Gabriels, D., Tanghe, S., Heirman, S., and Abdelli, F. 2005. Impact of water harvesting techniques on soil and water conservation: a case study on a micro catchment in southeastern Tunisia. *J. Arid Environments*. 61(2):297-313.

Seaby, L. P., Refsgaard, J. C., Sonnenborg, T. O., Stisen, S., Christensen, J. H., and Jensen, K.H. 2013. Assessment of robustness and significance of climate change signals for an ensemble of distribution-based scaled climate projections. *J. Hydrol*. 486:479-493.

Seager, R., Kushnir, Y., Ting, M., Cane, M., Naik, N., and Miller, J. 2008. Would advance knowledge of 1930s SSTs have allowed prediction of the dust bowl drought?. *J. Clim.* 21:3261-81.

Sen, O.L., Wang, Y., and Wang, B. 2004. Impact of Indochina deforestation on the East-Asian summer monsoon. *J. Clim.* 17:1366-1380.

Seneviratne, S.I., Corti, T., Davin, E.L., Hirschi, M., Jaeger, E.B., Lehner, I., Orlowsky, B., and Teuling, A.J. 2010. Investigating soil moisture-climate interactions in a changing climate: a review. *Earth-Sci. Reviews.* 99:125-161.

Sharpley, A. N. and Williams, J. R. 1990. *EPIC-Erosion Productivity Impact Calculator, 1.Model Documentation*.U.S. Department of Agriculture, Agricultural Research Service, Technical Bulletin 1768. 235 p.

Shoemaker, C.A., Haith, D.A., and Benaman, J. 2005. Calibration and validation of soil and water assessment tool on an agricultural watershed in upstate New York. *J. Hydrologic Eng.* (10):363-374.

Shrestha, S. and Htut, A.Y. 2016. Land use and climate change impacts on the hydrology of the Bago River basin, Myanmar. *Environ. Model. Assess*. 21:819-833.

Singh, A. and Gosain, A.K. 2011. Scenario generation using geographical information system (GIS) base hydrological modelling for a multi-jurisdictional Indian River basin. *J. Oceanogr. Mar. Sci.* 2:140-147.

Singh, J., Knapp, H.V., and Demissie, M. 2004. *Hydrologic Modeling of the Iroquois River Watershed Using HSPF and SWAT*; ISWS CR 2004-08. Illionois State Water Survey: Champaign, IL, USA.

Singh, V. P. 1995. *Computer Models of Watershed Hydrology.* Highlands Ranch, CO: Water Resources Publications.

Smith, R.E. and Scott, D.F. 1992. The effects of afforestation on low flows in various regions of South Africa. *Water SA.* 18(3):185-194.

Sorg, A., Bolch, T., Stoffel, M., Solomina, O., and Beniston, M. 2012. Climate change impacts on glaciers and runoff in Tien Shan (Central Asia). *Nat. Clim. Change*. 2(10):725-731.

Srinivasan, R., Ramanarayanan, T.S., Arnold, J.G., and Bednarz, S.T. 1998. Large area hydrologic modelling and assessment part II: model application. *J. Am. Water Resources Assoc.* 34(1):91-101.

Stonefelt, M. D., Fontaine, T. A., and Hotchkiss, R. H. 2000. Impacts of climate change on water yield in the upper Wind River basin. *J. Am. Water Resour. Assoc.* 36(2):321-336.

Sunandar, A.D., Suhendang, E., Hendrayanto., Jaya, I.N.S., and Marimin. 2014. Land use optimization in Asahan watershed with linear programming and SWAT model. *Int. J. Sci. Basic Appl. Res.*18:63-78.

Surendran, U., Kumar, V., Ramasubramoniam, S., and Raja, P. 2017. Development of Drought Indices for Semi-Arid Region Using Drought Indices Calculator (DrinC) – A Case Study from Madurai District, a Semi-Arid Region in India. *Water Resources Manag.* 31(11):3593-3605.

Tan, M.L., Ibrahim, A.L., Yusop, Z., Chua, V.P., and Chan, N.W. 2017. Climate change impacts under CMIP5 RCP scenarios on water resources of the Kelantan River basin, Malaysia. *Atmos. Res.* 189:1-10.

Tang, Q. and Lettenmaier, D. P. 2012. 21st century runoff sensitivities of major global river basins. *Geophys. Res. Letters.* 39(39):6403.

Tarigan, S., Wiegand, K., Sunarti., and Slamet, B. 2018. Minimum forest cover required for sustainable water flow regulation of a watershed: A case study in Jambi province, Indonesia. *Hydrol. Earth Syst. Sci*. 22:581-594.

Taylor, K. E., Stouffer, R. J., and Meehl, G. A. 2012. An overview of CMIP5 and the experiment design. *Bull. Amer. Meteor. Soc*. 93:485-498.

Tebaldi, C. and Knutti, R. 2007. The use of the multimodel ensemble in probabilistic climate projections. *Phil. Trans. R. Soc. A*. 365:2053-2075.

Tejaswini, V. and Sathian, K.K. 2018. Calibration and Validation of Swat Model for Kunthipuzha Basin Using SUFI-2 Algorithm. *Int. J. Curr. Microbiol. App. Sci.* 7(01):2162-2172.

Tesfaye. Y.G., Meerschaert, M.M., and Anderson, P.L. 2006. Identification of periodic autoregressive moving average models and their application to the modeling of river flows. *Water Resources Res.* 42:W01419.

Tessema, S. M. 2011. Hydrological modeling as a tool for sustainable water resources management: a case study of the Awash River basin. TRITA LWR. LIC 2056.

Teutschbein, C. and Seibert, J. 2012. Bias correction of regional climate model simulations for hydrological climate-change impact studies: Review and evaluation of different methods. *J. Hydrol.* 456:12-29.

Thom, H.C.S. 1958. A note on the gamma distribution. *Mon. Weather Rev*. 86: 117-122.

Tigkas, D. and Tsakiris, G. 2004. Medbasin: A Mediterranean rainfall-runoff software package. *European Water*. 5(6):3-11.

Tigkas, D., Vangelis, H., and Tsakiris, G. 2013. The RDI as a composite climatic index. *Eur. Water*. 41:17-22.

Tolson, B. A. and Shoemaker, C. A. 2007. Cannonsville reservoir watershed SWAT2000 model development, calibration, and validation. *J. Hydrol*. 337(1-2):68-86.

Trenberth, K. E. and Shea, D. J. 2005. Relationships between precipitation and surface temperature. *Geophys. Res. Lett*. 32:L14703.

Trenberth, K. E., Dai, A., Van Der Schrier, G., Jones, P.D., Barichivich, J., Briffa, K. R., and Sheffield, J. 2014. Global warming and changes in drought. *Nat. Clim. Change*. 4:17-22.

Tripathi, M. P., Panda, R. K., and Raghuwanshi, N. S. 2003. Identification and prioritisation of critical sub-watersheds for soil conservation management using the SWAT model. *Biosys. Eng.* 85(3):365-379.

Trzaska, S. and Schnarr, E. 2014. *A review of downscaling methods for climate change projections.* United States Agency for International Development, Burlington, Vermont: Tetra Tech ARD.

Tsakiris G. and Vangelis, H. 2005. Establishing a Drought Index Incorporating Evapotranspiration. *European Water*. 9(10):3-11.

Tsakiris G., Vangelis H., and Tigkas, D. 2010. Drought impacts on yield potential in rainfed agriculture. In: Proceedings of 2nd International conference on drought management 'economics of drought and drought preparedness in a climate change context', 4–6 March 2010, Istanbul, Turkey, pp. 191-197.

Tsakiris, G., Pangalou, D., and Vangelis, H. 2007. Regional drought assessment based on the Reconnaissance Drought Index (RDI). *Water Resource Manag.* 21:821-833.

Tsakiris, G., Pangalou, D., Tigkas, D., and Vangelis, H. 2007a. Assessing the Areal Extent of Drought. Proceedings of EWRA Symposium "Water Resources Management: New Approaches and Technologies", Chania - Greece, 14-16 June 2007, pp. 59-66.

Unnikrishnan Warrier, C. and Manjula, P. 2014. River– groundwater interaction of a tropical sub basin of bharathapuzha, kerala, india. *Int. J. Advanced Technol. Eng. Sci.* 2(07):2348-7550.

Vache, K.B., Eilers, J.M., and Santelmann, M.V. 2002. Water quality modelling of alternative agricultural scenarios in the U.S. Corn Belt. *J. Am. Water Resources Assoc.* 38(3):773-787.

Vaighan, A.A., Talebbeydokhti, N., and Bavani, A.M. 2017. Assessing the impacts of climate and land use change on streamflow, water quality and suspended sediment in the Kor River Basin, Southwest of Iran. *Environ. Earth Sciences*. 76(15):543.

Van der Walt, S., Colbert, S., and Varoquaux, G. 2011. The numpy array: A structure for efficient numerical computation. *Computing Sci. Eng.* 13:22-30.

Van Griensven, A. and Bauwens, W. 2003. Multiobjective autocalibration for semidistributed water quality models. *Water Resour. Res.* 39(12):1348-1356.

Van Griensven, A., Francos, A., and Bauwens, W. 2002. Sensitivity analysis and auto calibration of an integral dynamic model for river water quality. *Water Sci. Technol.* 45:325-332.

Van Liew, M. W. and Garbrecht, J. 2003. Hydrologic simulation of the Little Washita River experimental watershed using SWAT. *J. Am. Water Resour. Assoc.* 39(2):413-426.

Van Liew, M. W., Arnold, J. G., and Bosch, D. D. 2005. Problems and potential of autocalibrating a hydrologic model. *Trans. ASAE.* 48(3):1025-1040.

Van Liew, M. W., Garbrecht, J.D., and Arnold, J.G. 2003. Simulation of the impacts of flood retarding structures on streamflow for a watershed in southwestern Oklahoma under dry, average, and wet climatic conditions. *J. Soil Water Conser.* 58(6):340-348.

Varis, O., Kajander, T., and Lemmela, R. 2004. Climate and water: From climate models to water resources management and vice versa. *Climatic Change*. 66(3):321-344.

Venkatesh, B., Chandramohan, T., Purandara, B. K., Jose, M. K., and Nayak, P. C. 2018. Modeling of a River Basin Using SWAT Model. In: Singh V., Yadav S., Yadava R. (eds), *Hydrologic Modeling*. Water Science and Technology Library, vol 81. Springer, Singapore.

Verbist, K., Cornelis, W., Gabriels, D., Alaerts, K., and Soto, G. 2009. Using an inverse modelling approach to evaluate the water retention in a simple water harvesting technique. *Hydrol. Earth System Sciences Discussions*. 6 (3):4265-4306.

Verstraeten, G., Van Oost, K., Van Rompaey, A., Poesen, J., and Govers, G. 2002. Evaluating an integrated approach to catchment management to reduce soil loss and sediment pollution through modelling. *Soil Use Manag*. 18:386-394.

Wheater, H.S., Sharma, K. D., and Sorooshian, S. 2008. *Hydrological Modelling in Arid and Semi-Arid Areas*. Cambridge University Press, New York , 223 p.

White, K.L. and Chaubey, I. 2005. Sensitivity analysis, calibration, and validations for a multisite and multivariable swat model. *J. Am. Water Resour. Assoc.* 41(5):1077-1089.

Wilby, R. L., Charles, S. P., Zorita, E., Timbal, B., Whetton, P., and Mearns, L. O. 2004. *Guidelines for use of climate scenarios developed from statistical downscaling methods. Supporting material of the intergovernmental panel on climate change.* Prepared on behalf of Task Group on Data and Scenario Support for Impacts and Climate Analysis (TGICA). Retrieved from the Data Distribution Centre of the Intergovernmental Panel on Climate Change.

Williams, J. R., Jones, C. A., and Dyke, P. T. 1984. A modelling approach to determining the relationship between erosion and soil productivity. *Trans. Am. Soc. Agric. Eng*. 27(1):129-144.

Williams, J.R. and Berndt, H.D. 1977. Sediment yield prediction based on watershed hydrology. *Trans. ASAE.* 20:1100-1104.

Winchell, M., Srinivasan, R., Di Luzio, M., and Arnold, J. 2013. ArcSWAT (2013) interface for SWAT 2012 – User's guide. Blackland Research and Extention Center Texas Agrilife Research., Grassland, Soil and Water Laboratory USDA Agricultural Research Service, Available at: Temple, Texas, USA.

Winchell, M., Srinivasan, R., Di Luzio, M., and Arnold, J.G. 2010. ArcSWAT Interface for SWAT 2009 – User's Guide. Texas Agricultural Experiment Station and USDA Agricultural Research Service, Temple (Texas).

Wisser, D., Frolking, S., Douglas, E.M., Fekete, B.M., Schumann, A.H., and Vorosmarty, C.J. 2010. The significance of local water resources captured in small reservoirs for crop production–A global-scale analysis. *J. Hydrol.* 384 (3):264-275.

WWDR (World Water Development Report). 2018. Nature-based Solutions for Water. Published by the United Nations Educational, Scientific and Cultural Organization, New York, United States.

Xiong, K. G., Yang, J., Wan, S. Q., Feng, G. L., and Hu, J. G. 2009. Monte Carlo simulation of the record-breaking high temperature events of climate change. *Acta Phys. Sinica.* 58(4):2843-2852.

Yang, X.Y., Liu, Q., He, Y., Luo, X.Z., and Zhang, X.X. 2016. Comparison of daily and sub-daily SWAT models for daily streamflow simulation in the Upper Huai River Basin of China. *Stochastic Environ. Res. Risk Assess*. 33:959-972.

Yazdi, J. and Moridi, A. Interactive Reservoir-Watershed Modeling Framework for Integrated Water Quality Management. 2017. *Water Resour. Manag.* 31:2105-2125. https://doi.org/10.1007/s11269-017-1627-4.

Zabaleta, A., Meaurio, M., Ruiz, E., and Antiguedad, I. 2014. Simulation climate change impact on runoff and sediment yield in a small watershed in the Basque Country, northern Spain. *J. Environ. Qual.* 43:235-245. doi:10.2134/jeq2012.0209.

Zhang, B., Shrestha, N.K., Daggupati, P., Rudra, R., Shukla, R., Kaur, B., and Hou, J. 2018. Quantifying the Impacts of Climate Change on Streamflow Dynamics of Two Major Rivers of the Northern Lake Erie Basin in Canada. *Sustainability*. 10:2897.

Zhang, X., Srinivasan, R., and Van Liew, M. 2008. Multi-Site Calibration of the SWAT Model for Hydrologic Modeling. *Trans. ASABE*. 51(6):2039-2049.

Zhao, W. J., Sun, W., Li, Z. L., Fan, Y. W., Song, J. S., and Wang, L. R. 2013. A Review on SWAT Model for Stream Flow Simulation. *Advanced Mater. Res.* 726-731:3792-3798.

Zhou, X., Zhang, Y., Wang, Y., Zhang, H., Vaze, J., Zhang, L., Yang, Y., and Zhou, Y. 2012. Benchmarking global land surface models against the observed mean annual runoff from 150 large basins. *J. Hydrol*. 470-471:269-279.

Zorita, E. and von Storch, H. 1999. The analog method as a simple statistical downscaling technique: comparison with more complicated methods. *J. Clim*. 12(8):2474-2489.

Appendices

Appendix I. Monthly average Precipitation (mm) of Pattambi during 1989-2017

Year	Jan	Feb	Mar	Apr	May	Jun	Jul	Aug	Sep	Oct	Nov	Dec
1989	0.00	0.00	1.00	87.80	92.60	844.80	438.00	254.60	239.80	295.30	46.80	0.00
1990	1.00	0.00	0.00	16.60	386.20	530.00	730.00	308.10	33.60	446.30	99.50	0.00
1991	35.60	0.00	0.00	137.00	75.00	879.80	993.90	497.40	110.90	456.00	67.80	0.00
1992	0.00	0.00	0.00	37.20	89.80	799.60	788.20	469.90	244.30	318.50	238.50	0.00
1993	0.00	54.70	2.40	9.30	163.60	734.80	699.10	314.10	47.00	297.20	113.90	7.20
1994	0.00	0.00	32.10	249.60	66.10	825.50	1012.80	386.40	195.90	409.30	85.70	0.00
1995	0.00	0.00	6.50	76.60	185.90	583.20	836.80	383.90	248.70	140.00	189.20	0.00
1996	0.00	0.00	65.80	75.40	68.70	386.10	579.30	226.40	338.80	300.00	43.00	14.20
1997	0.00	0.00	7.10	5.60	80.70	510.10	1194.30	453.60	236.60	230.90	273.70	72.00
1998	0.00	0.60	0.00	40.20	134.20	679.00	590.70	397.30	448.30	316.80	44.10	37.30
1999	0.00	0.00	0.40	37.80	467.20	757.00	788.80	150.60	39.80	278.30	29.90	0.80
2000	0.00	9.50	0.00	56.40	47.40	602.60	327.00	518.20	146.10	197.60	82.30	52.86
2001	0.00	51.60	0.00	155.30	142.00	791.20	497.80	225.80	162.50	239.80	143.90	0.00
2002	0.00	0.00	2.70	57.90	222.60	471.90	376.40	422.70	51.60	376.30	70.80	0.00
2003	0.00	90.60	62.60	182.40	19.8	503.60	403.60	232.40	81.00	354.60	44.80	19.20
2004	0.00	0.00	4.10	105.00	463.30	689.70	337.10	486.00	122.20	305.20	42.60	0.00
2005	21.00	45.00	0.00	238.20	101.40	567.60	736.60	271.80	471.70	121.10	126.20	112.90
2006	0.00	0.00	36.10	16.70	396.60	690.40	470.90	431.20	500.60	352.90	133.90	0.00
2007	0.00	0.00	0.00	53.90	184.80	728.20	1303.50	469.40	599.00	297.40	34.40	6.00
2008	0.00	46.90	117.50	7.60	73.20	535.10	322.70	182.30	302.00	312.90	7.60	0.00
2009	0.00	0.00	57.00	42.20	125.60	278.60	1070.20	198.20	222.60	143.60	323.40	0.00
2010	0.00	0.00	0.00	114.50	130.50	681.20	572.50	273.40	174.10	430.90	245.10	10.50
2011	0.00	20.00	21.00	172.20	108.40	759.00	456.90	452.10	388.60	229.70	147.00	0.00
2012	0.00	0.00	0.30	104.40	42.50	459.70	297.80	489.30	220.20	234.90	74.60	6.20
2013	0.00	79.50	55.20	0.00	19.80	934.30	895.90	262.30	242.60	155.20	104.60	0.20
2014	0.00	0.00	0.00	23.80	167.40	423.00	623.70	608.40	238.20	360.70	78.30	0.00
2015	0.00	0.00	0.40	139.40	203.90	435.50	429.60	201.40	229.40	317.80	194.20	101.50
2016	0.00	0.00	0.00	0.30	191.70	480.60	344.60	120.20	92.80	59.60	4.10	34.30
2017	0.00	0.00	42.30	1.60	190.60	550.50	354.40	412.90	291.20	64.20	101.70	35.40

Appendix II. Monthly average Precipitation (mm) of Mannarkkad during 1989-2017

Year	Jan	Feb	Mar	Apr	May	Jun	Jul	Aug	Sep	Oct	Nov	Dec
1989	0.00	0.00	8.54	70.10	77.54	531.13	404.59	180.23	173.58	235.69	59.07	13.25
1990	20.65	0.00	7.50	32.80	287.55	464.46	609.48	263.77	40.09	328.20	81.65	0.00
1991	0.00	0.00	3.80	66.60	60.40	782.40	678.00	255.00	78.00	329.80	55.20	0.00
1992	0.00	0.00	0.00	63.00	132.00	330.60	385.10	423.40	227.20	87.00	73.00	0.00
1993	0.00	27.00	4.00	5.00	83.50	257.50	414.60	246.00	15.00	252.00	17.00	5.00
1994	13.00	10.00	13.00	74.00	28.00	233.00	563.70	274.10	144.90	521.30	67.00	0.00
1995	11.00	0.00	17.00	61.00	195.40	550.50	756.00	567.00	186.50	313.30	185.00	0.00
1996	0.00	0.00	9.00	399.00	25.00	457.00	585.60	234.20	384.40	452.00	86.00	66.00
1997	0.00	0.00	59.00	0.00	135.40	401.00	1112.00	277.00	230.00	304.00	430.80	33.00
1998	0.00	0.00	65.20	40.00	161.00	702.20	609.00	511.10	281.10	380.10	254.00	75.40
1999	0.00	42.80	0.00	12.30	230.40	290.70	642.00	145.00	77.00	765.00	15.00	0.00
2000	0.00	9.40	13.00	157.00	79.00	533.00	240.00	403.30	305.00	248.90	132.00	0.00
2001	3.00	43.00	0.00	341.00	97.00	401.00	408.00	243.40	191.00	279.00	391.00	0.00
2002	0.00	0.00	40.70	59.00	282.00	240.00	187.50	451.00	82.00	578.00	76.00	0.00
2003	0.00	11.00	66.30	148.00	126.00	476.00	396.00	202.00	37.00	415.00	29.00	0.00
2004	1.00	0.00	43.00	107.00	440.00	597.00	298.30	383.00	150.70	295.20	87.00	0.00
2005	25.00	0.00	15.00	320.00	79.00	931.00	1036.00	270.00	494.00	355.00	214.00	78.00
2006	4.00	0.00	37.00	131.00	646.10	504.00	504.00	352.00	684.00	393.00	181.70	0.00
2007	0.00	2.00	0.00	136.00	275.00	818.00	1040.00	629.80	530.10	313.00	70.00	16.00
2008	0.00	27.00	286.00	20.90	49.70	526.80	329.30	250.70	303.70	407.70	8.20	0.00
2009	0.00	0.00	98.00	55.20	145.50	374.20	817.10	268.70	291.80	235.90	245.50	96.80
2010	0.00	0.00	18.80	200.80	198.80	715.20	418.80	307.20	202.20	685.60	521.60	6.20
2011	0.00	63.20	1.60	144.90	89.60	791.60	394.20	369.60	435.80	412.00	176.30	2.40
2012	0.00	0.00	22.00	201.40	94.80	380.40	301.80	376.10	127.90	221.60	65.10	4.20
2013	0.00	2.10	27.40	9.00	144.20	680.90	684.30	237.20	529.40	292.50	77.80	5.80
2014	0.00	6.20	29.00	45.60	144.50	358.50	820.80	589.60	302.60	494.40	45.40	29.70
2015	0.00	0.00	4.20	177.00	305.30	561.70	190.40	197.70	230.90	164.80	309.40	25.20
2016	0.00	0.00	0.00	28.80	204.10	658.20	423.90	87.60	40.60	132.30	37.80	23.00
2017	0.00	0.00	102.70	12.30	146.60	441.10	259.00	489.70	829.60	207.50	1.80	81.00

Appendix III. Monthly average Maximum temperature (°C) of Pattambi during 1989-2017

Year	Jan	Feb	Mar	Apr	May	Jun	Jul	Aug	Sep	Oct	Nov	Dec
1989	34.49	36.36	36.95	36.02	34.19	30.01	29.74	29.79	30.16	30.89	32.42	33.05
1990	33.48	35.00	36.17	35.99	32.49	30.06	29.01	29.35	31.37	32.43	31.72	32.54
1991	33.54	35.61	36.82	35.57	34.84	29.89	29.46	29.23	31.73	31.07	31.70	32.19
1992	32.76	34.58	37.03	36.56	34.05	30.59	29.04	29.04	30.36	30.79	31.66	31.49
1993	42.45	34.51	35.53	36.42	34.85	30.45	29.12	29.47	31.05	31.23	31.60	31.56
1994	33.31	34.54	36.84	34.43	34.45	29.44	28.64	29.67	31.26	31.63	31.87	32.25
1995	32.92	34.85	36.76	36.16	32.77	30.89	28.75	29.61	30.51	32.14	31.62	32.48
1996	33.45	34.87	36.74	34.59	34.08	31.11	29.47	29.57	29.59	30.73	32.30	31.74
1997	32.79	34.74	36.31	36.10	34.94	31.41	28.82	29.24	31.50	32.41	32.10	32.28
1998	33.65	34.41	36.36	36.45	34.90	30.41	29.36	29.98	29.42	29.67	31.60	31.11
1999	32.81	35.18	35.96	33.84	30.81	29.89	28.41	30.05	31.69	30.68	31.79	32.14
2000	33.85	34.21	36.03	34.81	34.38	29.49	29.93	29.04	30.65	30.66	32.03	31.25
2001	33.11	34.31	35.20	34.41	32.99	29.33	29.27	29.53	31.61	31.15	31.82	31.87
2002	33.15	34.89	37.01	35.54	32.19	30.04	30.12	28.85	31.57	31.04	32.00	32.84
2003	33.27	35.16	35.18	34.76	33.73	31.11	29.82	30.14	31.23	31.17	31.87	32.65
2004	33.58	35.55	36.69	34.70	30.18	29.75	29.30	29.45	30.91	31.31	31.98	32.98
2005	33.78	35.35	36.26	34.01	34.06	30.50	28.98	29.76	29.77	31.32	31.53	32.18
2006	33.53	34.90	35.34	35.14	33.16	30.34	29.63	30.14	29.92	30.99	31.54	32.10
2007	33.13	34.65	36.49	36.37	33.84	30.20	28.26	29.62	29.41	30.52	32.09	32.12
2008	32.79	34.02	33.78	34.16	33.84	30.10	29.72	30.22	30.49	31.77	32.55	32.29
2009	32.82	33.23	33.75	34.08	33.04	30.48	28.20	29.50	29.65	31.60	31.77	32.47
2010	33.72	35.78	37.10	35.65	33.95	30.79	29.55	29.41	30.66	30.47	30.70	30.99
2011	33.12	34.34	35.56	34.55	33.66	29.84	29.43	29.64	30.17	32.14	31.52	32.44
2012	32.95	35.41	35.60	35.28	33.56	30.61	29.95	29.25	30.59	32.40	32.01	33.19
2013	34.44	35.10	36.01	35.75	34.93	28.96	28.72	29.83	30.36	30.97	32.39	31.96
2014	33.25	35.02	37.19	36.07	34.11	31.49	29.98	29.60	31.19	28.24	31.43	32.65
2015	33.18	34.79	35.88	33.40	32.95	31.20	30.50	31.00	31.80	32.45	32.04	32.54
2016	33.13	34.95	36.92	36.99	34.17	30.14	29.78	30.51	30.26	31.46	33.04	32.67
2017	34.13	35.80	35.78	35.75	34.46	29.65	30.17	29.71	30.91	31.24	32.18	31.87

Appendix IV. Monthly average Maximum temperature (°C) of Pulamanthole during 1989-2017

Year	Jan	Feb	Mar	Apr	May	Jun	Jul	Aug	Sep	Oct	Nov	Dec
1989	33.18	36.79	38.23	36.42	34.21	29.60	29.24	29.35	30.23	30.90	32.10	32.11
1990	33.18	35.05	37.16	36.22	31.76	28.77	27.35	28.11	30.72	30.87	28.85	30.53
1991	32.98	36.89	37.74	35.73	35.60	30.02	30.06	30.10	33.90	31.34	32.32	32.53
1992	34.05	35.16	37.06	37.35	34.95	30.27	29.24	29.24	30.70	30.89	32.08	33.00
1993	34.27	35.32	36.21	36.75	35.55	31.50	28.77	30.05	31.72	31.34	32.63	32.55
1994	34.11	35.86	37.48	35.28	35.16	28.78	28.03	29.90	31.83	31.87	33.43	33.79
1995	34.37	36.43	37.65	37.82	34.18	31.03	28.74	28.81	29.18	30.45	29.02	28.53
1996	29.47	31.69	33.94	32.63	32.50	30.12	28.37	29.31	29.20	29.10	29.27	27.66
1997	28.84	30.93	33.19	33.52	32.89	30.33	27.95	28.29	29.78	30.08	29.25	29.34
1998	29.23	31.80	33.73	34.82	33.66	29.18	28.29	28.95	27.88	28.05	28.67	28.00
1999	28.89	31.45	33.61	32.92	30.10	29.08	27.53	28.73	30.13	29.65	28.98	28.73
2000	30.19	31.00	33.39	32.90	32.98	28.98	29.10	28.71	29.73	28.76	29.00	28.00
2001	29.68	30.89	32.77	33.02	31.58	27.95	28.35	28.02	29.48	28.71	28.60	28.44
2002	29.52	31.50	33.26	33.47	31.87	29.13	29.05	28.24	30.38	29.10	29.48	27.81
2003	29.53	31.20	31.85	32.50	32.50	30.02	28.03	28.84	30.08	29.56	29.62	28.79
2004	30.58	32.16	34.61	33.23	29.61	28.27	28.65	29.08	29.43	29.81	28.97	29.15
2005	31.06	32.21	34.84	32.52	34.08	29.58	28.34	29.77	29.43	29.82	29.42	29.18
2006	30.47	32.30	33.69	34.22	32.79	29.90	28.61	29.00	29.12	29.03	29.52	29.34
2007	30.19	32.02	34.89	35.23	33.37	29.63	27.56	28.52	28.17	29.15	29.15	29.56
2008	29.82	31.81	33.69	36.22	35.68	31.73	30.78	31.40	31.43	31.68	31.88	31.42
2009	31.98	34.46	35.94	36.25	35.18	32.33	29.15	31.42	30.92	32.15	31.52	31.24
2010	31.98	34.68	37.39	36.92	35.79	32.07	30.48	31.08	31.57	30.53	30.17	29.65
2011	31.21	33.14	36.05	35.57	35.74	31.38	29.48	28.94	28.58	30.24	29.27	29.26
2012	29.31	31.50	32.66	33.00	32.61	29.57	29.37	28.81	29.40	31.24	30.80	31.53
2013	32.63	34.63	36.42	36.35	35.15	28.32	28.16	29.48	30.17	30.95	31.82	31.97
2014	33.58	20.52	37.11	35.88	33.35	30.55	28.56	28.69	30.05	30.71	30.57	29.47
2015	30.76	32.91	34.60	33.78	31.92	29.17	29.16	30.05	30.33	30.06	30.12	30.71
2016	31.81	33.31	35.00	35.80	33.29	28.65	28.37	29.24	29.40	29.84	30.57	30.69
2017	32.03	34.52	34.73	34.57	33.65	28.88	28.79	28.71	29.40	29.52	30.67	30.56

Appendix V. Monthly average Minimum temperature (°C) of Pattambi during 1989-2017

Year	Jan	Feb	Mar	Apr	May	Jun	Jul	Aug	Sep	Oct	Nov	Dec
1989	19.17	18.63	21.62	24.92	24.98	22.64	23.24	22.84	22.85	22.97	21.57	21.05
1990	17.31	17.51	19.01	20.97	20.37	19.17	20.03	22.70	23.44	23.34	22.18	21.92
1991	20.28	20.15	24.33	24.76	25.35	23.39	22.46	22.34	23.12	22.88	21.78	19.58
1992	18.76	20.84	21.83	23.73	23.95	22.65	22.17	28.86	22.35	21.84	21.54	19.47
1993	18.70	20.49	22.76	24.03	23.96	22.93	22.04	22.45	22.00	22.26	21.27	20.02
1994	19.77	19.90	21.29	22.13	22.75	21.20	20.33	20.88	20.47	20.66	20.15	19.39
1995	20.73	22.28	22.87	24.33	23.69	23.29	22.29	22.76	22.40	22.14	21.36	17.71
1996	18.47	19.60	21.17	23.50	24.03	23.49	22.33	22.36	22.54	21.67	21.45	19.57
1997	18.95	18.75	21.57	23.13	24.58	23.64	22.98	23.32	23.50	23.33	23.41	23.06
1998	22.00	22.29	36.18	26.02	25.82	23.62	23.47	23.79	23.36	23.00	22.73	21.18
1999	19.08	21.56	23.55	23.90	23.73	23.12	22.74	23.38	23.27	23.44	22.18	21.33
2000	21.69	22.09	23.47	24.93	24.55	23.03	22.75	22.52	23.06	22.23	21.32	18.93
2001	21.17	22.06	23.25	24.14	23.65	22.78	22.47	22.67	23.27	23.23	22.54	20.74
2002	21.15	21.59	23.84	24.90	24.12	22.63	23.40	23.25	23.22	23.67	23.07	19.72
2003	21.06	22.94	24.05	24.51	25.78	23.90	23.41	30.79	23.28	23.58	22.49	20.35
2004	20.81	21.27	23.73	25.08	24.20	23.49	23.53	23.20	23.57	23.23	22.14	21.00
2005	20.66	20.84	23.86	24.26	24.62	23.66	23.32	23.18	23.31	23.60	22.45	20.80
2006	21.04	20.57	23.35	24.61	24.72	24.09	23.47	23.48	23.42	23.44	23.18	21.17
2007	20.22	21.02	23.89	24.71	24.64	24.08	23.45	23.40	23.64	23.22	21.48	21.03
2008	19.67	21.72	22.14	24.87	24.94	23.69	23.74	23.90	23.29	23.42	22.82	20.22
2009	22.00	23.51	24.97	26.06	25.18	23.92	22.62	23.51	23.69	23.90	24.02	23.75
2010	21.42	22.86	24.21	25.29	25.66	24.24	23.51	23.65	23.63	23.45	23.15	21.09
2011	20.78	19.81	23.20	24.28	24.75	23.77	23.35	23.46	23.33	23.58	21.98	21.03
2012	20.01	21.14	23.89	25.01	25.48	24.13	23.87	23.78	23.66	23.65	22.30	21.70
2013	20.67	22.65	24.06	25.51	25.87	23.81	23.30	23.75	23.70	23.44	23.07	20.31
2014	21.27	21.18	23.05	25.35	24.96	24.33	23.27	23.26	23.24	26.25	23.07	21.79
2015	20.20	20.94	23.50	23.80	21.87	20.95	23.49	23.70	23.74	23.99	23.40	22.52
2016	21.41	22.30	24.97	26.50	25.18	23.88	23.83	23.88	23.56	23.14	22.58	21.47
2017	20.93	21.58	23.52	25.46	24.70	23.69	23.10	23.77	23.58	23.44	22.65	20.96

Appendix VI. Monthly average Minimum temperature (°C) of Pulamanthole during 1989-2017

Year	Jan	Feb	Mar	Apr	May	Jun	Jul	Aug	Sep	Oct	Nov	Dec
1989	19.98	19.66	22.23	20.32	24.55	22.18	22.89	22.60	22.93	23.06	21.62	21.15
1990	18.92	20.30	22.63	25.48	23.65	22.68	21.84	22.31	23.07	22.94	21.75	20.56
1991	19.89	19.98	23.84	24.05	25.19	23.28	22.15	22.15	22.77	19.05	21.95	19.23
1992	18.03	20.85	22.06	23.90	24.08	23.00	22.23	22.39	22.52	22.48	22.10	21.03
1993	17.79	19.82	22.56	24.12	24.16	23.07	22.08	22.81	22.85	22.63	22.02	20.85
1994	19.77	20.79	22.44	23.63	24.39	22.43	21.74	22.45	22.47	22.19	21.62	19.23
1995	19.73	21.54	22.58	24.02	23.71	23.52	23.34	25.92	25.50	25.87	24.83	22.45
1996	23.42	24.64	26.97	27.62	27.90	25.60	24.76	24.85	25.33	24.68	24.85	22.85
1997	23.56	24.27	26.73	27.98	27.68	26.48	24.15	24.55	25.23	24.84	24.60	25.31
1998	24.29	25.45	27.35	29.65	28.56	26.22	25.16	25.35	25.27	25.11	25.12	23.74
1999	22.53	24.55	26.61	27.05	25.81	25.00	24.81	25.65	26.03	25.55	24.57	23.89
2000	24.02	23.98	26.10	26.97	27.50	25.15	24.98	24.81	25.60	24.60	24.37	22.03
2001	23.79	24.71	26.61	27.05	26.98	24.80	24.76	24.89	25.48	25.15	25.03	23.55
2002	23.94	24.91	27.18	27.63	27.11	25.62	25.23	24.27	25.43	25.48	25.38	23.79
2003	23.65	25.04	26.50	27.38	28.10	26.18	24.39	25.48	25.75	25.47	24.78	23.06
2004	23.60	24.69	26.94	27.08	25.92	25.12	24.77	24.65	24.93	24.94	24.58	22.58
2005	23.32	24.45	26.55	26.90	27.77	25.27	24.16	24.61	24.47	24.56	23.95	22.58
2006	22.56	22.52	25.50	26.97	26.05	24.65	24.10	24.45	23.97	24.42	24.33	22.42
2007	22.40	23.23	26.32	27.03	26.82	24.82	23.66	24.15	23.92	24.02	22.93	22.82
2008	21.56	23.98	24.29	26.82	26.53	24.78	24.82	24.85	24.68	25.10	24.52	22.68
2009	22.68	24.02	26.37	27.20	26.97	25.78	24.05	25.39	25.55	25.58	25.12	24.00
2010	23.65	24.54	26.84	27.17	27.56	25.77	24.37	24.89	25.33	24.84	24.30	23.06
2011	22.60	22.80	25.74	26.38	26.68	24.48	25.45	25.55	25.68	26.61	25.33	24.45
2012	23.97	25.33	27.47	28.03	28.29	26.28	26.05	25.94	24.53	22.31	21.05	20.90
2013	20.55	21.02	23.18	24.43	24.65	22.27	21.84	22.56	22.40	21.87	22.22	20.82
2014	20.61	34.71	22.68	24.82	24.73	23.67	22.37	22.31	22.72	22.56	22.08	21.47
2015	21.37	21.32	22.82	23.82	22.98	23.08	22.92	22.82	23.07	23.19	22.60	21.94
2016	20.60	21.62	24.31	25.43	24.23	23.30	22.76	23.13	23.07	22.87	22.20	21.05
2017	20.08	21.36	23.24	25.22	24.39	23.52	22.87	23.29	23.35	23.39	22.58	21.34

Appendix VII. Monthly average Relative humidity (%) of Pattambi during 1989-2017

Year	Jan	Feb	Mar	Apr	May	Jun	Jul	Aug	Sep	Oct	Nov	Dec
1989	0.65	0.60	0.61	0.67	0.74	0.86	0.85	0.97	0.84	0.82	0.71	0.65
1990	0.68	0.63	0.66	0.69	0.80	0.86	0.86	0.85	0.77	0.78	0.79	0.67
1991	0.65	0.58	0.65	0.70	0.85	0.93	0.94	0.94	0.77	0.82	0.74	0.65
1992	0.55	0.63	0.60	0.67	0.75	0.83	0.86	0.86	0.82	0.81	0.78	0.63
1993	0.58	0.60	0.65	0.66	0.72	0.85	0.85	0.83	0.79	0.80	0.73	0.68
1994	0.60	0.61	0.62	0.74	0.70	0.86	0.88	0.82	0.79	0.79	0.70	0.60
1995	0.60	0.63	0.60	0.66	0.76	0.85	0.87	0.86	0.83	0.78	0.79	0.67
1996	0.60	0.57	0.61	0.73	0.72	0.81	0.86	0.86	0.85	0.82	0.77	0.70
1997	0.65	0.64	0.62	0.67	0.70	0.80	0.82	0.87	0.82	0.78	0.79	0.73
1998	0.62	0.63	0.66	0.68	0.74	0.86	0.87	0.84	0.86	0.84	0.77	0.70
1999	0.62	0.59	0.65	0.71	0.81	0.84	0.87	0.82	0.76	0.80	0.72	0.62
2000	0.56	0.62	0.61	0.70	0.69	0.85	0.83	0.86	0.80	0.83	0.72	0.65
2001	0.61	0.70	0.67	0.73	0.76	0.86	0.85	0.83	0.79	0.82	0.76	0.67
2002	0.61	0.70	0.67	0.73	0.76	0.86	0.85	0.83	0.79	0.82	0.76	0.67
2003	0.54	0.62	0.67	0.73	0.74	0.82	0.86	0.83	0.78	0.82	0.71	0.65
2004	0.59	0.54	0.62	0.71	0.84	0.84	0.84	0.84	0.81	0.79	0.70	0.61
2005	0.62	0.61	0.64	0.74	0.74	0.85	0.89	0.82	0.85	0.83	0.78	0.73
2006	0.63	0.54	0.67	0.69	0.74	0.84	0.86	0.83	0.84	0.82	0.76	0.63
2007	0.61	0.60	0.64	0.68	0.74	0.85	0.89	0.85	0.86	0.82	0.70	0.64
2008	0.63	0.65	0.67	0.70	0.70	0.84	0.83	0.81	0.81	0.78	0.74	0.65
2009	0.62	0.62	0.65	0.69	0.72	0.84	0.86	0.83	0.84	0.80	0.72	0.64
2010	0.61	0.61	0.64	0.68	0.71	0.83	0.85	0.82	0.83	0.79	0.71	0.63
2011	0.63	0.65	0.66	0.71	0.69	0.83	0.83	0.81	0.81	0.78	0.74	0.65
2012	0.61	0.58	0.67	0.69	0.74	0.83	0.83	0.85	0.81	0.76	0.74	0.65
2013	0.64	0.59	0.63	0.73	0.76	0.86	0.85	0.83	0.79	0.82	0.76	0.67
2014	0.75	0.85	0.81	0.82	0.88	0.93	0.94	0.95	0.94	0.94	0.92	0.87
2015	0.86	0.83	0.91	0.92	0.92	0.92	0.94	0.93	0.93	0.92	0.89	0.86
2016	0.81	0.86	0.85	0.85	0.90	0.94	0.93	0.93	0.92	0.92	0.88	0.87
2017	0.79	0.80	0.88	0.88	0.86	0.93	0.93	0.93	0.94	0.93	0.90	0.83

Appendix VIII. Monthly average Wind speed (m/s) of Pattambi during 1989-2017

Year	Jan	Feb	Mar	Apr	May	Jun	Jul	Aug	Sep	Oct	Nov	Dec
1989	1.39	1.16	0.90	1.50	1.39	1.09	1.54	1.47	1.00	0.77	1.24	2.21
1990	1.74	1.75	1.37	1.37	1.17	1.03	0.95	1.53	1.46	0.87	0.79	2.00
1991	1.62	1.47	1.35	1.19	1.08	1.02	1.17	1.14	1.23	0.78	1.13	1.61
1992	2.22	1.14	1.21	1.30	1.15	1.22	1.10	1.01	0.92	0.49	0.83	2.37
1993	1.69	1.80	1.26	1.16	1.23	0.94	1.10	1.33	1.03	0.66	0.91	1.58
1994	2.08	1.18	1.35	1.00	1.27	1.12	1.01	1.17	1.04	0.63	1.51	0.98
1995	0.70	1.68	1.28	1.21	1.09	0.91	1.01	1.07	1.14	0.75	0.24	1.65
1996	1.51	1.55	1.15	1.02	1.13	1.09	0.92	1.21	0.94	0.60	0.70	1.30
1997	1.42	1.03	1.19	1.17	1.19	0.66	0.56	0.01	0.76	0.75	0.71	1.19
1998	1.83	1.56	1.13	1.23	1.10	0.93	1.17	1.01	0.83	0.69	0.66	1.29
1999	1.58	1.44	1.08	1.44	1.03	0.96	1.12	1.18	1.04	0.59	0.98	1.87
2000	2.07	1.15	1.17	1.39	1.53	0.68	0.72	0.87	0.73	0.39	0.73	1.11
2001	1.37	0.77	1.01	0.80	0.98	0.87	0.99	1.17	1.10	0.90	0.92	1.93
2002	1.71	1.88	1.38	1.26	1.28	1.17	1.00	0.83	0.86	0.59	0.86	1.48
2003	1.82	1.14	0.96	0.83	1.14	0.84	0.71	0.90	0.89	0.44	1.54	1.34
2004	1.62	1.29	1.24	1.04	1.09	1.16	1.04	1.44	0.98	0.90	1.30	1.71
2005	1.34	1.34	1.23	0.97	1.01	0.83	1.05	0.99	0.92	0.57	0.82	0.94
2006	1.85	1.79	1.23	1.28	1.43	0.93	1.16	1.05	0.89	0.82	1.05	2.37
2007	2.00	1.57	1.24	1.25	1.19	1.06	0.93	1.05	0.82	0.86	0.91	1.78
2008	1.72	1.17	1.33	1.07	1.30	0.94	1.08	1.13	0.93	0.88	0.81	1.75
2009	1.98	1.32	1.22	0.83	1.07	0.77	0.66	0.62	0.61	0.67	0.90	1.70
2010	1.52	1.39	1.16	0.98	0.90	0.72	0.69	1.00	0.81	0.57	0.74	1.10
2011	1.37	1.18	1.18	1.01	0.96	0.63	0.53	0.58	0.46	0.47	0.71	0.95
2012	1.21	1.22	0.97	0.94	0.95	0.52	0.77	0.58	0.48	0.55	0.50	1.27
2013	1.16	1.34	1.00	0.95	1.10	0.74	0.70	1.05	0.74	0.64	0.77	1.15
2014	1.67	1.34	1.23	0.86	0.83	0.73	0.75	0.64	0.74	0.52	0.69	1.10
2015	1.51	1.54	1.57	0.72	0.57	0.65	0.72	0.75	0.58	0.46	0.84	1.47
2016	1.66	1.06	0.93	0.86	0.80	0.58	0.71	0.88	0.90	0.51	0.63	1.01
2017	1.52	1.58	0.94	0.92	0.93	0.84	1.18	1.47	1.24	0.75	0.94	2.09

Appendix IX. Monthly average Solar radiation (MJ/m²/day) of Pattambi during 1989-2017

Year	Jan	Feb	Mar	Apr	May	Jun	Jul	Aug	Sep	Oct	Nov	Dec
1989	28.90	34.28	21.08	28.97	28.92	10.20	15.92	22.59	19.38	22.19	30.32	33.76
1990	31.61	35.90	32.16	29.09	17.41	10.09	8.38	13.33	19.82	22.24	17.99	27.82
1991	30.59	35.40	31.12	28.84	28.65	7.79	7.72	9.45	27.54	14.86	24.26	30.02
1992	32.63	31.89	31.95	30.50	27.50	11.84	7.06	12.40	16.58	20.18	21.58	33.22
1993	30.31	34.02	30.39	31.99	27.74	12.88	9.20	18.07	22.64	17.69	22.20	26.21
1994	31.45	31.77	30.45	26.83	28.58	1.58	5.18	13.87	24.32	22.54	27.23	32.52
1995	30.89	34.23	32.24	33.14	25.42	15.23	7.46	18.33	23.20	25.05	23.41	35.33
1996	35.71	35.60	32.90	29.47	29.01	14.42	10.79	15.36	16.31	22.11	26.88	26.63
1997	33.75	32.86	33.00	33.17	28.07	21.43	10.23	12.44	25.36	24.97	24.35	27.49
1998	31.92	33.17	33.75	31.49	27.57	11.52	13.10	14.76	14.34	16.33	24.40	23.30
1999	31.89	31.65	30.44	23.99	18.55	17.63	8.02	20.10	24.52	16.54	28.45	31.20
2000	32.16	29.18	30.30	24.78	31.25	12.48	21.22	14.09	22.56	20.13	26.16	29.47
2001	29.71	30.24	31.23	25.28	25.44	10.45	12.76	16.06	22.93	18.62	24.23	31.68
2002	29.50	28.59	31.08	30.49	26.05	13.99	19.11	10.25	29.27	17.80	24.83	30.47
2003	32.95	31.73	31.73	27.24	26.36	18.14	8.64	17.50	27.11	27.63	26.06	32.16
2004	33.53	32.49	30.72	29.14	14.39	12.88	14.62	19.72	21.04	23.23	24.72	31.94
2005	30.08	34.98	32.86	28.42	29.75	13.37	8.62	20.14	18.43	17.77	17.51	28.14
2006	33.34	34.26	31.23	28.74	24.90	16.36	14.32	20.88	15.61	18.95	24.04	28.56
2007	29.30	33.74	30.67	28.74	27.50	14.93	5.38	14.06	10.14	18.30	27.76	26.09
2008	33.13	29.54	26.61	27.17	27.70	12.43	14.16	16.53	22.51	21.52	22.72	27.31
2009	32.32	33.20	29.89	24.60	24.00	17.69	6.60	19.28	15.96	21.63	21.38	27.15
2010	30.81	31.26	30.46	27.47	24.33	13.76	9.69	11.02	18.50	15.74	14.38	24.31
2011	29.03	29.67	31.82	25.31	26.92	10.84	9.49	10.02	16.87	22.12	22.12	26.00
2012	31.26	29.82	26.14	24.35	26.06	13.03	13.23	12.69	19.58	23.34	24.58	28.79
2013	29.09	29.49	28.88	27.10	18.60	5.54	3.39	15.18	14.86	17.79	19.88	27.36
2014	29.75	29.42	30.50	23.64	23.83	16.42	9.49	11.93	22.94	18.59	19.88	21.51
2015	31.82	31.43	30.09	26.27	20.40	10.91	17.55	22.88	22.58	17.86	18.67	25.99
2016	27.30	27.78	26.44	26.71	22.95	10.52	13.58	21.25	22.20	19.85	21.04	25.41
2017	28.32	30.28	27.91	24.58	21.66	9.84	12.91	12.37	17.62	17.33	21.76	26.55

Appendix X. Monthly average discharge (m^3/s) of Pulamanthole gauging station during 1989-2017

Year	Jan	Feb	Mar	Apr	May	Jun	Jul	Aug	Sep	Oct	Nov	Dec
1992	4.57	1.54	0.42	1.70	4.15	106.96	283.32	226.66	119.58	91.31	65.70	15.12
1993	6.19	4.09	2.99	2.09	7.89	55.37	148.80	137.09	42.90	114.37	34.11	11.65
1994	5.73	2.56	1.39	7.66	3.95	108.62	332.27	114.55	80.86	118.95	75.46	11.49
1995	5.51	2.43	1.74	2.37	14.83	49.45	181.70	138.15	134.15	50.29	70.76	11.05
1996	3.62	2.22	1.29	6.90	4.49	64.30	133.26	100.60	116.30	128.31	31.86	15.41
1997	5.68	3.16	2.12	3.02	2.91	18.10	276.65	177.67	88.39	55.22	91.96	27.40
1998	7.86	3.34	1.81	1.80	5.24	62.48	188.57	180.91	144.05	130.91	67.18	17.20
1999	6.11	4.64	2.20	2.75	22.37	153.73	191.43	131.93	22.50	152.09	34.50	14.04
2000	3.93	2.27	1.05	3.35	2.37	64.39	72.81	120.90	78.12	99.77	18.02	15.26
2001	4.82	3.69	1.52	9.26	6.89	129.77	135.25	90.88	47.92	80.36	90.12	14.38
2002	6.18	2.77	2.76	3.83	10.96	58.61	39.57	108.29	18.49	102.80	36.01	8.79
2003	3.09	3.19	5.56	4.35	4.63	34.62	69.17	54.00	22.24	46.89	14.25	6.66
2004	2.49	0.93	0.77	1.86	38.80	133.85	90.02	143.81	51.52	70.89	27.93	8.77
2005	2.36	2.06	0.58	10.44	4.40	68.69	257.03	122.96	133.74	80.12	51.46	22.02
2006	4.70	1.85	2.88	4.59	52.28	123.75	163.19	127.32	182.39	117.58	77.24	11.57
2007	4.50	3.51	3.31	3.87	7.01	101.99	393.43	187.87	189.16	102.85	43.09	8.18
2008	3.46	2.99	12.46	5.14	3.59	52.14	92.16	99.58	95.92	92.94	26.69	7.83
2009	2.18	0.00	0.74	0.00	2.92	18.79	286.40	84.23	120.55	78.60	60.06	11.91
2010	4.10	2.41	2.71	5.07	5.84	82.61	160.56	131.82	99.52	134.58	156.86	24.82
2011	8.01	3.42	3.08	12.52	5.40	183.97	145.21	159.30	187.94	72.87	67.51	12.68
2012	4.79	2.96	1.72	6.57	4.43	36.55	64.97	96.77	79.12	33.16	18.21	6.19
2013	3.14	1.04	1.27	0.59	1.69	160.85	254.16	133.08	134.13	62.63	23.52	10.52
2014	2.27	2.37	1.71	0.72	0.00	36.24	154.34	224.59	134.98	149.94	36.87	9.58
2015	2.19	1.40	2.32	4.07	16.08	84.14	78.84	48.72	35.73	39.94	43.71	14.03
2016	3.57	3.64	0.92	0.76	3.21	63.75	104.30	41.95	18.50	12.62	8.88	3.36
2017	1.29	0.00	0.00	0.00	0.28	30.73	60.39	93.87	245.96	75.13	17.26	8.96

Appendix XI. Annual Streamflow (Mm^3) of Pulamanthole gauging station during 1989-2017

Year	Streamflow (Mm^3)
1992	2452.28351
1993	1501.995312
1994	2287.882282
1995	1745.628624
1996	1618.455168
1997	2002.95504
1998	2146.872211
1999	1946.377037
2000	1282.777344
2001	1623.322426
2002	1051.831526
2003	703.8962208
2004	1514.684534
2005	2007.173088
2006	2298.409258
2007	2774.479824
2008	1298.388269
2009	1779.178176
2010	2155.133434
2011	2257.971898
2012	930.2487827
2013	2079.727204
2014	1997.399693
2015	988.4029536
2016	687.1636512
2017	1401.062746

Appendix XII. Bias corrected data of precipitation for different scenarios

Month	RCP4.5 2021-40	RCP4.5 2041-70	RCP8.5 2021-40	RCP8.5 2041-70	RCP6 2021-40	RCP6 2041-70
Jan	12.68	30.53	8.34	12.32	28.23	65.78
Feb	6.43	32.22	3.55	17.36	2.03	2.57
Mar	33.37	50.58	24.19	64.98	43.50	57.06
Apr	79.67	94.07	37.63	110.16	114.33	142.39
May	162.01	217.74	155.04	232.54	230.37	417.83
Jun	489.28	592.56	518.86	581.39	852.45	974.63
Jul	464.85	535.24	449.80	567.92	524.43	712.00
Aug	261.21	350.12	256.66	363.62	401.31	629.47
Sep	210.36	220.41	195.45	205.72	232.35	399.94
Oct	108.41	181.07	74.72	142.66	38.22	203.71
Nov	63.73	126.80	71.22	99.30	172.75	181.39
Dec	4.89	27.16	30.51	24.47	107.84	140.55

Appendix XIII. Bias corrected Maximum temperature (°C) data from 2021-70 under different scenarios

Month	**RCP_4.5**	**RCP_8.5**	**RCP_6**
Jan	34.90	35.09	31.80
Feb	35.79	35.90	33.54
Mar	37.15	37.68	37.97
Apr	36.28	36.41	38.37
May	34.62	34.65	36.59
Jun	31.62	31.66	32.40
Jul	30.83	30.84	30.86
Aug	30.64	30.50	30.93
Sep	31.65	31.79	32.09
Oct	31.98	32.21	32.21
Nov	32.93	32.99	32.05
Dec	33.33	33.26	31.04

Appendix XIV. Bias corrected Minimum temperature (°C) data from 2021-70 under different scenarios

Month	RCP_4.5	RCP_8.5	RCP_6
Jan	21.20	21.10	23.23
Feb	21.60	21.61	23.61
Mar	24.40	24.49	26.36
Apr	25.02	25.13	27.29
May	24.93	24.99	27.35
Jun	23.78	23.97	26.12
Jul	23.38	23.51	25.10
Aug	24.49	24.65	25.93
Sep	23.87	23.97	26.04
Oct	23.68	23.66	26.21
Nov	22.89	23.05	26.38
Dec	21.79	21.91	23.69

Appendix XV. Predicted annual streamflow under different scenario from 2021-40

Year	RCP_4.5	RCP_8.5	RCP_6
2021	3278.24	1319.93	2023.35
2022	3242.58	742.66	2634.29
2023	1434.45	2117.50	2106.06
2024	880.71	3922.52	3640.07
2025	1509.91	3368.33	3048.64
2026	1244.79	785.96	2430.38
2027	1918.06	834.27	2042.69
2028	2201.49	1229.14	3252.63
2029	1882.01	2065.38	2229.45
2030	1121.98	1301.16	2536.46
2031	1776.50	1447.91	3466.16
2032	2081.34	571.84	2057.17
2033	1077.61	3849.13	4093.65
2034	3269.20	1283.55	2217.28
2035	2774.13	1726.03	2957.75
2036	2050.29	3534.74	2238.18
2037	1292.49	2428.47	3359.37
2038	1460.40	1448.18	3121.39
2039	2179.75	2112.46	2016.84
2040	2200.78	1128.28	3733.66

Appendix XVI. Predicted annual streamflow (Mm^3) under different scenario from 2041-70

Year	RCP_4.5	RCP_8.5	RCP_6
2041	659.32	2030.11	3553.98
2042	1669.52	1577.09	1999.61
2043	1950.78	790.58	2418.35
2044	1044.72	3718.80	2121.34
2045	856.63	2698.40	1316.09
2046	873.74	1123.17	2438.29
2047	1551.65	2541.61	2825.19
2048	2779.26	931.49	2456.31
2049	1568.61	726.23	1193.47
2050	2849.24	2521.31	2314.18
2051	1352.92	1352.79	3567.66
2052	1713.70	2022.60	3600.49
2053	2026.93	1870.34	1964.01
2054	1529.89	2830.78	2196.51
2055	1899.72	1293.38	2341.23
2056	2033.47	2404.99	2302.83
2057	1028.38	1338.90	1888.38
2058	2467.13	1628.31	2041.08
2059	3106.07	1761.69	1804.84
2060	1865.33	1881.01	1825.21
2061	1908.89	1305.76	2615.23
2062	2898.38	1654.23	2484.95
2063	2138.85	3150.18	1934.86
2064	3470.26	2795.00	1732.20
2065	3216.00	2622.27	2926.88
2066	1887.57	2692.27	2231.71
2067	2684.96	2558.25	3224.03
2068	2029.71	1096.72	1430.46
2069	2404.77	2545.90	1951.25
2070	2069.48	2043.54	3796.77

Appendix XVII. Predicted monthly streamflow (Mm^3) under different scenario in comparison with observed from 2021-70

Month	RCP_4.5 2021-40	RCP_4.5 2041-70	RCP_8.5 2021-41	RCP_8.5 2041-70	RCP_6 2021-41	RCP_6 2041-70
Jan	39.78	41.86	31.35	32.33	56.92	60.52
Feb	20.31	21.11	15.76	18.90	33.31	54.62
Mar	9.47	10.84	7.97	9.21	15.54	25.19
Apr	35.35	36.60	19.98	33.24	38.40	55.98
May	70.28	54.46	44.99	29.81	72.10	82.82
Jun	299.66	370.18	425.73	478.07	545.94	615.87
Jul	390.66	400.75	464.78	521.25	499.80	583.14
Aug	345.75	346.94	319.36	347.93	370.39	410.06
Sep	264.73	265.77	194.32	186.83	272.20	314.87
Oct	237.57	203.52	160.82	152.67	250.40	286.49
Nov	143.25	144.39	107.92	110.74	139.09	170.05
Dec	87.03	88.11	67.87	62.63	55.82	100.65

Appendix XVIII. Predicted annual streamflow simulation (Mm^3) with and without conservation structures

Year	Without_structure	With_structure
1992	2129.37	2073.39
1993	1679.72	1627.06
1994	2339.85	2264.89
1995	1797.92	1741.50
1996	1341.85	1324.72
1997	2163.74	2089.33
1998	1972.51	1903.79
1999	1892.53	1826.69
2000	1300.41	1273.33
2001	1621.83	1564.53
2002	1337.13	1302.96
2003	1139.63	1112.40
2004	1787.70	1728.75
2005	1902.31	1836.69
2006	2254.35	2172.51
2007	2942.07	2825.87
2008	1218.13	1188.03
2009	1696.77	1643.22
2010	1798.27	1732.96
2011	2067.92	1990.08
2012	1305.81	1270.90
2013	2062.60	1985.25
2014	1863.43	1798.63
2015	1432.48	1383.37
2016	804.34	790.76
2017	1370.52	1328.91

Appendix XIX. Predicted monthly streamflow simulation (Mm^3) with and without conservation structures

Month	With_structure	Without_structure
Jan	27.89	18.64
Feb	17.27	3.26
Mar	19.65	2.35
Apr	20.03	4.19
May	30.51	27.38
Jun	311.79	318.57
Jul	416.18	418.12
Aug	286.53	287.12
Sep	218.91	219.80
Oct	206.39	206.93
Nov	123.54	120.39
Dec	60.66	57.11

Appendix XX. Predicted annual sediment yield (t/h) with and without conservation structures

Year	Without_structure	With_structure
1992	8.01	3.42
1993	3.82	2.15
1994	5.25	3.01
1995	5.75	1.93
1996	3.52	1.30
1997	6.06	1.55
1998	6.65	3.05
1999	4.87	1.82
2000	3.42	1.25
2001	3.82	1.69
2002	3.76	1.28
2003	2.19	1.11
2004	4.57	1.65
2005	5.17	2.47
2006	6.44	2.27
2007	8.76	3.58
2008	3.44	1.36
2009	4.07	1.71
2010	5.60	1.60
2011	5.53	2.01
2012	3.82	1.08
2013	6.60	2.55
2014	4.96	1.12
2015	3.78	1.19
2016	2.01	0.89
2017	3.46	1.37

Appendix XXI. Predicted monthly sediment yield (t/h) with and without conservation structures

Month	With_structure	Without_structure
Jan	0.024	0.019
Feb	0.015	0.009
Mar	0.029	0.003
Apr	0.060	0.041
May	0.020	0.014
Jun	0.568	1.848
Jul	0.376	1.011
Aug	0.332	0.770
Sep	0.172	0.672
Oct	0.133	0.338
Nov	0.072	0.053
Dec	0.062	0.045

MODELLING THE IMPACT OF CONSERVATION STRUCTURES AND CLIMATE CHANGE ON WATER YIELD IN A WATERSHED

by

FOUSIYA
(2018-18-001)

ABSTRACT OF THESIS

Submitted in partial fulfilment of the requirement for the degree of

MASTER OF TECHNOLOGY

IN

AGRICULTURAL ENGINEERING

(Soil and Water Engineering)

Faculty of Agricultural Engineering and Technology

Kerala Agricultural University

Department of Irrigation and Drainage Engineering

KELAPPAJI COLLEGE OF AGRICULTURAL ENGINEERING AND TECHNOLOGY

TAVANUR, MALAPPURAM- 679573

KERALA, INDIA

2020

ABSTRACT

Hydrological models have been increasingly used for the impact assessment of climate change and management practices on hydrological processes. In the Thuthapuzha watershed, where extreme events due to climate change and resulting changes in patterns of river flow predominate, proper management of water resources through soil and water conservation needs to be adapted in the future. In this research, SWAT model was used to simulate hydrological processes on a daily time-step in Thuthapuzha watershed, subbasin of Bharathapuzha located in Kerala, India. SWAT performs satisfactorily with Nash-Sutcliffe efficiency value (NSE) of 0.88, coefficient of determination (R^2) of 0.88 and Percent bias (PBIAS) of -1.4 for the calibration period (1989-2009) and R^2, NSE and PBIAS values of 0.8, 0.8 and 5.4 respectively for the validation period (2010-2017). The study concluded that the developed SWAT model can be used to predict streamflow from the watershed. So the developed model was then used for studying the impact of climate change and conservation structures on the hydrology of the watershed.

Quantification of changes in the water balance and soil erosion over a long period of time is necessary for watershed management. The developed SWAT model was used to understand the impact of conservation practices on hydrological processes. Major conservation practices in the study area were modelled as ponds and Kanjirapuzha reservoir within the study area was modelled as dam. The results obtained were analysed to study the impact of conservation structures on streamflow and found that monthly streamflow increased during summer season (9-17%) when the river has a very lean flow with the effect of conservation practices which helps in maintaining a better environmental flow regime. Conservation structures impact on sediment yield was also analysed by comparing the outputs with and without the addition of structures. In addition to the structural details, sediment yield analysis requires equilibrium sediment concentration value which is very difficult to estimate. Thus, a calibration process was again done for calibrating equilibrium sediment concentration using sediment yield output at the Pulamanthole gauging station (Jalowska and Yuan, 2018). For the study, it was assumed that the sediment yield output obtained from the calibrated model as the sediment yield with the addition of

structures. Monthly sediment yield showed a slight increase (0.001-0.04%) during the summer months whereas sediment yield decreased (0.2-1.3%) during peak flows with the addition of conservation structures.

Climate data are collected from CMIP5 and CORDEX-SA datasets of GFDL-CM3 climate model for RCP4.5, RCP6 and RCP8.5 scenarios and the bias corrected weather data were used as input in SWAT model. Comparison of streamflow and drought intensity based on predicted climate change scenarios is evaluated. The results of the future simulations of streamflow in SWAT reveal that, river flow increased under all RCP scenarios with predominant increase in RCP6 scenario (37-60%) followed by RCP4.5 (13-16%) and RCP8.5 (9-16%) from 2021-2070. Significant increase in streamflow was found during the end periods of simulation for all the scenarios taken for the study purpose. Results show the importance of climate change effect on water resources, where it does not have only an effect on precipitation and temperature, but the streamflow is also directly influenced by climate change. Thus, necessary steps should be taken to mitigate the extreme events due to streamflow increase during future periods.

In order to study the climatic condition in the Thuthapuzha watershed, drought intensity was calculated. Drought intensity was predicted using the SPI and RDI index for the period 1989-2017 and found that severely dry events have occurred once during 2015-16 when using SPI index. Comparison and regression analysis between both the indices showed that both were well correlated and similar trend with little variation in the drought period was observed. Thus, SPI index was selected for studying the impact of climate change on drought intensity and found that the wet years are more than drought years for all the RCP scenarios with RCP 8.5 shows more drought period followed by RCP4.5 and RCP6. For the projected period from 2021-70, extreme drought condition will occur only once and severe drought condition will occur six times for RCP8.5 whereas no extreme and severe drought conditions were observed for RCP4.5 and RCP6.

SWAT successfully achieved the aim of this research; to assess the impact of climate change and conservation practices in the Thuthapuzha watershed. Nevertheless, uncertainty cannot be avoided in this study since climate model datasets were used for making the future prediction. The results of the entire research work will give an insight to hydrologists in solving climate change related issues as well as provides water resources managers with an effective tool for the integrated catchment management.